Spring 2010

The role of pulmonary dendritic cells in regulating the antigen-specific CD8 T cell response following influenza virus infection

Jodi Lynn McGill
University of Iowa

THE ROLE OF PULMONARY DENDRITIC CELLS IN REGULATING THE ANTIGEN-SPECIFIC CD8 T CELL RESPONSE FOLLOWING INFLUENZA VIRUS INFECTION

by

Jodi Lynn McGill

An Abstract

Of a thesis submitted in partial fulfillment
of the requirements for the Doctor of
Philosophy degree in Immunology
in the Graduate College of
The University of Iowa

May 2010

Thesis Supervisor: Assistant Professor Kevin L. Legge

ABSTRACT

We have recently demonstrated in a model of influenza A virus (IAV) infection that the absence of specific pulmonary DC subsets, including plasmacytoid DC (pDC) and CD8α^+ DC, from the lungs leads to a significant decrease in the number of virus-specific CD8 T cells. Reconstitution of the lungs with physiologic numbers of pDC or CD8α^+ DC is able to restore the pulmonary IAV-specific CD8 T cell response to near normal levels via a mechanism that is dependent upon direct DC:T cell interactions, DC-expressed MHC I and the presence of viral antigen. Interestingly, however, this rescue is DC subset specific, as reconstitution with purified alveolar and airway DC or alveolar macrophages was unable to rescue the virus-specific CD8 T cell response. Following IAV infection there is an abundance of IAV antigen and MHC I expressing cells present in the lungs, including infected epithelial cells. Given this fact and the inability of all DC subsets to rescue the virus-specific CD8 T cell response, it suggested that there were additional, undefined requirements for pDC- and CD8α^+ DC-mediated rescue of the T cell response in the lungs. Further, although it was known that the reduction in virus-specific CD8 T cells in the lungs was a result of increased T cell apoptosis, it remained unclear what pathways of apoptosis were contributing to the increased cell death, and what mechanism pulmonary DC subsets were utilizing to rescue this defect.

Here, we demonstrate that in the absence of lung-resident DC subsets, virus-specific CD8 T cells undergo significantly increased levels of apoptosis via both extrinsic activation induced cell death and intrinsic activated cell-autonomous death pathways. Reconstitution of aDC depleted lungs with pulmonary pDC and CD8α^+ DC promotes increased T cell expression of the pro-survival molecule Bcl-2 and hence, increased T

cell survival and accumulation in the lungs. Our studies herein demonstrate that pulmonary DC subsets utilize a variety of mechanisms to promote the rescue of virus-specific CD8 T cells in the lungs. Blockade of the costimulatory molecules CD70, and in some cases, 4-1BBL and OX40L, ablates the pulmonary DC mediated rescue of CD8 T cell numbers in the lungs, suggesting that late costimulation is one essential mechanism that pulmonary DC use to regulate CD8 T cell immunity following IAV infection. Further, we demonstrate that the absence of DC following IAV infection results in significantly reduced levels of IL-15 in the lungs and that pulmonary DC-mediated rescue of virus-specific CD8 T cell responses in the lungs requires the trans-presentation of IL-15 via DC-expressed IL-15Rα. In addition to the role of pulmonary DC mediated costimulation and IL-15 trans-presentation, we further demonstrate a previously unrecognized role for viral antigen in regulating the accumulation of both pulmonary DC and virus-specific CD8 T cells in the lungs, suggesting that viral load can dictate the nature of the inflammatory environment in the lungs and thus, regulate the character of the ensuing IAV-specific immune response.

Collectively, the results detailed here demonstrate a previously unrecognized role for pulmonary DC in regulating primary IAV-specific CD8 T cell immunity, and hence, promoting enhanced viral clearance and recovery from disease.

Abstract Approved: _____
Thesis Supervisor

_____
Title and Department

_____
Date

THE ROLE OF PULMONARY DENDRITIC CELLS IN REGULATING THE ANTIGEN-SPECIFIC CD8 T CELL RESPONSE FOLLOWING INFLUENZA VIRUS INFECTION

by

Jodi Lynn McGill

A thesis submitted in partial fulfillment
of the requirements for the Doctor of
Philosophy degree in Immunology
in the Graduate College of
The University of Iowa

May 2010

Thesis Supervisor: Assistant Professor Kevin L. Legge

Graduate College
The University of Iowa
Iowa City, Iowa

CERTIFICATE OF APPROVAL

_____

PH.D. THESIS

_____

This is to certify that the Ph.D. thesis of

Jodi Lynn McGill

has been approved by the Examining Committee
for the thesis requirement for the Doctor of Philosophy
degree in Immunology at the May 2010 graduation.

Thesis Committee: _____
Kevin L. Legge, Thesis Supervisor

_____
John T. Harty

_____
Wendy J. Maury

_____
Annette J. Schlueter

_____
Thomas J. Waldschmidt

TABLE OF CONTENTS

LIST OF TABLES

Table

LIST OF FIGURES

Figure

LIST OF ABBREVIATIONS

APC: antigen presenting cell

aDC: airway and alveolar dendritic cells

aMϕ: alveolar macrophage

ACAD: activated cell-autonomous death

AICD: activation induced cell death

CL-4: Clone-4 T cell receptor transgenic cells

CTL: cytotoxic T lymphocytes

DC: dendritic cell

EIU: egg infectious unit

HA: hemagglutinin

HSV: herpes simplex virus

IAV: influenza A virus

iDC: interstitial dendritic cell

IFN: interferon

iNOS: inducible nitric oxide synthase

LCMV: lymphocytic choriomeningitis virus

LN: lymph node

LNDC: lymph node resident dendritic cell

MFI: mean fluorescence intensity

NK cell: natural killer cell

NP: nucleocapsid

NS-1: nonstructural 1

pDC: plasmacytoid dendritic cell

p.i.: post infection

rDC: respiratory dendritic cell

RSV: respiratory syncitial virus

TCIU: tissue culture infectious unit

TCR: T cell receptor

TipDC: TNF-/inducible nitric oxide synthase producing dendritic cell

TLR: toll like receptor

TNF: tumor necrosis factor

TRAIL: tumor necrosis factor related apoptosis-inducing ligand

VSV: vesicular stomatitis virus

CHAPTER I INTRODUCTION

Influenza virus infection

Influenza A virus (IAV) infections represent a major public health threat, particularly in the case of children, the elderly and those with underlying diseases, all of whom are at an increased risk for disease complications and death following IAV infection (1-3). Seasonal outbreaks alone cause an estimated 200,000 hospitalizations and over 30,000 deaths annually in the United States (4). In addition to typical seasonal infections, IAV can also undergo substantial changes (through recombination/ antigenic shift) that leave us with little to no protective immunity and increase influenza's mortality rate even among healthy young adults (5-8). In the last century alone we have observed three major pandemics: the 1918 Spanish flu, 1957 Asian flu and the 1968 Hong Kong flu; with the 1918 pandemic being the most devastating, causing an estimated 30-50 million deaths worldwide (5, 9). Furthermore the recent appearance of IAV strains with pandemic potential, such as H5N1 avian influenza, have highlighted the importance of research into IAV infections and the innate and adaptive immune responses that control and eliminate infection.

Influenza Virus

Influenza viruses have a negative sense, single stranded, segmented RNA genome and are member of the Orthomyxoviridae family of viruses (10, 11). There are three groups of influenza virus, A, B, and C and, while all three groups are associated with human disease, only group A influenza has an extended host range. The segmented RNA genome encodes eleven proteins, including the hemagglutinin (HA) and neuraminidase (NA) proteins that are essential for infection and often used to classify the virus into subtypes, as well as nucleoprotein (NP), M1, M2, NS1, NS2, PA, PB1, PB1-F2 and PB2 (10, 11). In humans, IAV is transmitted via respiratory droplets and primarily involves

infection of the epithelial mucosa of the respiratory tract (10, 11), although other cell types, including dendritic cells (DC), can become infected (12). Much of our current knowledge of the immune response to IAV is based on the well-characterized mouse model of IAV infection, which accurately recapitulates many aspects of the human disease (13-16). Like human IAV infection, IAV in mice primarily results in infection of the epithelial mucosa of the respiratory tract, although other cell types including DC and lymphocytes can become infected (17), albeit with reduced efficiency and limited productivity.

During the initial steps of replication, IAV uses its hemagglutinin protein to recognize and bind sialic acid residues located on the surface of epithelial cells that line the nose, throat and lungs (10, 16). The hemagglutinin is proteolytically cleaved and the virus is imported into the cell by endocytosis. Once in the endosome, the hemagglutinin protein fuses the viral envelope to the vacuole membrane, and the M2 ion channel allows acidification of the viral core, causing disassembly and release of the viral RNA and core proteins (10, 16). Amantadine, one of the antiviral drugs shown to be effective against IAV, targets the M2 ion channel, thus preventing viral disassembly and replication (10, 16). Next, the viral RNA and core proteins form a complex that is transported into the cell nucleus, where the RNA polymerase transcribes positive-sense viral RNA which will then be exported to the cytoplasm to be translated into new viral proteins, or will remain in the nucleus to be packaged into new viral particles (10, 16). During replication, newly assembled viral RNA is packed into a new virion together with the RNA-dependent polymerase and viral core proteins. The virion then buds from the cell in part of the host cell phospholipid membrane, simultaneously acquiring newly assembled HA and NA proteins which were secreted through the golgi apparatus to the cell surface following translation (10, 16). The mature virus is released from the host cell when its neuraminidase cleaves the sialic acid residues binding it. Oseltamivir, an antiviral drug

commonly used during IAV infection, inhibits neuraminidase, thus preventing the release of new infectious viruses (10, 16).

Viruses are known to use a variety of immune evasion strategies to avoid detection and elimination by the immune system. Type I IFNs possess potent antiviral properties and are critical to the control of IAV infection. IFN stimulation induces transcription of several IFN-responsive genes, many of which can protect and interfere with the establishment of IAV infection in uninfected cells (18, 19). Further IFN stimulation can regulate innate and adaptive immune responses through its ability enhance DC maturation and antigen cross-priming by CD8α^+ DC; and promote the survival and development of effector functions by activated CD8 T cells (20-31). Given the importance of type I IFN in regulating antiviral immunity, it is not surprising that IAV has evolved to produce a potent IFN antagonist, the NS1 protein. NS1 has been shown to inhibit type I IFN production by infected cells, including classical DC (32-36); and also to inhibit rDC maturation *in vitro*, resulting in a poor ability to stimulate virus-specific CD8 T cell responses (32, 33). In addition to immune evasion via NS-1, IAV also uses antigenic shift, the result of RNA polymerase replication errors that yield minor antigenic changes, and antigen drift, the result of major viral reassortment following co-infection with multiple IAV strains, as mechanisms to infect new host species and avoid protective immunity.

Dendritic cells

DC play a key role in bridging innate and adaptive immune responses following IAV infection. In the naïve steady-state, DC are located throughout the respiratory tract including the airway epithelium, lung parenchyma and the alveolar spaces of the lung (37-45) where they constantly survey for invading pathogens or foreign material. Lung-resident DC are a heterogeneous population with respect to surface phenotype and function, however, the predominant DC in the naïve lungs are airway and alveolar DC

(aDC), characterized as being $CD11c^{+}MHC\ II^{+}CD11b^{neg}CD4^{neg}CD8^{neg}$, and interstitial DC (iDC) characterized as being $CD11c^{+}MHC\ II^{+}CD11b^{hi}CD4^{neg}CD8^{neg}$ (38, 39, 46-48). Following a pulmonary insult or infection there is an influx of $CD11c^{+}MHC\ II^{+}$ DC into the lungs. This increase is due to both an increase in aDC and iDC numbers as well as the recruitment of additional subsets such as inflammatory monocyte-derived DC, plasmacytoid DC (pDC) and $CD8\alpha^{+}$ DC (47-55).

DC activation following IAV infection

Activated cytotoxic T lymphocytes (CTLs) are critical for clearance of a primary IAV infection in the lungs (56-59). Induction of adaptive IAV-specific CD8 T cell responses requires the presentation of peptide antigens by MHC molecules on the surface of mature APCs within the draining LN (60-63). Therefore, early studies were focused on identifying the primary cell population involved in initiating virus-specific T cell immunity following IAV infection. *In vitro* exposure of DC to IAV was shown to be sufficient to stimulate a primary virus-specific CD8 T cell response from LN-purified T cells (64-68). Further, IAV-infected DC were particularly potent inducers of IAV-specific immunity relative to other APC subsets and could trigger effective CD8 T cell responses without the addition of exogenous cytokines (64, 67). Together, these results suggested that DC are likely to be the primary population responsible for the induction of virus-specific CD8 T cell responses.

Prior to their interactions with naïve T cells in the LN, however, DC within the lungs must acquire IAV-antigen and mature. Although the primary route of DC antigen acquisition *in vivo* remains unclear, it is likely that DC acquire antigen via two distinct mechanisms: through direct infection with IAV (17, 64, 67, 68) or through phagocytosis of either dead or dying epithelial cells (60, 62, 69-74). Early *in vitro* studies demonstrated that DC are susceptible to direct infection by IAV and that IAV infection induces robust maturation and confers DC with the ability to induce potent virus-specific

T cell responses (64, 67, 68). Interestingly a fraction of respiratory DC (rDC) examined directly *ex vivo* from draining LN contain intact IAV NP antigen (75), as well as the non-structural IAV protein NS1 (76), and early studies have suggested the presence of plaqueable virus in DC isolated from the LN (17), together indicating that a direct infection of DC by IAV may occur *in vivo*. In support of this idea, recent studies in our laboratory using rt-PCR analysis to examine IAV NS2 mRNA expression in rDC purified from the draining LN suggest that ~5-10% of DC migrating from the lungs to the LN may be directly infected with virus (VanOosten and Legge, unpublished results).

In addition to the route of direct infection, DC can also acquire antigen through phagocytosis of dead or dying epithelial cells (60, 62, 69-74). Infection with IAV induces apoptosis of the respiratory epithelium (70, 71, 77). Encounter of naïve T cells with influenza antigen-bearing immature DC does not drive T cell activation but rather induces tolerance to viral antigens (78, 79). However, coupled with IAV-induced inflammation, DC uptake and present apoptosis-derived IAV antigens, mature and initiate an effective adaptive immune response (60, 62, 72, 73). Albert *et al.* demonstrated that human DC were able to acquire IAV antigen from apoptotic bodies and induce potent CD8 T cell responses *in vitro* (69, 80). Importantly, neither model of antigen acquisition is mutually exclusive and it is likely that both direct infection and uptake of apoptotic bodies from dying, virally-infected epithelial cells contributes to the ability of rDC to acquire and present viral antigens on their surface.

Following infection by or encounter with IAV, DC initiate production of proinflammatory cytokines and chemokines that can include IL-6, IL-12, TNF-α, IL-8, IP-10, RANTES, MIP-1β, and most importantly, type 1 interferons (IFNα and IFNβ) (61). Type I IFNs possess potent antiviral properties and are critical to the control of IAV infection. IFN stimulation induces transcription of several IFN-responsive genes, many of which can protect and interfere with the establishment of IAV infection in uninfected cells (18, 19). Further IFN stimulation can regulate innate and adaptive immune

responses through its ability to enhance rDC maturation and antigen cross-priming by CD8α^+ DC; and promote the survival and development of effector functions by activated CD8 T cells (20-31).

DC migration from the lungs to the LN

Migration of rDC from the lungs to the LN is a key step in the initiation of adaptive immune responses following IAV infection. Most studies examining DC trafficking have utilized intranasal or intra-tracheal installation of fluorescent dyes (51, 81), fluorescent dye-tagged latex particles or beads (82), or fluorescently-coupled macromolecules (40, 83, 84) to track cell migration out of the lungs to the draining LN. Under steady-state conditions, DC migrate continuously, but at low levels, from the lungs to the draining LN, and arrive therein in a semi-mature state (51, 85). This continual migration is thought to be important in promoting tolerance to innocuous antigens (39, 44, 45, 86, 87).

Following IAV infection or treatment with TLR agonists, we and others have demonstrated that DC trafficking from the lungs to the LN is rapidly enhanced, inducing an influx of mature, lung-derived DC into the draining LN (51, 81, 84). Using i.n. CFSE administration, we demonstrated that this rapid augmentation of DC migration into the LN is transient, however, peaking within 18 hours post infection (p.i.) and returning to baseline levels by 48 hours p.i. (51, 88). Contrasting reports have demonstrated a slightly longer period of enhanced DC migration from the lungs to the LN, sometimes as long as 5-7 days p.i. (81, 84), suggesting that the period of enhanced migration may be dependent upon the strain of IAV and the dose of infection.

DC and the induction of adaptive immune responses

Although rDC migration from the lungs to the LN is key for the initiation of adaptive immune responses, as blockade (51, 81) or depletion of rDC (89) prior to IAV infection inhibits activation of naïve IAV-specific CD8 T cells, rDC alone are not the

only DC population responsible for activating virus-specific T cell responses. Belz et al. recently examined the ability of migratory rDC, CD8α$^+$ LN resident, CD8α$^-$ LN resident or pDC purified from the lung draining LN of IAV infected mice to activate naïve, virus-specific CD8 T cells *in vitro*. These experiments revealed that both rDC that had migrated from the lungs to the LN, and CD8α$^+$ LN resident DC (LNDC) were able to activate naïve virus-specific CD8 T cells (81, 90-92). It is likely that the CD8α$^+$ LNDC, which are known to cross-present antigens, acquired viral antigens from the migrating rDC populations, thus allowing them to initiate IAV-specific CD8 T cell responses in the LN (91, 92). Several subsequent publications examining herpes simplex virus-1 (HSV) (81, 92-94), vaccinia virus (90), lymphocytic choriomeningitis virus (LCMV) and *Listeria monocytogenes* (95) have supported the hypothesis that migrating DC subsets transfer antigen to CD8α$^+$ LNDC upon arrival in the draining LN, suggesting that this may be a more global mechanism of promoting robust primary effector T cell responses.

Interestingly this transfer of antigen may have role outside of simply increasing the number of DC presenting viral antigen in the LN as Belz *et al*. have recently shown a division of labor between migratory rDC and CD8α$^+$ LNDC in activating naïve and memory virus-specific CD8 T cells following secondary virus challenge (96). Following IAV infection, both naïve and memory CD8 T cells responded to antigen-bearing CD8α$^+$ DC within the LN, but only naïve CD8 T cells responded to lung-derived migratory rDC. This diminished capacity of pulmonary DC to promote memory CD8 T cell expansion during subsequent challenge infections may be dependent upon expression of CD70, as LNDC promoted memory CD8 T cell expansion through CD70/CD27 interactions, while rDC stimulation of naive T cells was CD70 independent (96). Importantly these results suggest a unique mechanism for continually promoting naïve CD8 T cell expansion even in the face of preexisting memory. Unlike CD8 T cell activation, naïve IAV-specific CD4 T cells appear to instead be limited to activation via migratory DC populations (97). Importantly while the ability to present antigen to IAV-specific T cells is limited to only

a few distinct subsets of DC, it appears that IAV antigens are transferred from migratory rDC to several DC subsets within the LN (89). Therefore in the future, it will be important to more clearly elucidate the mechanisms and implications of this division of labor between DC subsets in priming/expansion of adaptive immune cells during primary, secondary, tertiary, etc. IAV challenges and following vaccination and boosting responses against IAV.

The kinetics of antigen presentation following IAV infection continues to remain a controversial subject. Antigen presentation and early activation of IAV-specific CD8 T cells in the lung-draining LN initiates at low levels as early as 1-2 days p.i. (81, 88, 98), consistent with the data suggesting that the influx of rDC from the lungs peaks at 18 hours p.i. (51, 88). However, the peak of antigen-presentation within the LN is thought to occur at day 3 p.i. and can be sustained out to at least 9 days p.i. (81), lending support to the evidence that migratory rDC transfer antigen to LN-resident $CD8\alpha^+$ DC and suggesting that the predominant antigen-presenting population at these later time points is, in fact, the $CD8\alpha^+$ LNDC subset (81, 90-92). Until recently, IAV was thought to cause an acute infection in immunologically competent hosts, and several groups using a variety of approaches including direct analysis for plaqueable virus, PCR for IAV genome or probing for MHC-IAV peptide complexes, have shown that IAV antigen is undetectable in the host by 15-18 days p.i. (13, 17, 99-103). However, recent data utilizing the adoptive transfer of IAV-specific T cells has suggested that, while undetectable by PCR, low levels of IAV-antigen may persist in the host for extended periods of time p.i. and, more importantly, that this persistent antigen pool is sufficient to generate/maintain virus-specific T cell responses for several months after infection (101, 102, 104, 105). In contrast, using a similar approach, Mintern *et al.* have convincingly demonstrated that IAV-peptide-MHC complexes do not persist at later times (i.e. days 30+) following IAV infections (103). In the coming years it will be important to resolve the differences in these findings as knowledge of the length of antigen presentation

following IAV infections is essential to our understanding of the initiation and maintenance of effector and memory adaptive IAV-specific immunity.

Role of pulmonary DC in the regulation of adaptive CD8 T cell responses in the lungs

Following IAV infection or encounter with foreign antigen, we and others have demonstrated a massive recruitment of $CD11c^+MHC\ II^+$ conventional DC and pDC into the lungs for at least 6 days p.i. (49, 51, 53-55, 89, 106). These recruited DC subsets do not subsequently migrate to the draining LN (51, 81), suggesting that they do not participate in the initiation of adaptive immune responses. However, there is accumulating evidence suggesting that these DC may be playing a role in shaping the ensuing adaptive immune response in the lungs.

We recently described a novel role for lung-recruited pulmonary DC subsets, particularly pDC and $CD8\alpha^+$ DC in promoting increased virus-specific CD8 T cells in the lungs (53) (Figure 1). Depletion of aDC at 48 hr post IAV infection (i.e. following the conclusion of DC trafficking from the lungs to the LN) resulted in increased mortality, increased pulmonary viral titers and reduced virus-specific CD8 T cells in the lungs (53). Further, aDC depletion resulted in reduced recruitment of pDC and $CD8\alpha^+$ DC to the lungs. Importantly, reconstitution of the lungs with purified pDC and $CD8\alpha^+$ was able to rescue the IAV-specific CD8 T cell response. This reconstitution of the virus-specific CD8 T cell response required direct cell-to-cell interactions between DC and T cells in the lungs and required MHC I and viral antigens on the reconstituted DC (53). At that time, it was unclear what additional mechanisms were contributing to the enhanced accumulation of virus-specific CD8 T cells in the lungs following pulmonary DC reconstitution. However, we have subsequently demonstrated that pulmonary DC provide key survival signals to virus-specific CD8 T cells in the lungs, as, in their

absence, the T cells undergo increased levels of apoptosis. This topic will be discussed further in Chapters III through V.

In accordance with our findings, Aldridge *et al*. recently demonstrated that TNF-/inducible nitric oxide synthase (iNOS)- producing DCs (TipDCs) that accumulate in the lungs following IAV infection interact directly with effector CD8 T cells in the lungs to promote increased CD8 T cell accumulation therein (107). In this model $CCR2^{-/-}$ mice, which fail to recruit TipDC to the lungs following infection, have a reduced virus-specific CD8 T cell response compared to wildtype controls. However, reconstitution of $CCR2^{-/-}$ lungs with purified TipDC promoted increased CD8 T cell accumulation in a manner that required IAV antigen (107).

In further agreement, using a model of RSV infection, Smit *et al*. have recently demonstrated a requirement for pDC in the lungs in promoting virus-specific CD8 T cell responses therein (108). In their model, Flt3L-induced expansion of pDC in the lungs resulted in increased virus-specific CD8 T cell responses in the lungs, while a specific depletion of pDC resulted in a reduction in the magnitude of the T cell response (108), together confirming an important role for lung-recruited pDC in shaping the magnitude of the RSV-specific CD8 T cell response. Overall, the above studies indicate an emerging role for pulmonary DC in regulating the magnitude and character of the adaptive CD8 T cell response in the lungs following infection by both IAV and other respiratory pathogens.

Alveolar Macrophages

The lung contains two primary phagocyte populations, DC and alveolar macrophages (aMϕ), with the latter being the predominant APC population in the airways during steady-state conditions. Classically, aMϕ are thought to have a regulatory phenotype in the lungs, existing in a relatively quiescent state during homeostasis (109). These resting aMϕ produce only low levels of inflammatory cytokines and are less

phagocytic than their counterparts in other tissues (109). Importantly, aMϕ have also been shown to suppress the induction of innate and adaptive immunity (110-113). *In vivo* depletion of aMϕ by clodronate-liposome administration leads to excessive inflammation and immunity to otherwise harmless inhaled antigens (113), while *in vitro* incubation of antigen-presenting DC in the presence of aMϕ can suppress T cell activation via a mechanism that involves nitric oxide (NO), IL-10, transforming growth factor-β (TGF-β) and prostaglandins (110). More recently, it has become evident that one of the primary mechanisms of aMϕ-mediated suppression is inhibition of DC maturation through the production of NO (110, 111).

Despite this role as a regulatory cell during steady-state conditions, the inhibitory phenotype of aMϕ can be overcome in the face of IAV infection in order to mount potent antiviral immune responses. Following activation, aMϕ convert into highly phagocytic cells that produce robust amounts of inflammatory cytokines including IL-6 and TNFα (114). In addition to aMϕ activation, IAV infection induces significant recruitment of inflammatory monocytes via CCR2 (115), that differentiate into monocyte-derived DC (moDC) and inflammatory "exudate" macrophages (52, 116-119). While initially inflammatory cells during the course of infection, emerging evidence suggests that these exudate macrophages will eventually develop the suppressor phenotype of lung-resident aMϕ, helping to restore preinfection homeostasis in the lungs over the course of a few days (120, 121). Although aMϕ were originally described as the cell type responsible for pulmonary monocyte recruitment during IAV infection, a recent study by Herold *et al*. suggests that instead the majority of the recruitment results from alveolar epithelial cells that produce high levels of CCL2 (MCP-1), a ligand for CCR2, following infection (119).

In addition to their role in immunity to more "seasonal" strains of IAV, infection with highly pathogenic IAV are also known to induce significant recruitment of aMϕ to the lungs (122-124). Although this excessive inflammation was initially thought to contribute to the pathogenicity of the virus, a recent report by Tumpey *et al*. demonstrates

an essential role for these macrophages in regulating anti-viral immunity in mice (124). Depletion of aMϕ prior to, but not 3 or 5 days following, IAV infection results in uncontrolled viral replication and a significant increase in IAV-associated mortality (124). These results suggest that macrophages play a key role in the early control of virus infection prior to the induction of adaptive responses. In accordance with this idea, Kim *et al*. have demonstrated a similar essential role for aMϕ following IAV infection of swine (125). In this model, although no mortality was observed, swine depleted of aMϕ prior to IAV infection exhibited increased respiratory stress, increased induction of IL-10 and a significant reduction in pulmonary TNFα levels. Further, aMϕ depletion resulted in reduced antibody titers and reduced numbers of virus-specific CD8 T cells in the lungs at later time points p.i. (125). It has been suggested that aMϕ phagocytosis is the key mechanism through which these cells regulate IAV infection, as clearance of apoptotic host cells is essential to limit virus spread. Therein, not surprisingly, inhibition of aMϕ and neutrophil phagocytosis in the lungs following IAV infection results in increased viral titers and IAV-associated mortality (126). Together, the results above suggest an important role for macrophages in the innate immune response in the lungs following IAV infection.

Despite the apparently beneficial role that these cells play in controlling early viral replication, several contrasting reports have demonstrated a more deleterious role for aMϕ following IAV infection. Excessive inflammation in the lung is detrimental following a variety of respiratory challenges (127, 128). The majority of immunopathology associated with IAV infection has been attributed to NOS2 and TNFα, as IAV infection of mice deficient in either exhibit decreased mortality (129-131) and antioxidant treatment (which inhibits NOS2) of IAV-infected mice results in improved lung function and accelerated disease resolution (132). Importantly, both cytokines appear to contribute to pulmonary damage and destruction, but have little effect in controlling viral replication (133, 134).

Until recently, the phenotype of the cells that produced the majority of NOS2 and TNFα in the lungs following IAV infection was unknown. However recent work has demonstrated that IAV infection of CCR2-deficient mice results in decreased monocyte/macrophage recruitment to the lungs, as well as reduced lung pathology and mortality compared to wildtype controls (115, 119, 135). Similarly a dependence on CCL2 for recruitment of macrophages was observed in mice constitutively overexpressing the CCR2 ligand, CCL2. IAV-infection of these mice significantly increased monocyte/macrophage recruitment to the lungs, immunopathology and mortality (52). Finally, Lin *et al*. have demonstrated that the moDC and exudate macrophages recruited to the lungs during IAV infections via CCR2 are responsible for the majority of NOS2 and TNFα production in the lungs following infection. Together these studies suggest that macrophages may be a predominant cell population contributing to IAV-associated immunopathology (52).

In addition to their role in promoting cytokine-associated immunopathology, Herold *et al.* have shown a direct role for macrophages in promoting increased lung epithelial apoptosis following IAV infection. Exudate macrophages express increased levels of tumor necrosis factor-related apoptosis-inducing ligand (TRAIL) in the lungs following IAV infection (135), and the abrogation of TRAIL signaling by exudate macrophages results in a significant reduction in epithelial cell apoptosis in the lungs, decreased immunopathology and decreased IAV-associated mortality. Together, these results suggest that macrophage-derived TRAIL may play an important role in promoting epithelial cell apoptosis and lung immunopathology (135).

The above results accentuate the importance of a balanced immune response, particularly in a delicate tissue such as the lungs. Although several groups have demonstrated an essential role for macrophage-derived innate immunity following IAV infection, excessive inflammatory cytokine production and immune cell recruitment

resulting from activated macrophages can result in increased immunopathology and increased susceptibility to virus-associated mortality.

Mechanisms of CD8 T cell apoptosis

Following initiation of an immune response, primary, virus-specific CD8 T cells undergo massive proliferation and differentiation to activated effector cells (59). Following clearance of the pathogen, however, these activated effector cells must be eliminated. Activated, effector CD8 T cells are known to undergo apoptosis via 2 broad mechanisms, the first being activation induced cell death (AICD) and the second being activated T cell autonomous death (ACAD) (20, 136, 137). AICD occurs during TCR stimulation without appropriate costimulation, and, while not required, most often occurs in the presence of death receptors and ligands (e.g. CD95 on apoptotic T cells and CD95L on killer cells) (138). ACAD is intrinsic, cell death-receptor independent and occurs during cytokine and growth factor withdrawal (139). It is likely that both AICD and ACAD cooperate to eliminate effector T cells during the contraction phase of an immune response (20, 136, 137).

If AICD proceeds downstream of a death receptor (i.e. CD95, etc.), it occurs via one of two pathways: the extrinsic type I cell-death pathway or the extrinsic type II cell death pathway (20, 136, 137) (see Figure 2). In the extrinsic type II cell death pathway, apoptosis proceeds downstream from the death receptor via active caspase 8 and Bid, through the mitochondria and Bax aggregation to cytochrome c release, which stimulates apoptosome formation and activation of caspase 9, followed by activation of caspase 3/6/7 and ultimately, death (20, 136, 137). This type of signaling can be blocked by expression of anti-apoptotic Bcl-2 which binds to Bax or Bak to prevent apoptosis (20, 136, 137). The extrinsic type I cell-death pathway again proceeds from the death receptor to active caspase 8 but then bypasses the apoptosome, Bid, Bax, etc. and proceeds

directly to activating the effector caspases 3/6/7 (20, 136, 137). Unlike the extrinsic type II cell death pathway this pathway is not blocked by Bcl-2.

ACAD, which occurs during cytokine and growth factor withdrawal, is intrinsic and cell death-receptor independent (20, 136, 137) (see Figure 3). Apoptosis through this pathway proceeds independent of active capase-8 through Bim to the mitochondria and cytochrome c release, which stimulates formation of the apoptosome and activation of caspase 9. Caspase 9 stimulates activation of caspase 3/6/7, which leads to subsequent cell death. Like the extrinsic type II cell-death pathway, the ACAD pathway is inhibited by Bcl-2 and may in fact initiate due to a reduction in the ratio of anti-apoptotic Bcl-2 to pro-apoptotic Bim within a cell (20, 136, 137).

Sensitivity to both ACAD, and, in particular, AICD, is strictly controlled and is thought to depend upon the activation status of the T cell (20, 136, 137). During the activation and expansion phase, the T cell is thought to be resistant to apoptosis, but this resistance declines later in the effector phase and renders the T cell susceptible to death. In the case of AICD, while not entirely understood, it is thought that signals via the T cell receptor (TCR) can induce upregulation of both anti-apoptotic molecules such as c-FLIP, Bcl-2 and Bcl-X_L and pro-apoptotic molecules such as CD95L, Bim and Nur77 (140-142). T cell fate is then determined by the balance between these molecules and is largely dependent upon the types of signals received by the cell and the cytokine milieu present at the time of TCR stimulation. For example, IL-2, while an important survival factor for effector T cells, is also necessary for sensitization to AICD (143, 144). IL-2 will induce downregulation of both the survival factor c-FLIP and upregulation of the pro-apoptotic molecule CD95 (145). Additionally, stimulation of effector T cells via their TCR in the presence of IL-2 and IL-4 (146) or IFNγ (147) induces increased degradation of c-FLIP and hence, increased apoptosis by AICD. In contrast, stimulation via the TCR in the presence of IL-2 and IL-15 instead inhibits apoptosis by AICD (148-150), likely as a result of IL-15 mediated Bcl-X_L upregulation (151, 152). Together,

these results suggest that T cell survival depends upon a delicate balance of pro- and anti-apoptotic signals to the cell that are delivered via cytokine and TCR signals. Given the intricate mechanisms involved in regulating T cell survival, it suggests that during infection even small changes in the antigen load or inflammatory milieu can disrupt the balance between survival and death, potentially resulting in impaired and ineffective T cell responses, or in contrast, overly robust and elongated responses that may result in damaging immunopathology.

Interleukin 15

The cytokine interleukin-15 has been demonstrated to play a key role in promoting lymphoid homeostasis, particularly with respect to CD8 T cells (153, 154). IL-15 is a member of the common γ-chain family of cytokines and has been demonstrated to share many similarities with both IL-2 and IL-7. IL-15 can bind with high-affinity to IL-15Rα and moderate-affinity to the IL-2/IL15Rβ-common γ-chain complex. IL-15 was initially thought to signal similar to IL-2, whereby IL-15Rα formed a heterotrimeric complex with IL-2/IL15Rβγ for high affinity signaling. While this model appears to hold true in certain situations, recent reports have demonstrated a unique, alternative signaling model, termed trans-presentation. In this model, IL-15Rα is required for the processing and presentation of active IL-15 in trans to cells expressing the IL-2/IL15Rβγ complex (155-157). Through a series of adoptive transfer experiments utilizing combinations of IL-15 and IL-15Rα deficient donor and host cells, it has been shown that T cell responsiveness to IL-15 requires only the moderate affinity IL-2/IL15Rβγ complex, but not the high-affinity chain. However, processing and presentation of IL-15 requires the presence of IL-15Rα (158). This model is consistent with the observation that IL-15Rα transcripts are widely expressed by many cell types, suggesting that these cells may play a role in presenting IL-15, but do not necessarily respond to the cytokine signal. (158)

At this time, it is unclear which specific cells serve as the primary trans-presenting cells in the face of an immune response, however, several lines of evidence have indicated that DC may be playing an important role (159, 160). It appears that radiation-sensitive hematopoietic cells are most effective at promoting IL-15 mediated responses (160, 161), and the cells appear to be myeloid in origin, as hematopoietic cells from $RAG^{-/-}$ or wildtype mice are equally effective at mediating IL-15 signals (159, 161). It is known that DC express both IL-15 and IL-15Rα, and that stimulation by IFNαβ (162) or IFNγ (163, 164), as well as double-stranded RNA, LPS, bacterial or viral infection leads to further upregulation (154, 162, 165, 166). In addition, DC are responsive to IL-15 levels, providing a positive feedback loop that leads to increased IL-15 production as well as upregulation of costimulatory molecules CD80, CD40, and MHC I and II (162) and enhanced production of IL-12 (167). Given these changes, it is not surprising that DC matured in the presence of IL-15 have been demonstrated to promote enhanced antigen-specific CD8 T cell proliferation (162, 168) and a robust Th1 skewing *in vivo* (169). In addition to IL-15's role in promoting DC maturation, it has also been demonstrated to promote DC survival. $IL\text{-}15^{-/-}$ and $IL\text{-}15R\alpha^{-/-}$ mice have reduced numbers of DC in both the blood and spleen, a defect which can be partially rescued with exogenous IL-15 treatment (165).

Although it has been demonstrated to play a minor role in maintaining the homeostasis of naïve CD8 T cells, IL-15 has been best characterized for its role in maintaining memory CD8 T cell homeostasis. Memory CD8 T cells express increased levels of IL-2/IL15Rβ relative to naïve CD8 T cells (150), and it has been demonstrated that mice lacking IL-15 or the high-affinity IL-15Rα have depleted numbers of memory CD8 T cells following challenge (160, 170-172). While these mice initially generate normal memory CD8 T cell responses, their numbers gradually decrease over time concurrent with decreased BrdU incorporation, suggesting that IL-15 plays an important role in promoting memory CD8 T cell basal proliferation (160, 170-172).

More recently, there has been increasing evidence that IL-15 is also important for promoting effector CD8 T cell responses (151, 152, 170, 173-175). Surface expression of both IL-15Rα and IL-2/IL15Rβ increase following TCR activation (174) and the addition of exogenous IL-15 has been demonstrated to promote increased survival of activated CD8 T cells both *in vitro* and *in vivo* following challenge with Staphylococcal Enterotoxin A (174), *Mycobacterium tuberculosis* (173) and Vesicular Stomatitis virus (VSV) infection (155). Interestingly, it appears the requirements for IL-15 by effector CD8 T cells may differ depending upon the type of immune response. IL-15$^{-/-}$ mice are able to mount a robust CTL response against LCMV (171), but exhibit an ~50% reduction in the primary CD8 T cell response to VSV (170). Several studies have suggested that IL-15 is crucial for survival of activated CD8 T cells (152, 174, 175). An examination of the molecular basis for IL-15 mediated protection suggested that while IL-15 signaling did not inhibit the expression of the pro-apoptotic molecules Bax or Bcl-xS, it promoted strong induction of the important anti-apoptotic molecules Bcl-2 and Bcl-xL (152). Bcl-2 has been demonstrated to play a critically important role in activated CD8 T cell survival (20, 136, 137), suggesting that IL-15 mediated signaling may be one of the important factors promoting its upregulation following T cell activation.

Together, the above studies suggest a particularly important role for IL-15 in the generation and maintenance of an appropriate immune response. It is still unclear what role IL-15 may be playing during the effector phase of the response and in what context it is promoting activated T cell survival. Further, although IL-15 has been demonstrated to induce effective DC maturation, it is unclear what influence this has on the course and outcome of the immune response *in vivo*. This topic will be further explored in Chapter IV.

Costimulatory molecules and their role in regulating CD8 T cell immunity

Activation and differentiation of naïve CD8 T cells requires an encounter with a mature, antigen-bearing dendritic cell that is capable of presenting peptide in the context of MHC I and accompanying costimulatory molecules (60-63). Costimulation is required for the T cell to achieve full activation and survival, as TCR stimulation in the absence of costimulation results in tolerance, rather than immunity (78, 79). CD28 is widely considered to be the primary costimulatory receptor for initiation of T cell expansion and survival (176, 177). Recently, however, several additional costimulatory molecules have been identified that, while usually not capable of acting independently of CD28 costimulation, can regulate T cell expansion and survival later during the effector phase of the response. Amongst these "late" costimulatory molecule pairs (T/DC), OX40 (CD134 and TNFRSF4) /OX40L (CD252 and TNFSF4), 4-1BB (CD134 and TNFRSF9)/ 4-1BBL (TNFSF9) and CD27 (TNFRSF7)/CD70 (TNFSF7) have all been demonstrated to promote increased CD8 T cell activation, survival and expansion following pathogen challenge (178-180).

DC activation and maturation is induced following encounter with a variety of signals, including TLR agonists and inflammatory cytokines (60, 61). In the presence of these signals, ligation of CD40 on the DC surface, (i.e. by CD4 T cell expressed CD40L), leads to increased activation, enhanced survival and upregulation of several key costimulatory molecules, including CD80 (B7.1), CD86 (B7.2), 4-1BBL, OX40L and CD70 (176, 181-186). As a key regulator of APC activation, CD40 can indirectly influence the development of the ensuing CD8 T cell response, making it an important costimulatory molecule (187). While CD40 costimulation has a well defined role in germinal center formation, antibody class switching and promoting CD4 T cell responses (187), its role is less understood in the context of CD8 T cell responses and viral infections. For example, CD40 is dispensible following primary infection with VSV,

LCMV or HSV-1 (188, 189), but the absence of CD40 results in impaired memory response to LCMV (188). In contrast, following a primary IAV infection, CD40 licensing is necessary for optimal CD8 T cell responses (190), but not via a direct mechanism. Rather, CD40 is required on non-CD8 T cells in order to achieve effective cellular immunity to IAV, supporting the classical model of CD4 T cell help and DC licensing (190).

CD28 is widely considered to be the primary costimulatory molecule for initial expansion and survival of both CD4 and CD8 T cells (176, 177). CD28 is constitutively expressed by naïve T cells, and its binding to CD80 or CD86 on the surface of activated DC results in delivery of a strong costimulatory signal to T cells activated via their TCR (176, 177, 191). While a few models of infection appear to be CD28 independent (192-196), the majority of viral models, including VSV (197, 198), HSV-1 and 2 (189, 199), vaccinia (194, 195) and IAV infection (166, 181, 200-204) require CD28 costimulation in order to mount protective CD8 T cell responses. Primary infection of $CD28^{-/-}$ or $CD80^{-/-}$ $CD86^{-/-}$ mice with the aforementioned viruses results in delayed clearance and increased disease. Interestingly, these effects appear to be limited to the primary response, as there is no additional loss of T cell numbers over time and recall responses are not impaired in the absence of CD28 costimulation (198, 205, 206).

4-1BB is a member of the TNFR superfamily that is most highly expressed by activated CD8 T cells, but can also be found on the surface of several other cell types including DC, monocytes, NK cells and activated CD4 T cells (178-180, 207). 4-1BBL is primarily expressed by activated DC, macrophages and B cells, but can be expressed by non-immune cell types at sites of inflammation (178-180, 207). While it has been shown to induce resting CD4 and CD8 T cell proliferation and cytokine production (208-211), it appears that the major physiological role for 4-1BB signaling is to enhance T cell survival. Importantly, most evidence suggests that 4-1BB stimulation is most effective for regulating CD8, rather than CD4, T cell survival and accumulation. For example, 4-

1BB stimulation can prevent AICD in effector T cells (212), and systemic administration of agonistic anti-4-1BB can prolong CD8 T cell, but not CD4 T cell, survival following superantigen administration (213). It is likely that 4-1BB stimulates expression of the pro-survival factors Bcl-X_L and Bfl-1 (214), thus promoting increased and prolonged CD8 T cell survival. In the context of pathogen challenge, the absence of 4-1BB or 4-1BBL results in mildly impaired primary CD8 T cell responses to several acute viral infections including VSV, LCMV and IAV (215-217). Interestingly, this requirement appears to vary with antigen load and the severity of infection, as the absence of 4-1BB signaling during infection with low dose LCMV (215) or low virulence IAV (218), resulted in only a minor reduction in the CD8 T cell response, while the absence of 4-1BB signaling during high dose LCMV challenge (216) or infection with highly virulent IAV (218), resulted in severely impaired CD8 T cell responses and increased mortality. Together, these results suggest that 4-1BB may play a specialized role in regulating CD8 T cell survival during highly stringent challenges, but may be dispensable following less severe infection.

Like 4-1BB, OX40 is also a member of the TNFR superfamily that is primarily expressed by activated T cells, while its ligand, OX40L is expressed by activated B cells and DC (178-180, 207). In contrast to 4-1BB however, OX40 is more prominently expressed by activated CD4 T cells than by CD8 T cells (178-180, 207), suggesting an important role for OX40 on helper T cells. In agreement, mice deficient in OX40 or its ligand consistently show defects in CD4 T cell responses with reduced Th1 and Th2 cytokine production and decreased contact sensitivity (183, 219-221), but little affect on the accompanying CTL response (219-221). Treatment of IAV-infected mice with OX40-Ig results in prolonged CD4 T cell survival in the lungs, but does not alter CD8 T cell responses (222). Despite this, there is some evidence suggesting that OX40 can directly regulate CD8 T cell responses, as systemic administration of agonistic anti-OX40 can induce proliferation and IL-2 production by both CD4 and CD8 T cells (223-226),

and can prolong both CD4 and CD8 T cell survival following systemic superantigen administration (227).

CD27 is a stimulatory member of the TNFR superfamily that is expressed by both naïve and activated T cells (178, 179, 207, 228). Expression of its ligand, CD70, is highly regulated and restricted primarily to activated T cells, B cells and DC (178, 179, 207, 228). Mice deficient in CD27 exhibit reduced CD4 and CD8 T cell responses following primary and secondary IAV infection (204, 229), while young mice transgenic for CD70 exhibit enhanced CD8 T cell responses to IAV as a result of both increased cell numbers and increased effector function per cell (230). Interestingly, the effects of CD70 deficiency or over-expression observed following IAV infection are most apparent in the lungs, rather than the spleen or draining LN (204, 229), suggesting that CD70 may also be important for accumulation in peripheral tissues. CD27 signaling does not lead to increased proliferation, but has instead been shown to promote prolonged T cell survival following viral infection (204). In the case of IAV, blocking CD70 at the later stages of the effector phase results in reduced numbers of virus-specific CD8 T cells and increased T cell sensitivity to Fas-mediated apoptosis (231). Additionally, while recall CD8 T cell responses do not directly require CD27 stimulation, blockade of CD70 at the later stages of the primary response indirectly affects the quality of IAV-specific memory responses as a result of increased and accelerated contraction during the primary response (231). Together, these results suggest that while CD27 costimulation is not required at the priming phase of the CTL response, CD27/CD70 interactions are required by CD8 T cells in the lungs during the later phase of the response in order to prolong their survival and promote the development of effective virus-specific memory responses.

Purpose of Study

Previous studies have shown that the absence of or reduced recruitment of pulmonary DC in the lungs results in impaired CD8 T cell responses following IAV infection. This defect is a result of increased CD8 T cell apoptosis, and can be rescued by reconstitution with purified pulmonary pDC and CD8α^+ DC via a mechanism that requires MHC I and viral antigen. It was unclear what mechanisms were contributing to the increased pulmonary T cell death following aDC depletion and what additional signals mediated via pulmonary DC were necessary to promote the survival and accumulation of effector CD8 T cells in the lungs following IAV infection. The purpose of this study was to answer the following questions:

1) Do costimulatory molecules contribute to the pulmonary DC mediated rescue of virus-specific CD8 T cell responses in the lungs of aDC depleted mice?
2) What is the role and pathway of increased CD8 T cell apoptosis in the lungs of IAV-infected and aDC depleted mice?
3) What is the role of ACAD and how does IL-15 regulate antigen-specific CD8 T cell responses in the lungs following IAV infection?
4) What is the role of AICD and how does antigen load and death receptor signaling regulate antigen-specific CD8 T cell responses in the lungs following IAV infection and aDC depletion?

Figure 1. The role of DC in the initiation and regulation of adaptive CD8 T cell responses following IAV infection. 1) rDC lining the airways and alveolar spaces of the lungs acquire influenza antigen either through direct infection or uptake of apoptotic bodies from infected epithelial cells. rDC undergo maturation and migration to the lung draining LN. 2) Once in the LN, rDC pass on antigen to LN-resident $CD8\alpha^+$ DC. Both LN-resident $CD8\alpha^+$ DC and rDC interact with naïve antigen-specific CD8 T cells in the LN and initiate a program of activation, proliferation and differentiation into cytotoxic effector cells. 3) Activated effector CD8 T cells migrate from the LN to the lungs. 4) CD8 T cells undergo a second direct interaction with MHC I expressing, viral antigen-presenting pulmonary pDC, $CD8\alpha^+$ DC or TiP DC in order to accumulate to sufficient numbers to mediate viral clearance and protection.

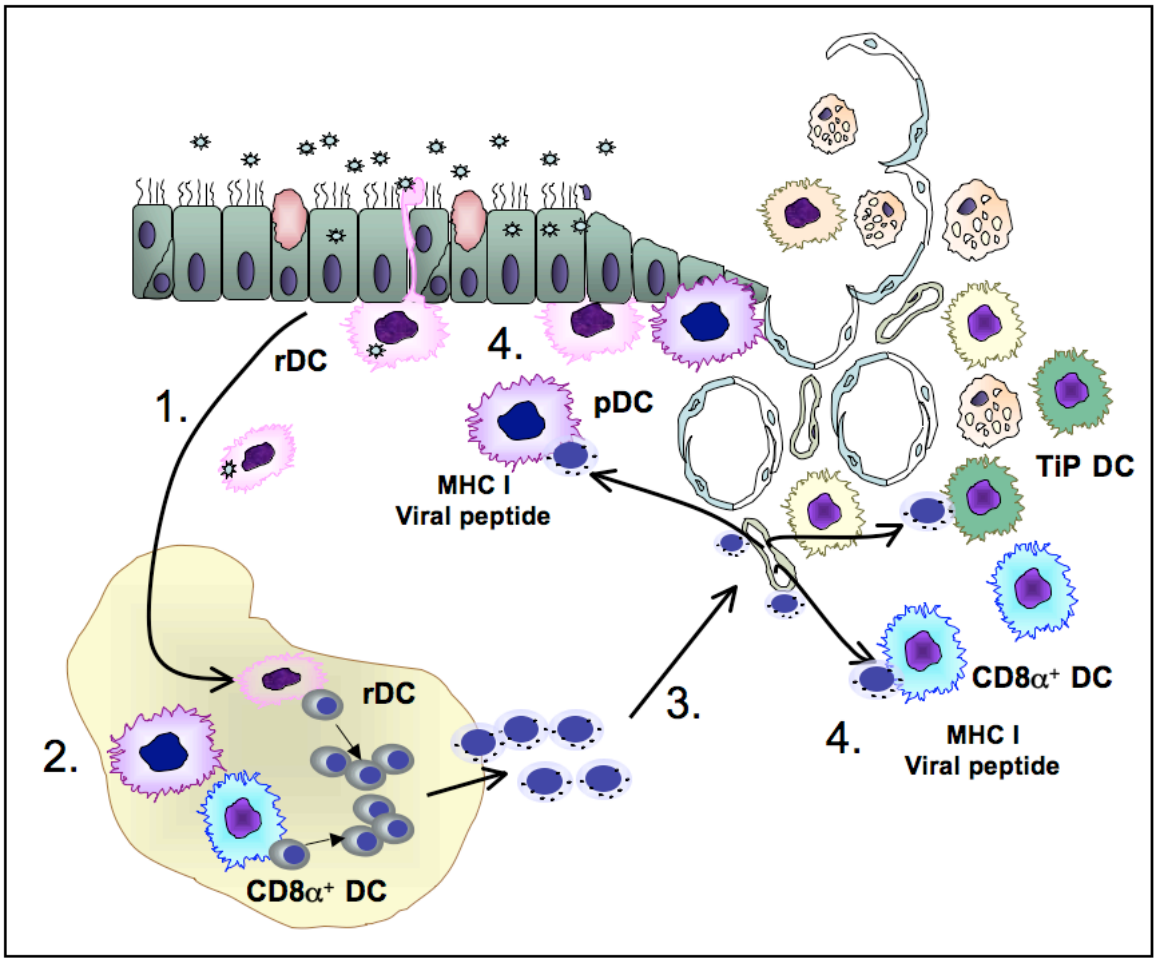
rDC
1.
4.
pDC
MHC I
Viral peptide
TiP DC
CD8α⁺ DC
4.
MHC I
Viral peptide
3.
2.
rDC
CD8α⁺ DC

Figure 2. Activation Induced Cell Death: Extrinsic cell death pathways I and II. Ligation of CD95 (Fas) leads to formation of the DISC and subsequent cleavage of Pro-caspase 8 or 10 to active caspase 8 or 10. In type I cells, active caspase 8 can directly lead to the activation of the effector caspases 3/6/7, and subsequent death. In type II cells, active caspase 8 cleaves BID to its active form truncated BID (tBID). tBID then releases cytochrome C from the mitochondria, which results in formation of the apoptosome and activation of the initiator pro-caspase 9. Active caspase 9 then activates the effector caspases 3/6/7, ultimately resulting in cell death. The type II cell death pathway can be inhibited by the pro-survival factor Bcl-2, while the type I cell death pathway cannot. Figure 2 was adapted from a figure created by R. A. Langlois.

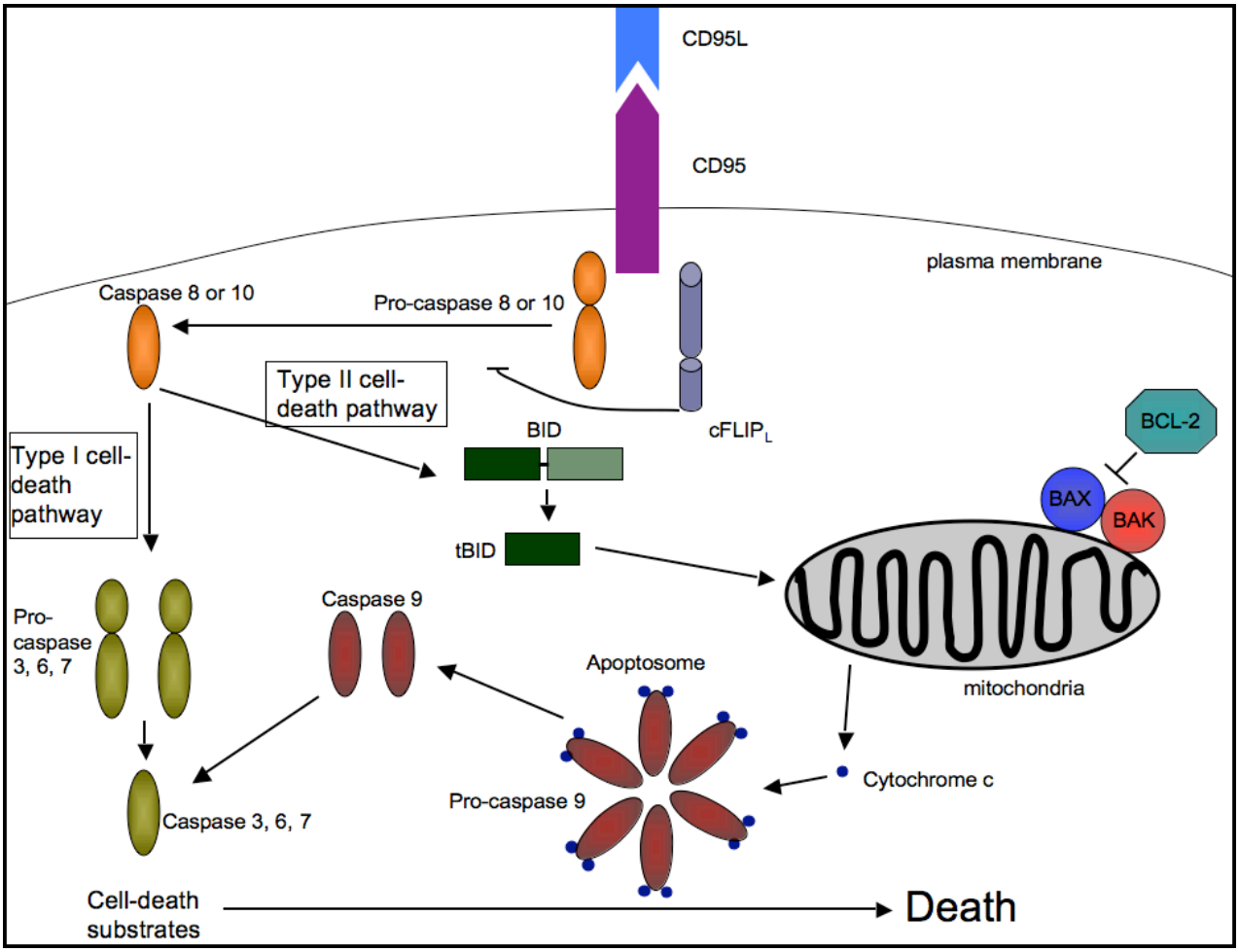
CD95L
CD95
plasma membrane
Caspase 8 or 10
Pro-caspase 8 or 10
Type II cell-death pathway
cFLIP$_L$
BID
BCL-2
BAX
BAK
Type I cell-death pathway
tBID
Pro-caspase 3, 6, 7
Caspase 9
Apoptosome
mitochondria
Cytochrome c
Pro-caspase 9
Caspase 3, 6, 7
Cell-death substrates
Death

Figure 3. Activated Cell-Autonomous Death: Intrinsic cell death pathway. The intrinsic cell death pathway can be activated by a variety of signals including cytokine and growth factor deprivation or DNA damage. BAX and BAK are normally bound to Bcl-2, sequestering them in an inactive state at the outer mitochondrial membrane. Following stimulation, pro-apoptotic molecules Bim and PUMA are activated and move to the mitochondrial membrane, displacing Bcl-2 from BAX and BAK and leading to release of cytochrome c from the mitochondria. Cytochrome c proceeds to activate the apoptosome and subsequent cleavage of pro-caspase 9. Active caspase 9 goes on to activate the effector caspases 3/6/7, which ultimately leads to cell death. Figure 3 was adapted from a figure created by R.A. Langlois.

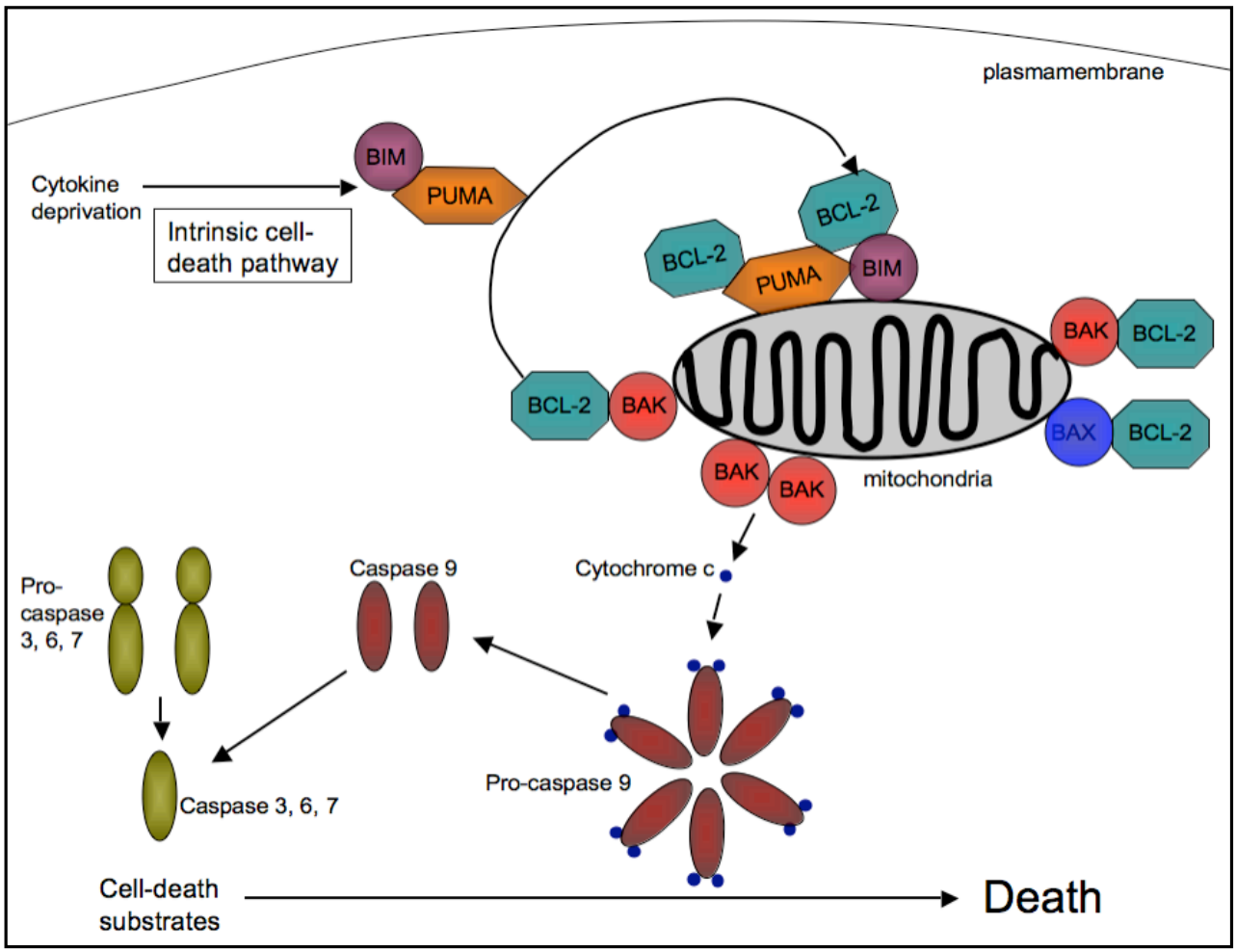
plasmamembrane
Cytokine deprivation
Intrinsic cell-death pathway
BIM
PUMA
BCL-2
BCL-2
PUMA
BIM
BAK
BCL-2
BCL-2
BAK
BAX
BCL-2
BAK
BAK
mitochondria
Cytochrome c
Caspase 9
Pro-caspase 3, 6, 7
Caspase 3, 6, 7
Pro-caspase 9
Cell-death substrates
Death

CHAPTER II ROLE OF DC MEDIATED COSTIMULATION IN REGULATING VIRUS-SPECIFIC CD8 T CELL RESPONSES IN THE LUNGS FOLLOWING INFLUENZA VIRUS INFECTION

Introduction

Clearance of a primary IAV infection is known to require killing of virus-infected host cells by activated, antigen-specific CD8 T cells in the lungs (58). Until recently, antigen-specific CD8 T cells were thought to undergo programmed activation, whereby a single, brief interaction with a mature, antigen-bearing DC in the LN was sufficient to induce a full program of activation, division and differentiation from naïve to mature, cytotoxic CD8 T cells (232, 233). Increasing evidence has suggested, however, that activation of antigen-specific CD8 T cells is not as simple as previously thought, and multiple factors including cytokine signals such as IL-2 (234), IFNα (21, 22, 28) and IL-12 (235-237), and late costimulatory signals such as CD70 (231) and 4-1BBL (201, 218) can regulate and fine-tune the magnitude and duration of the effector response, as well as the nature of the ensuing memory T cell population.

We have recently demonstrated in a model of IAV infection that the absence of specific pulmonary DC subsets, including pDC and CD8α^+ DC, from the lungs leads to a decrease in the number of virus-specific CD8 T cells (53). Reconstitution of the lungs with physiologic numbers of pDC or CD8α^+ DC is able to restore the pulmonary IAV-specific CD8 T cell response to near normal levels via a mechanism that is dependent upon direct DC:T cell interactions, DC-expressed MHC I and the presence of viral antigen (see Figure 1). Interestingly, however, this rescue is DC subset specific, as reconstitution with purified aDC or alveolar macrophages (aMϕ) is unable to rescue the virus-specific CD8 T cell response (53). Following IAV infection there is an abundance of IAV antigen and MHC I expressing cells present in the lungs, including infected

epithelial cells. Given this fact and the inability of all DC subsets to rescue the virus-specific CD8 T cell response, it suggested that there were additional, undefined requirements for pDC- and CD8α^+ DC-mediated rescue of the T cell response in the lungs.

Following initial infection by or encounter with IAV, DC activate and mature, initiating production of several proinflammatory cytokines and chemokines (61) and upregulating key costimulatory molecules including CD80 and CD86 (61). The unique ability of DC to provide signal 1 (antigen in the context of MHC I) and signal 2 (CD28 costimulation) enables them to prime virus-specific CD8 T cells in the LN and initiate a robust IAV-specific cellular response (60, 61).

Given the key role for costimulatory molecules in the early priming interactions between antigen-bearing DC and virus-specific CD8 T cells in the LN, as well as the unique and important functions for "late" costimulatory molecules in promoting increased T cell expansion and/or survival later in the response (178-180, 207), we hypothesized that the additional, undefined requirement for pulmonary DC mediated rescue of the CD8 T cell response in the lungs of aDC depleted mice is costimulation.

Materials and Methods

Mice

6-12 week old female BALB/c mice and 6-12 week old male C57BL/6 mice were purchased from the National Cancer Institute (Frederick, MD). BALB/c CD40$^{-/-}$ (CNCr.129P2-*Cd40*^{tm1Kik}/J) mice were purchased from Jackson Laboratories (Bar Harbor, Maine). BALB/c CD80$^{-/-}$CD86$^{-/-}$ double deficient mice (C.129-*Cd80*^{tm1Shr} *Cd86*^{tm1Shr}/Mmmh) were a kind gift of Dr. Arlene Sharpe and obtained via the Mutant Mouse Regional Research Centers (MMRRC) database. All mice were housed, bred and maintained in the animal care facility at the University of Iowa. Experiments were

conducted according to federal and institutional guidelines and were approved by the University of Iowa Animal Care and Use Committee.

Virus infection

Mouse-adapted influenza A viruses A/PuertoRico/8/34 and A/JAPAN/305/57 were grown in the allantoic fluid of 10-day old embryonated chicken eggs for 2 days at 37°C, as previously described (76). Allantoic fluid was harvested and stored at -80°C. BALB/c and C57BL/6 mice were anesthetized with isofluorane and infected i.n. with either 5875 TCIU or 587 TCIU of mouse-adapted A/JAPAN/305/57 or 1066 TCIU of A/PR/8/34, respectively, in 50 μl of Iscove's media as previously described (76).

Clodronate-liposome treatment

Pulmonary DC and macrophage depletion was performed by treatment with liposomes containing dichloromethylene bisphosphonate (Clodronate) (53). Clodronate was a gift of Roche Diagnostics GmbH, Mannheim, Germany. It was encapsulated in liposomes as described previously (238). Phosphatidylcholine (LIPOID E PC) was obtained from Lipoid GmbH, Ludwigshafen,Germany. Cholesterol was purchased from SIGMA Chem.Co. USA. At 48 hours p.i., mice were anesthetized by isofluorane inhalation and administered 75 μl of Clodronate-liposomes or PBS-liposomes i.n.

Peptides

Influenza virus peptides $HA_{204-212}$ (LYQNVGTYV), $HA_{529-537}$ (IYATVAGSL), and $NP_{147-155}$ (TYQRTRALV) for BALB/c and PA_{224} (SSLENFRAYV) and NP_{366}(ASNENMETM) for C57BL/6 were synthesized by BioSynthesis Incorporated (Lewisville, TX).

MHC I tetramers

Tetramers HA_{204} (H-2K(d)/LYQNVGTYV), HA_{529} (H-2K(d)/IYATVAGSL), and NP_{147} (H2K(d)/TYQRTRALV) for BALB/c, and PA_{224} (H2D(b)/SSLENFRAYV) and

NP_{366}(H2D(b)/ASNENMETM) for C57BL/6 were obtained from National Institute of Allergy and Infectious Disease MHC Tetramer Core Facility (Atlanta, GA).

Preparation of cells

Lungs were pressed through wire mesh to obtain a single cell suspension, which was then enumerated by trypan blue exclusion. For DC preparations, lungs were digested for 25 minutes at 25° C in media containing 1 mg/ml Collagenase (Sigma) and 0.02 mg/ml DNase (Sigma) before single cell preparation. DC for reconstitution experiments were purified from the lungs of day 6 A/JAPAN/305/57 infected control BALB/c, $CD40^{-/-}$ or $CD80^{-/-}CD86^{-/-}$ donors or A/PR/8/34 infected C57BL/6 donors respectively using MACS technology (Miltenyi Biotech) according to manufacturer's instructions or by fluorescence activated cell sorting (FACS) as has been previously described (53). Purified cells were resuspended in Iscove's DMEM and $2.5x10^4$ cells in 50 ul were adoptively transferred i.n. to host mice on day 3 p.i. (53).

Antibodies and reagents

The following reagents were used for these studies: rat anti-mouse CD3ε (145-2C11), rat anti-mouse CD8α (53-6.7), rat anti-mouse IA/IE (M5/114.15.2), rat anti-mouse CD11b (M1/70), hamster anti-mouse CD11c (HL3), rat anti-mouse IFNγ (XMG1.2), rat anti-mouse CD70 (FR70) purchased from Becton Dickinson; rat anti-mouse CD45R (RA3-6B2) purchased from Caltag; rat anti-mouse OX40-L (RM134L) and rat anti-mouse 4-1BBL (TKS-1) purchased from BioLegend or eBioscience; polyclonal goat anti-mouse CD27L (CD70) purchased from R&D Systems. For surface staining, isolated cells (10^6) cells were stained with antibody or tetramer for 30 minutes at 4° C and then fixed using BD FACS Lysing Solution (BD Biosciences). For intracellular cytokine staining, fixed cells were permeabilized and labeled with antibodies in FACS buffer containing 0.5% Saponin (Acros Organics, NJ) for 1 hour at 4° C. All flow cytometry data were acquired on a BD FACS Calibur or BD FACS Canto II (BD

Immunocytometry Systems) and analyzed using FlowJo software (TreeStar, Ashland, OR). A minimum of $1x10^6$ cells were collected for DC analysis experiments and a minimum of $7x10^5$ cells were collected for T cell analysis experiments.

Statistical analysis

Statistical significance of the difference between two sets of data was assessed using an unpaired, one-tailed *t*-test or a paired *t*-test for control and experimental data groups that could be paired. Differences were considered to be statistically significant at $p<0.05$.

Results

Pulmonary pDC and CD8α^+ DC express the costimulatory molecules CD40, CD80 and CD86

CD40, CD80 and CD86 are all key costimulatory molecules that play essential roles in regulating the immune response following viral infection (176, 177, 187). DC are known to express CD40, CD80 and CD86 following IAV infection, however, the level of their expression on pulmonary pDC and CD8α^+ DC is not well defined (176, 177, 187). To confirm that pulmonary pDC and CD8α^+ DC express CD40, CD80 and CD86 in the lungs at these time points p.i., we infected groups of BALB/c mice with a sublethal dose of IAV. On day 6 p.i., the mice were sacrificed and their lungs were analyzed by flow cytometry for pDC and CD8α^+ DC expression of the costimulatory molecules CD40, CD80 and CD86. As demonstrated in Figure 4, both pDC and CD8α^+ DC express these important costimulatory molecules on their surface, suggesting they are capable of receiving signals via CD40 ligation and delivering CD28 costimulation to T cells in the lungs via CD80 or CD86.

CD40 costimulation is not required to rescue virus-specific CD8 T cell responses in the lungs of aDC depleted mice

CD40 is important for promoting full DC maturation and upregulation of several key costimulatory molecules including CD80, CD86, 4-1BBL, OX40L and CD70 (176, 181-186). Given the importance of CD40 ligation in regulating downstream immune responses, and the knowledge that both pDC and CD8α^+ DC express high levels of CD40 in the lungs following IAV infection (Figure 4), we wanted to test the role of CD40 on pulmonary DC subsets and their ability to rescue virus-specific CD8 T cell responses in the lungs of aDC depleted mice. To this end, we infected BALB/c mice with a 0.1 LD_{50} dose of IAV and aDC depleted groups of mice at 48 hours p.i. On day 3 p.i., mice were reconstituted with $2.5x10^4$ pulmonary pDC or CD8α^+ DC purified from the lungs of day 6 IAV-infected wildtype or CD40$^{-/-}$ donor mice. One group of control mice received IAV but was not aDC depleted, while a second group of mice was infected and aDC depleted, but not reconstituted. On day 6 p.i., mice were sacrificed and their lungs examined by flow cytometry for the frequency (Figure 5A) and total numbers (Figure 5B) of virus-specific CD8 T cells as measured by MHC I tetramers or ICS for IFNγ (not shown). As seen in Figure 5, aDC depletion at 48 hours p.i. results in a reduced number of tetramer$^+$ virus-specific CD8 T cells, while pulmonary DC reconstitution with wildtype pDC or CD8α^+ DC rescues the numbers of virus-specific CD8 T cells in the lungs of aDC depleted mice. Interestingly, we observed that CD40 deficiency on pulmonary DC does not ablate the rescue of virus-specific CD8 T cell responses in aDC depleted mice (Figure 5), suggesting that CD40 ligation is not required for pulmonary DC mediated rescue of virus-specific CD8 T cell responses in the lungs following IAV infection.

CD80 and CD86 costimulation is not required to rescue virus-specific CD8 T cell responses in the lungs of aDC depleted mice

CD80 and CD86 stimulation of CD28 is necessary for the induction of a primary CD8 T cell response in the LN (176, 177). While it is likely that the virus-specific CD8 T cells in the lungs of aDC depleted mice have received CD28 costimulation during their priming in the LN, it remains unclear if the T cells have fully differentiated prior to their arrival in the lungs, or if additional CD28 costimulation is required therein to promote full differentiation and acquisition of effector functions. Preliminary results indicate that CD8 T cells from aDC depleted lungs may be slightly reduced in their per-cell ability to kill targets (data not shown), suggesting that they may require additional costimulation in order to achieve full effector functions. Further, our preliminary results suggest that pulmonary DC isolated from naïve or day 3 infected donor mice, which are known to express lower surface levels of the costimulatory molecules CD80 and CD86, are not able to rescue the virus-specific T cell response in the lungs of aDC depleted mice (data not shown). Together, these data suggest that CD80 and CD86 costimulation of CD28 may be required by aDC depleted T cells in the lungs in order to fully mature and accumulate therein. To test this hypothesis, we infected groups of BALB/c mice with a sublethal dose of IAV +/- aDC depletion at 48 hours p.i.. On day 3 p.i., mice were reconstituted i.n. with $2.5x10^4$ pulmonary pDC or $CD8\alpha^+$ DC purified from the lungs of day 6 IAV-infected wildtype or $CD80^{-/-}CD86^{-/-}$ donor mice. One group of control mice received IAV but was not aDC depleted, while a second group of control mice was infected and aDC depleted, but not DC reconstituted. On day 6 p.i., mice were sacrificed and their lungs examined by flow cytometry for the frequency (Figure 6A) and total numbers (Figure 6B) of virus-specific CD8 T cells. As seen in Figure 6, pulmonary DC subsets that are deficient in CD80 and CD86 are able to rescue the virus-specific CD8 T cell response in the lungs of aDC depleted mice to levels similar to that of their wildtype

counterparts, suggesting that CD28 costimulation by pulmonary DC subsets is not required to promote the accumulation of virus-specific CD8 T cells in the lungs following IAV infection.

The role of "late" OX40 and 4-1BB costimulation in the lungs following influenza virus infection

The late costimulatory molecules OX40L and 4-1BBL have both been described to play important roles in promoting the expansion and survival of virus-specific CD4 and CD8 T cells following viral infection (178-180, 207). Given that virus-specific CD8 T cells undergo increased apoptosis in the lungs following aDC depletion at 48 hours p.i., we next hypothesized that pulmonary pDC and CD8α^+ DC were promoting the rescue of virus-specific T cells in the lungs via "late" 4-1BBL or OX40L mediated costimulation. Expression of both OX40L and 4-1BBL has been described on activated splenic or bone marrow-derived DC (178-180, 207), but it was unknown whether pulmonary pDC or CD8α^+ DC specifically express these molecules, and the timing of their expression in the lungs following IAV infection is not well described. Therefore, we undertook experiments to determine if pulmonary pDC and CD8α^+ DC express the late costimulatory molecules OX40L and 4-1BBL in the lungs following IAV infection. To this end, groups of BALB/c and C57BL/6 mice were infected with a sublethal dose of IAV. On day 6 p.i., (i.e. the same day that pulmonary pDC and CD8α^+ DC are harvested for adoptive transfer to aDC depleted host mice), the mice were sacrificed and their lungs analyzed by flow cytometry for pulmonary pDC and CD8α^+ DC expression of 4-1BBL and OX40L. As seen in Figure 7, both pDC and CD8α^+ DC express 4-1BBL and OX40L in the lungs following IAV infection, suggesting that they are capable of utilizing these costimulatory molecules to regulate and promote virus-specific CD8 T cell responses therein.

In order to test the functional role of pulmonary DC-expressed 4-1BBL and OX40L in promoting virus-specific T cell responses in the lungs following IAV infection, we again utilized our depletion/pulmonary DC adoptive transfer approach. Groups of BALB/c mice were infected with a sublethal dose of IAV +/- aDC depletion at 48 hours p.i.. On day 3 p.i. (i.e. 24 hours post-depletion) pulmonary pDC or $CD8\alpha^+$ DC were purified and then coated *in vitro* with anti-mouse 4-1BBL or anti-mouse OX40L blocking antibodies prior to their adoptive transfer into aDC depleted host mice. On day 6 p.i., the mice were sacrificed and their lungs examined by flow cytometry for total numbers of virus-specific CD8 T cells as measured by MHC I tetramer staining. As expected, the adoptive transfer of control pDC or $CD8\alpha^+$ DC results in increased virus-specific CD8 T cell responses in the lungs of aDC depleted mice (Figure 8A). Surprisingly, however, the adoptive transfer anti-4-1BBL or anti-OX40L antibody coated pDC or $CD8\alpha^+$ DC into aDC depleted lungs also promotes increased IAV-specific CD8 T cell responses to levels similar to control pulmonary DC subsets. These results suggest that neither 4-1BBL nor OX40L mediated costimulation is necessary for pulmonary DC to promote the rescue of virus-specific CD8 T cell responses in the lungs of aDC depleted mice.

Given the large body of literature describing a role for both 4-1BBL and OX40L in regulating effector T cell responses following viral infection (178-180, 207, 217, 218), we were particularly surprised by their lack of effect in our model of aDC depletion and pulmonary DC reconstitution. Further investigation revealed that much of the literature examining 4-1BBL and OX40L has focused upon a C57BL/6 model of pathogen challenge, rather than a BALB/c model. In an effort to resolve our results with those of the literature, we next used our model of aDC depletion/pulmonary DC reconstitution in a C57BL/6 model of IAV infection. Groups of C57BL/6 host mice were infected with a sublethal dose of A/PR/8/34 and aDC depleted at 48 hours p.i.. 24 hours later, (i.e. day 3 p.i.) pulmonary pDC or $CD8\alpha^+$ DC were purified from day 6 IAV infected C57BL/6

donor mice and coated *in vitro* with anti-mouse 4-1BBL or anti-mouse OX40L blocking antibodies prior to their adoptive transfer into aDC depleted host mice. Control mice received pulmonary pDC or CD8α^+ DC that remained uncoated with blocking antibodies. On day 7 p.i., the mice were sacrificed and their lungs examined by flow cytometry for total numbers of virus-specific CD8 T cells as measured by MHC I tetramer staining. Like those results observed in the BALB/c model of aDC depletion, IAV infection of C57BL/6 mice induces a robust virus-specific CD8 T cell response that is significantly reduced following aDC depletion at 48 hours p.i. (Figure 8B). Further, as in the BALB/c model, the adoptive transfer of control non-antibody-coated pDC or CD8α^+ DC on day 3 p.i. is able to rescue the IAV-specific CD8 T cell response in the lungs of aDC depleted mice. In contrast, however, blocking 4-1BBL or OX40L on the surface of pDC prior to their adoptive transfer results in significantly reduced virus-specific CD8 T cell responses in the lungs of aDC depleted mice (Figure 8B). Together, these results suggest that the requirements of virus-specific CD8 T cells in the lungs following IAV infection may differ depending upon the mouse strain utilized, and further suggest that C57BL/6 pulmonary pDC, but not C57BL/6 CD8α^+ DC or BALB/c pulmonary DC subsets, may utilize the late costimulatory molecules 4-1BBL or OX40L to promote IAV-specific immunity in the lungs.

The role of "late" CD27 costimulation in the lungs following influenza virus infection

Like OX40 and 4-1BB, CD27 is a costimulatory molecule that is known to promote prolonged and enhanced survival of both CD4 and CD8 T cells (178-180, 207). In particular, CD27/CD70 interactions have a well-described role in the lungs following IAV infection. A deficiency in CD27 results in a systemic reduction in the numbers of antigen-specific CD8 T cells following IAV infection (204, 229), with this reduction being most pronounced in the lungs themselves. In support of these results, transgenic

over-expression of CD70 results in enhanced antigen-specific CD8 T cell responses following IAV infection (230), while blockade of CD70 at the late stages of the effector response results in reduced numbers of IAV-specific CD8 T cells (231), likely as a result of increased sensitivity to Fas-mediated apoptosis.

CD70 is expressed by activated DC (178-180, 207), but it was unknown whether pulmonary pDC and CD8α^+ DC specifically express CD70, and the timing of its expression in the lungs following IAV infection is not well described. Therefore, we undertook experiments to determine if pulmonary pDC and CD8α^+ DC express the late costimulatory molecule CD70 in the lungs following IAV infection. To this end, groups of BALB/c and C57BL/6 mice were infected with a sublethal dose of IAV. On day 6 p.i., (i.e. the same day that pulmonary pDC and CD8α^+ DC are harvested for adoptive transfer to aDC depleted host mice), the mice were sacrificed and their lungs analyzed by flow cytometry for pulmonary pDC and CD8α^+ DC expression of CD70. As seen in Figure 9, a fraction of both pDC and CD8α^+ DC express CD70 in the lungs at this time point following IAV infection, suggesting that these cells would be capable of providing CD27-mediated costimulation to regulate and promote virus-specific CD8 T cell responses therein.

Given the described role of CD70 in the lungs following IAV infection (204, 229) we next wanted to determine if pulmonary DC subsets were promoting the increased accumulation of virus-specific CD8 T cells in the lungs of aDC depleted mice via a mechanism involving CD27 costimulation. Therefore, groups of BALB/c mice were infected with a sublethal dose of IAV +/- aDC depletion at 48 hours p.i.. On day 3 p.i. (i.e. 24 hours post-depletion) pulmonary pDC or CD8α^+ DC were purified from day 6 IAV-infected donors and then coated *in vitro* with anti-mouse CD70 blocking antibodies prior to their adoptive transfer into aDC depleted host mice. On day 6 p.i., the mice were sacrificed and their lungs examined by flow cytometry for total numbers of virus-specific CD8 T cells as measured by MHC I tetramer staining. While the adoptive transfer of

control pDC or CD8α^+ DC to aDC depleted lungs resulted in rescued virus-specific CD8 T cell responses therein (Figure 10A), the blockade of CD70 on the surface of pulmonary DC subsets prior to their adoptive transfer *in vivo* resulted in a reduced ability to rescue CD8 T cell responses in the lungs of aDC depleted mice (Figure 10A). Similarly, although not statistically significant, in the C57BL/6 model, blocking CD70 on the surface of pulmonary DC subsets prior to their adoptive transfer resulted in a reduction in their ability to rescue the virus-specific CD8 T cell response in the lungs of aDC depleted mice. Together, these results support our hypothesis that pulmonary pDC and CD8α^+ DC utilize CD70 to promote increased virus-specific CD8 T cell responses in the lungs of aDC depleted mice, and suggest that CD27 costimulation is necessary for regulating IAV-specific CD8 T cell responses following a primary infection.

Discussion

Here we have demonstrated that pulmonary DC subsets do not require CD40, CD80 or CD86 costimulation in order to rescue antigen-specific CD8 T cells in the lungs following IAV infection; however, it appears that, depending upon the host genetic background, pulmonary DC subsets may utilize the late costimulatory molecules 4-1BBL, OX40L and/or CD70 in order to promote increased accumulation of virus-specific CD8 T cells in the lungs of aDC depleted mice. In recent years, it has become increasingly apparent that late costimulation via these members of the TNFR superfamily can play an essential role in regulating CD8 T cell immunity at various stages of the response including during differentiation and acquisition of effector functions, survival and transition to memory cells (178-180, 207). While 4-1BBL and CD70 both have well described functions in regulating the CD8 T cell response following viral infection, and in particular IAV infection (204, 215, 217, 218, 229-231), the role of OX40L in regulating CD8 T cell immunity is less clear. OX40 has been predominantly described to promote CD4 helper T cell immunity following viral infections, primarily via its ability

to prolong T cell survival subsequent to CD28 costimulation (178-180, 207). For example, mice deficient in OX40 or its ligand show striking defects in both the primary and memory CD4 T cell response to IAV or LCMV, but exhibit no changes in the CD8 T cell response (219-221). In contrast to these data however, systemic administration of agonist anti-OX40 can induce proliferation of both CD8 and CD4 T cells, demonstrating that CD8 T cells are capable of responding to signals from OX40L (223-226). Further, administration of soluble OX40-Ig fusion protein following IAV infection results in a reduction in disease severity as measured by weight loss, and decreased lung pathology (222). This reduced disease severity was accompanied by a decrease in both CD4 and CD8 T cell responses, suggesting that OX40 may be capable of regulating CD8 T cell responses in some instances (222). Here we lend further support to this argument, demonstrating that, in the C57BL/6 model, blocking OX40L on pDC prior to their adoptive transfer *in vivo* is able to ablate their ability to rescue virus-specific CD8 T cell responses in the lungs following IAV infection. At this time it is unclear what signals OX40L may be providing to CD8 T cells to promote their increased accumulation in the lungs, but the literature suggests that OX40L signals are able to induce upregulation of Bcl-2 and Bcl-X_L expression by CD4 T cells (239, 240). In the future, it will be important to determine if pulmonary DC- mediated OX40L signals are inducing CD8 T cell accumulation via a similar mechanism.

Given that C57BL/6 mice and BALB/c mice behave relatively similarly in our model of IAV infection and aDC depletion, and exhibit similar requirements for pulmonary pDC and CD8α^+ DC mediated regulation of CD8 T cell immunity in the lungs, it is particularly interesting that blockade of 4-1BBL and OX40L on C57BL/6 pDC, but not BALB/c pulmonary pDC, is able to prevent the rescue of virus-specific CD8 T cell responses in the lungs of aDC depleted mice. Arguably, staining for OX40L and 4-1BBL revealed slightly higher levels of expression on C57BL/6 pulmonary pDC compared to BALB/c pulmonary pDC (Figure 7); however, it is unclear if this minor

change in expression would translate into a functional difference in the ability to costimulate CD8 T cells in the lungs between the two mouse strains. The magnitude and character of the adaptive T cell response is governed by multiple factors including MHC (241-248), TCR affinity/avidity (244, 245, 247, 249), T cell clonality (250, 251) and T cell repertoire availability (241-243); changes in all of which could account for the differential costimulation requirements between the CD8 T cells of the C57BL/6 and BALB/c strains. Further, this is not the first instance where differences in the requirements for CD8 T cell costimulation have been attributed to different genetic backgrounds. For example, in a model of skin transplant tolerance, C57BL/6 mice exhibit increased sensitivity to transplant rejection relative to C3H mice via a mechanism of CD8 T cell costimulation that is independent of CD28 and CD40 signaling (252). While the alternative forms of costimulation that were promoting the graft-specific CD8 T cell response were not identified (252), it is possible that 4-1BBL or OX40L mediated costimulation was important for promoting the increased CD8 T cell responses in the C57BL/6 mice, but not the C3H mice. These results would coincide well with our own suggesting that C57BL/6 pDC, but not BALB/c pDC, utilized the alternative costimulatory molecules 4-1BBL and OX40L to regulate CD8 T cell immunity in the lungs following IAV infection.

We demonstrate here that blockade of OX40L and 4-1BBL on C57BL/6 pulmonary pDC, but not C57BL/6 CD8α^+ DC prevents the rescue of virus-specific CD8 T cells in the lungs of aDC depleted mice. Traditionally, pDC and CD8α^+ DC differ in their tissue localization following pathogen challenge, as well as their ability to prime CD8 T cell responses *in vivo:* CD8α^+ DC localize to lymphoid tissues (46) and are able to cross-present antigens (90, 94), thus initiating robust CD8 T cell responses and Th1 skewing *in vivo* (253-257); while pDC are far better known for their robust production of type I IFN (258-261). Therefore, it is not particularly surprising that they would differ in the mechanism by which they were able to rescue virus-specific CD8 T cell responses in

the lungs of aDC depleted mice. However, our previous studies have not identified any differences between the ability of the two subsets to regulate CD8 T cell immunity in the lungs. The ability to costimulate CD8 T cells via 4-1BBL or OX40L is the first suggestion of a mechanism that pDC, but perhaps not CD8α^+ DC, may use to rescue the T cell response in the lungs. Of note, the surface levels of OX40L and 4-1BBL on pDC and CD8α^+ DC are relatively similar (Figure 7), suggesting that the discrepancy in pDC vs. CD8α^+ DC use of OX40L and 4-1BBL is not likely to be attributed to differences in expression levels. Further, it is not likely that signals from OX40L and 4-1BBL are additive, nor are they able to compensate for each other on the surface of pulmonary DC subsets, as simultaneous blockade of both molecules did not result in a significant reduction in the ability of CD8α^+ DC to rescue virus-specific CD8 T cell responses, nor did it result in a synergistic reduction in the ability of pDC to rescue virus-specific CD8 T cell responses in the lungs of aDC depleted mice (data not shown). In the future, it will be interesting to further characterize the differences between pDC and CD8α^+ DC and identify additional unique mechanisms that allow them to promote virus-specific CD8 T cell responses in the lungs following IAV infection.

The requirement for 4-1BBL mediated costimulation following viral infection is thought to depend upon the antigen load and severity of infection (215, 216, 218). Mice that lack 4-1BB or its ligand exhibit only a minor phenotype following infection with a low dose of LCMV (215) or the relatively nonvirulent strain, HK/x31, of IAV (218). In contrast, a deficiency in 4-1BB costimulation results in significantly reduced CD8 T cell responses, increased disease severity and increased mortality following infection with high doses of LCMV (216), or the more virulent A/PR/8/34 strain of IAV (218). Interestingly, 4-1BBL is upregulated transiently and to only a low level following HK/x31 infection, but is upregulated to much higher levels and sustained for longer periods following the PR/8 infection (218). The infections used in our model are sublethal to control mice, but are relatively stringent, inducing ~20-25% weight loss and

significant lung pathology. Following aDC depletion, however, this same dose results in severe lung pathology, sustained high pulmonary viral loads and 100% mortality by day 8 p.i. (53). Given that aDC depleted mice are undergoing such a severe infection, it suggests that, in the case of the C57BL/6 strain, the requirement for pDC-mediated 4-1BBL costimulation may be unique to the model of aDC depletion, rather than a global requirement for effective CD8 T cell responses in the lungs following IAV infection. A detailed kinetic analysis of 4-1BB/4-1BBL expression in the lungs will be necessary to detemine if aDC depletion induces strong and sustained 41BB/4-1BBL expression in the lungs compared to non-depleted controls.

CD70 has been described to promote increased CD8 T cell survival in the lungs following IAV infection (231). Mice lacking CD27 have severely reduced primary and recall CD8 T cell responses following IAV infection (204, 229), and the specific blockade of CD70 in the lungs at late time points post-IAV infection results in reduced primary CD8 T cell numbers and enhanced AICD-mediated CD8 T cell apoptosis (231). Additionally, young mice that over-express CD70 demonstrate enhanced primary CD8 T cell responses in the lungs following IAV infection (230). Together, these results suggest a key role for CD27-CD70 interactions in the lungs following IAV infection. In these previous models, it was hypothesized, but not clearly demonstrated, that CD27 costimulation was being mediated by CD70-expressing DC in the lungs at the time of infection. Here, we demonstrate a direct role for CD70 on the surface of pulmonary DC subsets in promoting the accumulation of virus-specific CD8 T cells in the lungs at the time of infection. The mechanism through which pulmonary DC subsets use CD70 to promote increased antigen-specific T cell responses in the lungs of aDC depleted mice remains unclear. However, given the previous reports suggesting that CD70 interactions are important for overcoming Fas-mediated AICD (231), it is likely that this is also an important mechanism of promoting aDC depleted CD8 T cell responses following IAV

infection. Future studies should be aimed at exploring this mechanism of CD70-mediated CD8 T cell rescue in more detail.

Figure 4. Pulmonary DC subsets express the costimulatory molecules CD80, CD86 and CD40. Mice were infected with a sublethal dose of IAV, sacrificed on day 6 p.i. and their lungs analyzed by flow cytometry for $CD8\alpha^+$ DC (top panels) and pDC (bottom panels) expression of CD80 (left panels), CD86 (middle panels) and CD40 (right panels). Isotype controls are included as filled grey lines. Shown are representative histograms of 2 independent experiments, n= 4-6 mice/group

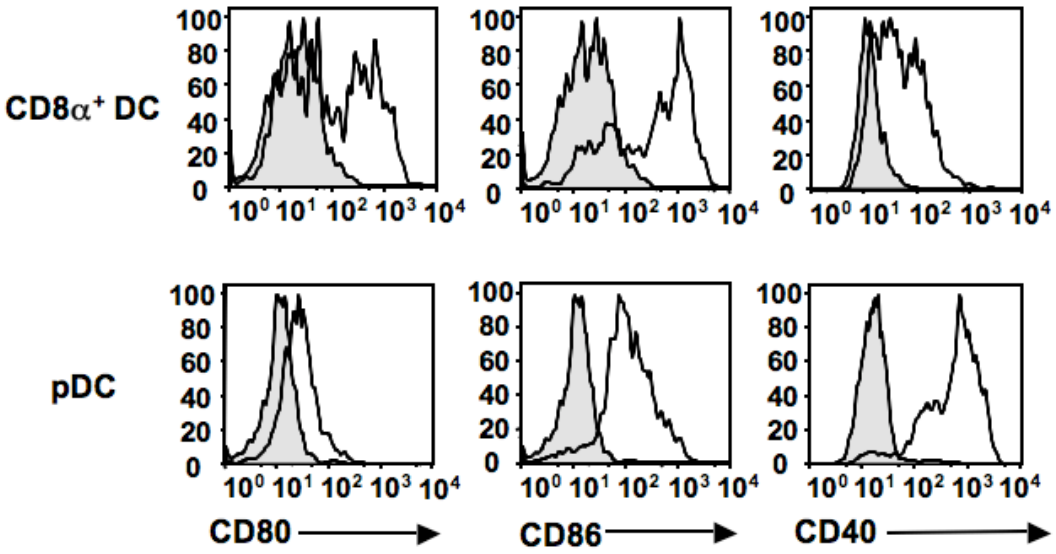
CD8α+ DC
pDC
100
80
60
40
20
0
10^0 10^1 10^2 10^3 10^4
CD80
CD86
CD40

Figure 5. Pulmonary pDC and CD8α^+ DC mediated rescue of IAV-specific CD8 T cell responses from aDC depleted mice does not require CD40. Groups of BALB/c mice were infected with a sublethal dose of IAV and aDC depleted at 48 hours p.i. (black bars), while controls remained undepleted (white bars). On day 3 p.i., groups of aDC-depleted mice were then reconstituted i.n. with $2x10^4$ purified pulmonary pDC (light grey bars) or CD8α^+ DC (dark grey bars) that were purified from IAV-infected BALB/c CD40$^{-/-}$ (KO) or wildtype CD40$^{+/+}$ donors. On day 6 p.i., the number of pulmonary IAV-specific CD8 T cells in the lungs was enumerated by tetramer staining. Representative flow plots are gated on CD3$^+$CD8$^+$ T cells. Numbers of Tetramer$^+$ CD8 T cells in the lungs were determined by subtracting background staining using the Media Control (A, top). Data are representative of 3 independent experiments and represent means ± SEM. n= 3 mice/group. *p≤0.05 relative to influenza only controls

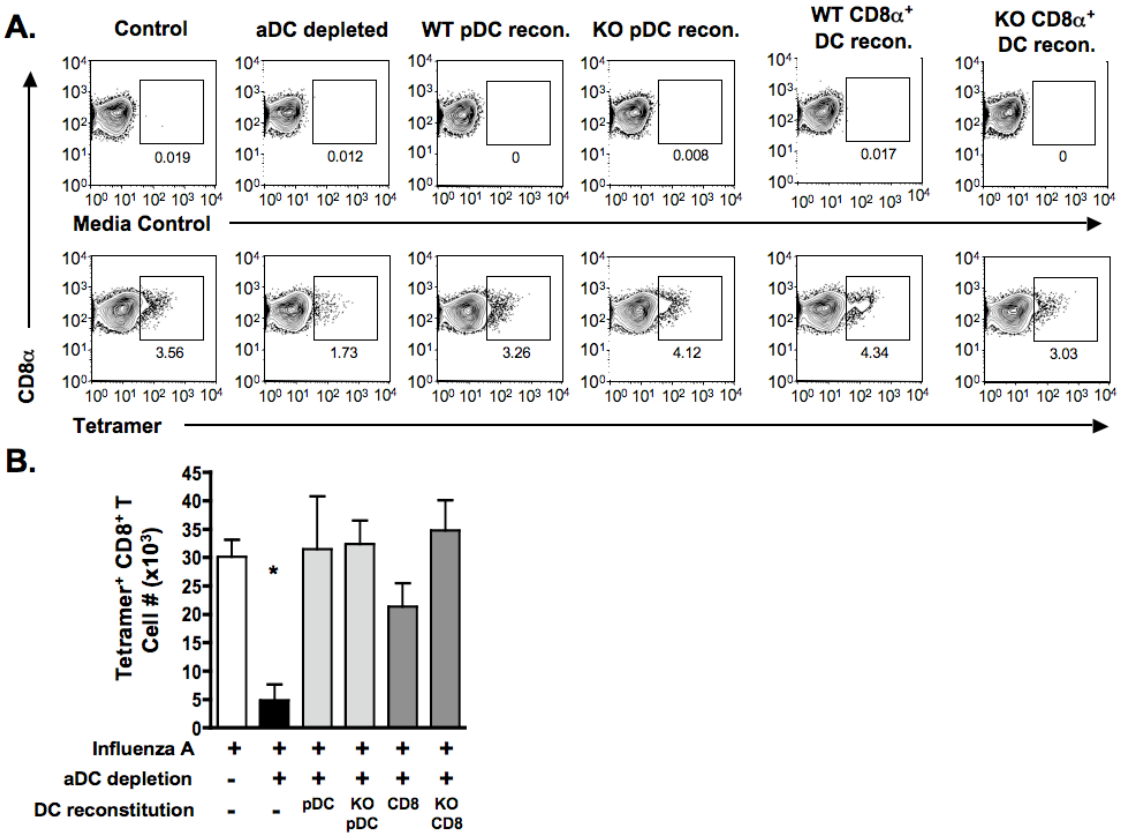
A.
Control
aDC depleted
WT pDC recon.
KO pDC recon.
WT CD8α+ DC recon.
KO CD8α+ DC recon.
0.019
0.012
0
0.008
0.017
0
Media Control
3.56
1.73
3.26
4.12
4.34
3.03
CD8α
Tetramer
B.
Tetramer+ CD8+ T Cell # (x10³)
45
40
35
30
25
20
15
10
5
0
*
Influenza A + + + + + +
aDC depletion - + + + + +
DC reconstitution - - pDC KO pDC CD8 KO CD8

Figure 6. Pulmonary pDC and CD8α^+ DC mediated rescue of IAV-specific CD8 T cell responses from aDC depleted mice does not require CD80 or CD86. Groups of BALB/c mice were infected with a sublethal dose of IAV and aDC depleted at 48 hours p.i. (black bars), while controls remained undepleted (white bars). On day 3 p.i., groups of aDC-depleted mice were then reconstituted i.n. with $2x10^4$ purified pulmonary pDC (light grey bars) or CD8α^+ DC (dark grey bars) that were purified from IAV-infected BALB/c $CD80^{-/-}86^{-/-}$ (KO) or wildtype $CD80^{+/+}86^{+/+}$ donors. On day 6 p.i., the number of pulmonary IAV-specific CD8 T cells in the lungs was enumerated by tetramer staining. Representative flow plots are gated on $CD3^+CD8^+$ T cells. Numbers of $Tetramer^+$ CD8 T cells in the lungs were determined by subtracting background staining using the Media Control (A, top). Data are representative of 3 independent experiments and represent means ± SEM. n= 3 mice/group. *$p \leq 0.05$ relative to influenza only controls

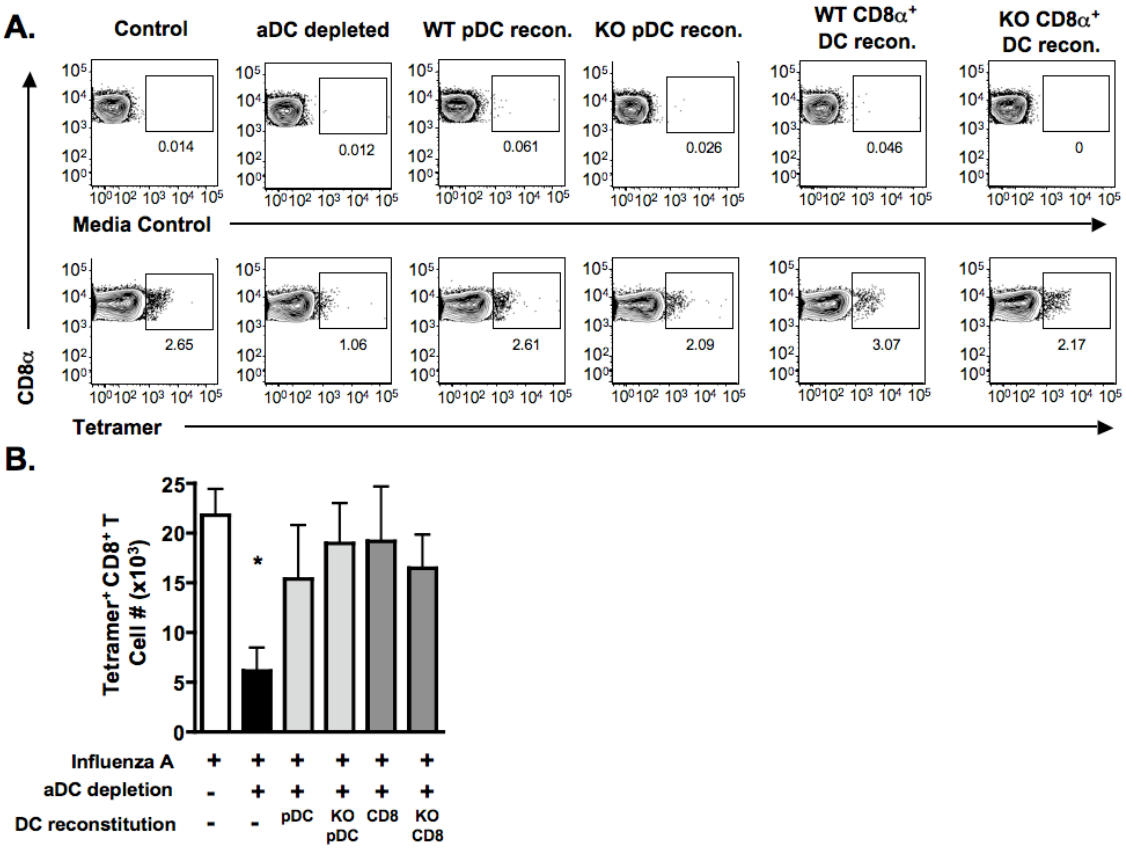
A.
Control
aDC depleted
WT pDC recon.
KO pDC recon.
WT CD8α+ DC recon.
KO CD8α+ DC recon.
Media Control
0.014
0.012
0.061
0.026
0.046
0
2.65
1.06
2.61
2.09
3.07
2.17
CD8α
Tetramer
B.
Tetramer+ CD8+ T Cell # (x10³)
25
20
15
10
5
0
*
Influenza A + + + + + +
aDC depletion - + + + + +
DC reconstitution - - pDC KO pDC CD8 KO CD8

Figure 7. Pulmonary DC subsets express the late costimulatory molecules 4-1BBL and OX40L. Groups of BALB/c mice were infected with influenza A/JAPAN/305/57 and groups of C57BL/6 mice were infected with influenza A/PR/8/34, then sacrificed on day 6 p.i. and their lungs analyzed by flow cytometry for $CD8\alpha^+$ DC (top panels) and pDC (bottom panels) expression of 4-1BBL (left panels) and OX40L (right panels). Isotype controls are included as filled grey lines. Shown are representative histograms of 2-3 independent experiments, n= 2-5 mice/group.

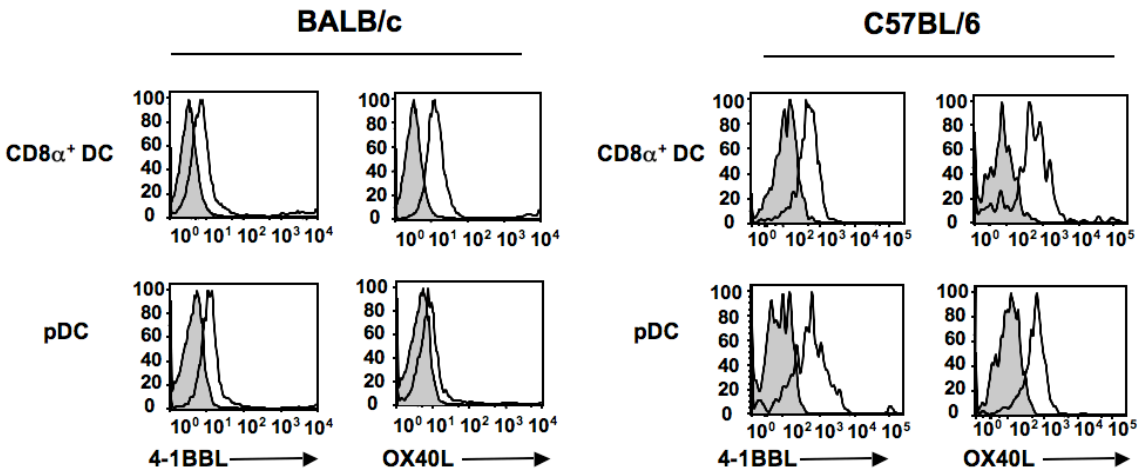
BALB/c
C57BL/6
CD8α+ DC
pDC
CD8α+ DC
pDC
100
80
60
40
20
0
10^0 10^1 10^2 10^3 10^4
10^0 10^2 10^3 10^4 10^5
4-1BBL
OX40L
4-1BBL
OX40L

Figure 8. Role of OX40L and 4-1BBL in the pulmonary pDC and CD8α^+ DC mediated rescue of IAV-specific CD8 T cell responses from aDC depleted mice. (A) Groups of BALB/c mice were infected with a sublethal dose of IAV +/- aDC depletion. On day 3 p.i., groups of aDC-depleted mice were reconstituted i.n. with $2x10^4$ purified pulmonary pDC (light grey bars) or CD8α^+ DC (dark grey bars) that were left untreated or blocked *in vitro* with anti-4-1BBL antibody or anti-OX40L antibody prior to adoptive transfer. On day 6 p.i., the number of pulmonary antigen-specific CD8 T cells was enumerated by tetramer staining. Data are pooled from three independent experiments and represent means ± SEM. n= 9-11 mice/group. (B) Groups of C57BL/6 mice were infected with a sublethal dose of IAV and aDC depleted at 48 hours p.i. (black bars), while controls remained undepleted (white bars). On day 3 p.i., groups of aDC-depleted mice were then reconstituted i.n. with $2x10^4$ purified pulmonary pDC (light grey bars) or CD8α^+ DC (dark grey bars) that were left untreated or blocked *in vitro* anti-4-1BBL antibody or anti-OX40L antibody prior to adoptive transfer. On day 7 p.i., the number of pulmonary antigen-specific CD8 T cells was enumerated by tetramer staining. Data are pooled from six independent experiments and represent means ± SEM. n= 11-16 mice/group. *$p \leq 0.05$ relative to influenza only controls, ‡$p \leq 0.05$ relative to untreated control pDC

A.

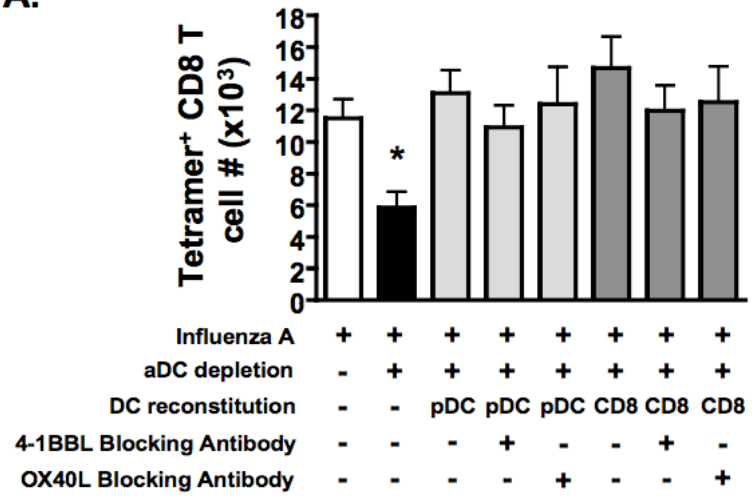
Tetramer+ CD8 T cell # (x10³)
18
16
14
12
10
8
6
4
2
0
*
Influenza A + + + + + + + +
aDC depletion - + + + + + + +
DC reconstitution - - pDC pDC pDC CD8 CD8 CD8
4-1BBL Blocking Antibody - - - + - - + -
OX40L Blocking Antibody - - - - + - - +

B.

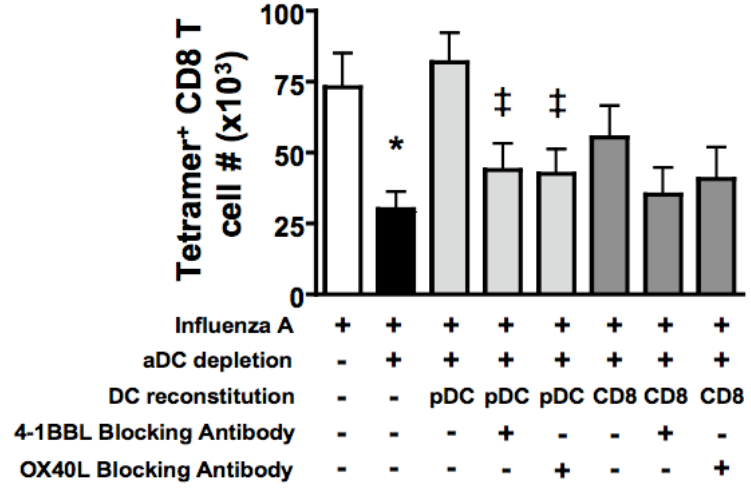
Tetramer+ CD8 T cell # (x10³)
100
75
50
25
0
*
‡
‡
Influenza A + + + + + + + +
aDC depletion - + + + + + + +
DC reconstitution - - pDC pDC pDC CD8 CD8 CD8
4-1BBL Blocking Antibody - - - + - - + -
OX40L Blocking Antibody - - - - + - - +

Figure 9. Pulmonary DC subsets express the late costimulatory molecule CD70. Groups of BALB/c mice were infected with influenza A/JAPAN/305/57 and groups of C57BL/6 mice were infected with influenza A/PR/8/34, then sacrificed on day 6 p.i. and their lungs analyzed by flow cytometry for $CD8\alpha^+$ DC (top panels) and pDC (bottom panels) expression of CD70. Isotype controls are included as filled grey lines. Shown are representative histograms of 1 experiment, n= 2-3 mice/group.

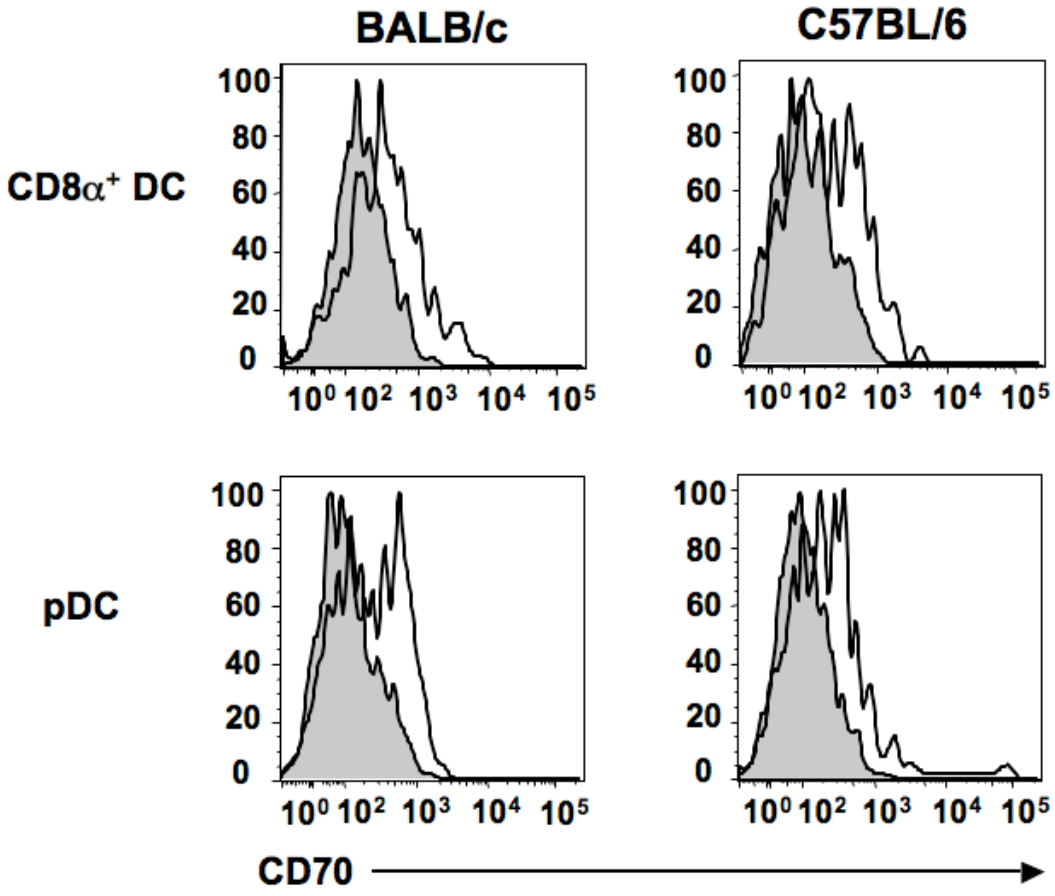
BALB/c
C57BL/6
CD8α+ DC
pDC
100
80
60
40
20
0
10^0 10^2 10^3 10^4 10^5
CD70

Figure 10. Role of CD70 in the pulmonary pDC and CD8α^+ DC mediated rescue of IAV-specific CD8 T cell responses from aDC depleted mice. (A) Groups of BALB/c mice were infected with a sublethal dose of IAV +/- aDC depletion. On day 3 p.i., groups of aDC-depleted mice were reconstituted i.n. with $2x10^4$ purified pulmonary pDC (light grey bars) or CD8α^+ DC (dark grey bars) that were left untreated or blocked *in vitro* with anti-CD70 antibody prior to adoptive transfer. On day 6 p.i., the number of pulmonary antigen-specific CD8 T cells was enumerated by tetramer staining. Data are pooled from two independent experiments and represent means ± SEM. n= 5-8 mice/group. (B) Groups of C57BL/6 mice were infected with a sublethal dose of IAV and aDC depleted at 48 hours p.i. (black bars), while controls remained undepleted (white bars). On day 3 p.i., groups of aDC-depleted mice were then reconstituted i.n. with $2x10^4$ purified pulmonary pDC (light grey bars) or CD8α^+ DC (dark grey bars) that were left untreated or blocked *in vitro* anti-CD70 antibody prior to adoptive transfer. On day 7 p.i., the number of pulmonary antigen-specific CD8 T cells was enumerated by tetramer staining. Data are representative of two independent experiments and represent means ± SEM. n=4 mice/group. *$p \leq 0.05$ relative to influenza only controls, ‡$p \leq 0.05$ relative to untreated DC reconstituted mice

A.

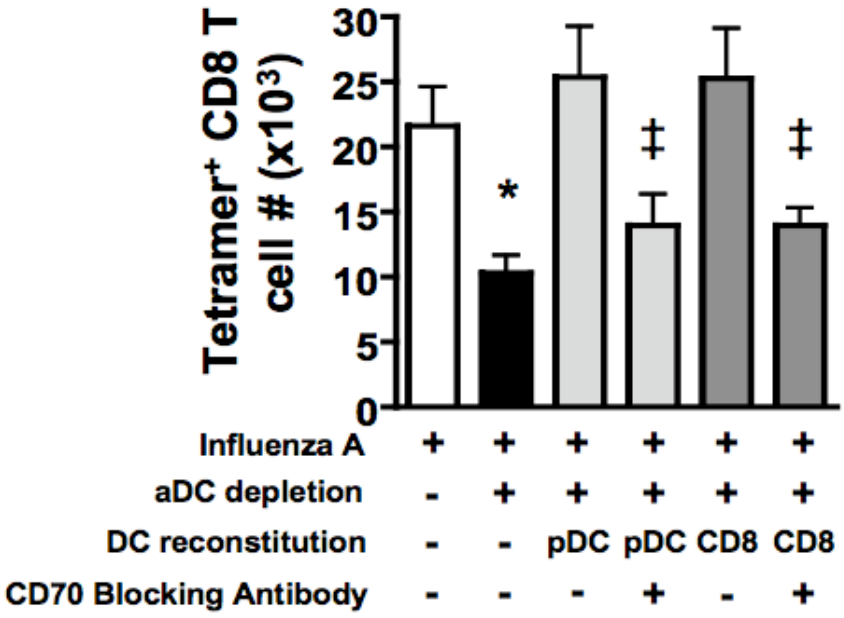
Tetramer+ CD8 T cell # (x10³)
30
25
20
15
10
5
0
*
‡
‡
Influenza A + + + + + +
aDC depletion - + + + + +
DC reconstitution - - pDC pDC CD8 CD8
CD70 Blocking Antibody - - - + - +

B.

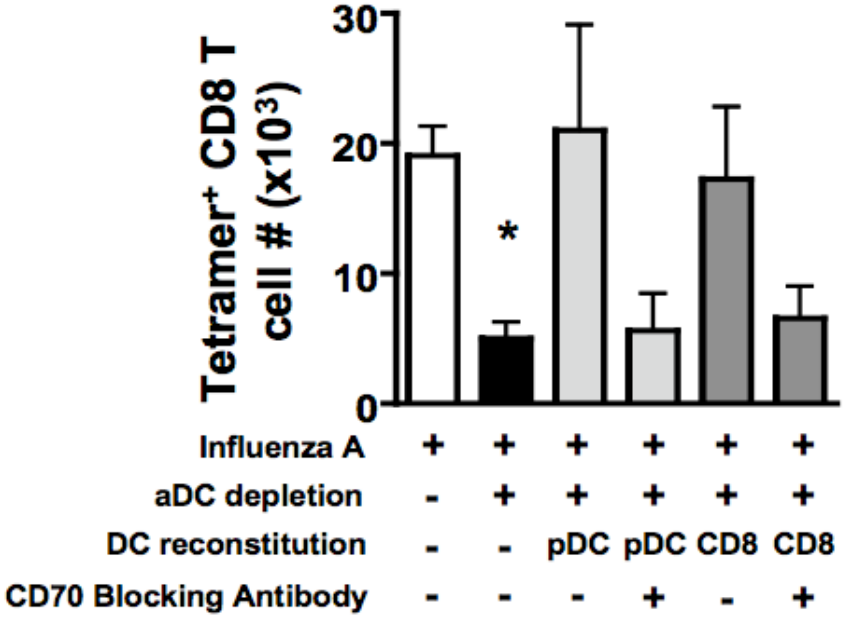
Tetramer+ CD8 T cell # (x10³)
30
20
10
0
*
Influenza A + + + + + +
aDC depletion - + + + + +
DC reconstitution - - pDC pDC CD8 CD8
CD70 Blocking Antibody - - - + - +

CHAPTER III THE MECHANISMS REGULATING ANTIGEN-SPECIFIC CD8 T CELL RESPONSES IN THE LUNGS FOLLOWING INFLUENZA VIRUS INFECTION

Introduction

As discussed in Chapter I, the absence of specific pulmonary DC subsets, including pDC and CD8α^+ DC, from the lungs leads to a decrease in the number of virus-specific CD8 T cells (53). Reconstitution of the lungs with physiologic numbers of pDC or CD8α^+ DC is able to restore the pulmonary IAV-specific CD8 T cell response to near normal levels via a mechanism that is dependent upon direct DC:T cell interactions, DC-expressed MHC I and the presence of viral antigen. Importantly, we have demonstrated that the reduction in T cell numbers observed in the lungs of aDC depleted mice following IAV challenge results not from impaired proliferation within the lungs, but instead is due to increased levels of apoptosis by virus-specific CD8 T cells compared to non-depleted controls.

Virus-specific CD8 T cells are known to undergo apoptosis by 2 broad mechanisms: AICD and ACAD (see Chapter I for more details) (20, 136). AICD proceeds downstream from the death receptor (i.e. CD95, etc) via the extrinsic type I cell-death pathway or the extrinsic type II cell death pathway (Figure 2) (20, 136). The type II cell death pathway can be blocked by expression of anti-apoptotic Bcl-2 which binds to Bax to prevent apoptosis (20, 136), while the type I death pathway cannot be blocked by Bcl-2. ACAD is intrinsic and cell death-receptor independent (Figure 3) (20, 136). Apoptosis through this pathway proceeds independent of active capase 8 and, like the type II cell-death pathway, is inhibited by Bcl-2 (20, 136).

While it was clear the virus-specific CD8 T cells were undergoing increased levels of apoptosis in the lungs of aDC depleted mice compared to non-depleted controls,

the pathway and mechanism by which these cells were dying remained unclear. It was previously known that aDC depleted mice have significantly increased pulmonary viral titers in the lungs, suggesting an increased possibility for virus-specific CD8 T cells to encounter viral antigen in the absence of appropriate costimulation, enhancing the risk for death via AICD (see Chapter V). It is also known, however, the aDC depleted mice have reduced numbers of DC in the lungs which may provide important survival cytokines (i.e. IL-15, see Chapter IV) leading the virus-specific CD8 T cells to die as a result of cytokine deprivation or ACAD. Therefore, we undertook studies to determine the primary pathway of virus-specific CD8 T cell apoptosis in the lungs of aDC depleted mice.

Materials and Methods

Mice

6-12 week old female BALB/c mice and 6-12 week old male C57BL/6 CD45.1$^+$ congenic mice were purchased from the National Cancer Institute (Frederick, MD). Clone-4 (CL-4) TCR transgenic mice (H-2^d, CD90.1$^+$) were purchased from The Jackson Laboratory (Bar Harbor, ME), and CL-4 TCR transgenic mice (H-2^d; CD90.2$^+$) were a kind gift from Dr. Linda Sherman (Scripps Research Institute). Both CL-4 transgenic strains are specific to the $HA_{533-541}$/$HA_{529-537}$ epitope of H1 and H2 IAV, respectively. BALB/c CD90.1$^+$ congenic mice were a kind gift of Dr. Richard Enelow (Dartmouth College) and Dr. John Harty (University of Iowa). C57BL/6 VavP-Bcl-2 transgenic mice (H-2^b, CD45.2$^+$) were a kind gift from Dr. Annette Schlueter (University of Iowa). All mice were housed, bred and maintained in the animal care facility at the University of Iowa. Experiments were conducted according to federal and institutional guidelines and were approved by the University of Iowa Animal Care and Use Committee.

Virus infection

Mouse-adapted influenza A viruses A/PuertoRico/8/34 and A/JAPAN/305/57 were grown in the allantoic fluid of 10-day old embryonated chicken eggs for 2 days at 37°C, as previously described (76). Allantoic fluid was harvested and stored at -80°C. BALB/c and C57BL/6 mice were anesthetized with isofluorane and infected i.n. with either 5875 TCIU or 587 TCIU of mouse-adapted A/JAPAN/305/57 or 1066 TCIU of A/PR/8/34, respectively, in 50 μl of Iscove's media as previously described (76).

Clodronate-liposome treatment

Pulmonary DC and macrophage depletion was performed by treatment with liposomes containing dichloromethylene bisphosphonate (Clodronate) (53). Clodronate was a gift of Roche Diagnostics GmbH, Mannheim, Germany. It was encapsulated in liposomes as described previously (238). Phosphatidylcholine (LIPOID E PC) was obtained from Lipoid GmbH, Ludwigshafen,Germany. Cholesterol is purchased from SIGMA Chem.Co. USA. At 48 hours p.i., mice were anesthetized by isofluorane inhalation and administered 75 μl of Clodronate-liposomes or PBS-liposomes i.n.

MHC I tetramers

Tetramers HA_{204} (H-2K(d)/LYQNVGTYV), HA_{529} (H-2K(d)/IYATVAGSL), and NP_{147} (H2K(d)/TYQRTRALV) for BALB/c, and PA_{224} (H2D(b)/SSLENFRAYV) and NP_{366}(H2D(b)/ASNENMETM) for C57BL/6 were obtained from National Institute of Allergy and Infectious Disease MHC Tetramer Core Facility (Atlanta, GA).

Preparation of cells

Lungs were pressed through wire mesh to obtain a single cell suspension, which was then enumerated by trypan blue exclusion. For DC preparations, lungs were digested for 25 minutes at 25° C in media containing 1 mg/ml Collagenase (Sigma) and 0.02 mg/ml DNase (Sigma) before single cell preparation. Dendritic cells for reconstitution

experiments were purified from the lungs of day 6 A/JAPAN/305/57 infected BALB/c donors respectively using MACS technology (Miltenyi Biotech) according to manufacturer's instructions or by fluorescence activated cell sorting (FACS) as has been previously described (53). Purified cells were resuspended in Iscove's DMEM and $2.5x10^4$ cells in 50 ul were adoptively transferred i.n. to host mice on day 3 p.i. (53).

Purification and adoptive transfer of naïve CD8 T cells

Single cell suspension of splenic cells from CL-4 mice or VavP-Bcl-2 transgenic mice were labeled with CD8α Microbeads (MB) and purified according to manufacturers instructions (Miltenyi Biotec). Purified $CD90.2^+$ CL-4 CD8 T cells were adoptively transferred ($5x10^5$) i.v. into BALB/c $CD90.1^+$ congenic mice, purified $CD90.1^+$ CL-4 cells were adoptively transferred ($5x10^5$) i.v. into BALB/c $CD90.2^+$ mice or purified $CD45.2^+$ VavP-Bcl-2 transgenic cells were adoptively transferred (10^7) into C57BL/6 $CD45.1^+$ mice. 24 hrs later the host mice were infected with influenza as described above.

Immunoblotting

Single cell suspensions were prepared as above from the lungs of day 5 IAV-infected control and aDC depleted CL-4 host mice. CL-4 CD8 T cells were purified based on CD3, CD8 and CD90.1/CD90.2 expression using MACS technology (Miltenyi Biotech) according to manufacturer's instructions or by fluorescence activated cell sorting (FACS) as has been previously described (53).

Equivalent numbers of purified CL-4 cells (10 ul volume) were lysed 10 minutes at 4° C in Triton X-100 buffer (1% Triton X-100, 20 mM Tris (pH 7.5), 1% EDTA, plus Complete Mini *EASYpack* Protease Inhibitor Cocktail Tablets (Roche)). Lysates were then centrifuged for at 16,000xg for 10 min. Supernatants were mixed with 10 uL of 2x sample buffer (0.5 M Tris-HCl (pH 6.8), 10% SDS, 0.1 % bromophenol blue, 10% glycerol, 5% 2-mercaptoethanol) and loaded on individual lanes of a 12% or 4-20%

gradient Tris-glycine gel (Invitrogen). Proteins were separated by electrophoresis, transferred to a nitrocellulose membrane (Bio-Rad) and blotted with the following antibodies (1 ug/mL): monoclonal rat anti-mouse Bid (91508) and monoclonal rat anti-mouse Bcl-2 (121529) from R&D Systems, polyclonal rabbit anti-mouse caspase 9 from Cell Signaling Technology, polyclonal rabbit anti-mouse Bim from BD Pharmingen, polyclonal rabbit anti-mouse caspase 8 and monoclonal mouse anti-mouse Bcl-xL (7B2.5) from Abcam, and monoclonal mouse anti-mouse GAPDH (6C5) from Millipore. Bands were visualized using HRP-conjugated goat anti-rabbit, goat anti-mouse or goat anti-rat (1:20,000 dilution) with the SuperSignal West Pico Chemiluminescent Substrate (ThermoScientific) or the SuperSignal West Femto Maximum Sensitivity Substrate (ThermoScientific). When necessary, membranes were stripped for 5 minutes at room temperature with the Re-Blot Plus Mild Solution (Millipore).

Antibodies and reagents

The following flow cytometry reagents were used for these studies: rat anti-mouse CD3ε (145-2C11), rat anti-mouse CD8α (53-6.7), rat anti-mouse IA/IE (M5/114.15.2), rat anti-mouse CD11b (M1/70), mouse anti-rat CD90.1 (OX-7), hamster anti-mouse CD11c (HL3), hamster anti-mouse Bcl-2 (3F11), hamster IgG isotype control (A19-3), mouse anti-mouse CD45.2 (104), mouse anti-human Ki-67 (B56) and 7-AAD purchased from Becton Dickinson; mouse anti-mouse CD90.2 (5a-8), rat anti-mouse CD45R (RA3-6B2), recombinant human Annexin-V purchased from Caltag. Intranasal CFSE labeling was performed as previously described (51, 262, 263). BrdU incorporation was analyzed using the BrdU Flow Kit (BD Pharmingen) according to manufacturer's instructions, as previously described (262, 263). Vybrant FAM caspase 3/7 and caspase 8 kits were purchased from Invitrogen and used according to manufacturer's instructions. For surface staining, isolated cells (10^6) cells were stained with antibody or tetramer for 30 minutes at 4° C and then fixed using BD FACS Lysing Solution (BD Biosciences). For intracellular

cytokine staining, fixed cells were permeabilized and labeled with antibodies in FACS buffer containing 0.5% Saponin (Acros Organics, NJ) for 1 hour at 4° C. All flow cytometry data were acquired on a BD FACS Calibur or BD FACS Canto II (BD Immunocytometry Systems) and analyzed using FlowJo software (TreeStar, Ashland, OR).

Statistical analysis

Statistical significance of the difference between two sets of data was determined using an unpaired, one-tailed *t*-test or a paired *t*-test for control and experimental data groups that could be paired. Differences were considered to be statistically significant at $p<0.05$.

Results

aDC depletion at 48 hours p.i. does not alter proliferation of transgenic CL-4 CD8 T cells in the lungs

We have previously demonstrated that aDC depletion at 48 hours following IAV infection results in increased virus-associated mortality, increased pulmonary viral titers and significantly reduced numbers of virus-specific CD8 T cells in the lungs on day 6 p.i. (26). Further, we have demonstrated that IAV-specific CD8 T cells undergo increased apoptosis in the absence of pulmonary DC subsets (264). Our previous experiments testing the effects of aDC depletion on CD8 T cell immunity were performed examining the endogenous polyclonal CD8 T cell response. However, in order to perform a detailed analysis of the cell death pathways contributing to the increased apoptosis observed in the lungs of aDC depleted mice, we needed a plentiful source of IAV-specific CD8 T cells that could be easily identified and isolated. To this end, we chose to utilize transgenic CL-4 CD8 T cells, which are specific to the HA protein of IAV. The transgenic T cell adoptive transfer model allows us to easily identify IAV-specific CD8 T cells using a

congenic mismatch system, and results in increased numbers of CD8 T cells in the lungs, allowing for easier purification and analysis. However, in order to determine the cell death pathways contributing to the increased apoptosis observed in the lungs of aDC depleted mice, we first needed to confirm that our transgenic IAV-specific CL-4 T cells (specific to the HA_{529} epitope of IAV) exhibit a similar phenotype following aDC depletion to that observed in the endogenous response. As seen in Figure 11, the endogenous IAV-specific response is reduced in the lungs of aDC depleted mice as early as day 4 p.i. (i.e. when CD8 T cells are first beginning to arrive in the lungs (13, 14)) and significantly reduced by day 5 p.i.. In experiments that utilized the adoptive transfer of transgenic, IAV-specific CL-4 CD8 T cells, we observed a similar reduction in the numbers of CL-4 CD8 T cells in the lungs of aDC depleted host mice relative to non-depleted controls on days 4 and 5 p.i., suggesting that the transgenic CL-4 model faithfully replicates the model of aDC depletion observed using the polyclonal endogenous response.

We have previously demonstrated using the endogenous polyclonal model, that aDC depletion at 48 hours p.i. results in increased apoptosis of virus-specific CD8 T cells in the lungs, and subsequently, reduced T cell numbers therein (26). We wanted to confirm that a similar mechanism was contributing to the reduced numbers of transgenic CL-4 CD8 T cells in the lungs following aDC depletion. Therefore, we first examined proliferation of CL-4 CD8 T cells in the lungs of aDC depleted mice compared to non-depleted controls. Our laboratory has previously developed a novel i.n. CFSE/BrdU dual-labeling technique that allows one to specifically measure cell division by T cells in the lungs (262, 263). Briefly, CFSE was administered i.n. to day 4 and 5 infected control and aDC depleted CL-4 host mice, followed 2 hours later by i.n. BrdU. Using the gating strategy outlined in Figure 12A, lung-resident CL-4 T cell proliferation was analyzed 4 hours after BrdU administration by measuring BrdU incorporation by $CFSE^+$ $CD90.2^+$ CD8 T cells present in the lungs at the time of assay. As seen in Figure 12B, the

frequency of CL-4 CFSE$^+$ CD8 T cells that incorporated BrdU in the lungs during the time of assay was the same between aDC depleted and non-depleted control mice on days 4 and 5 p.i.. Similarly, no difference in Ki67 staining was observed between the transgenic CL-4 T cell response from aDC-depleted and non-depleted mice (Figure 13). Together these results suggest that, like our previous studies using the endogenous polyclonal response, the proliferative capacity of transgenic CL-4 CD8 T cells is the same between control and aDC depleted host groups, and therefore the reduction in CD8 T cell numbers in the lungs is likely not a result of differences in lung-resident T cell expansion.

aDC depletion at 48 hours p.i. results in increased apoptosis of transgenic CL-4 CD8 T cells

Having confirmed that aDC depletion did not alter the levels of lung-resident, CL-4 CD8 T cell proliferation during IAV infection, we next wanted to verify that the decrease in CL-4 CD8 T cell numbers in the lungs of aDC depleted mice was a result of increased CD8 T cell apoptosis following their arrival in the lungs. To this end, CL-4 CD90.2$^+$ CD8 T cells were adoptively transferred into CD90.1$^+$ hosts and, 24 hours later, the mice were infected +/- aDC depletion as above. On days 4 and 5 p.i., the lungs were analyzed for CL-4 CD8 T cell apoptosis, as measured by the presence of active caspase 3/7. As seen in Figure 14, aDC depletion at 48 hours p.i. results in increased frequencies of active caspase 3/7$^+$ pulmonary CL-4 CD8 T cells on both days 4 and 5 p.i., confirming that CL-4 CD8 T cells from aDC depleted mice are undergoing increased levels of apoptosis in the lungs relative to CL-4 CD8 T cells from non-depleted controls. These data confirm that aDC depletion at 48 hours p.i. results in increased apoptosis of CL-4 transgenic CD8 T cells in the lungs on days 4 and 5 p.i. and suggest that, with respect to T cell apoptosis, this model will faithfully replicate those results observed using the endogenous polyclonal response to study the effects of aDC depletion.

aDC depletion at 48 hours p.i. results in reduced expression of pro-survival molecules by virus-specific CD8 T cells

Survival of activated effector T cells is thought to depend upon a delicate balance between pro- and anti- apoptotic molecules including CD95L, Bim, Bcl-X_L and, of particular importance, Bcl-2 (20, 136). Bcl-2 is an important pro-survival factor that, if present at high enough levels, can inhibit both the intrinisic (Figure 3) and the extrinsic type II cell death pathway (Figure 2). Given its importance in both AICD- and ACAD-mediated cell death pathways, we next initiated studies examining levels of Bcl-2 expression by virus-specific CD8 T cells in the lungs of aDC depleted mice. To this end, groups of mice were infected with a sublethal dose of IAV and half were aDC depleted as above. On days 4 and 5 p.i., the frequency and level (as measured by change in MFI) of Bcl-2 expression was measured in virus-specific CD8 T cells from the lungs. While we did not observe a significant change in the frequency of antigen-specific CD8 T cells expressing Bcl-2 in control vs. aDC depleted lungs (data not shown), there was a reduction in the levels of Bcl-2 expressed by CD8 T cells from aDC depleted mice on day 4 and a significant reduction by day 5 compared to non-depleted control mice (Figure 15A). Further, we observed a similar reduction in Bcl-2 expression by virus-specific CD8 T cells in the lungs of aDC depleted mice when we utilized our transgenic CL-4 T cell adoptive transfer method (Figure 15B).

While the differences in Bcl-2 expression between aDC depleted and control CD8 T cells appear minor, CD8 T cells have been shown to be sensitive to even slight fluctuations in Bcl-2 protein levels (133-135). Additionally, while flow cytometric reagents are reliable for detecting the presence of Bcl-2 in CD8 T cells, they are not as sensitive as alternative methods for the quantification of protein levels of Bcl-2 or other factors regulating apoptosis in CD8 T cells. Therefore, we chose to confirm our flow cytometry data by performing the more sensitive method of western blot analysis for Bcl-2 expression. Having confirmed that CL-4 transgenic T cells behave similarly to the

endogenous IAV-specific CD8 T cell response in the lungs of aDC depleted mice, we felt confident employing this model to obtain a more plentiful and easily identifiable source of purified virus-specific CD8 T cells from the lungs. Therefore, naïve CL-4 CD90.2$^+$ CD8 T cells were adoptively transferred i.v. into naïve CD90.1$^+$ congenic host mice as in Figures 12-15. 24 hours later, the host mice were infected with a sublethal dose of IAV and half were depleted of aDC at 48 hours p.i.. On day 5 p.i., CD90.2$^+$ CL-4 CD8 T cells were isolated and cell lysates were prepared as described in the Materials and Methods. As seen in Figure 16, control CL-4 CD8 T cells express robust levels of Bcl-2 protein in the lungs at this early time point p.i.. Similar to our results using flow cytometric analysis, CL-4 T cells from aDC depleted lungs express reduced levels of the pro-survival factor Bcl-2 compared to CL-4 T cells from control lungs. In fact, densitometric analysis demonstrated that CD8 T cells from aDC depleted lungs express ~25% less Bcl-2 compared to CD8 T cells from control lungs (Figure 16B). Together, these results suggest that pulmonary CD8 T cells from aDC depleted mice may undergo increased apoptosis as a result of reduced Bcl-2 expression.

Bcl-X_L is another pro-survival member of the Bcl-2 family that is important for regulating survival and apoptosis of effector CD8 T cells (20, 136, 137). Like Bcl-2, effector cells are particularly sensitive to the relative levels of Bcl-X_L in the cell, and its over-expression is sufficient to rescue CD8 T cells from AICD and ACAD mediated apoptosis. Therefore, we next examined levels of Bcl-X_L in control vs. aDC depleted CL-4 CD8 T cells. As seen in Figure 17, control CL-4 CD8 T cells express high levels of Bcl-X_L protein at this early time point p.i.. In contrast, however, CL-4 CD8 T cells isolated from the lungs of aDC depleted mice (Figure 17) express ~25% less Bcl-X_L than their control counterparts (Figure 17B). Together with the above results, it is likely that aDC depleted virus-specific CD8 T cells are undergoing increased apoptosis as a result of reduced expression of several key survival molecules.

aDC depletion at 48 hours p.i. results in altered Bim:Bcl-2 expression ratios by CL-4 CD8 T cells in the lungs

ACAD mediated CD8 T cell apoptosis is dependent upon the balance between Bcl-2 and the pro-apoptotic molecule Bim, rather than absolute levels of each protein (133, 134). This would suggest that slightly deceased levels of Bcl-2 expression in aDC depleted CD8 T cells, coupled with increased, or even stable, levels of Bim, would be sufficient to induce increased levels of apoptosis. Therefore, we next analyzed Bim vs. Bcl-2 expression in CL-4 T cell lysates from day 5 IAV-infected control and aDC depleted mice. Similar to our results in Figure 16, we observed reduced levels of Bcl-2 expression by CL-4 T cells from aDC depleted lungs relative to those from control non-depleted lungs (Figure 18A). Interestingly, we also observed stable and even slightly increased levels of the pro-apoptotic protein Bim in CL-4 T cell lysates from aDC depleted mice compared to non-depleted control T cell lysates (Figure 18A). A densitometric analysis of the ratios between Bim:Bcl-2 revealed that while CL-4 T cells from control lungs express a Bim:Bcl-2 ratio of less than 1 in the lungs following IAV infection, CL-4 T cells from aDC depleted lungs express a Bim:Bcl-2 ratio of greater than 1 (Figure 18B). Overall, these results suggest that reduced levels of Bcl-2 and stable, or even increased, levels of Bim may play an important role in regulating the apoptosis of virus-specific CD8 T cells in the lungs of aDC depleted mice. Further, given the important role of Bim in initiating the ACAD pathway, these results suggest that aDC depleted cells are undergoing apoptosis at least partially due to death by neglect, or ACAD.

Virus-specific CD8 T cells from aDC depleted mice undergo apoptosis via both ACAD and AICD mediated pathways

Thus far, we have demonstrated that aDC depleted CD8 T cells express reduced levels of the pro-survival molecules Bcl-2 and Bcl-X_L, and increased levels of the pro-apoptotic molecule Bim, indicating that they may be undergoing apoptosis as a result of ACAD. Given that Bcl-2 can play a role in regulating both ACAD and AICD mediated cell death, we next directly examined members of both pathways to determine which type of apoptosis was contributing to the decreased CD8 T cell numbers in the lungs of aDC depleted mice. Formation of active caspase 9 is one of the final steps in both the intrinsic ACAD pathway and the extrinsic type II cell death pathway, prior to the activation of the effector caspases 3/6/7 (Figures 2 and 3). Therefore, we first determined if CD8 T cells from aDC depleted mice expressed increased levels of caspase 9 compared to their control counterparts. To this end, cell lysates of CL-4 T cells isolated from control and aDC depleted mice on day 5 p.i. were probed for the presence of full-length and cleaved, active caspase 9. As seen in Figure 19A, while control CL-4 CD8 T cells express robust levels of uncleaved, pro-caspase 9 and relatively low levels of active caspase 9 in the lungs at this time point, CL-4 CD8 T cells from aDC depleted mice have almost no pro-caspase 9, but express high levels of the active, cleaved forms of caspase 9. A densitometric analysis of the ratio between full-length pro-caspase 9 and active, cleaved caspase 9 confirmed that over 50% of the caspase 9 detected in control CD8 T cells is present in its inactive pro-form, while less than 20% of the caspase 9 detected in aDC depleted T cells exists in its inactive form (Figure 19B). Together, these results confirm that CD8 T cells from aDC depleted mice are likely undergoing apoptosis via the intrinsic ACAD-mediated pathway, and further suggest that the extrinsic type II cell death pathway may also contribute to their death.

One of the key signaling events that differentiate between ACAD and the type II extrinsic cell death pathway is the activation of caspase 8. Caspase 8 is one of the first molecules to be activated in the AICD pathway following ligation of a death receptor such as Fas (Figure 2). We have previously determined that aDC depleted lungs contain an increased frequency of virus-specific CD8 T cells that express activated caspase 8 as measured by flow cytometry (53, 264); however, we next confirmed this data using the more sensitive approach of western blotting. CL-4 T cell lysates were prepared as in Figure 16 and probed for expression of the active form of caspase 8. As seen in Figure 20, similar to our results using flow cytometry (53, 264), virus-specific CD8 T cells from aDC depleted lungs express increased levels of active caspase 8 compared to their non-depleted counterparts (Figure 20A). Densitometric analysis of the western blots in Figure 20A reveal that CD8 T cells from aDC depleted lungs express ~10% more active caspase 8 than their control counterparts (Figure 20B).

The extrinsic type II cell death pathway (Figure 2) proceeds from the activation of caspase 8 to the cleavage of full-length BID to its active form, tBID. tBID then proceeds downstream to the mitochondria to interact Bax and Bak and induce the release of cytochrome c, which induces the activation of caspase 9 and then the subsequent activation of the effector caspases. Together, the presence of active caspase 9 (Figure 19) and active caspase 8 (Figure 20A) suggests that virus-specific CD8 T cells from aDC depleted mice are undergoing increased apoptosis via the type II cell death pathway. Therefore, we next attempted to confirm these results by examining the levels of active tBID that were present in virus-specific CD8 T cells from aDC depleted lungs. As seen in Figure 20C, cell lysates from both control and aDC depleted CL-4 CD8 T cells express robust levels of the full-length form of BID; however, we were unable to detect the presence of active tBID in virus-specific CD8 T cells from either control or aDC depleted lungs (Figure 20C). In contrast, we were able to detect both full-length BID and active tBID in positive control samples that included cell lysates from splenocytes that were

stimulated with the agonistic anti-Fas antibody Jo-2 in soluble form (Figure 20D, lane 1) or plate-bound form (Figure 20D, lane 2), as well as splenocytes treated directly with recombinant caspase 8 (Figure 20D, lane 3), which is known to induce cleavage of BID to tBID. Together, these results suggest that the type II extrinsic cell death pathway is not likely to be a primary pathway contributing to the apoptosis of CD8 T cells in the lungs of aDC depleted mice.

The result of our western blot analysis have been summarized in Figure 21. Overall, it is likely that virus-specific CD8 T cells from aDC depleted lungs undergo apoptosis via two primary mechanisms: intrinisic ACAD-mediated cell death and extrinsic type I AICD-mediated cell death. The presence of active caspase 8 suggests that some cells are receiving signals via Fas or other death receptors; however, the undetectable levels of active tBID suggests that the extrinsic pathway is mostly bypassing activation of the type II cell death pathway and instead primarily activating the effector caspases, hence the type I cell death pathway (Figure 21A). However, the presence of active caspase 9, as well as the imbalance in the Bim:Bcl-2 ratio in aDC depleted T cells suggests that some of the cells are also dying via ACAD as a result of neglect or cytokine starvation (Figure 21B). Overall, these results suggest that multiple mechanisms of cell death are at play in the lungs of aDC depleted mice, and that likely, some cells are dying by ACAD, while others are dying by AICD. In the following chapters we will more directly address the functional role of each pathway in regulating T cell death in the lungs following IAV infection and aDC depletion.

Transgenic over-expression of Bcl-2 is sufficient to rescue virus-specific CD8 T cells from apoptosis in the lungs of aDC depleted mice

As we demonstrated in Figures 15, 16 and 18, aDC depletion results in reduced expression of Bcl-2 by virus-specific CD8 T cells in the lungs. Bcl-2 is able to block

both the intrinsic ACAD pathway and the type II AICD pathway by sequestering the pro-apoptotic molecules Bax and Bak away from the mitochondria (20, 136). Therefore, we reasoned that if the reduction in Bcl-2 was functionally contributing to the decrease in virus-specific CD8 T cells in the lungs of aDC depleted mice via its regulation on the ACAD pathway, then over-expression of Bcl-2 should be sufficient to rescue these T cells from death. To test this hypothesis, we isolated $CD45.2^+$ CD8 T cells from the spleens of VavP-Bcl-2 transgenic mice, which over-express Bcl-2 under control of the Vav promoter, and adoptively transferred 10^7 cells i.v. to congenic $CD45.1^+$ host mice. 24 hours later, the mice were infected with a sublethal dose of IAV+/- aDC depletion at 48 hours p.i.. On day 7 p.i., the lungs were analyzed by flow cytometry for the total numbers of endogenous $CD45.1^+CD3^+CD8^+Tetramer^+$ virus-specific CD8 T cells (Figure 22A) and adoptively transferred, Bcl-2 transgenic $CD45.2^+CD3^+CD8^+Tetramer^+$ virus-specific CD8 T cells (Figure 22B). As expected, aDC depletion at 48 hours p.i. results in a significant reduction in the numbers of endogenous virus-specific CD8 T cells in the lungs. In contrast, however, over-expression of the pro-survival molecule Bcl-2 is able to rescue virus-specific CD8 T cells in the lungs of aDC depleted mice, as we observe no differences between the numbers of adoptively transferred Bcl-2 transgenic CD8 T cells in the lungs of aDC depleted mice compared to non-depleted control lungs (Figure 22B). These results suggest a functional contribution for the reduced levels of Bcl-2 expression observed in T cells from control vs. aDC depleted mice, as overcoming this reduction is able to reverse the phenotype of increased apoptosis in the lungs. Further, these results suggest that while T cells from aDC depleted mice die by both ACAD and AICD mediated mechanisms, over-expression of the pro-survival molecule Bcl-2 is able to protect and overcome these pathways of apoptosis, resulting in the selective survival and accumulation of virus-specific CD8 T cells in the lungs of aDC depleted mice.

Discussion

We demonstrate here that virus-specific CD8 T cells from the lungs of aDC depleted mice are likely undergoing increased apoptosis via both ACAD- and AICD-mediated mechanisms (See Figure 21 for a summary). Interestingly, while we were able to detect high levels of active caspase 8 in T cells from aDC depleted mice (Figure 20A and B), we were unable to detect the presence of tBID (Figure 20C), a finding which would indicate virus-specific CD8 T cells were dying via the extrinsic type II cell death pathway. The result of our positive control experiments (Figure 20D) indicate that the anti-BID antibody is specific and able to detect the truncated form of BID, suggesting that the inability to detect tBID in our freshly isolated CD8 T cells is not due to a technical problem with the detection antibody. However, it is likely that the levels of tBID are abnormally high under the *in vitro* culture conditions utilized in these positive control experiments, given the uniform and simultaneous triggering of apoptosis during culture, as well as the strong apoptotic signals delivered by both recombinant caspase 8 and the anti-Fas antibody. The half-life of tBID has been estimated to be as short as 1.5 hours (265). In our experiments in Figure 20 we are analyzing a small population of heterogeneous cells that are at various stages of life and death, and therefore, are unlikely to simultaneously express detectable levels of tBID. Given the possibility that its short half-life makes tBID undetectable in the cells obtained during these analyses, it is difficult to definitively conclude that tBID is absent from virus-specific CD8 T cells in the lungs of aDC depleted mice.

Cleavage of BID by active caspase 8 during initiation of the type II cell death pathway results in the induction of both caspase dependent and independent apoptosis pathways (Figure 2, Figure 21A); therefore, tBID formation is an important amplification step that is necessary for cells that are relatively resistant to apoptosis (20, 136, 137). Newly activated CD8 T cells express high levels of pro-survival molecules such as c-FLIP, Bcl-2 and Bcl-X_L, and thus, are resistant to apoptosis (137). The signal

amplification afforded by the type II cell death pathway is though to be unnecessary following induction of apoptosis in a cell population that is already more prone to death, i.e. CD8 T cells at the later stages of the effector response (137). While we are examining CD8 T cells at relatively early time points following infection, we have already demonstrated that the balance of pro- and anti-apoptotic molecules expressed by aDC depleted CD8 T cells renders them highly susceptible to apoptosis. This suggests that perhaps activation of the type II cell death pathway at the population level of virus-specific CD8 T cells in the lungs is largely unnecessary. Overall, it is probable that both the type I and type II extrinsic cell death pathways are contributing to the apoptosis of virus-specific CD8 T cells at the single-cell level in the lungs of aDC depleted mice. However, at the population level, given the undetectable levels of tBID, the type II cell death pathway is not likely to be the primary pathway being utilized by virus-specific CD8 T cells in the lungs of aDC depleted mice.

While activation of caspase 8 is primarily thought to occur during the initiation of apoptosis, it has also been described to play an important role during T cell activation (266). Blockade of caspase 8 activation during CD3- or IL-2-mediated T cell activation results in impaired T cell expansion *in vitro* (267, 268), while mice containing a T cell-specific deficiency in caspase 8 exhibit increased susceptibility to infection with LCMV as a result of an impaired CD8 T cell responses *in vivo* (269). Together, these results indicate that the expression of active caspase 8 does not definitively indicate that a cell is apoptotic. For this reason, we have used multiple parameters of analysis including measuring for the presence of active caspase 3/7 ((53, 264) and Figure 14), the presence of active caspase 8 and staining for Annexin-V and 7-AAD (53, 264), to conclude that aDC depleted CD8 T cells are indeed undergoing increased apoptosis compared to control cells. Further, given that T cells from both control and aDC depleted mice are isolated from IAV-infected lungs at an early time point p.i., it is unlikely that aDC depleted T cells exist in a higher activation status, and thus are expressing more active

caspase 8 than their control counterparts. Therefore, while it is formally possible that the presence of active caspase 8 is not indicative of apoptosis, taken together, our results suggest that indeed, virus-specific CD8 T cells from aDC depleted lungs are undergoing apoptosis via an AICD-mediated mechanism. In Chapter V we will more definitively explore a functional role for AICD and demonstrate that the extrinsic cell death pathway is contributing to the apoptosis of virus-specific CD8 T cells in the lungs of aDC depleted mice.

In Chapter II we demonstrated that the late costimulatory molecules CD70 and, in some cases, OX40L and 4-1BBL, are playing a role in the pulmonary DC mediated rescue of virus-specific CD8 T cells in the lungs of aDC depleted mice. All of these members of the TNFR superfamily have been to described to promote increased T cell survival (178-180, 207). Further, CD27 and 4-1BB costimulation have both been demonstrated to induce upregulation of pro-survival molecules such as Bcl-2, Bcl-X_L and Bfl1, and prevent Fas-mediated AICD (213, 214, 231). While it is currently unknown what molecular mechanisms pulmonary DC subsets are using to rescue virus-specific CD8 T cells in the lungs following aDC depletion, it is possible that they are promoting upregulation of the Bcl-2 or Bcl-X_L via costimulation of 4-1BB, OX40 or CD27, or, as we will discuss in Chapter IV, via trans-presentation of IL-15. Our western blot results suggest that both ACAD, which can be blocked by Bcl-2 (20, 136, 137), and AICD extrinsic cell death pathway I, which cannot be blocked by Bcl-2 (20, 136, 137), are contributing to CD8 T cell death in the lungs of aDC depleted mice. However, our results using Bcl-2 transgenic CD8 T cells (Figure 22) suggest that over-expression of Bcl-2 is sufficient to promote a complete rescue of CD8 T cell numbers in the lungs of aDC depleted mice. Similarly, blockade of 4-1BBL, OX40L and, in particular, CD70, is sufficient to ablate the effect of pulmonary DC transfer (Chapter II). Together, these results suggest that signals from pulmonary DC may be sufficient to overcome both pathways, or, just as likely, it is possible that rescuing even a few virus-specific CD8 T

cells (i.e. the portion that are undergoing apoptosis via ACAD, and thus can be rescued by Bcl-2 over-expression) at this early stage of infection is sufficient to allow accumulation and rescue of virus-specific CD8 T cell response to control levels.

While it is accepted that elimination of effector CD8 T cells occurs via both ACAD and AICD, it has been suggested that which program gets activated is largely dependent upon the quantity of antigen (137). For example, at the end of an immune response to a foreign pathogen, antigen concentrations are extremely low and the likelihood of reactivating a T cell via its TCR, a requirement for AICD, is low. Therefore, CD8 T cells are more likely to undergo intrinsic ACAD. In contrast however, during a chronic infection or autoimmune disease, antigen is present at high levels and CD8 T cells are more likely to receive signals via their TCR and undergo apoptosis via AICD (137). In our model of IAV infection followed by aDC depletion at 48 hours p.i., we are severely altering both the antigen and the inflammatory cytokine environment in the lungs (53); thus, it is not surprising that both types of T cell death are occurring therein. aDC depleted mice express significantly higher viral titers in the lungs compared to their non-depleted control counterparts (53), suggesting an increased likelihood for virus-specific CD8 T cells to encounter antigen in the absence of the proper costimulatory molecules. In Chapter V we will demonstrate that indeed, the high antigen burden present in the lungs of aDC depleted mice contributes to the increased CD8 T cell apoptosis observed therein, suggesting an important functional role for AICD in regulating the magnitude of the pulmonary effector response. Further, depletion of aDC at 48 hours p.i. results in impaired recruitment of several pulmonary DC subsets including pDC and CD8α^+ DC (53). The impaired recruitment of these and other pulmonary subsets likely results in reduced levels of inflammatory cytokines and growth factors, thus rendering virus-specific CD8 T cells more susceptible to ACAD. In Chapter IV we will demonstrate that aDC depleted mice express reduced levels of the cytokine IL-15 compared to non-depleted controls, and suggest that the absence of pulmonary DC-

mediated IL-15 trans-presentation contributes functionally to ACAD-mediated apoptosis by virus-specific CD8 T cells in the lungs.

Figure 11. aDC depletion at 48 hours p.i. results in reduced numbers of IAV-specific CD8 T cells in the lungs on days 4 and 5 p.i. (A and B) Groups of BALB/c mice were infected with a sublethal dose of IAV. Half of the mice were aDC depleted at 48 hours p.i. (aDC depleted, black bars), while the other half remained non-depleted (Control, white bars). On days 4 and 5 p.i., the frequency (A) and number (B) of antigen-specific tetramer$^+$ CD8 T cells in the lungs was enumerated. Representative FACS plots are gated on CD3$^+$CD8$^+$ T cells. Numbers of Tetramer$^+$ CD8 T cells in the lungs were determined by subtracting background staining using the Media Control. Data are pooled from 2 separate experiments and represent means ± SEM. n=5-9 mice/group. (C and D) Influenza-specific, CD90.2$^+$ CL-4 T cells were adoptively transferred into groups of CD90.1$^+$ BALB/c mice as described in the Materials and Methods. 24 hours later, mice were infected with a sublethal dose of IAV. Half of the mice were aDC depleted at 48 hours p.i. (aDC depleted), while the other half remained non-depleted (Control). On days 4 and 5 p.i., the frequency (C) and number (D) of CD90.2$^+$, adoptively transferred CL-4 T cells were determined by flow cytometry. Representative FACS plots are gated on CD3$^+$CD8$^+$ T cells. Data are representative of 3 separate experiments and represent means± SEM. n=3-4 mice/group.

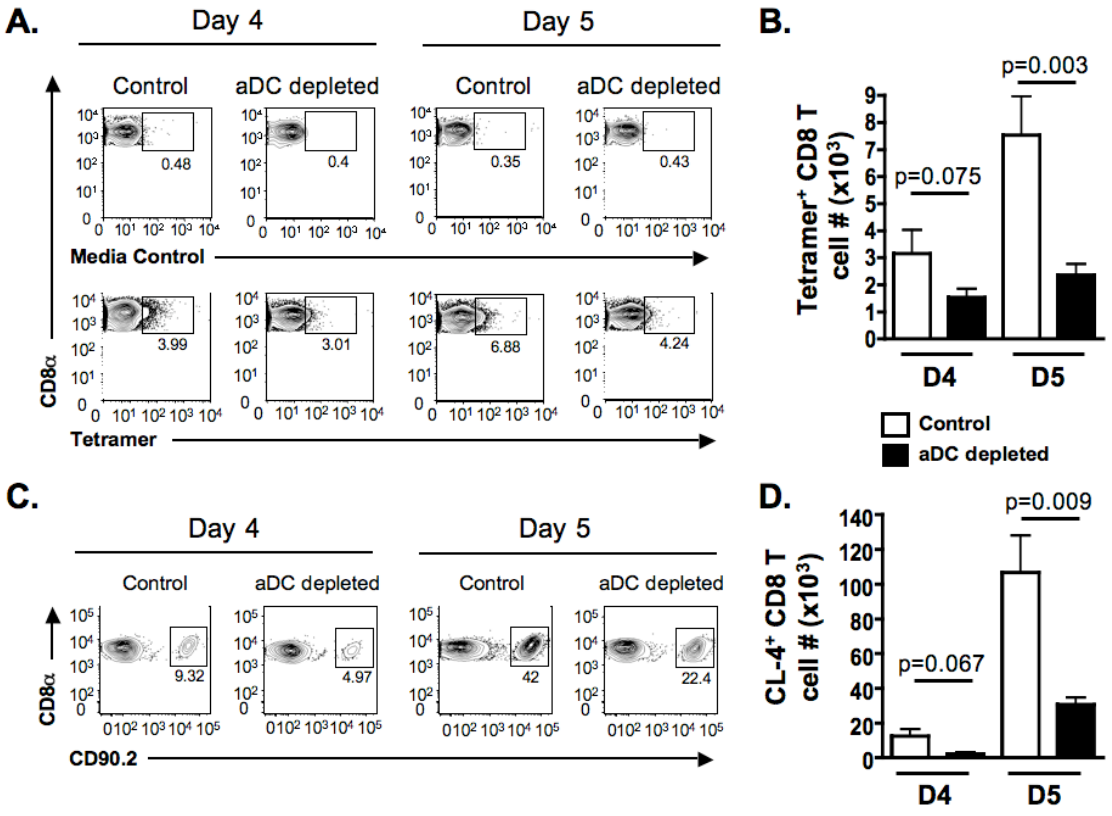
A.
Day 4
Day 5
Control
aDC depleted
Control
aDC depleted
0.48
0.4
0.35
0.43
Media Control
3.99
3.01
6.88
4.24
CD8α
Tetramer
B.
p=0.003
p=0.075
Tetramer+ CD8 T cell # (x10³)
D4
D5
Control
aDC depleted
C.
Day 4
Day 5
Control
aDC depleted
Control
aDC depleted
9.32
4.97
42
22.4
CD8α
CD90.2
D.
p=0.009
p=0.067
CL-4+ CD8 T cell # (x10³)
D4
D5

Figure 12. aDC depletion at 48 hours p.i. does not alter IAV-specific transgenic CD8 T cell proliferation in the lungs. (A) Representative gating strategy for i.n. BrdU-CFSE labeling of virus-specific CD8 T cells. Influenza-specific, $CD90.2^+$ CL-4 T cells were adoptively transferred into groups of $CD90.1^+$ BALB/c mice as in Figure 11C. 24 hours later, mice were infected with a sublethal dose of IAV +/- aDC depletion. On days 4 and 5 p.i., mice were treated with i.n. CFSE, followed 2 hours later by i.n. BrdU as described in the Materials and Methods. 4 hours after BrdU administration, mice were sacrificed and their lungs analyzed by flow cytometry for the frequency of $BrdU^+$ cells among $CFSE^+CD8^+CD90.2^+$ T cells using the shown representative gating strategy. (B) Proliferation, as measured by BrdU incorporation, of lung-resident $CFSE^+CD90.2^+$ CD8 T cells was assessed by flow cytometry using the gating strategy outlined in A. Data are representative of 1 experiment and represent means± SEM. n=3-5 mice/group. NS=No statistical difference was observed between the analyzed groups.

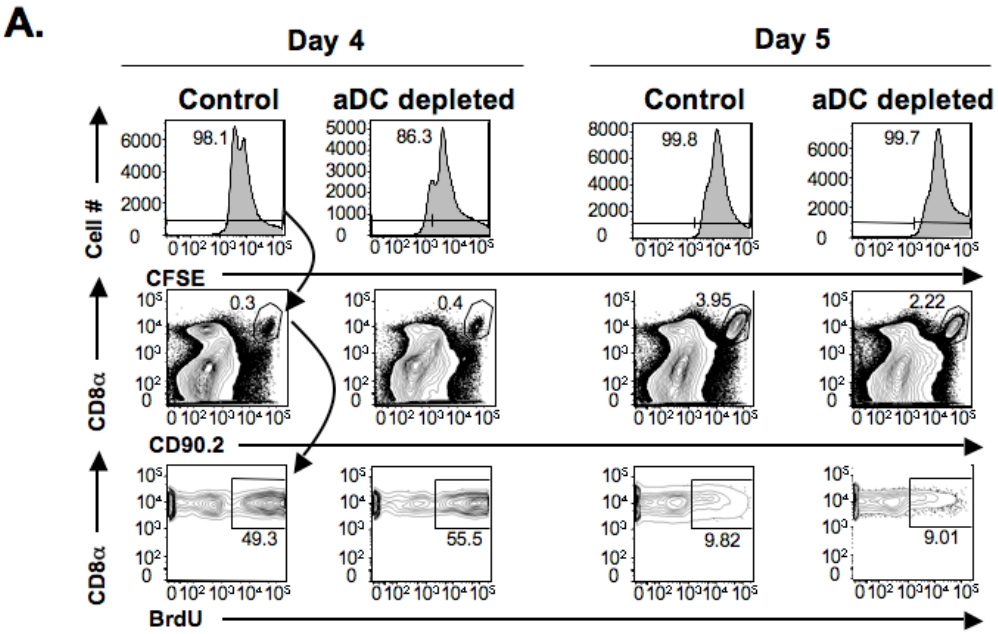
A.
Day 4
Day 5
Control
aDC depleted
Control
aDC depleted
Cell #
98.1
86.3
99.8
99.7
CFSE
CD8α
0.3
0.4
3.95
2.22
CD90.2
CD8α
49.3
55.5
9.82
9.01
BrdU

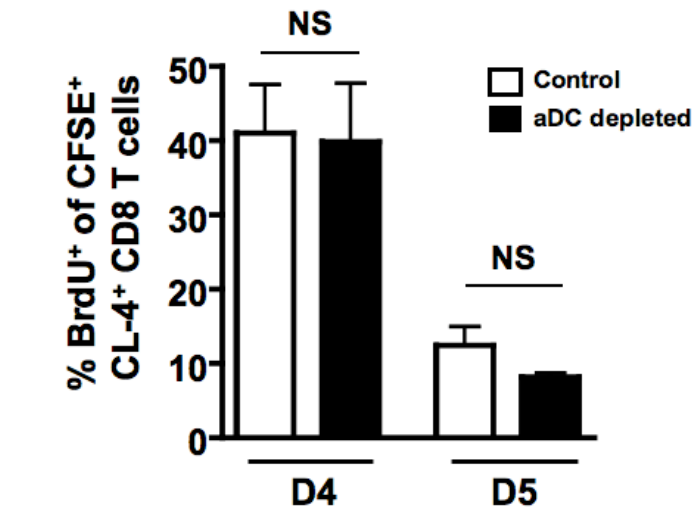
B.
NS
NS
Control
aDC depleted
% BrdU+ of CFSE+ CL-4+ CD8 T cells
50
40
30
20
10
0
D4
D5

Figure 13. aDC depletion at 48 hours p.i. does not alter the proliferation of IAV-specific CD8 T cells in the lungs. Influenza-specific, $CD90.2^+$ CL-4 T cells were adoptively transferred to groups of $CD90.1^+$ BALB/c mice as in Figure 11C. 24 hours later, mice were infected with a sublethal dose of IAV +/- aDC depletion. On days 4 and 5 p.i., mice were sacrificed and proliferation, as measured by Ki67 expression, of adoptively transferred $CD90.2^+$ CL-4 T cells was analyzed by flow cytometry. (A) Shown are representative isotype (grey fill) or Ki67 staining (black lines) for control non-depleted and aDC depleted mice on days 4 and 5 p.i. Data in A and B are representative of 3 experiments and represent mean± SEM. n=3-4 mice/group.

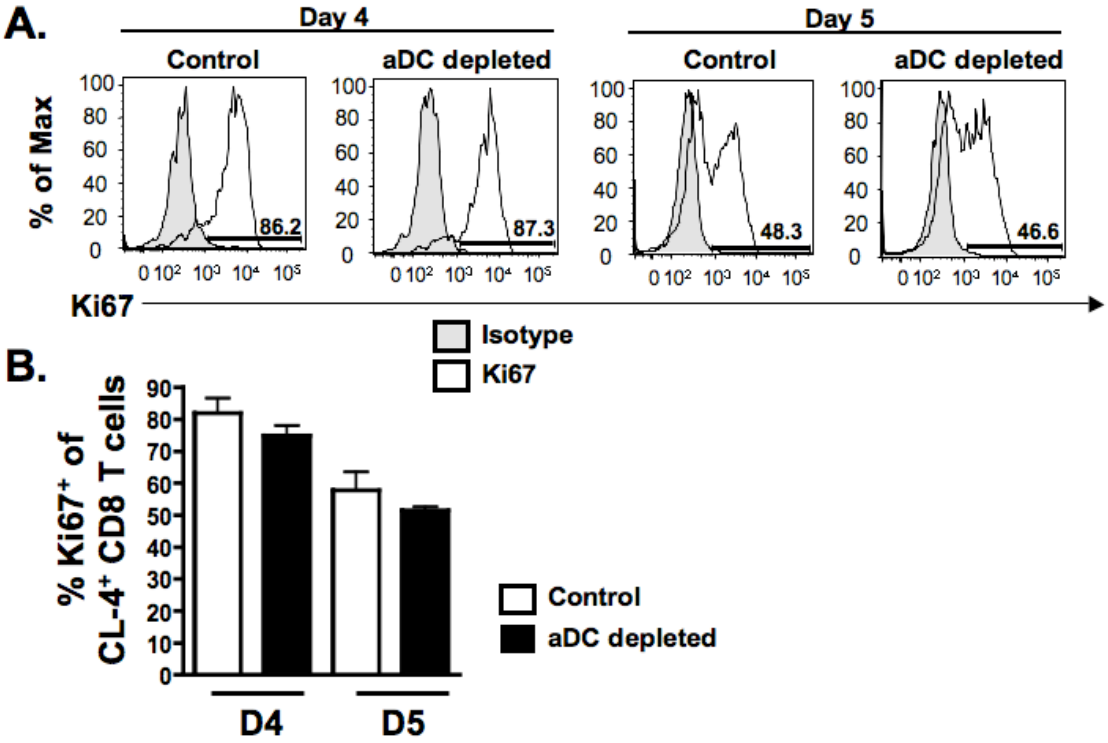
A.
Day 4
Day 5
Control
aDC depleted
Control
aDC depleted
% of Max
86.2
87.3
48.3
46.6
Ki67
Isotype
Ki67
B.
% Ki67+ of CL-4+ CD8 T cells
Control
aDC depleted
D4
D5

Figure 14. aDC depletion at 48 hours p.i. results in increased apoptosis by virus-specific CD8 T cells. Influenza-specific, $CD90.2^+$ CL-4 T cells were adoptively transferred into groups of $CD90.1^+$ BALB/c mice. 24 hours later, mice were infected with a sublethal dose of IAV +/- aDC depletion. On days 4 and 5 p.i., mice were sacrificed and apoptosis, as measured by the presence of active caspase 3/7, in $CD90.2^+$ CL-4 T cells was measured by flow cytometry. (A) Shown are representative FACS plots from day 4 and 5 p.i. gated on $CD3^+CD8^+$ T cells. Data in A and B are representative of 3 separate experiments with n=3-4 mice/group. Shown are means ± SEM.

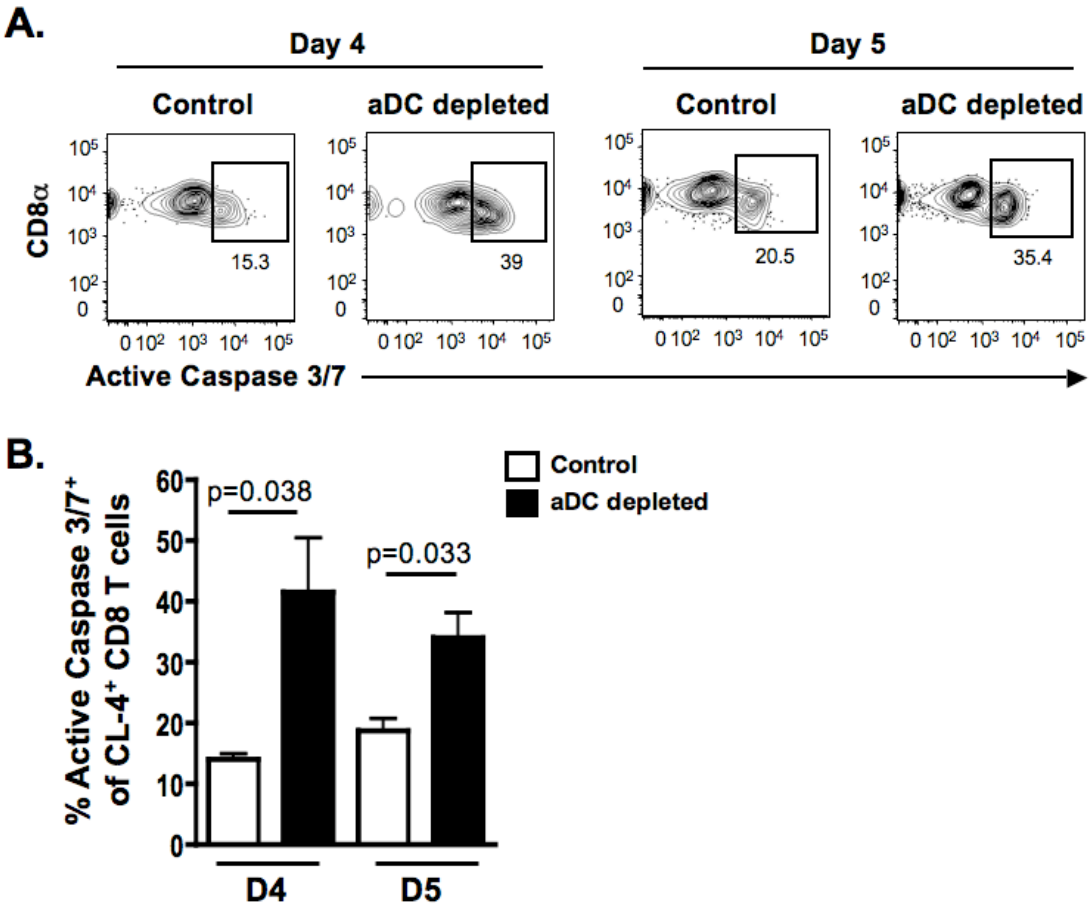
A.
Day 4
Day 5
Control
aDC depleted
Control
aDC depleted
CD8α
15.3
39
20.5
35.4
Active Caspase 3/7
B.
Control
aDC depleted
% Active Caspase 3/7+ of CL-4+ CD8 T cells
p=0.038
p=0.033
D4
D5

Figure 15. aDC depletion at 48 hours p.i. results in decreased levels of Bcl-2 expression by IAV-specific CD8 T cells. (A) Mice were infected with a sublethal dose of IAV +/- aDC depletion at 48 hours p.i.. Mice were sacrificed on days 4 and 5 p.i. and their lungs examined by flow cytometry for $CD3^+CD8^+Tetramer^+$ CD8 T cell expression of Bcl-2 as measured by Mean Fluorescence intensity (MFI). MFI was calculated by subtracting the MFI of the isotype from that of the stained samples. Data are pooled from 2 independent experiments and represent means±SEM. n=4-6 mice/group (B) Influenza-specific, $CD90.2^+$ CL-4 T cells were adoptively transferred into groups of $CD90.1^+$ BALB/c mice as in Figure 11C. 24 hours later, mice were infected with a sublethal dose of IAV +/- aDC depletion at 48 hours p.i.. On days 4 and 5 p.i., mice were sacrificed and analyzed for pulmonary $CD3^+CD8^+CD90.2^+$ CD8 T cell expression of Bcl-2 as measured by Mean Fluorescence intensity (MFI). MFI was calculated by subtracting the MFI of the isotype from that of the stained samples. Data are pooled from 3 independent experiments and represent means± SEM. n=8-9 mice/group

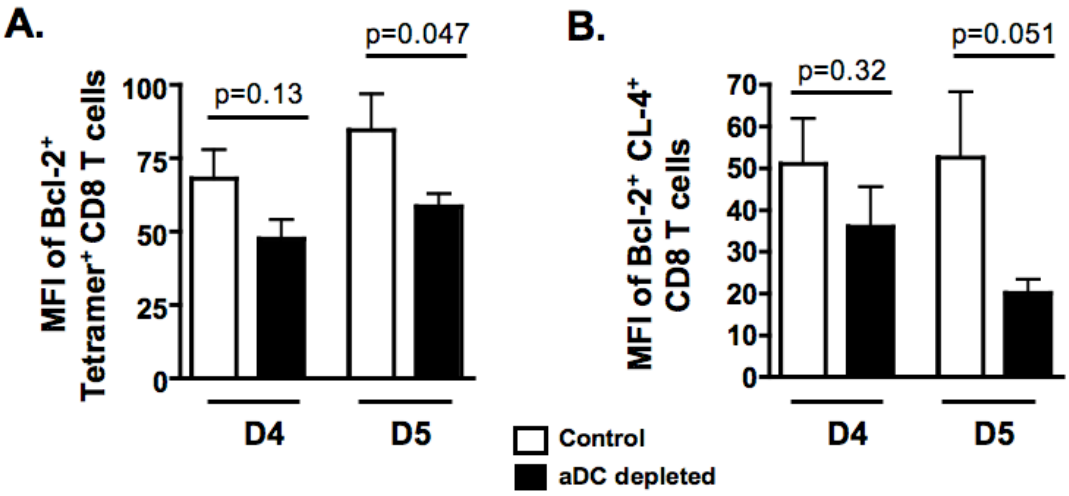
A.
MFI of Bcl-2+ Tetramer+ CD8 T cells
100
75
50
25
0
p=0.13
p=0.047
D4
D5
B.
MFI of Bcl-2+ CL-4+ CD8 T cells
70
60
50
40
30
20
10
0
p=0.32
p=0.051
D4
D5
Control
aDC depleted

Figure 16. aDC depletion at 48 hours p.i. results in decreased levels of Bcl-2 expression in IAV-specific CD8 T cells in the lungs. IAV-specific, CD90.2^{+} CL-4 T cells were adoptively transferred to groups of CD90.1^{+} BALB/c mice as in Figure 11C. 24 hours later, mice were infected with a sublethal dose of IAV +/- aDC depletion at 48 hours p.i.. On day 5 p.i., whole cell lysates were prepared from 6x10^{5} transgenic CL-4^{+} CD8 T cells that were isolated from the lungs of control and aDC depleted mice and resolved on a 4-20% Tris-HCl gradient gel. Cell lysates were then probed by western blot for Bcl-2 expression (26 kD) and GAPDH expression (40 kD) as a loading control. (B) Densitometric analysis was performed on the western blots shown in A. Control samples were normalized to 1 and data are expressed as a ratio of Bcl-2:GAPDH. Data are representative of 3 independent experiments.

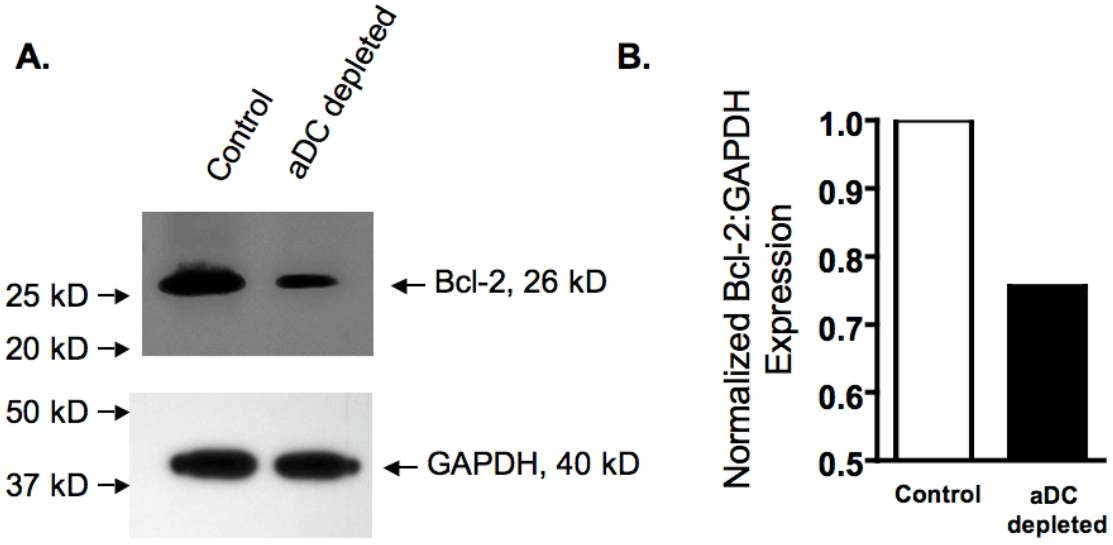
A.
Control
aDC depleted
25 kD
20 kD
Bcl-2, 26 kD
50 kD
37 kD
GAPDH, 40 kD
B.
Normalized Bcl-2:GAPDH Expression
1.0
0.9
0.8
0.7
0.6
0.5
Control
aDC depleted

Figure 17. aDC depletion at 48 hours p.i. results in decreased levels of Bcl-X_L expression by IAV-specific CD8 T cells in the lungs. Cell lysates were prepared from $4x10^5$ CL-4 T cells that were isolated from the lungs of control and aDC depleted mice as in Figure 16 and resolved on a 12% Tris-HCl gel. Cell lysates were then probed by western blot for Bcl-X_L expression (29 kD) and GAPDH expression (40 kD) as a loading control. (B) Densitometric analysis was performed on the western blots shown in A. Control samples were normalized to 1 and data are expressed as a ratio of Bcl-X_L:GAPDH. Data are representative of 2 independent experiments.

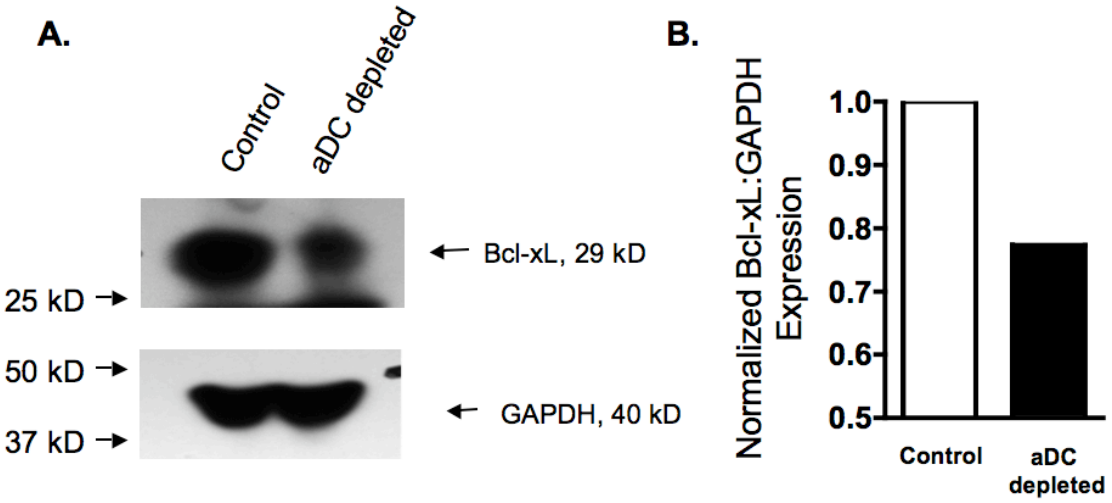
A.
Control
aDC depleted
Bcl-xL, 29 kD
25 kD
50 kD
37 kD
GAPDH, 40 kD
B.
Normalized Bcl-xL:GAPDH Expression
1.0
0.9
0.8
0.7
0.6
0.5
Control
aDC depleted

Figure 18. aDC depletion at 48 hours p.i. results in an altered ratio of Bim:Bcl-2 expression by IAV-specific CD8 T cells in the lungs. On day 5 p.i., whole cell lysates were prepared from $5x10^5$ transgenic CL-4^+ CD8 T cells from control and aDC depleted lungs as in Figure 16 and resolved on a 4-20% Tris-HCl gradient gel. Cell lysates were then probed by western blot for Bcl-2 expression (26 kD), Bim expression (23 kD) and GAPDH expression (40 kD) as a loading control. (B) Densitometric analysis was performed on the western blots shown in A. Data are normalized to GAPDH and expressed as a ratio of Bim:Bcl-2 expression. Data are representative of 2 independent experiments.

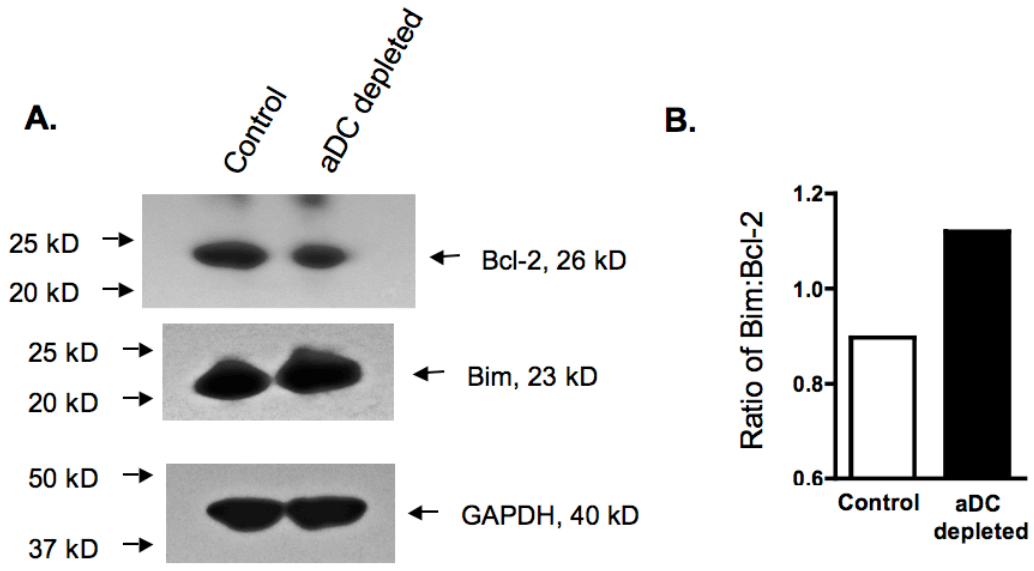
A.
Control
aDC depleted
25 kD
20 kD
Bcl-2, 26 kD
25 kD
20 kD
Bim, 23 kD
50 kD
37 kD
GAPDH, 40 kD
B.
Ratio of Bim:Bcl-2
1.2
1.0
0.8
0.6
Control
aDC depleted

Figure 19. aDC depletion at 48 hours p.i. results in increased levels of active caspase 9 in virus-specific CD8 T cells in the lungs. (A) CL-4 T cell lysates ($6x10^5$) were prepared from control and aDC depleted lungs as in Figure 16, resolved on a 4-20% Tris-HCl gradient gel and probed by western blot for the presence of full-length caspase 9 (49 kD) and active, cleaved caspase 9 (35, 37 kD), as well as for GAPDH (40 kD) as a loading control. (B) Densitometric analysis was performed on the western blot shown in A. Data are expressed as a ratio of Full:Cleaved caspase 9. Data are representative of 2 independent experiments.

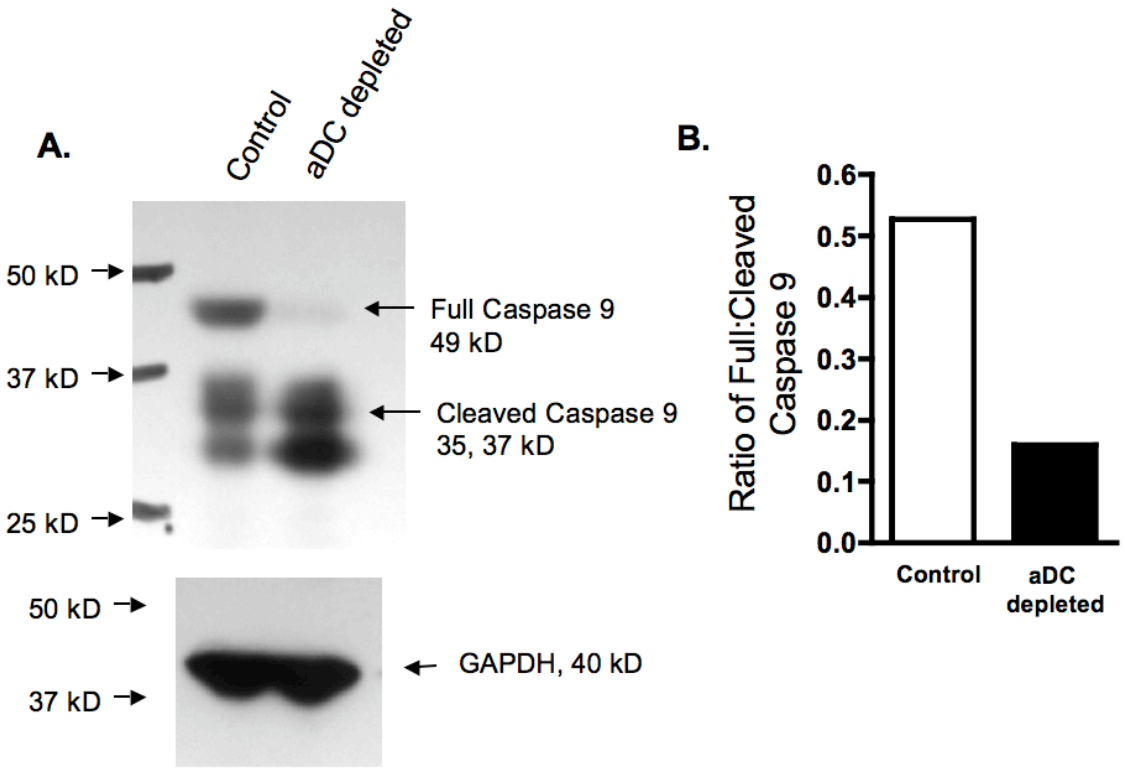
A.
Control
aDC depleted
50 kD
37 kD
25 kD
Full Caspase 9
49 kD
Cleaved Caspase 9
35, 37 kD
50 kD
37 kD
GAPDH, 40 kD
B.
Ratio of Full:Cleaved Caspase 9
0.6
0.5
0.4
0.3
0.2
0.1
0.0
Control
aDC depleted

Figure 20. aDC depletion at 48 hours p.i. results in increased levels of active caspase 8, but not tBID, in IAV-specific CD8 T cells in the lungs. (A and C) Control and aDC depleted CL-4 T cell lysates (A: $4x10^5$, B: $6x10^5$) were prepared as in Figure 16. Cell lysates were then probed by western blot for the presence of (A) active, cleaved caspase 8 (18 kD), or (C) the presence of full-length BID (21 kD) and active tBID (15 kD), as well as for GAPDH (40 kD) as a loading control. Samples in A were resolved on a 12% Tris-HCl gel; samples in B were resolved on a 4-20% Tris-HCl gradient gel. Data in A are representative of 2 independent experiments. Data in B are representative of 3 independent experiments. (B) Densitometric analysis was performed on the western blots shown in A. Control samples were normalized to 1 and data are expressed as a ratio of active caspase 8:GAPDH. (D) BALB/c mice were infected with a sublethal dose of IAV. On day 6 p.i., mice were sacrificed and $5x10^6$ whole splenocytes cultured for 8 hours in the presence of 2 μg/mL of soluble anti-Fas (Jo-2) (lane 1), 2 μg/mL plate-bound anti-Fas (Jo-2) (lane 2) or in the presence of 500 ng/mL recombinant caspase 8. Splenocytes were then washed and whole cell lysates were prepared as described in the Materials and Methods. Lysates were then resolved on a 4-20% Tris-HCl gradient gel and probed for the presence of full length BID (21 kD) and active, tBID (15 kD). Data are representative of 1 experiment.

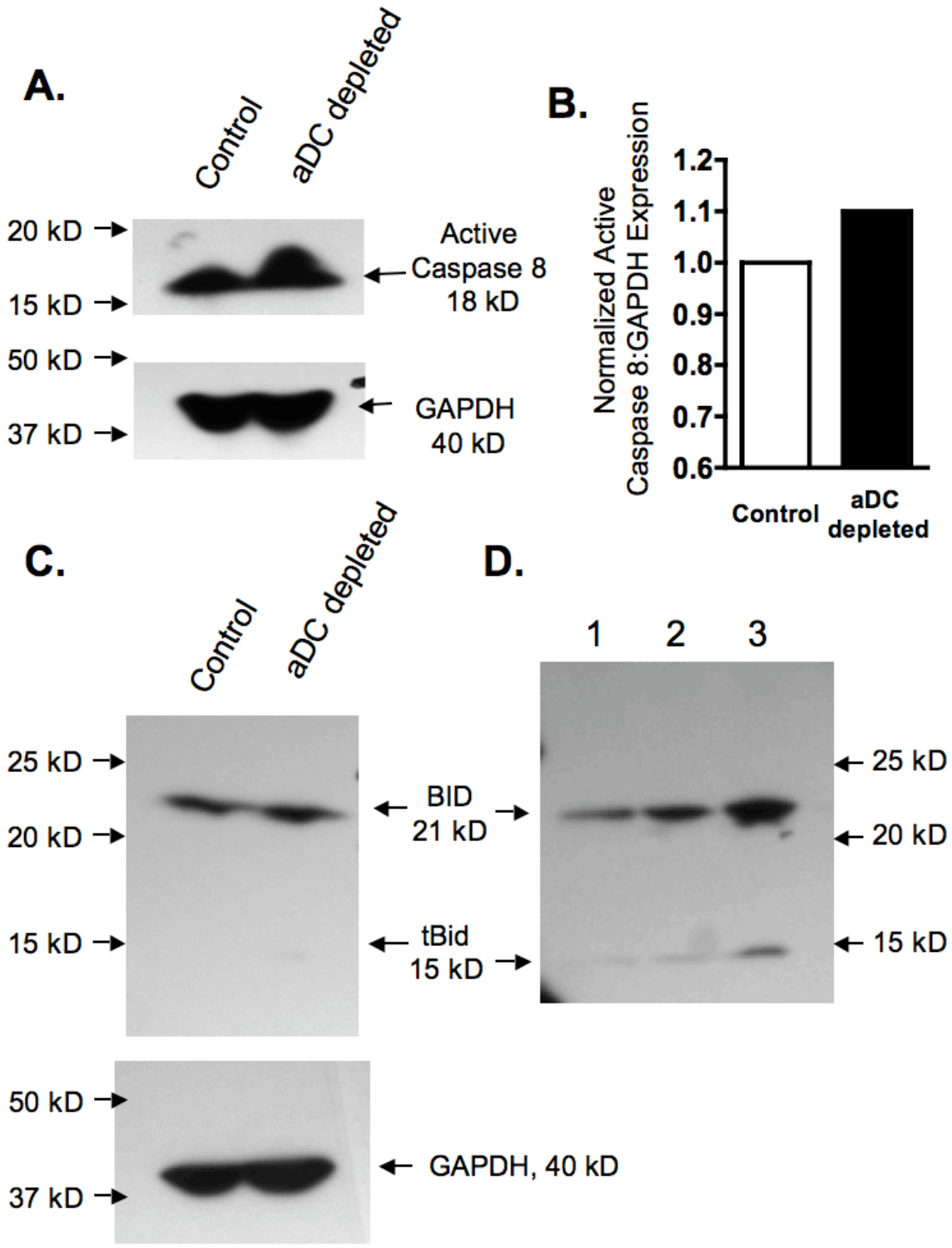
A.
Control
aDC depleted
20 kD
15 kD
Active
Caspase 8
18 kD
50 kD
37 kD
GAPDH
40 kD
B.
Normalized Active
Caspase 8:GAPDH Expression
1.2
1.1
1.0
0.9
0.8
0.7
0.6
Control
aDC
depleted
C.
Control
aDC depleted
25 kD
20 kD
15 kD
BID
21 kD
tBid
15 kD
50 kD
37 kD
GAPDH, 40 kD
D.
1
2
3
25 kD
20 kD
15 kD

Figure 21. Summary of Chapter III analyses: IAV-specific CD8 T cells from aDC depleted mice undergo apoptosis via both ACAD- and AICD-mediated mechanisms. (A) Virus-specific CD8 T cells from aDC depleted mice express increased levels of active caspase 8 compared to non-depleted control T cells, suggesting that they are receiving signals via a death receptor such as CD95L (FasL). However, aDC depleted CD8 T cells do not express detectable levels of tBID, suggesting that they are primarily utilizing the extrinsic type I cell death pathway, as opposed to the type II cell death pathway which depends upon the cleavage of BID and activation of the mitochondrial pathway. (B) aDC depleted CD8 T cells express increased levels of Bim and reduced levels of Bcl-2 and Bcl-X_L, as well as increased levels of active caspase 9, suggesting that they are also undergoing apoptosis via intrinsic ACAD. Together, the results from Chapter III suggest that virus-specific CD8 T cells from aDC depleted mice are utilizing multiple cell death pathways and likely undergoing apoptosis as a result of both AICD (A) and ACAD (B). Figure 21 was adapted from a figure created by R.A. Langlois.

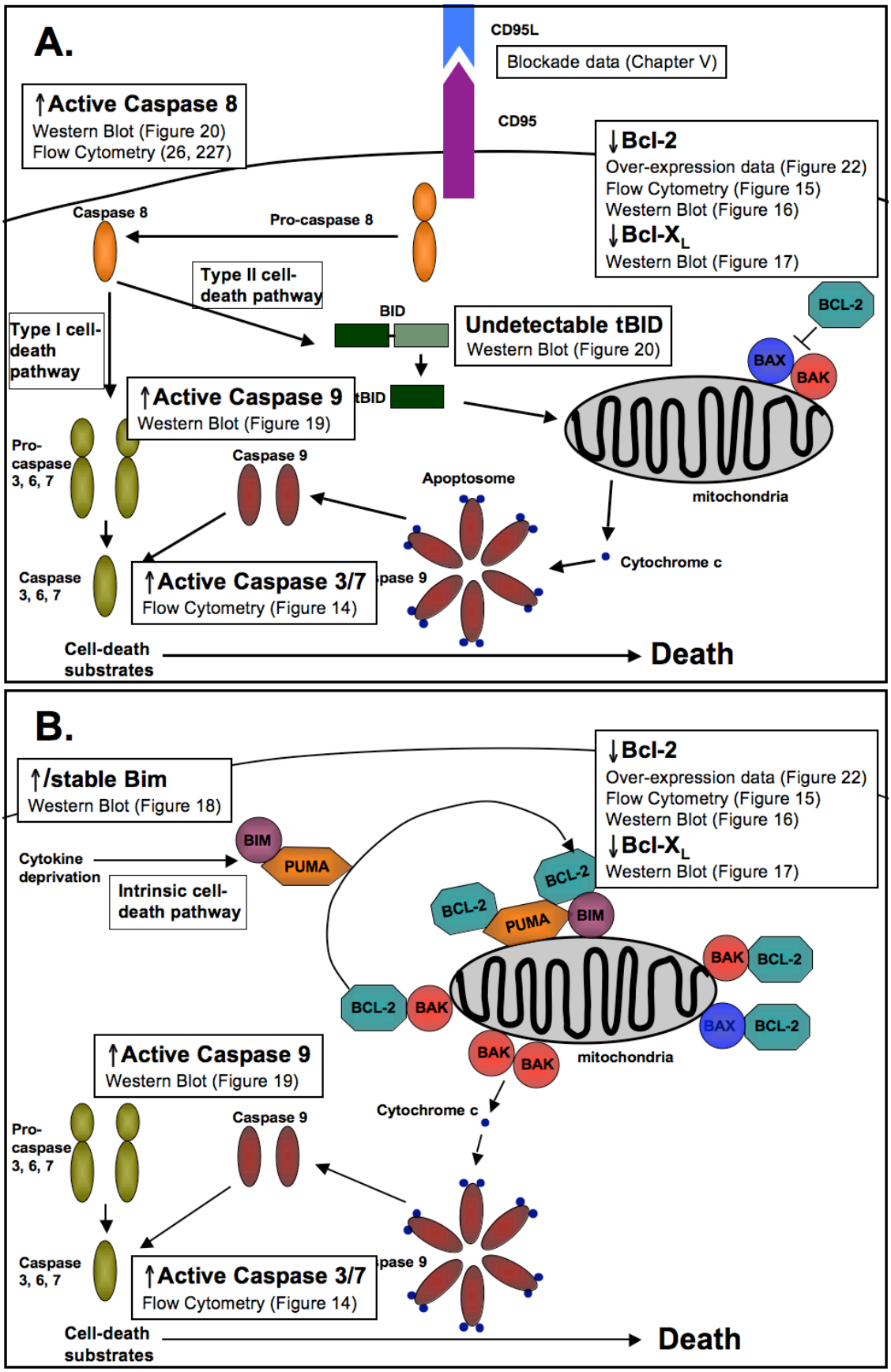
A.
CD95L
Blockade data (Chapter V)
↑Active Caspase 8
Western Blot (Figure 20)
Flow Cytometry (26, 227)
CD95
↓Bcl-2
Over-expression data (Figure 22)
Flow Cytometry (Figure 15)
Western Blot (Figure 16)
↓Bcl-XL
Western Blot (Figure 17)
Caspase 8
Pro-caspase 8
Type II cell-death pathway
Type I cell-death pathway
BID
Undetectable tBID
Western Blot (Figure 20)
BCL-2
BAX
BAK
↑Active Caspase 9
Western Blot (Figure 19)
tBID
Pro-caspase 3, 6, 7
Caspase 9
Apoptosome
mitochondria
Caspase 3, 6, 7
↑Active Caspase 3/7
Flow Cytometry (Figure 14)
pase 9
Cytochrome c
Cell-death substrates
Death
B.
↑/stable Bim
Western Blot (Figure 18)
↓Bcl-2
Over-expression data (Figure 22)
Flow Cytometry (Figure 15)
Western Blot (Figure 16)
↓Bcl-XL
Western Blot (Figure 17)
BIM
PUMA
Cytokine deprivation
Intrinsic cell-death pathway
BCL-2
BAK
BAX
mitochondria
↑Active Caspase 9
Western Blot (Figure 19)
Cytochrome c
Pro-caspase 3, 6, 7
Caspase 9
Caspase 3, 6, 7
↑Active Caspase 3/7
Flow Cytometry (Figure 14)
pase 9
Cell-death substrates
Death

Figure 22. Transgenic over-expression of Bcl-2 is sufficient to rescue virus-specific CD8 T cells from apoptosis in the lungs of aDC depleted mice. 10^7 CD8 T cells were isolated from the spleens of CD45.2$^+$ C57BL/6 VavP-Bcl-2 transgenic mice and adoptively transferred i.v. to naïve, congenic CD45.1$^+$ C57BL/6 host mice. 24 hours later, mice were infected with a sublethal dose of IAV and half were aDC depleted at 48 hours p.i. On day 7 p.i., the mice were sacrificed and their lungs analyzed by flow cytometry for total numbers of endogenous CD45.1$^+$CD3$^+$CD8$^+$tetramer$^+$ virus-specific CD8 T cells (A) and adoptively transferred, Bcl-2 transgenic CD45.2$^+$CD3$^+$CD8$^+$tetramer$^+$ virus-specific CD8 T cells (B). Data are pooled from 3 independent experiments and represent means±SEM. n=8-12 mice/group

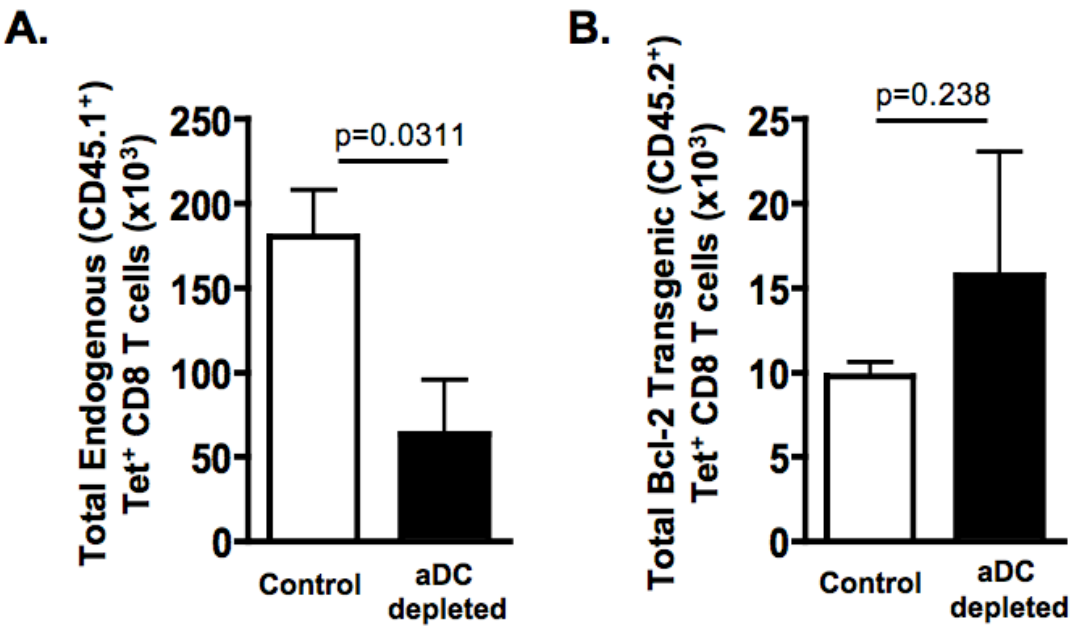
A.
Total Endogenous (CD45.1+) Tet+ CD8 T cells (x10³)
250
200
150
100
50
0
p=0.0311
Control
aDC depleted
B.
Total Bcl-2 Transgenic (CD45.2+) Tet+ CD8 T cells (x10³)
25
20
15
10
5
0
p=0.238
Control
aDC depleted

CHAPTER IV THE ROLE OF IL-15 TRANS-PRESENTATION BY PULMONARY DENDRITIC CELLS IN THE LUNGS FOLLOWING INFLUENZA VIRUS INFECTION

Introduction

As demonstrated in Chapter III, in the absence of pulmonary pDC or CD8α^+ DC, virus-specific CD8 T cells undergo increased levels of apoptosis via both ACAD and AICD mediated pathways. AICD is often induced when T cells encounter MHC I and viral antigen in the absence of appropriate costimulatory molecules, while ACAD is often induced in the absence of key survival factors, including cytokines (20, 136, 137). Given that both types of T cell apoptosis were occurring in the lungs of aDC depleted mice, we next sought to explore the functional role for each pathway and determine the additional mechanisms by which pulmonary DC reconstitution acts to rescue CD8 T cell numbers and apoptosis. To this end, Chapter IV will explore the role of DC-presented cytokine survival signals, specifically IL-15, in rescuing virus-specific CD8 T cell apoptosis in the lungs of aDC depleted mice. Chapter V will explore the role of excess antigen presentation that occurs in the absence of pulmonary DC subsets and how this contributes to AICD mediated T cell apoptosis.

IL-15 has been best characterized for its role in maintaining memory CD8 T cell homeostasis, primarily through promoting enhanced basal proliferation (170-172). More recently, however, there is accumulating evidence that IL-15 is also important for promoting primary effector CD8 T cell responses (151, 152, 170, 173-175). Surface expression of both IL-15Rα and IL-2/IL15Rβ is upregulated following TCR activation (174) and IL-15 has been proposed to enhance activated CD8 T cell survival following challenge with staphylococcal enterotoxin A (174), *Mycobacterium tuberculosis* (173) and VSV infection (155). Together, the above studies suggest a particularly important

role for IL-15 in the generation and maintenance of an appropriate immune response; however, it remains unclear what role IL-15 plays during the effector phase of the immune response or in what context IL-15 contributes to activated CD8 T cell survival *in vivo*.

Here, we demonstrate a previously unrecognized role for pulmonary DC-mediated IL-15 trans-presentation in regulating virus-specific CD8 T cell responses in the lungs following IAV infection. IAV infection induces upregulation of both IL-15 mRNA and protein in the lungs, while depletion of aDC at 48 hours p.i. results in a significant reduction in pulmonary IL-15 expression. We demonstrated in Chapter III that pulmonary DC reconstitution prevents virus-specific CD8 T cell apoptosis. Here, we show that this rescue requires DC mediated trans-presentation of IL-15, as blockade of IL-15 or IL-15Rα on the surface of pulmonary DC prior to adoptive transfer, or transfer of IL-15$^{-/-}$ pulmonary DC subsets ablates the rescue of the virus-specific CD8 T cell response in the lungs of aDC depleted mice.

Materials and Methods

Mice

6-12 week old female BALB/c mice and 6-12 week old male and female C57BL/6 mice were purchased from the National Cancer Institute (Frederick, MD). C57BL/6 IL-15$^{-/-}$ (C57BL/6NTac-*IL15*^{tm1Imx}) mice were purchased from Taconic Farms, Inc (Hudson, NY). CL-4 TCR transgenic mice (H-2^{d}, CD90.1^{+}) were purchased from The Jackson Laboratory (Bar Harbor, ME), and CL-4 TCR transgenic mice (H-2^{d}; CD90.2^{+}) were a kind gift from Dr. Linda Sherman (Scripps Research Institute). Both CL-4 transgenic strains are specific to the $HA_{533-541}$/$HA_{529-537}$ epitope of H1 and H2 Influenza A viruses, respectively. BALB/c CD90.1^{+} congenic mice were a kind gift of Dr. Richard Enelow (Dartmouth College) and Dr. John Harty (University of Iowa). All mice were housed, bred and maintained in the animal care facility at the University of Iowa.

Experiments were conducted according to federal and institutional guidelines and were approved by the University of Iowa Animal Care and Use Committee.

Virus infection

Mouse-adapted influenza A viruses A/PuertoRico/8/34 and A/JAPAN/305/57 were grown in the allantoic fluid of 10-day old embryonated chicken eggs for 2 days at 37°C, as previously described (76). Allantoic fluid was harvested and stored at -80°C. BALB/c and C57BL/6 mice were anesthetized with isofluorane and infected i.n. with either 5875 TCIU or 587 TCIU of mouse-adapted A/JAPAN/305/57 or 1066 TCIU of A/PR/8/34, respectively, in 50 μl of Iscove's media as previously described (76).

Clodronate-liposome treatment

Pulmonary DC and macrophage depletion was performed by treatment with liposomes containing dichloromethylene bisphosphonate (Clodronate) (53). Clodronate was a gift of Roche Diagnostics GmbH, Mannheim, Germany. It was encapsulated in liposomes as described previously (238). Phosphatidylcholine (LIPOID E PC) was obtained from Lipoid GmbH, Ludwigshafen,Germany. Cholesterol is purchased from SIGMA Chem.Co. USA. At 48 hours p.i., mice were anesthetized by isofluorane inhalation and administered 75 μl of Clodronate-liposomes or PBS-liposomes i.n.

Peptides

Influenza virus peptides $HA_{204-212}$ (LYQNVGTYV), $HA_{529-537}$ (IYATVAGSL), and $NP_{147-155}$ (TYQRTRALV) for BALB/c and PA_{224} (SSLENFRAYV) and NP_{366}(ASNENMETM) for C57BL/6 were synthesized by BioSynthesis Incorporated (Lewisville, TX).

MHC I tetramers

Tetramers HA_{204} (H-2K(d)/LYQNVGTYV), HA_{529} (H-2K(d)/IYATVAGSL), and NP_{147} (H2K(d)/TYQRTRALV) for BALB/c, and PA_{224} (H2D(b)/SSLENFRAYV) and

NP_{366}(H2D(b)/ASNENMETM) for C57BL/6 were obtained from National Institute of Allergy and Infectious Disease MHC Tetramer Core Facility (Atlanta, GA).

Preparation of cells

Lungs were pressed through wire mesh to obtain a single cell suspension, which was then enumerated by trypan blue exclusion. For DC preparations, lungs were digested for 25 minutes at 25° C in media containing 1 mg/ml Collagenase (Sigma) and 0.02 mg/ml DNase (Sigma) before single cell preparation. Dendritic cells for reconstitution experiments were purified from the lungs of day 6 A/JAPAN/305/57 or A/PR/8/34 infected BALB/c or IL-$15^{+/+}$ and IL-$15^{-/-}$ C57BL/6 donors respectively using MACS technology (Miltenyi Biotech) according to manufacturer's instructions or by fluorescence activated cell sorting (FACS) as has been previously described (53). Purified cells were resuspended in Iscove's DMEM and $2.5x10^4$ cells in 50 ul were adoptively transferred i.n. to host mice on day 3 p.i. (53).

Purification and adoptive transfer of CL-4 T cells

Single cell suspension of splenic cells from CL-4 mice were labeled with CD8α Microbeads (MB) and purified according to manufacturers instructions (Miltenyi Biotec). Purified $CD90.2^+$ CL-4 cells were then adoptively transferred ($5x10^5$) i.v. into BALB/c $CD90.1^+$ congenic mice, or purified $CD90.1^+$ CL-4 cells were adoptively transferred ($5x10^5$) i.v. into BALB/c $CD90.2^+$ mice. 24 hrs later the host mice were infected with influenza as described above.

Antibodies and reagents

The following reagents were used for these studies: rat anti-mouse CD3ε (145-2C11), rat anti-mouse CD8α (53-6.7), rat anti-mouse IFNγ (XMG1.2), rat anti-mouse IA/IE (M5/114.15.2), rat anti-mouse CD11b (M1/70), mouse anti-rat CD90.1 (OX-7), hamster anti-mouse CD11c (HL3) purchased from Becton Dickinson; mouse anti-mouse

CD90.2 (5a-8), rat anti-mouse CD45R (RA3-6B2) purchased from Caltag; polyclonal goat anti-mouse IL-15Rα and polyclonal goat anti-mouse IL-15 were purchased from R&D Systems. Vybrant FAM caspase 3/7 kits were purchased from Invitrogen and used according to manufacturer's instructions. For surface staining, isolated cells (10^6) cells were stained with antibody or tetramer for 30 minutes at 4° C and then fixed using BD FACS Lysing Solution (BD Biosciences). For intracellular cytokine staining, fixed cells were permeabilized and labeled with antibodies in FACS buffer containing 0.5% Saponin (Acros Organics, NJ) for 1 hour at 4° C. All flow cytometry data were acquired on a BD FACS Calibur or BD FACS Canto II (BD Immunocytometry Systems) and analyzed using FlowJo software (TreeStar, Ashland, OR).

IL-15 ELISA

The IL-15 ELISA Duo kit was purchased from R&D Systems. Control and aDC depleted lungs were harvested on day 6 p.i., homogenized in 0.5 mL ELISA diluent (1% BSA in PBS) plus Complete Mini *EASYpack* Protease Inhibitor Cocktail Tablets (Roche) and plated in 100 ul aliquots. ELISA plates were incubated overnight at 4° C. ELISAs were then read according to manufacturer's instructions.

Quantitative real-time RT-PCR analysis for IL-15 mRNA expression

Total RNA was isolated from whole lung homogenates or from FACS-purified pulmonary DC subsets using TRIzol according to manufacturer's instructions (Invitrogen). cDNA was transcribed from 1 ug RNA using 1 uM 18-mer Oligo dT primer and 1 U/ul AMV reverse transcriptase (Promega) in the presence of 1 U/ul RNase OUT (Invitrogen), 10 mM dNTP, 25 mM MgCl and 10x ThermoStart PCR reaction buffer (ThermoScientific) at 42° C for 60 min in a 20 ul reaction volume. The qRT-PCR was performed using the ABI-prism 7000 Sequence Detector Apparatus (Perkin Elmer/Applied Biosystems, Foster City, CA, USA) for 40 cycles in a two-temperature

profile: a denaturation period of 15 s at 94°C followed by a 1 min annealing/extension period at 60°C. All PCR reactions were carried out in 25 μl final volumes comprising the following components: 100 ng cDNA, TaqMan Universal PCR Master Mix, 450 nM primers and 125 nM probes. The following primers and probes were utilized (270, 271):

IL-15 Forward: CAT CCA TCT CGT GCT ACT TGT GTT

IL-15 Reverse: CAT CTA TCC AGT TGG CCT CTG TTT

IL-15 Probe: FAM-AGG GAG ACC TAC ACT GAC ACA GCC CAA AA-BHQ

GAPDH Forward: TTC ACC ACC ATG GAG AAG GC

GAPDH Reverse: GGC ATG GAC TGT GGT CAT GA

GAPDH Probe: FAM - TGC ATC CTG CAC CAC CAA CTG CTT AG - BHQ

Comparisons were made by the comparative threshold cycle (Ct) method, with GAPDH serving as the comparator. For whole lung homogenates, data are presented as fold change relative to naïve lung samples, which are set to a value of 1.

IL-15Rα/Fc treatment

Recombinant mouse IL-15Rα/Fc chimera was purchased from R&D Systems and control human Fc fragments were purchased from Jackson Laboratories. Mice were anesthetized using isofluorane and administered 5 μg of IL-15Rα-Fc or control-Fc i.n. on days 3, 4 and 5 p.i..

Statistical analysis

Statistical significance of the difference between two sets of data was assessed using an unpaired, one-tailed *t*-test or a paired *t*-test for control and experimental data groups that could be paired. Differences were considered to be statistically significant at $p<0.05$.

Results

Pulmonary DC reconstitution promotes increased lung-resident, virus-specific CD8 T cell survival following aDC depletion

We have demonstrated in Chapter III that aDC depletion at 48 hours p.i. induces increased apoptosis of virus-specific CD8 T cells via a mechanism involving both AICD and ACAD mediated apoptosis. It remained unclear, however, what mechanism pulmonary DC subsets were using in the lungs to promote rescue of virus-specific CD8 T cell responses. Therefore, we next determined if pulmonary DC reconstitution 24 hours after aDC depletion was resulting in increased accumulation of CD8 T cells in the lungs by promoting their increased survival therein. To this end, groups of mice were IAV infected +/- aDC depletion. 24 hours post-DC depletion, mice were reconstituted i.n. with purified pulmonary pDC or CD8α^+ DC as in Figure 5. On day 5 p.i., the lungs were then assessed for frequencies (Figure 23A) and total numbers of tetramer$^+$ CD8 T cells (Figure 23C), as well as the frequency of tetramer$^+$ CD8 T cell apoptosis as measured by active caspase 3/7 expression (Figure 23B and 23D). Similar to our previous results, we observed a rescue in the frequency and number of pulmonary tetramer$^+$ CD8 T cells following reconstitution with purified pDC or CD8α^+ DC relative to non-reconstituted aDC depleted control mice (Figure 23A and 23C). Consistent with the rescue of pulmonary IAV-specific CD8 T cell numbers, we also observed a significant reduction in the frequency of apoptotic CD8 T cells in the lungs on day 5 p.i. following reconstitution with either pDC or CD8α^+ DC (Figure 23B and 23D), with levels of CD8 T cell apoptosis being similar to that of non-depleted control CD8 T cells. A similar trend was also seen when examining the frequency of active caspase 8$^+$ T cells (226). Together, these results suggest that virus-specific CD8 T cell interactions with pulmonary pDC and

CD8α^+ DC provides key survival signals, allowing T cells to accumulate to high numbers in the lungs following IAV infection.

To further confirm our hypothesis that pulmonary pDC and CD8α^+ DC were providing survival signals to CD8 T cells in the lungs of aDC depleted mice and thus promoting their accumulation therein, we next chose to examine levels of the pro-survival molecule Bcl-2 and determine if pulmonary DC reconstitution resulted in its upregulation by virus-specific CD8 T cells in the lungs. To this end, groups of mice were IAV infected +/- aDC depletion. 24 hours post-DC depletion, mice were reconstituted i.n. with purified pulmonary pDC or CD8α^+ DC as in Figure 5. On day 5 p.i., the lungs were then analyzed by flow cytometry for virus-specific CD8 T cell expression of Bcl-2 as measured by MFI. As expected, aDC depletion at 48 hours p.i. results in a significant reduction in the levels of Bcl-2 expressed by virus-specific CD8 T cells in the lungs compared to non-depleted controls (Figure 24). However, reconstitution of aDC depleted lungs with purified pulmonary pDC or CD8α^+ DC resulted in an upregulation of Bcl-2 expression by antigen-specific CD8 T cells within the lungs to levels similar to that of their non-depleted counterparts. These results further support the hypothesis that virus-specific CD8 T cells are acquiring key survival signals from pulmonary DC subsets present in the lungs following IAV infection, and that these signals promote upregulation of anti-apoptotic molecules such as Bcl-2, thus supporting CD8 T cell accumulation therein.

aDC depletion at 48 hours p.i. results in decreased pulmonary IL-15 expression

Given our results suggesting that virus-specific CD8 T cells were undergoing apoptosis as a result of ACAD or neglect, and that donor pulmonary DC were positively regulating virus-specific CD8 T cell responses in the lungs of aDC depleted mice through the promotion of increased CD8 T cell survival (Figure 23) and upregulation of Bcl-2

(Figure 24), we next sought to identify what additional survival signal(s) the pDC and CD8α^+ DC were providing. Therefore, we performed focused microarray analysis on whole lung homogenates from day 6 infected control and aDC depleted lungs as well as on purified pulmonary DC subsets. As seen in Table 1, aDC depletion at 48 hours p.i. results in several changes in gene expression in the lungs. Interestingly, one of the changes we observed was decreased expression of IL-15 mRNA in aDC depleted lungs. Further, IL-15 mRNA expression was more robustly expressed by pDC and CD8α^+ DC (data not shown), the two DC subsets reduced in the lungs of aDC depleted mice and known to restore pulmonary CD8 T cell responses upon reconstitution (53). Similar to our initial array results, quantitative real-time PCR analysis for IL-15 expression by naïve, day 6 p.i. control IAV infected and day 6 p.i. aDC depleted lung homogenates showed that IAV infection induces an ~5-fold increase in pulmonary IL-15 mRNA expression relative to naïve control lungs (Figure 25A). Strikingly, however, aDC depletion at 48 hours p.i. resulted in a significant reduction in IL-15 mRNA expression, with expression levels reduced to approximately 2-fold gene induction over naïve (Figure 25A). This change in mRNA expression was reflected at the protein level, as we observed a significant reduction in IL-15 protein expression by aDC depleted lungs relative to non-depleted controls (Figure 25B). Together, these results demonstrated that aDC depletion at 48 hours p.i. results in a reduction in the expression of IL-15 message and protein in the lungs during IAV infection.

Pulmonary pDC and CD8α^+ DC express IL-15 mRNA and surface IL-15Rα

Given the previously described role for IL-15 in promoting effector CD8 T cell responses (151, 152, 170, 173-175), its potential ability to promote CD8 T cell survival (151, 152, 173-175), and the ability of the purified pulmonary DC subsets that express robust levels of IL-15 mRNA to rescue IAV-specific CD8 T cells from apoptosis in the

lungs following aDC depletion, we next determined if these subsets were indeed capable of making and presenting IL-15 to IAV-specific CD8 T cells in the lungs. We first confirmed the results of our arrays by performing qRT-PCR for IL-15 mRNA expression on DC subsets purified from the lungs of day 6 p.i. donors. As seen in Figure 26A, both pDC and CD8α^+ DC express high levels of IL-15 mRNA. In contrast, aMϕ, another prevalent APC population in the lungs during IAV infection that is incapable of rescuing IAV-specific CD8 T cell responses, expressed lower levels of IL-15 mRNA (~60% of pDC/ CD8α^+ DC).

Since the ability to trans-present IL-15 to other cells requires surface expression of IL-15Rα, we next verified that both pDC and CD8α^+ DC expressed detectable levels of the receptor. As seen in Figure 26B, pDC, CD8α^+ DC and aMϕ all expressed IL-15Rα on their surface, suggesting they could potentially trans-present IL-15 to other cell types.

IL-15 presented on the surface of pulmonary DC subsets promotes increased accumulation of IAV-specific CD8 T cells in the lungs of aDC depleted mice

Having demonstrated that pDC and CD8α^+ DC have the potential to trans-present IL-15 to other cell types, that aDC depleted lungs express reduced levels IL-15 protein and that reconstitution with pDC or CD8α^+ DC is able to rescue CD8 T cell responses in the lungs of aDC depleted mice, we next directly determined the role of pulmonary DC-expressed IL-15 and IL-15Rα in our aDC depletion/reconstitution system. To this end, BALB/c mice were infected with a sublethal dose of IAV +/- aDC depletion at 48 hours p.i.. On day 3 p.i., pulmonary pDC or CD8α^+ DC were purified and then coated *in vitro* with anti-mouse IL-15Rα (Figure 27A) or IL-15 (Figure 27B) blocking antibodies prior to adoptive transfer into aDC depleted host mice. As seen in Figure 27A, while adoptive transfer of control pDC or CD8α^+ DC into aDC depleted lungs promotes increased IAV-

specific CD8 T cell responses as measured by tetramer staining or intracellular staining for IFNγ, adoptive transfer of pDC or CD8α$^+$ DC coated with anti-IL-15Rα blocking antibodies ablates the rescue of pulmonary IAV-specific CD8 T cell responses in the lungs of DC reconstituted mice. Similarly, using our CL-4 adoptive transfer system, we observed that reconstitution with pDC or CD8α$^+$ DC rescued the numbers of virus-specific CL-4 T cells in the lungs, but blockade of IL-15Rα on the DC prior to their adoptive transfer prevented the DC-mediated rescue of CL-4 CD8 T cell numbers in the lungs of aDC depleted mice (Figure 28). Like the results observed in Figure 27A, if pulmonary DC subsets are instead coated with anti-IL-15 blocking antibodies prior to their transfer into aDC depleted lungs, there is again an ablation of the rescue effect mediated by control pulmonary pDC or CD8α$^+$ DC (Figure 27B). Although coating of DC with IL-15 or IL-15Rα blocking antibodies prior to their adoptive transfer *in vivo* could potentially result in their clearance and hence a shortened half-life, we did not observe differences in DC recovery from the lungs when comparing uncoated, anti-IL-15 or anti-IL-15Rα Ab coated pDC or CD8α$^+$ DC (Figure 29). This suggests that differences observed in the ability of the DC to promote IAV-specific CD8 T cell rescue in this experiment were not a result of enhanced clearance of the DC *in vivo* due to Fc-mediated mechanisms.

However, given this potential limitation of our *in vivo* antibody blocking approach, we confirmed our results using the adoptive transfer of IL-15$^{-/-}$ pulmonary DC subsets. To this end, we infected wildtype C57BL/6 host mice with a sublethal dose of IAV strain A/PR/8/34 (H1N1). Mice were then aDC depleted at 48 hours p.i., followed by i.n. reconstitution on day 3 p.i. with pulmonary pDC or CD8α$^+$ DC subsets purified from the lungs of day 6 IAV A/PR/8/34 infected wildtype or IL-15$^{-/-}$ C57BL/6 donor mice. On day 7 p.i., the numbers of IAV PA_{224}-specific and NP_{366}-specific CD8 T cells (Figure 27C) in the lungs were measured by tetramer staining and ICS for IFNγ. In agreement with our results using the IL-15 or IL-15Rα blocking antibodies (Figures 27A

and 27B), reconstitution with IL-15$^{-/-}$ pulmonary DC ablated donor DC rescue of the IAV-specific CD8 T cell response (Figure 27C). Importantly, given that these experiments were performed in IL-15$^{+/+}$ mice, this trans-presentation must be mediated specifically by pulmonary pDC or CD8α^+ DC, as the presence of other IL-15 expressing cells in the lungs could not compensate for the absence of the IL-15$^{+/+}$ pulmonary DC subsets.

IL-15 presented on the surface of pulmonary DC subsets promotes increased survival of IAV-specific CD8 T cells in the lungs of aDC depleted mice

Given our observation that blocking IL-15 or IL-15Rα on the surface of pDC and CD8α^+ DC prior to their adoptive transfer ablated the rescue of virus-specific CD8 T cell responses in the lungs of aDC depleted mice, and the documented role of IL-15 in promoting effector CD8 T cell survival *in vitro*, we next hypothesized that DC IL-15 induced signaling may be providing survival signals to activated CD8 T cells *in vivo*, therein allowing increased accumulation of IAV-specific CD8 T cell responses in the lungs of aDC depleted mice. Therefore, we infected BALB/c mice with IAV, depleted aDC at 48 hours p.i. and reconstituted with purified control pulmonary DC subsets, anti-IL-15 blocking antibody coated pulmonary DC subsets or anti-IL-15Rα blocking antibody coated DC subsets as in Figure 27A and Figure 27B, respectively. On day 5 p.i., the frequency of active caspase 3/7 by tetramer$^+$ CD8 T cells in the lungs was measured as in Figures 14 and 23. Similar to our previous results, we observed significantly increased levels of apoptosis as measured by an increased frequency of active caspase 3/7$^+$ cells among the lung tetramer$^+$ CD8 T cell population of aDC depleted mice compared to non-depleted controls (Figure 30). Reconstitution with IL-15 or IL-15Rα antibody coated pulmonary pDC or CD8α^+ DC did not result in a reduction

in the frequency of apoptotic, IAV-specific CD8 T cells in the lungs of aDC depleted mice.

Our results thus far suggest a model whereby pulmonary DC trans-present IL-15 to effector CD8 T cells in order to prevent ACAD mediated T cell apoptosis in the lungs and promote T cell survival and accumulation therein. We have examined the role of IL-15 by utilizing an aDC depletion and pulmonary DC reconstitution approach, whereby we eliminate a variety of pulmonary DC mediated signals and examine the role of IL-15 in this context. We next sought to determine the role of IL-15 alone, in an otherwise pulmonary DC sufficient environment, in promoting effector CD8 T cell survival following IAV infection. To this end we chose to block IL-15 presentation in the lungs through the use of recombinant mouse IL-15Rα/Fc fusion protein. Therefore we infected BALB/c mice with a sublethal dose of IAV, treated groups of mice i.n. on days 3, 4 and 5 p.i. with mouse IL-15Rα/Fc fusion protein or control human Fc fragments and then analyzed the lungs on day 6 p.i. for the frequency (Figure 31A) and total number (Figure 31C) of tetramer^{+} IAV-specific CD8 T cells as well as the frequency of apoptotic IAV-specific CD8 T cells (Figure 31B and 31D). In agreement with our results using the aDC depletion/reconstitution system (Figure 27), the administration of the blocking mouse IL-15Rα/Fc fusion protein resulted in reduced numbers of pulmonary influenza-specific CD8 T cells compared to mice receiving control Fc fragments. Additionally, we observed a significantly increased frequency of IAV-specific CD8 T cell apoptosis in IL-15Rα/Fc chimera treated lungs relative to control treated lungs. In agreement with our results blocking IL-15 trans-presentation using the IL-15Rα/Fc chimera, IAV infection of IL-15$^{-/-}$ mice also resulted in reduced frequencies and numbers of IAV-specific CD8 T cells in the lungs (Figure 32), further confirming an important role for IL-15 trans-presentation in regulating the magnitude of the pulmonary effector CD8 T cell response. Importantly, these results demonstrate a novel role for pulmonary IL-15 signaling in regulating the magnitude of antigen-specific CD8 T cell responses in the lungs following IAV infection,

and lend support to our results suggesting that pulmonary DC are providing these IL-15-mediated signals to CD8 T cells during infection via direct cell-to-cell contact and trans-presentation via IL-15Rα. Taken together, these results suggest that the DC-mediated rescue of IAV-specific CD8 T cells from ACAD mediated-death in the lungs of aDC depleted mice requires IL-15 trans-presentation by pulmonary DC subsets. These results further suggest a model whereby IAV-specific CD8 T cells require a two-hit model of priming in order to accumulate to sufficient numbers to control IAV infection; the first interaction being that of LN priming to initiate programmed activation, differentiation and proliferation, and the second interaction occurring in the lungs with pDC or CD8α$^+$ DC bearing MHC class I and IAV-derived antigen as well as IL-15Rα trans-presented IL-15.

Discussion

Our previous studies have demonstrated that the ability to rescue IAV-specific CD8 T cell responses in the lungs of aDC depleted mice was specific to pulmonary pDC, CD8α$^+$ DC and iDC, as adoptive transfer of aDC or aMϕ or the presence of MHC I-viral antigen bearing epithelial cells in the lungs of aDC depleted mice is not sufficient to rescue the T cell response therein (53). While it remains unclear why aDC and aMϕ are not sufficient to rescue IAV-specific CD8 T cell responses in the lungs, our preliminary results showed that aDC and aMϕ express reduced levels of IL-15 (Figure 26 and data not shown) when compared to pDC and CD8α$^+$ DC which express high levels of IL-15 mRNA. Further our preliminary experiments suggest that following addition of exogenous IL-15, adoptively transferred aDC may be able to rescue IAV-specific CD8 T cell responses in aDC depleted mice. These results suggest that the reduced levels of IL-15 expression by aMϕ and aDC may be a key factor in preventing aMϕ and aDC from rescuing the T cell response in DC depleted mice.

In addition to the important role that pDC and CD8α^+ DC play in regulating IAV-specific T cell immunity, Aldrige *et al.* have recently demonstrated an important role for TipDC in interacting with antigen-specific CD8 T cells following IAV infection (107). Elimination of TipDC recruitment to the lungs using a CCR2$^{-/-}$ mouse, resulted in a reduction in the number of virus-specific CD8 T cells in the lungs after infection. Reconstitution of the lungs with purified TipDC restored the virus-specific CD8 T cell response in the lungs via a mechanism that required viral antigen. These results expand upon our previously published findings and suggest that, in addition to iDC, pDC and CD8α^+ DC, TipDC are also capable of interacting with pulmonary CD8 T cells to promote increased effector responses in the lungs. It remains unclear, however, what mechanism is responsible for increased CD8 T cell responses following TipDC reconstitution, and it will be important to determine if TipDC are likewise promoting increased CD8 T cell survival via IL-15 trans-presentation, or if TipDC use a unique mechanism to promote CD8 T cell accumulation in the lungs (107).

While this report suggests a novel role for pulmonary DC IL-15 trans-presentation to CD8 T cells in the lungs following IAV infection, previous reports have shown that IL-15 can regulate CD8 T cell responses both *in vivo* and *in vitro*. For example, IL-15$^{-/-}$ mice undergoing a primary infection by VSV have an ~50% reduction in the CD8 T cell response compared to wildtype controls (170). Similarly, IL-15$^{-/-}$ mice infected with *Mycobacterium tuberculosis* exhibit reduced numbers of CD8 T cells in the lungs and mediastinal LN (173). Importantly, while these cells were shown to undergo similar rates of proliferation compared to wild-type CD8 T cells as measured by BrdU incorporation, Annexin-V staining revealed a significant increase in the level of apoptosis in IL-15$^{-/-}$ CD8 T cells relative to wildtype controls (173). These results are in accordance with several other reports suggesting that IL-15 is crucial for promoting the survival of activated murine CD8 T cells both *in vitro* and *in vivo.* These include experiments demonstrating the importance of IL-15 following cytokine starvation induced by IL-2

withdrawal (152), following *in vitro* activation with the superantigen staphylococcal enterotoxin A (174), and following systemic administration of the anti-Fas monocolonal antibody Jo2 (175). Interestingly, however, IL-15$^{-/-}$ mice infected with LCMV mount a robust primary CTL response (171). Together, these results suggest the requirement for IL-15 by effector CD8 T cells may differ depending upon the infectious agent and type of ensuing immune response.

At this time, the molecular mechanisms regulating the IL-15-mediated rescue of virus-specific CD8 T cells by pulmonary DC subsets in the lungs remain unclear. Previous reports examining the molecular basis for IL-15 mediated protection from apoptosis following IL-2 withdrawal *in vitro* suggested that while IL-15 signaling did not inhibit the expression of the pro-apoptotic molecules Bax or Bcl-xS (152), it promoted strong induction of the important anti-apoptotic molecules Bcl-2 and Bcl-XL (151, 152). As discussed in Chapters I and III, Bcl-2 has been demonstrated to play a critical role in activated CD8 T cell survival, and the balance between pro-apoptotic Bim and Bcl-2 is key in regulating activated CD8 T cell survival in a variety of model systems (20). These results coordinate well with our own results suggesting that pulmonary virus-specific CD8 T cells from aDC depleted mice express lower levels of Bcl-2 (Chapter III, Figures 15, 16, 18, 24), but increased levels of Bim compared to CD8 T cells from non aDC depleted mice (Chapter III, Figure 18), and that increased levels of Bcl-2 can rescue CD8 T cell apoptosis in aDC depleted mice (Chapter III, Figure 22). In accordance with these results, we have further demonstrated that reconstitution of aDC depleted lungs with pulmonary DC subsets results in increased Bcl-2 expression by virus-specific CD8 T cells in the lungs (Figure 24), suggesting that pulmonary DC are trans-presenting IL-15 and thus promoting increased Bcl-2 expression. These results further demonstrate an important functional role for ACAD mediated T cell death in regulating CD8 T cell numbers in the lungs following IAV infection and suggest IL-15 is a key survival factor in promoting T cell accumulation and hence, viral clearance.

Table 1. Gene expression in whole lung homogenates and purified pulmonary DC subsets following IAV infection.

Symbol	Whole Lung Homogenates		Purified Pulmonary Dendritic Cells				
	Control	*aDC depleted*	*aDC*	*iDC*	*aMφ*	*pDC*	*CD8α+ DC*
Gapdh	1.00	1.00	1.00	1.00	1.00	1.00	1.00
Areg	0.63	0.57	-0.26	-0.10	-0.03	0.26	0.04
Arts1	0.48	0.17	-0.58	-0.21	-0.42	0.09	0.28
Bmp1	0.35	0.02	-0.48	-0.15	-0.39	0.04	0.68
Bmp10	0.40	-0.03	-0.73	-0.11	-0.40	0.01	0.10
Bmp15	0.48	-0.02	-0.81	-0.35	-0.38	0.15	0.17
Bmp2	0.60	0.06	-0.84	-0.10	-0.27	0.30	0.04
Bmp3	0.61	0.15	-0.81	-0.04	-0.24	0.33	0.31
Bmp4	0.63	0.30	0.01	0.17	0.08	0.15	0.22
Bmp5	0.50	0.03	-0.36	0.01	-0.26	0.03	0.08
Bmp6	0.42	-0.01	-0.47	-0.27	-0.45	0.03	0.37
Bmp7	0.32	0.04	-0.49	-0.32	-0.48	0.04	0.53
Bmp8b	0.33	-0.03	-0.69	-0.32	-0.48	0.02	0.10
Csf1	0.37	0.57	-0.55	-0.30	-0.22	0.18	0.24
Csf2	0.38	0.01	-0.52	0.07	-0.31	0.18	0.13
Csf3	0.91	0.60	0.86	0.99	0.89	0.88	0.70
Ctf1	0.68	0.12	0.29	0.30	0.28	0.20	0.08
Ctf2	0.60	0.02	-0.38	0.06	-0.16	0.05	0.06
Eda	0.56	-0.03	-0.43	-0.26	-0.41	0.02	0.83
Fbs1	0.62	0.19	-0.16	-0.19	0.11	0.29	0.36
Fgf10	0.34	-0.02	-0.69	-0.23	-0.39	0.06	0.03
Flt3l	0.38	-0.04	-0.70	-0.29	-0.30	0.08	0.30
Gdf1	0.51	0.11	-0.47	0.13	-0.02	0.25	0.21
Gdf10	0.68	0.12	-0.44	0.36	-0.13	0.36	0.32
Gdf11	0.70	0.07	-0.23	0.12	-0.04	0.19	0.05
Gdf15	0.76	0.48	0.56	0.86	0.78	0.76	0.32
Gdf2	0.54	0.01	-0.63	-0.23	-0.34	0.08	0.50
Gdf3	0.40	-0.08	-0.80	-0.19	-0.43	0.24	0.10
Gdf5	0.38	-0.02	-0.41	-0.20	0.05	0.28	0.02
Gdf8	0.35	-0.04	-0.72	-0.34	-0.31	0.17	0.15
Gdf9	0.54	0.17	0.28	-0.16	0.50	0.58	0.29
Gpi1	0.73	0.76	0.94	0.99	0.95	0.97	0.89
Grn	0.75	0.73	0.91	1.00	0.97	1.00	0.99
Ifna1	0.59	0.13	-0.10	0.26	0.41	0.39	0.44
Ifna12	0.47	-0.02	-0.68	-0.14	-0.26	0.03	0.17

Table 1. Continued

Ifna13	0.42	-0.02	-0.86	-0.18	-0.40	0.01	0.04
Ifna2	0.48	0.15	-0.60	-0.19	-0.20	0.28	0.03
Ifna4	0.34	-0.04	-0.52	-0.33	-0.15	0.08	0.62
Ifna5	0.34	0.03	-0.48	-0.30	-0.05	0.27	0.16
Ifna6	0.63	0.09	-0.30	0.23	-0.09	0.42	0.25
Ifna7	0.67	0.09	-0.38	0.11	-0.09	0.11	0.03
Ifnb1	0.51	0.02	-0.33	0.06	-0.11	0.02	0.22
Ifng	0.44	0.58	0.85	0.94	0.88	0.88	0.15
Ik	0.40	0.34	-0.68	-0.10	-0.26	0.05	0.03
Il10	0.68	0.43	0.88	0.97	0.92	0.95	0.31
Il11	0.20	-0.01	-0.37	-0.34	-0.05	0.10	0.04
Il12a	0.64	0.58	0.98	0.99	0.97	0.97	0.95
Il12b	0.65	0.54	0.70	0.50	0.82	0.86	0.52
Il13	0.62	0.02	-0.25	0.50	0.25	0.10	0.01
Txlna	0.50	0.11	0.66	0.95	0.85	0.80	0.20
Il15	0.38	0.07	-0.48	0.18	-0.11	0.05	0.12
Il16	0.36	-0.07	-0.50	-0.04	-0.02	0.03	0.02
Il17a	0.41	-0.05	-0.45	-0.29	-0.12	0.05	0.00
Il17b	0.16	-0.04	-0.36	-0.31	0.03	0.12	0.02
Il17c	0.28	-0.05	-0.30	0.26	-0.01	0.28	0.09
Il25	0.57	0.04	-0.31	0.41	0.00	0.54	0.30
Il17f	0.62	-0.02	-0.47	0.40	-0.02	0.03	0.03
Il18	0.50	0.57	0.32	0.95	0.95	0.95	0.97
Il19	0.39	-0.06	-0.48	0.28	-0.14	0.02	0.01
Il1a	0.41	-0.04	-0.48	0.11	-0.25	0.03	0.00
Il1b	0.55	0.80	0.71	0.77	0.78	0.96	0.79
Il1f10	0.18	-0.06	-0.31	0.08	-0.15	0.13	0.02
Il1f5	0.26	-0.01	-0.26	0.51	-0.10	0.35	0.26
Il1f6	0.51	0.07	-0.30	0.74	-0.01	0.57	0.22
Il1f8	0.55	0.04	-0.33	0.48	-0.08	0.03	0.02
Il1f9	0.45	-0.03	-0.53	0.38	-0.03	0.00	0.03
Il1rn	0.41	0.01	-0.44	0.56	-0.10	0.03	0.01
Il2	0.91	0.61	-0.15	0.40	0.12	0.27	0.22
Il20	0.34	-0.02	-0.37	0.35	-0.23	0.01	0.00
Il21	0.15	-0.03	-0.16	0.45	-0.07	0.16	0.01
Il22	0.29	-0.01	-0.24	0.51	-0.15	0.34	0.07
Il24	0.51	0.06	-0.23	0.66	-0.02	0.55	0.09
Il27	0.54	0.07	0.05	0.83	0.65	0.42	0.01
Il3	0.49	0.25	0.79	0.97	0.90	0.92	0.39
Il4	0.33	0.01	-0.44	0.33	0.00	0.04	0.02
Il5	0.33	-0.01	-0.43	0.51	-0.04	0.09	0.02

Table 1. Continued

Il6	0.24	0.30	-0.23	0.37	-0.06	0.08	0.00
Il7	0.12	-0.04	-0.19	0.52	-0.06	0.19	0.00
Il9	0.12	-0.03	-0.32	0.70	-0.05	0.28	0.08
Kitl	0.29	0.03	-0.44	0.38	-0.08	-0.03	0.01
Lefty1	0.25	0.07	0.63	0.31	0.10	0.65	0.62
Lif	0.12	0.12	-0.27	0.30	-0.15	0.00	-0.01
Ifnz	0.10	0.07	-0.12	0.38	0.04	0.24	0.00
Lta	0.26	0.21	0.18	0.55	0.12	0.42	0.70
Ltb	0.44	0.33	0.57	0.73	0.29	0.91	0.94
Mif	0.69	0.64	0.94	1.00	0.98	0.98	0.98
Nodal	0.34	0.10	0.01	0.53	0.36	0.22	0.01
Nrg1	0.29	-0.02	-0.28	0.23	-0.06	-0.03	0.00
Oit1	0.21	-0.04	-0.27	0.13	-0.09	-0.03	0.00
Osm	0.19	0.00	-0.24	0.30	0.11	0.08	-0.01
S100a11	0.37	0.98	0.89	0.98	0.94	0.99	0.97
Scgb3a1	0.07	0.57	-0.22	0.52	0.06	0.29	0.06
Scye1	0.46	0.15	-0.15	0.60	0.08	0.36	0.03
Spp1	0.48	0.67	0.17	0.66	0.23	0.62	0.01
Thpo	0.39	0.13	0.74	0.96	0.88	0.82	0.02
Tnf	0.43	0.31	0.61	0.96	0.82	0.95	0.25
Tnfrsf11b	0.25	0.04	-0.10	0.21	0.11	0.07	0.00
Tnfsf10	0.44	0.55	0.95	0.99	0.94	0.96	0.72
Tnfsf11	0.17	0.19	-0.05	0.37	0.22	0.14	0.00
Tnfsf12	0.09	-0.04	-0.27	0.49	0.01	0.22	0.04
Tnfsf13	0.39	0.28	0.06	0.69	0.27	0.65	0.08
Tnfsf13b	0.38	0.53	0.30	0.58	0.40	0.51	0.01
Tnfsf14	0.29	0.18	0.16	0.41	0.00	0.00	0.00
Tnfsf15	0.31	0.00	-0.01	0.14	-0.03	0.00	0.01
Tnfsf18	0.26	-0.06	-0.11	0.07	-0.01	-0.03	0.01
Tnfsf4	0.13	-0.05	-0.06	0.11	0.10	0.03	0.00
Cd40lg	0.02	-0.04	-0.22	0.36	-0.02	0.05	0.00
Fasl	0.06	0.04	-0.14	0.70	0.41	0.29	0.01
Cd70	0.38	0.07	-0.04	0.47	0.33	0.46	0.06
Tnfsf8	0.12	0.08	0.21	0.06	0.08	0.03	0.00
Tnfsf9	0.24	0.19	0.68	0.90	0.88	0.82	0.01

Note: Groups of BALB/c mice were infected with a sublethal dose of IAV +/- aDC depletion as in Figure 5. On day 4 p.i., total RNA was isolated from the lungs and analyzed by microarray for general cytokine expression. Separate groups of BALB/c mice were infected with a sublethal dose of IAV. On day 6 p.i., DC subsets were purified from the lungs and total RNA was isolated and analyzed by microarray for general cytokine expression. GAPDH was normalized to 1 and data are expressed as expression relative to GAPDH.

Figure 23. Pulmonary DC reconstitution of aDC depleted mice results in decreased apoptosis of IAV-specific CD8 T cells in the lungs. Groups of BALB/c mice were infected with a sublethal dose of IAV +/- aDC depletion as in Figure 5. On day 3 p.i., groups of aDC depleted mice were then reconstituted i.n. with $2x10^4$ pulmonary pDC (light grey bars) or $CD8\alpha^+$ DC (dark grey bars) purified from the lungs of IAV-infected donors. On day 5 p.i., the frequency (A) and number of $tetramer^+$ CD8 T cells (C), and the frequency of apoptotic, $tetramer^+$ CD8 T cells (B, D) per lung were measured. Data in A are representative FACS plots gated on $CD3^+CD8^+$ T cells. Numbers of $Tetramer^+$ CD8 T cells in the lungs were determined by subtracting background staining using the Media Control (A, top). Data in B are representative FACS plots gated on $CD3^+CD8^+Tetramer^+$ T cells. Data in C and D are pooled from 2 separate experiments with n=6 mice/group. Shown are means ± SEM. *$p \leq 0.05$ relative to non-depleted control group

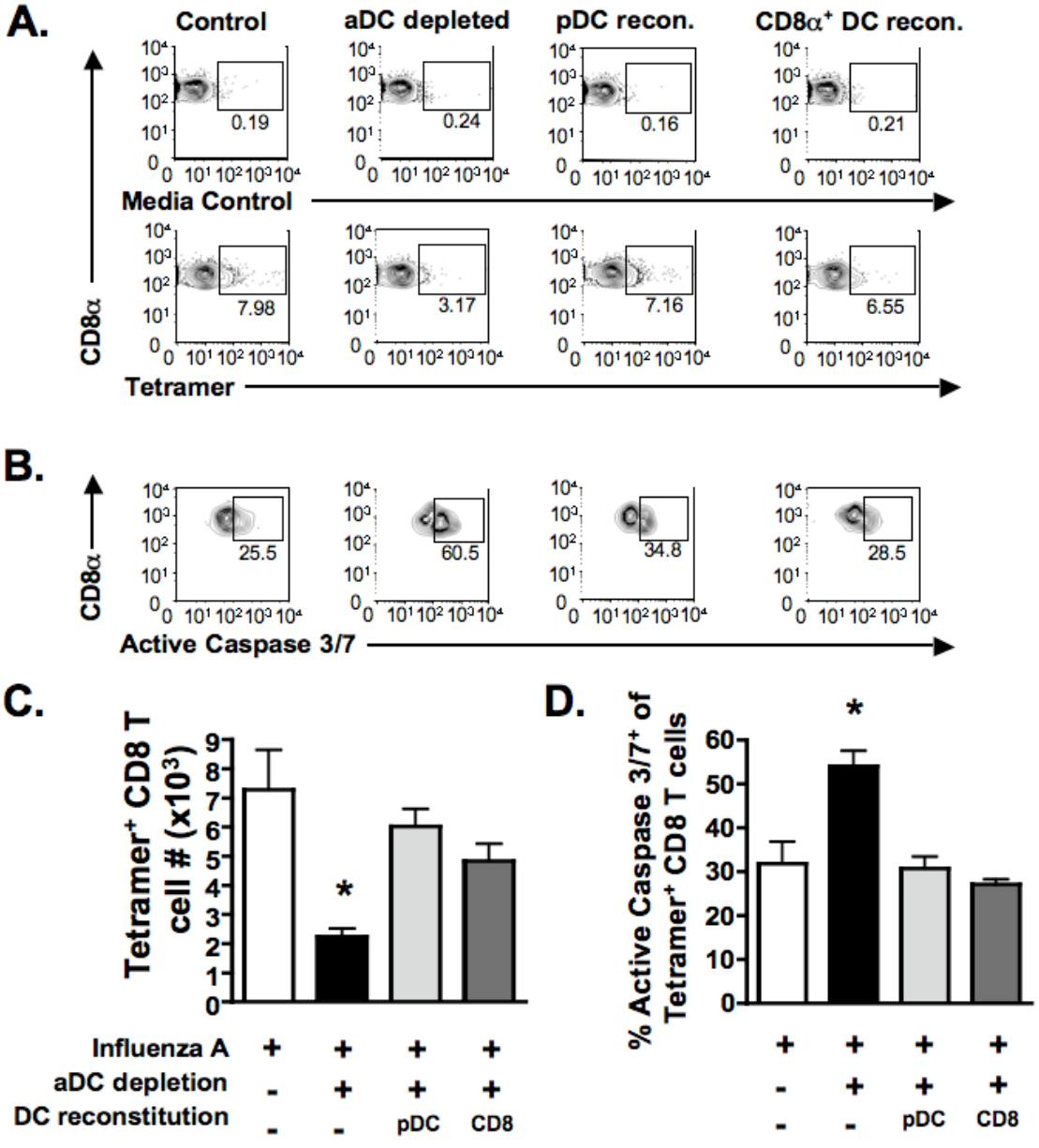
A.
Control
aDC depleted
pDC recon.
CD8α⁺ DC recon.
0.19
0.24
0.16
0.21
Media Control
7.98
3.17
7.16
6.55
CD8α
Tetramer
B.
25.5
60.5
34.8
28.5
CD8α
Active Caspase 3/7
C.
Tetramer⁺ CD8 T cell # (x10³)
Influenza A
aDC depletion
DC reconstitution
pDC
CD8
D.
% Active Caspase 3/7⁺ of Tetramer⁺ CD8 T cells
pDC
CD8

Figure 24. Pulmonary DC reconstitution of aDC depleted mice results in increased Bcl-2 expression by IAV-specific CD8 T cells in the lungs. Groups of BALB/c mice were infected with a sublethal dose of IAV +/- aDC depletion as in Figure 5. On day 3 p.i., groups of aDC depleted mice were then reconstituted i.n. with $2x10^4$ pulmonary pDC (light grey bars) or $CD8\alpha^+$ DC (dark grey bars) purified from the lungs of IAV-infected donors. On day 5 p.i., the mice were sacrificed and their lungs examined by flow cytometry for $CD3^+CD8^+Tetramer^+$ CD8 T cell expression of Bcl-2 as measured by Mean Fluorescence intensity (MFI). MFI was calculated by subtracting the MFI of the isotype from that of stained samples. Data are pooled from 2 independent experiments and represent means±SEM. n=6-7 mice/group

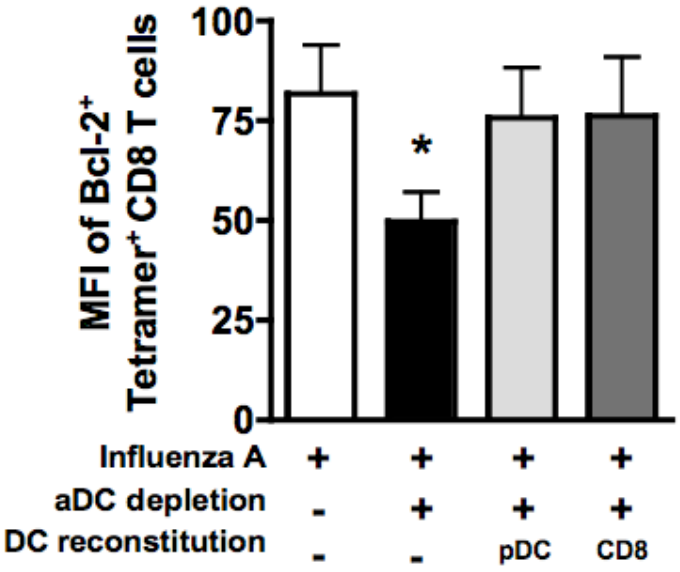
MFI of Bcl-2+ Tetramer+ CD8 T cells
100
75
50
25
0
*
Influenza A + + + +
aDC depletion - + + +
DC reconstitution - - pDC CD8

Figure 25. aDC depletion at 48 hours p.i. results in decreased pulmonary IL-15 mRNA and protein expression. Groups of BALB/c mice were infected with a sublethal dose of IAV +/- aDC depletion as in Figure 5. (A) On day 6 p.i., lungs were removed and analyzed using qRT-PCR analysis for IL-15 expression. Results were normalized to GAPDH expression, then to expression of IL-15 mRNA by naïve lungs to calculate the ΔΔCt. Data are pooled from 2 separate experiments and represent means ± SEM. n=3-6 mice/group. (B) On day 6 p.i., lung homogenates from groups of naïve, control and aDC depleted mice were analyzed for IL-15 protein expression by ELISA as described in Materials and Methods. The dotted line represents the limit of detection of the assay. ND= not detected. Data are representative of 4 separate experiments and represent means ± SEM. n=5 mice/group.

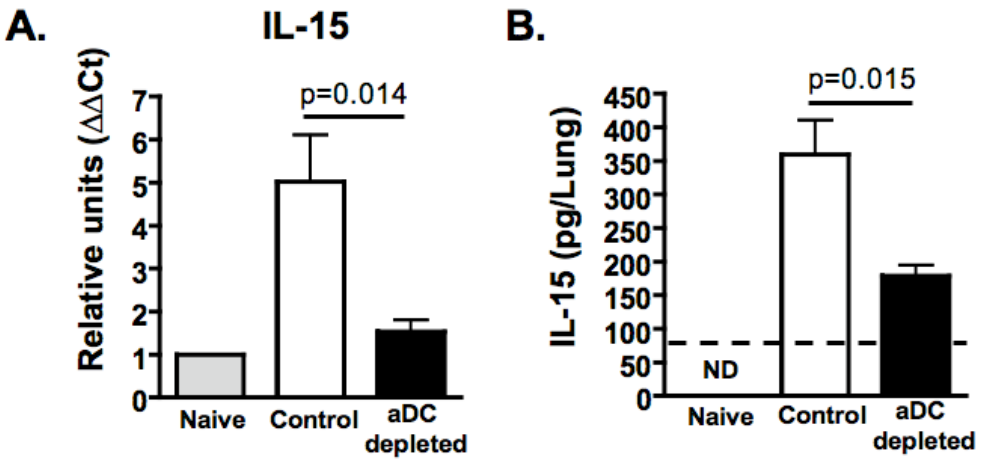
A.
IL-15
Relative units (ΔΔCt)
p=0.014
0
1
2
3
4
5
6
7
Naive
Control
aDC depleted
B.
IL-15 (pg/Lung)
p=0.015
0
50
100
150
200
250
300
350
400
450
ND
Naive
Control
aDC depleted

Figure 26. Pulmonary pDC and CD8α^+ DC express IL-15 and IL-15Rα. (A) Groups of BALB/c mice were infected with a sublethal dose of IAV. On day 6 p.i., lungs were pooled and pDC, CD8α^+ DC and aMϕ were FACS purified and analyzed by qRT-PCR analysis for IL-15 expression. Results were normalized to GAPDH expression. Data are pooled from three separate experiments and represent means ± SEM (B) Groups of BALB/c mice were infected with a sublethal dose of IAV. On day 6 p.i., pDC, CD8α^+ DC and aMϕ in the lungs were analyzed for surface expression of IL-15Rα (black line) vs. isotype control (filled grey) by flow cytometry. Data are representative of 3 separate experiments.

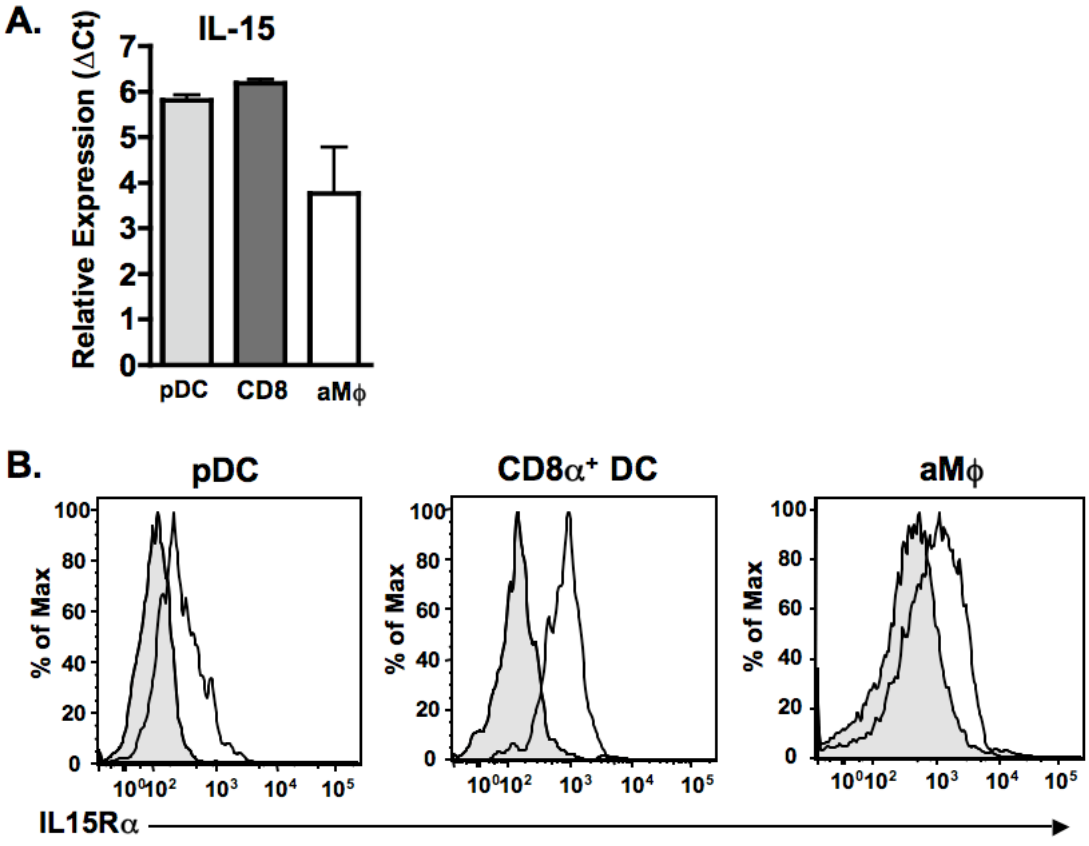
A.
IL-15
Relative Expression (ΔCt)
0
1
2
3
4
5
6
7
pDC
CD8
aMϕ
B.
pDC
CD8α+ DC
aMϕ
% of Max
0
20
40
60
80
100
10^0 10^2 10^3 10^4 10^5
IL15Rα

Figure 27. Pulmonary pDC and CD8α^+ DC mediated rescue of IAV-specific CD8 T cell responses from aDC depleted mice requires IL-15 trans-presentation. Groups of BALB/c mice were infected with a sublethal dose of IAV +/- aDC depletion as in Figure 5. On day 3 p.i., groups of aDC-depleted mice were reconstituted i.n. with $2x10^4$ purified pulmonary pDC (light grey bars) or CD8α^+ DC (dark grey bars) that were left untreated or blocked *in vitro* with (A) anti-IL-15Rα antibody or (B) anti-IL-15 antibody prior to adoptive transfer. On day 6 p.i., the number of pulmonary antigen-specific CD8 T cells was enumerated by tetramer staining (left panels) or ICS for IFNγ (right panels). Data are pooled from three separate experiments and represent means ± SEM. n= 9-12 mice/group. (C) Groups of C57BL/6 mice were infected with a sublethal dose of IAV and aDC depleted at 48 hours p.i. (black bars), while controls remained undepleted (white bars). On day 3 p.i., groups of aDC-depleted mice were then reconstituted i.n. with $2x10^4$ purified pulmonary pDC (light grey bars) or CD8α^+ DC (dark grey bars) that were purified from IAV-infected C57BL/6 IL-$15^{-/-}$ (KO) or wildtype IL-$15^{+/+}$ donors. On day 7 p.i., the number of pulmonary IAV-specific CD8 T cells was enumerated by tetramer staining (left panels) or ICS for IFNγ (right panels). Data are pooled from two separate experiments and represent means ± SEM. n= 6-7 mice/group. *$p \leq 0.05$ relative to undepleted control group

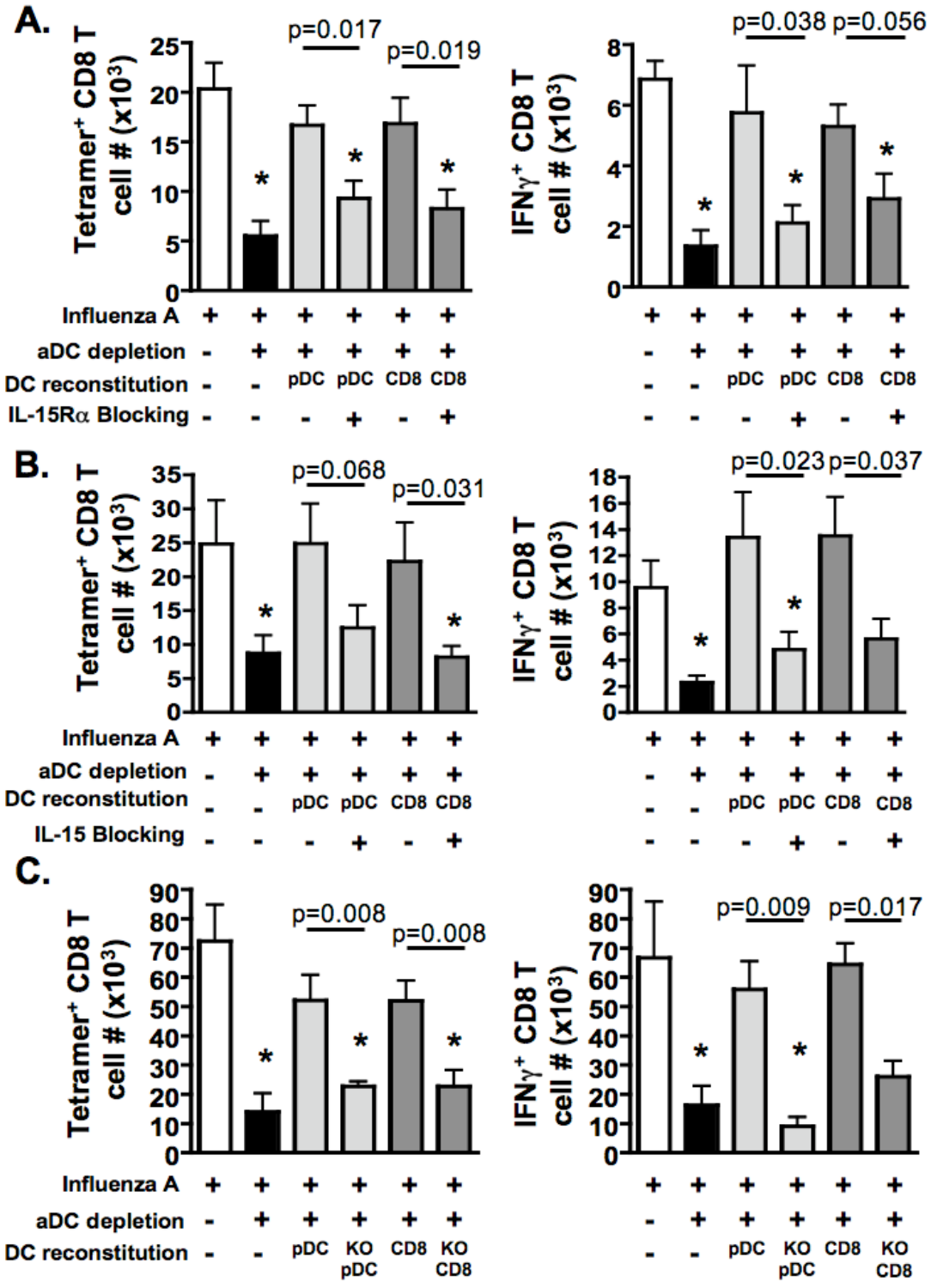
A.
Tetramer+ CD8 T cell # (x10³)
p=0.017
p=0.019
IFNγ+ CD8 T cell # (x10³)
p=0.038
p=0.056
Influenza A
aDC depletion
DC reconstitution
IL-15Rα Blocking
pDC
CD8
B.
Tetramer+ CD8 T cell # (x10³)
p=0.068
p=0.031
IFNγ+ CD8 T cell # (x10³)
p=0.023
p=0.037
Influenza A
aDC depletion
DC reconstitution
IL-15 Blocking
pDC
CD8
C.
Tetramer+ CD8 T cell # (x10³)
p=0.008
p=0.008
IFNγ+ CD8 T cell # (x10³)
p=0.009
p=0.017
Influenza A
aDC depletion
DC reconstitution
pDC
KO pDC
CD8
KO CD8

Figure 28. Pulmonary pDC and CD8α^+ DC mediated rescue of IAV-specific CD8 T cell responses from aDC depleted mice requires IL-15 trans-presentation. Influenza-specific, CD90.1$^+$ CL-4 T cells were adoptively transferred to groups of CD90.2$^+$ BALB/c mice as described in Materials and Methods. 24 hours later, mice were infected with a sublethal dose of IAV +/- aDC depletion as outlined in Figure 5. On day 3 p.i., groups of aDC-depleted mice were reconstituted i.n. with 2x10^4 purified pulmonary pDC (light grey bars) or CD8α^+ DC (dark grey bars) that were left untreated or blocked *in vitro* with anti-IL-15Rα antibody. On day 6 p.i., the number of pulmonary adoptively transferred, CD90.1$^+$ CL-4 CD8 T cells was enumerated by flow cytometry. Data are pooled from 2 separate experiments and represent means ± SEM. n= 7-8 mice/group.

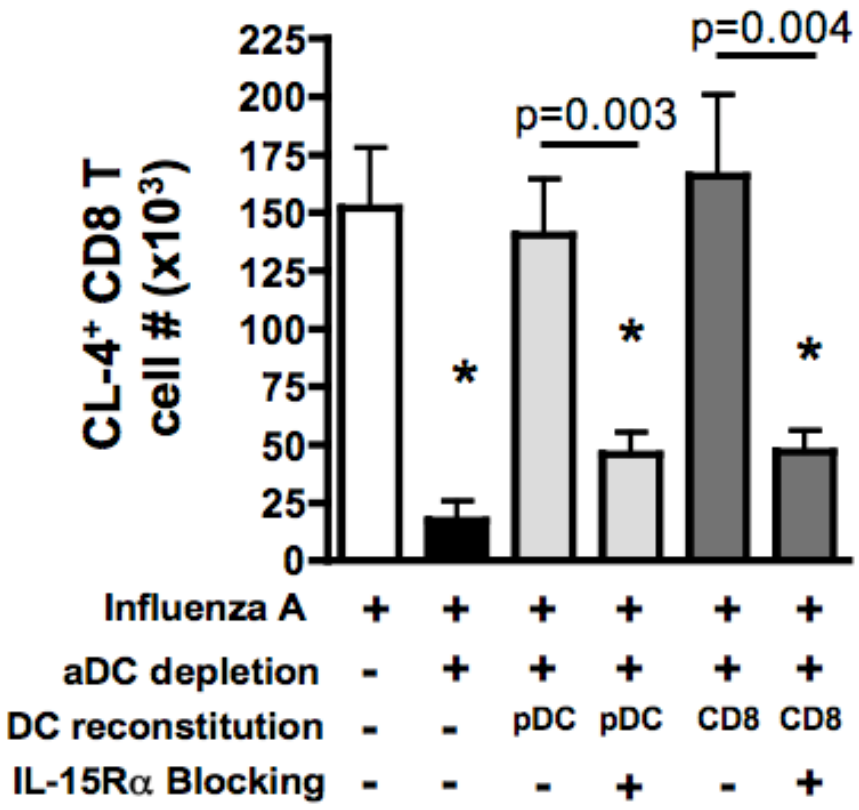
CL-4+ CD8 T cell # (x10³)
225
200
175
150
125
100
75
50
25
0
p=0.003
p=0.004
*
*
*
Influenza A + + + + + +
aDC depletion - + + + + +
DC reconstitution - - pDC pDC CD8 CD8
IL-15Rα Blocking - - - + - +

Figure 29. IL-15Rα antibody coating does not alter DC survival in the lungs of aDC depleted mice. Groups of BALB/c mice were infected with a sublethal dose of IAV and aDC depleted at 48 hours p.i.. On day 3 p.i., groups of aDC-depleted mice were reconstituted i.n. with $2x10^4$ CFSE-labeled, purified pulmonary pDC (white bars) or $CD8\alpha^+$ DC (grey bars) that were left untreated or blocked *in vitro* with anti-IL-15Rα antibody. 18 hours after reconstitution, mice were sacrificed and their lungs examined by flow cytometry for the numbers of $CFSE^+$ adoptively-transferred pulmonary DC subsets in the lungs. Data are pooled from 2 separate experiments, n=4 mice/group. NS= No statistical significance was detected between analyzed groups.

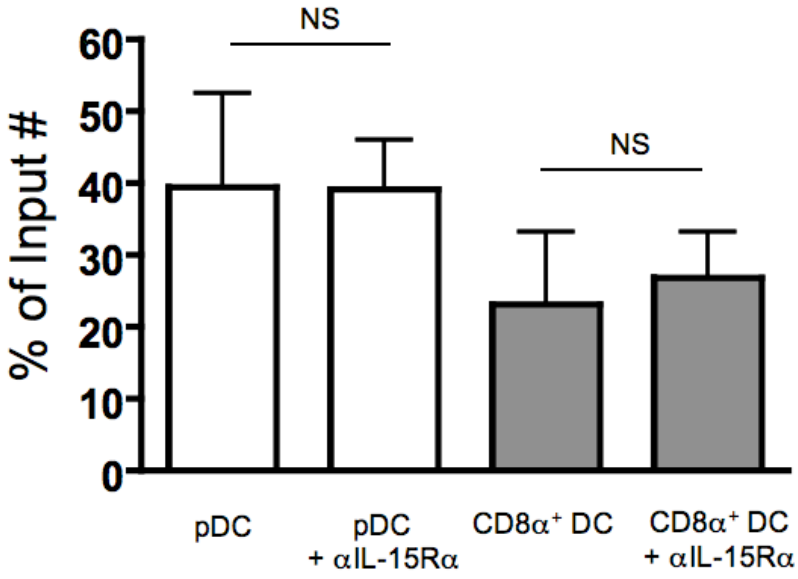
NS
NS
60
50
40
30
20
10
0
% of Input #
pDC
pDC
+ αIL-15Rα
CD8α+ DC
CD8α+ DC
+ αIL-15Rα

Figure 30. Blocking IL-15 or IL-15Rα on the surface of pulmonary DC subsets prior to adoptive transfer ablates pulmonary DC mediated rescue of IAV-specific CD8 T cell apoptosis in the lungs of aDC depleted mice. Groups of BALB/c mice were infected with a sublethal dose of IAV +/- aDC depletion as in Figure 5. On day 3 p.i., groups of aDC depleted mice were then reconstituted i.n. with $2x10^4$ purified pulmonary pDC (light grey bars) or $CD8\alpha^+$ DC (dark grey bars) that were blocked *in vitro* with anti-IL-15 (15) or anti-IL-15Rα (15R) antibody prior to adoptive transfer. On day 5 p.i., the lungs were analyzed for the frequency of apoptosis of $tetramer^+$ CD8 T cells. Data are representative of 2 separate experiments and represent means ± SEM. n=3-4 mice/group. *$p \leq 0.05$ relative to influenza virus infection only controls

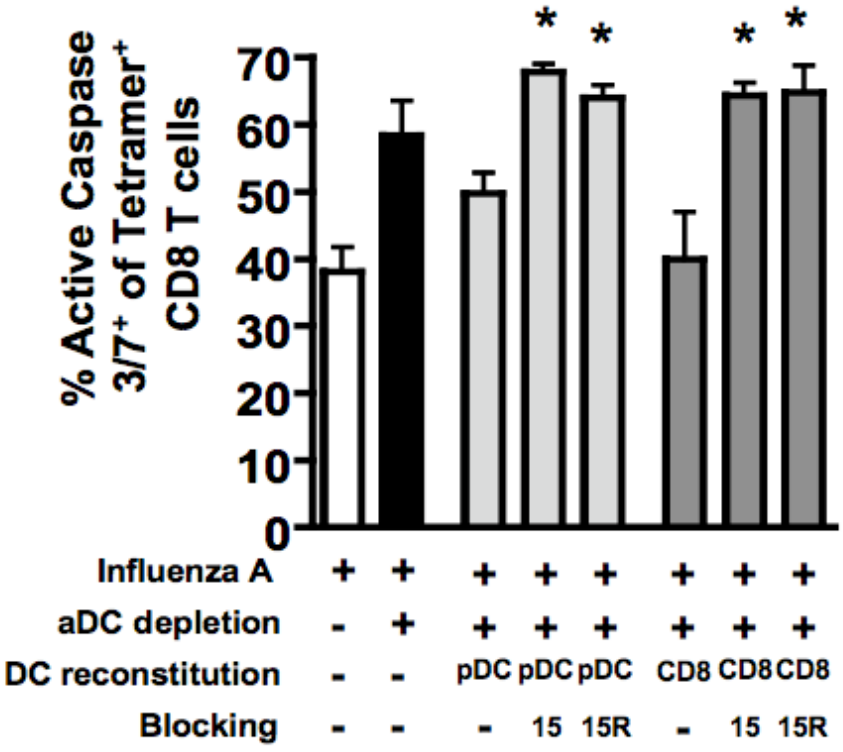
% Active Caspase 3/7+ of Tetramer+ CD8 T cells
70
60
50
40
30
20
10
0
*
*
*
*
Influenza A + + + + + + + +
aDC depletion - + + + + + + +
DC reconstitution - - pDC pDC pDC CD8 CD8 CD8
Blocking - - - 15 15R - 15 15R

Figure 31. IL-15Rα-Fc administration results in reduced IAV-specific CD8 T cell responses and increased CD8 T cell apoptosis in the lungs following IAV infection. Groups of BALB/c mice were infected with a sublethal dose of IAV. On days 3, 4 and 5 p.i., mice were i.n. administered IL-15Rα-Fc (black bars) or control human Fc fragments (white bars). On day 6 p.i., the lungs were analyzed for (A) the frequency and (C) number of tetramer$^+$ CD8 T cells or (B and D) for apoptosis of tetramer$^+$ CD8 T cells. Representative FACS plots are gated on (A) CD3$^+$CD8$^+$ T cells or (B) CD3$^+$CD8$^+$Tetramer$^+$ T cells. Numbers of Tetramer$^+$ CD8 T cells in the lungs were determined by subtracting background staining using the Media Control (A, left). Data are representative of 2 separate experiments and represent means ± SEM. n=3-5 mice/group.

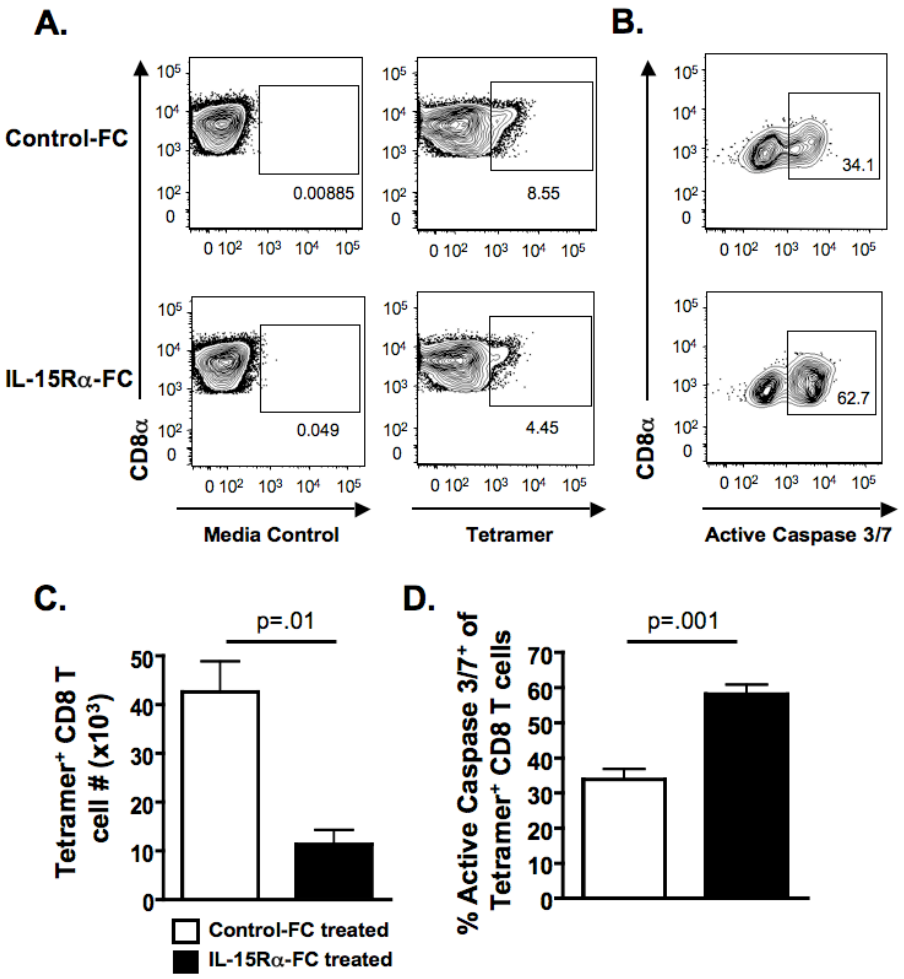
A.
B.
Control-FC
IL-15Rα-FC
CD8α
0.00885
8.55
34.1
0.049
4.45
62.7
Media Control
Tetramer
Active Caspase 3/7
C.
p=.01
Tetramer+ CD8 T cell # (x10³)
Control-FC treated
IL-15Rα-FC treated
D.
p=.001
% Active Caspase 3/7+ of Tetramer+ CD8 T cells

Figure 32. IL-15$^{-/-}$ mice exhibit reduced IAV-specific CD8 T cell numbers in the lungs following IAV infection. Groups of IL-15$^{-/-}$ and wildtype control IL-15$^{+/+}$ C57BL/6 mice were infected with a sublethal dose of IAV. On day 8 p.i., the (A) frequency and (B) number of virus-specific CD8 T cells in the lungs was measured by tetramer (left) or ICS for IFNγ (right). Representative FACS plots in A are gated on CD3^{+}CD8^{+} T cells. Numbers of Tetramer^{+} or IFNγ^{+} CD8 T cells in the lungs were determined by subtracting background staining using the Media Control (A, top panel). Data are representative of 2 separate experiments and represent means ± SEM. n= 4-5 mice/group. *$p \leq 0.05$ relative to IAV infection only controls

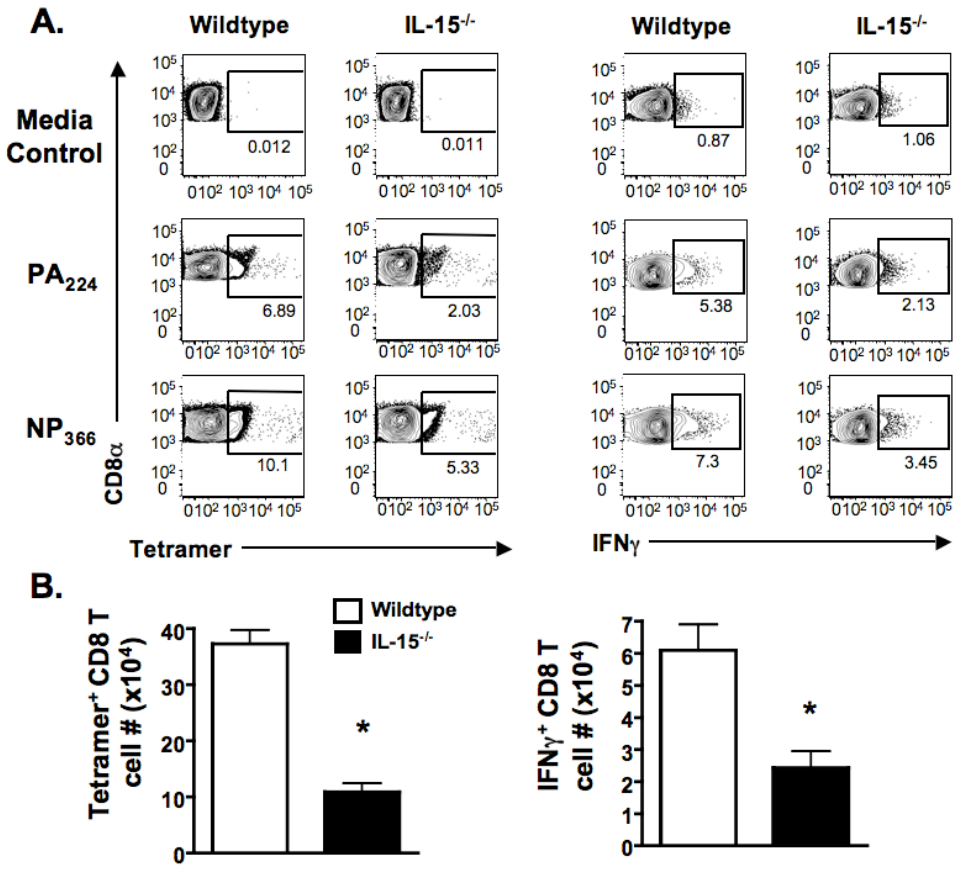
A.
Wildtype
IL-15-/-
Wildtype
IL-15-/-
Media Control
PA224
NP366
CD8α
Tetramer
IFNγ
0.012
0.011
0.87
1.06
6.89
2.03
5.38
2.13
10.1
5.33
7.3
3.45
B.
Wildtype
IL-15-/-
Tetramer+ CD8 T cell # (x10^4)
IFNγ+ CD8 T cell # (x10^4)
*
*

CHAPTER V AICD AND ITS ROLE IN CD8 T CELL APOPTOSIS FOLLOWING ADC DEPLETION

Introduction

We demonstrated in Chapter III that virus-specific CD8 T cells undergo increased apoptosis in the lungs of aDC depleted mice as a result of both ACAD and AICD mediated mechanisms. In Chapter IV we explored a functional role for the pulmonary DC mediated trans-presentation of IL-15 in preventing ACAD by virus-specific T cells in the lungs following IAV infection. Here, we will further determine if there is a functional role for AICD in regulating virus-specific CD8 T cell death in the lungs of aDC depleted mice.

AICD occurs when effector CD8 T cells receive stimulation via their TCR in the absence of appropriate costimulation (20, 136, 137). We have previously demonstrated that aDC depleted mice have consistently higher viral titers compared to their non-depleted counterparts (53), and a reduction in the numbers of antigen presenting cells in the lungs following IAV infection (53). Together these results suggest that, in the lungs of aDC depleted mice, virus-specific CD8 T cells are at an increased likelihood for encountering viral antigen on the surface of non-antigen presenting cells in the absence of appropriate costimulation or the necessary survival signals. Although not absolutely required, AICD most often occurs in the presence of death receptor signaling, for example, following ligation of Fas or the TRAIL receptor, DR-5 (20, 136, 137). The results of our western blots (Chapter III) suggest that indeed, pathways of AICD are contributing to the apoptosis of T cells in the lungs of aDC depleted mice. In particular, the increased presence of active caspase 8 (Figure 20A), suggests that death receptor signaling (i.e. ligation of Fas) is a primary contributing factor. Given these data, we next chose to examine the effects of pulmonary antigen load and death receptor signaling in

the lungs following IAV infection to elucidate a functional role for AICD-mediated CD8 T cell death.

Materials and Methods

Mice

6-12 week old female BALB/c mice were purchased from the National Cancer Institute (Frederick, MD). All mice were housed and maintained in the animal care facility at the University of Iowa. Experiments were conducted according to federal and institutional guidelines and were approved by the University of Iowa Animal Care and Use Committee.

Virus infection

Mouse-adapted influenza A virus A/JAPAN/305/57 was grown in the allantoic fluid of 10-day old embryonated chicken eggs for 2 days at 37°C, as previously described (76). Allantoic fluid was harvested and stored at -80°C. BALB/c mice were anesthetized with isofluorane and infected i.n. with either 5875 TCIU or 587 TCIU of mouse-adapted A/JAPAN/305/57, in 50 μl of Iscove's media as previously described (76). For experiments using a second dose of live IAV on day 3 p.i., experimental mice received $2.35x10^6$ TCIU of mouse-adapted A/JAPAN/305/57 in 50 ul of stock virus allantoic fluid, while control mice received 50 ul of allantoic fluid from uninfected eggs.

Clodronate-liposome treatment

Pulmonary DC and macrophage depletion was performed by treatment with liposomes containing dichloromethylene bisphosphonate (Clodronate) (53). Clodronate was a gift of Roche Diagnostics GmbH, Mannheim, Germany. It was encapsulated in liposomes as described previously (238). Phosphatidylcholine (LIPOID E PC) was obtained from Lipoid GmbH, Ludwigshafen, Germany. Cholesterol was purchased from

SIGMA Chem.Co. USA. At 48 hours p.i., mice were anesthetized by isofluorane inhalation and administered 75 μl of Clodronate-liposomes or PBS-liposomes i.n.

Oseltamivir Phosphate treatment

The neuraminidase-inhibitor pro-drug oseltamivir phosphate (oseltamivir) [ethyl(3R,4R,5S)-4-acetamido-5-amino-3-(1-ethylpropoxy)-1-cyclohexene-1-carboxylate] was provided by Roche Pharmaceuticals. Mice were anesthetized by isofluorane inhalation and administered osteltamivir (2 mg/kg/day) diluted in sterile, distilled water once a day by oral gavage on days 2, 3 and 4 p.i..

Pulmonary virus titer

Lungs from infected mice were rapidly homogenized and viral titers determined using an endpoint dilution assay and expressed as Tissue Culture Infections $Dose_{50}$ ($TCID_{50}$). Briefly, 10-fold dilutions of homogenized and clarified lung from IAV-infected mice were mixed with 10^5 MDCK cells in DMEM. After 24 hours incubation at 37ºC, the inoculum was removed and DMEM media containing 0.0002% L-1-(tosylamido-2-phenyl)ethyl chloromethyl ketone (TPCK)-treated trypsin (Worthington Diagnostics, Freehold, NJ) and penicillin (100U/ml)/streptomycin (100mg/ml) was added to each well. After 3 days incubation at 37°C in a humidified atmosphere of 5% CO_2, supernatants were mixed with an equal volume of 0.5% chicken RBC, the agglutination pattern read, and the $TCID_{50}$ values calculated.

MHC I tetramers

Tetramers HA_{204} (H-2K(d)/LYQNVGTYV), HA_{529} (H-2K(d)/IYATVAGSL), and NP_{147} (H2K(d)/TYQRTRALV) for BALB/c were obtained from National Institute of Allergy and Infectious Disease MHC Tetramer Core Facility (Atlanta, GA).

Preparation of cells

Lungs were pressed through wire mesh to obtain a single cell suspension, which was then enumerated by trypan blue exclusion. For DC preparations, lungs were digested for 25 minutes at 25° C in media containing 1 mg/ml Collagenase (Sigma) and 0.02 mg/ml DNase (Sigma) before single cell preparation. Dendritic cells for reconstitution experiments were purified from the lungs of day 6 A/JAPAN/305/57 infected BALB/c donors using MACS technology (Miltenyi Biotech) according to manufacturer's instructions or by fluorescence activated cell sorting (FACS) as has been previously described (53). Purified cells were resuspended in Iscove's DMEM and $2.5x10^4$ cells in 50 ul were adoptively transferred i.n. to host mice on day 3 p.i. (53).

Antibodies and reagents

The following reagents were used for these studies: rat anti-mouse CD3ε (145-2C11), rat anti-mouse CD8α (53-6.7), rat anti-mouse IFNγ (XMG1.2), rat anti-mouse IA/IE (M5/114.15.2), rat anti-mouse CD11b (M1/70), hamster anti-mouse CD11c (HL3) purchased from Becton Dickinson; rat anti-mouse CD45R (RA3-6B2) purchased from Caltag. Vybrant FAM caspase 3/7 kits were purchased from Invitrogen and used according to manufacturer's instructions. For surface staining, isolated cells (10^6) were stained with antibody or tetramer for 30 minutes at 4° C and then fixed using BD FACS Lysing Solution (BD Biosciences). For intracellular cytokine staining, fixed cells were permeabilized and labeled with antibodies in FACS buffer containing 0.5% Saponin (Acros Organics, NJ) for 1 hour at 4° C. All flow cytometry data were acquired on a BD FACS Calibur or BD FACS Canto II (BD Immunocytometry Systems) and analyzed using FlowJo software (TreeStar, Ashland, OR).

Fas:Fc treatment

Recombinant human Fas:Fc chimeric fusion protein was purchased from BD Pharmingen and control human Fc fragments were purchased from Jackson Laboratories.

Mice were anesthetized using isofluorane and administered 8 μg of Fas:Fc or Control:Fc i.n. on days 4 and 5 p.i..

Statistical analysis

Statistical significance of the difference between two sets of data was assessed using an unpaired, one-tailed *t*-test or a paired *t*-test for control and experimental data groups that could be paired. Differences were considered to be statistically significant at $p<0.05$.

Results

Pulmonary DC reconstitution of aDC depleted lungs results in reduced pulmonary viral titers

We have previously demonstrated that aDC depletion at 48 hours post-IAV infection results in a profound increase in viral titers in the lungs (53). It is thought that this increase is a result of the reduced numbers of virus-specific CD8 T cells that accumulate in the lungs following aDC depletion. Reconstitution of aDC depleted lungs results in increased numbers of virus-specific CD8 T cells therein; however, it was unclear what effect this rescue of CD8 T cell responses had on the pulmonary viral titer. Therefore, we next determined if pulmonary DC reconstitution resulted in reduced pulmonary viral titers in the lungs of aDC depleted mice. To this end, groups of mice were IAV infected +/- aDC depletion at 48 hours p.i.. On day 3 p.i., mice were reconstituted with pulmonary pDC or $CD8\alpha^+$ DC as in Figure 5. On days 4, 5 and 6 p.i., the mice were sacrificed and their lungs analyzed for pulmonary virus titers using an endpoint dilution assay as described in Materials and Methods. As seen in Figure 33, although not significant, pulmonary DC reconstitution of aDC depleted lungs with both pDC and $CD8\alpha^+$ DC results in reduced viral titers in the lungs, particularly on days 5 and 6 p.i.. While it is formally possible that the adoptively transferred DC subsets are directly

promoting a reduction in pulmonary viral titers, these results are unlikely given our data suggesting that pulmonary DC subsets from B/Lee infected or $\beta 2M^{-/-}$ donors are unable to promote the same effect (53). Instead, it is likely that pulmonary DC are able to provide survival signals, by providing IL-15 (Chapter IV) and or costimulation (Chapter II), to the T cells that block AICD, and that the protected CD8 T cells then kill virus-infected cells thereby lowering non-APC mediated antigen presentation as well as virus titers.

The effects of manipulating antigen load in the lungs following IAV infection

We next wanted to determine if the increased viral titers in the lungs of aDC depleted mice were directly contributing to the increased apoptosis of the antigen-specific CD8 T cells therein. To this end, we chose to alter the antigen environment in the lungs of control non-depleted mice to more closely mimic the increased antigen load in the lungs of aDC depleted mice, and, in parallel experiments, reduce the antigen load of aDC depleted lungs to more closely mimic the environment in the lungs of non-depleted, IAV-infected control mice. To this end, groups of BALB/c mice were infected with a sublethal dose of IAV +/- aDC depletion at 48 hours p.i.. Starting 12 hours later, on days 2, 3 and 4 p.i. the aDC depleted mice were treated by oral gavage with the IAV neuraminidase inhibitor, Oseltamivir. This treatment regime is able to knockdown the pulmonary antigen load, as measured by ELISA for the IAV NP protein, in aDC depleted lungs to levels similar to that of non-depleted, IAV infected control mice (Figure 34). A separate group of mice was IAV infected, but received a second dose of live IAV i.n. ($2.35x10^6$ TCIU) on day 3 p.i.. Mice were harvested on day 5 p.i. and their lungs analyzed by flow cytometry for total numbers of virus-specific CD8 T cells (Figure 35A) and the frequency of apoptotic CD8 T cells in the lungs as measured by the presence of active caspase 3/7 (Figure 35B). As seen in Figure 35, mice that received a second dose

of live IAV, and hence an increased antigen load in the lungs, exhibit a trend towards reduced numbers of virus-specific CD8 T cells (Figure 35A) and have significantly increased frequencies of apoptotic CD8 T cells in the lungs (Figure 35B) compared to control IAV-infected mice that did not receive a second infection. aDC depleted mice that were treated with the anti-viral drug Oseltamivir exhibit a significant rescue in the numbers of T cells in their lungs (Figure 35A) and a reduction in the frequencies of virus-specific CD8 T cells undergoing apoptosis therein (Figure 35B). This result suggests that the Oseltamivir-mediated reduction in the viral titers of aDC depleted mice is able to reduce the frequency of viral antigen presentation by non-professional antigen presenting cells, and therein reduces AICD-mediated apoptosis of IAV-specific CD8 T cells in the lungs. Similarly, the increase in viral antigen afforded by a second infection with live IAV on day 3 p.i. likely results in an increased frequency of viral-antigen presentation by non-professional APCs and, subsequently, increased AICD- mediated apoptosis of virus-specific CD8 T cells in the IAV-infected environment.

We have previously described that the magnitude of the CD8 T cell response relates inversely to the initial dose of infection, i.e. increased viral inoculum results in reduced CD8 T cell responses (76). This inverse correlation is a result of increased LNDC-mediated death of CD8 T cells in the LN following lethal doses of infection ((76), and R. A. Langlois, manuscript submitted). Therefore, we further wanted to confirm that the reduced CD8 T cell responses observed in the lungs of mice receiving the second dose of live IAV was a result of altered CD8 T cell survival in the lungs and not a result of reduced CD8 T cell output from the LN. To this end, groups of mice were infected with a sublethal dose of IAV, followed on day 3 p.i. by a second dose of live IAV as in Figure 35. A control group was included that received only the initial sublethal IAV infection. On day 5 p.i., the total numbers of virus-specific CD8 T cells within the draining LN were determined. As seen in Figure 36, there is no significant change in the numbers of virus-specific CD8 T cells in the LN of mice receiving a second infection

with live IAV on day 3 p.i. compared to control LN. This result suggests that the reduced numbers of CD8 T cells observed in the lungs of mice receiving a 2nd dose of live IAV are not due to decreased CD8 T cell output from the LN, but are likely an effect of the increased viral burden in the lungs. However, an additional complication to interpreting these experiments is that altering the viral load in the lungs following IAV infection also appears to alter the numbers of pulmonary DC that are recruited to the lungs following IAV infection. As seen in Figure 37, a second dose of live IAV results in significantly reduced numbers of pulmonary pDC (Figure 37A) and CD8α^+ DC (Figure 37B) in the lungs, while Oseltamivir treatment of aDC depleted mice as in Figure 35, results in a increase in these subsets (Figure 37, A and B) compared to non-Oseltamivir treated, aDC depleted controls. We observed a similar trend in the numbers of lung-resident pulmonary DC subsets, with a reduction in aDC (Figure 37C) and iDC (Figure 37D) numbers in the lungs of mice receiving a second live IAV infection, and a significant increase in aDC and iDC numbers in the lungs of aDC depleted mice receiving Oseltamivir treatment (Figure 37). We have previously demonstrated that the presence of pulmonary pDC and CD8α^+ DC is integral to regulating virus-specific CD8 T cell immunity in the lungs following IAV infection (53). Further, it is thought that aDC and iDC play a key role in promoting pDC and CD8α^+ DC recruitment to the lungs (264), together suggesting that alterations in the pulmonary viral burden have important effects on the cellular infiltrate present in the lungs following IAV infection. In summary, the relationship between antigen load, pulmonary DC recruitment and virus-specific CD8 T cell numbers in the lungs following IAV infection remains unclear. However, our results demonstrate an important role for antigen levels in regulating accumulation of both the innate and adaptive components of the immune response and suggest that the inflammatory environment resulting from excess antigen in the lungs can have severe consequences on CD8 T cell survival and subsequent disease severity, survival and recovery following IAV infection.

Blocking Fas/FasL interactions in the lungs of aDC depleted mice rescues pulmonary virus-specific CD8 T cell responses

Given the complications inherent with directly altering antigen loads in the lungs following IAV infection, we next chose to use an alternative approach for investigating the role of AICD in the lungs following IAV infection. AICD most often occurs in the presence of death-receptor signaling, with Fas/FasL being the most common example (20, 136, 137). If virus-specific CD8 T cells were undergoing increased apoptosis in the lungs of aDC depleted mice as a result of Fas/FasL-mediated AICD, we reasoned that blockade of this interaction should result in reduced AICD and subsequently increased survival and accumulation of virus-specific CD8 T cells in the lungs. To this end, mice were infected with a sublethal dose of IAV+/- aDC depletion at 48 hours p.i.. On days 4 and 5 p.i., (i.e. when virus-specific CD8 T cells are just beginning to enter the lungs (13, 14)) mice were treated i.n. with Fas:Fc chimeric fusion protein, which is known to block Fas/FasL interactions *in vivo* (272), or control Fc fragments. On days 5 (Figure 38, A and B) and 6 (Figure 38C) p.i., the lungs were examined for the frequency of virus-specific CD8 T cells undergoing apoptosis was measured by the presence of active caspase 3/7 (Figure 38A), as well as for total numbers of virus-specific CD8 T cells (Figure 38, B and C). As seen in Figure 38A, administration of Fas:Fc, but not control Fc fragments, results in a reduction in the frequency of virus-specific CD8 T cells undergoing apoptosis in the lungs of aDC depleted mice on day 5 p.i.. Further, this reduction in T cell apoptosis mediated by blocking Fas/FasL interactions translates into an increase in the numbers of antigen-specific CD8 T cells in the lungs on day 5 p.i. (Figure 38B) and a significant increase in T cell numbers by day 6 p.i. (Figure 38C) compared to control Fc treated, aDC depleted lungs. Of note, we observed no changes in virus-specific CD8 T cell apoptosis or total numbers in the lungs between control, non-depleted mice given control Fc fragments and non-depleted control mice given Fas:Fc

(data not shown). Together, these results suggest that Fas/FasL interactions in the lungs of aDC depleted mice are at least partially responsible for the increased apoptosis and reduced CD8 T cell numbers observed therein.

Discussion

We demonstrate here that blockade of Fas:FasL interactions in the lungs of aDC depleted mice results in a significant reduction in virus-specific CD8 T cell apoptosis and increased CD8 T cell accumulation therein (Figure 38). AICD-mediated cell death is generally associated with death receptor signaling, with Fas:FasL being the most common example (20, 136, 137). Therefore, it is not surprising that blockade of Fas:FasL was an effective approach for preventing CD8 T cell death in the lungs of aDC depleted mice. However, there are other death receptor pairs that have been described to mediate AICD, including TNF Receptor 1 (TNFR1) and the TRAIL receptor, DR-5 (20, 136, 137). A role for TRAIL in promoting death of aDC depleted CD8 T cells seems unlikely, as it has primarily been described to play a role in the elimination of "helpless" CD8 T cells (273-275). However, TNFR1 has been shown to promote AICD of mature, peripheral CD8 T cells (276, 277), and may play a partially redundant role with Fas (277). IAV infection results in high concentrations of TNFα in the lungs (107, 127) and conceivably, TNF/TNFR interactions, in addition to Fas/FasL interactions, could also be playing an important role in regulating pulmonary CD8 T cell apoptosis. Further, although death-receptor ligation is the primary route of caspase 8 activation and AICD initiation, other pathways can also activate caspase 8. For example, Granzyme B can directly activate caspase 8 and initiate AICD independent of death-receptor ligation (278). Thus, while our results suggest an integral role for Fas:FasL interactions in regulating AICD- mediated apoptosis of virus-specific CD8 T cells in the lungs, alternative routes of AICD activation may also account for increased pulmonary T cell death following IAV infection and should be explored in future experiments.

The results of our western blot analysis of virus-specific CD8 T cells from the lungs of aDC depleted mice suggest that both ACAD and AICD mediated pathways of apoptosis are contributing to the reduced CD8 T cell responses therein (Chapter III). From these analyses, it was difficult to determine how each type of death was functionally contributing to the reduced CD8 T cell response in the lungs following aDC depletion. AICD is thought to occur when activated effector cells receive antigen re-stimulation via their TCR in the absence of the appropriate costimulation (20, 136, 137). This is most likely to occur in an environment that has an abundance of antigen and a shortage of professional APCs capable of presenting the antigen in the presence of the necessary T cell survival signals; very much like the environment that is created in our model, following depletion of pulmonary DC subsets from the lungs of IAV-infected mice (53). Therefore, in an attempt to elucidate the functional contribution of AICD-mediated apoptosis in the lungs following IAV infection, we developed an experimental approach to alter the levels of antigen present in the lungs following IAV infection, and hence, alter the likelihood of virus-specific CD8 T cells encountering cognate antigen on the surface of non-professional APCs and undergoing apoptosis by AICD. We demonstrate here that alterations in the viral burden in the lungs following IAV infection result in profound changes in the subsequent innate and adaptive immune response therein. Treatment of aDC depleted mice with Oseltamivir to knockdown levels of viral antigen in the lungs resulted in an increase in the pulmonary virus-specific CD8 T cell response, while administration of a second dose of live IAV on day 3 p.i. yielded a significant reduction in the virus-specific T cell response in the lungs (Figure 35). From the results here, it is difficult to ascertain whether the effects on the CD8 T cell response are solely a result of changes in protein antigen load, or a result of changes in the live, replicating pathogen itself. Administration of a second dose of UV-inactivated IAV (data not shown), rather than the live IAV, did not result in the same reduction in virus-specific CD8 T cell numbers in the lungs, suggesting that viral replication may be required in

order to promote AICD-mediated CD8 T cell apoptosis. One caveat to these experiments is that the concentration of NP antigen in a dose of UV-inactivated IAV is only ~60% of that in the initial dose of live IAV; therefore, in the future it will be necessary to increase the dose of UV-inactivated IAV that is given, to match the antigen concentration to that of the second dose, live IAV. However, because live IAV can actively initiate production of more viral proteins, it is highly likely that, regardless of the NP concentration in the initial inoculum, the antigen burden reaches higher levels in the lungs following administration of live IAV than the levels achieved with a single administration of UV-inactivated IAV. Therefore, to more definitively separate the role of protein antigen from the role of a replicating pathogen in promoting AICD-mediated CD8 T cell apoptosis, in the future, it will be necessary to compare the levels of IAV NP that are present in the lungs at time points following administration of UV-inactivated IAV vs. administration of live, replicating IAV. Regardless, our results suggest that increased viral burden in the lungs can promote increased AICD-mediated CD8 T cell apoptosis and suggest that this mechanism may contribute to the reduced numbers of virus-specific CD8 T cells observed in the lungs following aDC depletion.

We demonstrate here that altering the viral burden in the lungs of IAV-infected mice leads to differential accumulation of pDC and CD8α^+ DC to the lungs. Knocking down the levels of viral antigen and viral replication in the lungs of aDC depleted mice resulted in increased pDC and CD8α^+ DC numbers in the lungs (Figure 37), while increasing viral titers in the lungs of IAV infected mice by administration of a second dose of live IAV resulted in a reduction in pulmonary pDC and CD8α^+ DC numbers (Figure 37). It is interesting to note that a similar phenotype arises in the lungs following a lethal vs. sublethal challenge with IAV (264). Mice infected with a lethal dose inoculum of IAV exhibit a significant reduction in the numbers of pDC and CD8α^+ DC that accumulate in the lungs compared to mice infected with a sublethal dose inoculum (264). At this time, the mechanism contributing to this change in pulmonary DC

accumulation in the lungs following IAV infection remains unclear. However, it is possible that alterations in the pulmonary antigen load are contributing to a differential recruitment of these cells to the lungs, particularly since these changes in viral burden undoubtedly alter the inflammatory environment in the lungs of IAV infected mice. We have demonstrated that lung-resident aDC play an important role in recruiting pDC to the lungs, while lung-resident iDC are critical for recruiting CD8α^+ DC to the lungs following IAV infection (264). While it is currently unclear what specific factors contribute to pulmonary DC subset recruitment, our preliminary experiments suggest that aDC may recruit pDC via CXCL12 and CXCL1 interactions with CXCR4 and CXCR3, respectively, while iDC may recruit CD8α^+ DC via CCL2 interactions with CCR5 and CCRL-1 (data not shown). We demonstrate in Figure 37 that, relative to pDC and CD8α^+ DC numbers, there are similar changes in the numbers of aDC and iDC present in the lungs following administration of a second dose of live IAV or Oseltamivir treatment, suggesting that alterations aDC- and iDC-produced CXCL12, CXCL1 and CCL2 may translate into changes in pDC and CD8α^+ DC recruitment to the lungs.

Another possible explanation for the differential accumulation of pulmonary DC subsets that we observe following administration of a second dose of live IAV or Oseltamivir treatment is that the alterations in the lung environment resulting from increased antigen burden or increased viral replication induce increased death of these cells therein. IL-15 levels are decreased in the lungs following aDC depletion (Figure 25). While it is currently unknown what effects the changes in pulmonary viral burden and inflammation have on the local levels of IL-15, based upon our results in Chapter IV, a reduction in pulmonary pDC and CD8α^+ DC numbers is likely also resulting in a reduction in IL-15 levels in the lungs. In addition to its role as a survival factor for effector CD8 T cells, IL-15 has also been described to promote increased survival of DC (165). Together, these results suggest that the reduced accumulation of pulmonary pDC and CD8α^+ in the lungs of second dose IAV mice (Figure 37) or lethal dose IAV mice

(264) may result from reduced levels of IL-15, or, conceivably, other essential DC survival factors. Along these lines, although it is currently unknown what effect UV-inactivated IAV administration has on pulmonary pDC and CD8α^+ DC accumulation, a potential explanation for why administration of UV-inactivated IAV does not result in a change in virus-specific CD8 T cell numbers is because UV-inactivated IAV does not mediate the same inflammatory changes in the lungs as live IAV (76, 279), and thus may not as drastically alter the inflammatory cytokine/chemokine environment or the innate cellular infiltrate therein. Ultimately, the role of antigen burden/inflammation in regulating the accumulation of both pulmonary DC and virus-specific CD8 T cells in the lungs remains unclear; however, our results suggest that alterations in IAV load may play an important functional role in regulating AICD-mediated apoptosis and the magnitude of the virus-specific CD8 T cell response in the lungs following IAV infection.

Figure 33. Pulmonary DC reconstitution of aDC depleted mice results in decreased viral titers in the lungs. Groups of BALB/c mice were infected with a sublethal dose of IAV +/- aDC depletion as in Figure 5. On day 3 p.i., groups of aDC depleted mice were then reconstituted i.n. with $2x10^4$ pulmonary pDC (light grey bars) or $CD8\alpha^+$ DC (dark grey bars) purified from the lungs of IAV-infected donors. On days 4, 5 and 6 p.i., the lungs were examined for viral titers using endpoint dilution assay. Data are pooled from 2-3 separate experiments with n=6-8 mice/group. Shown are means ± SEM.

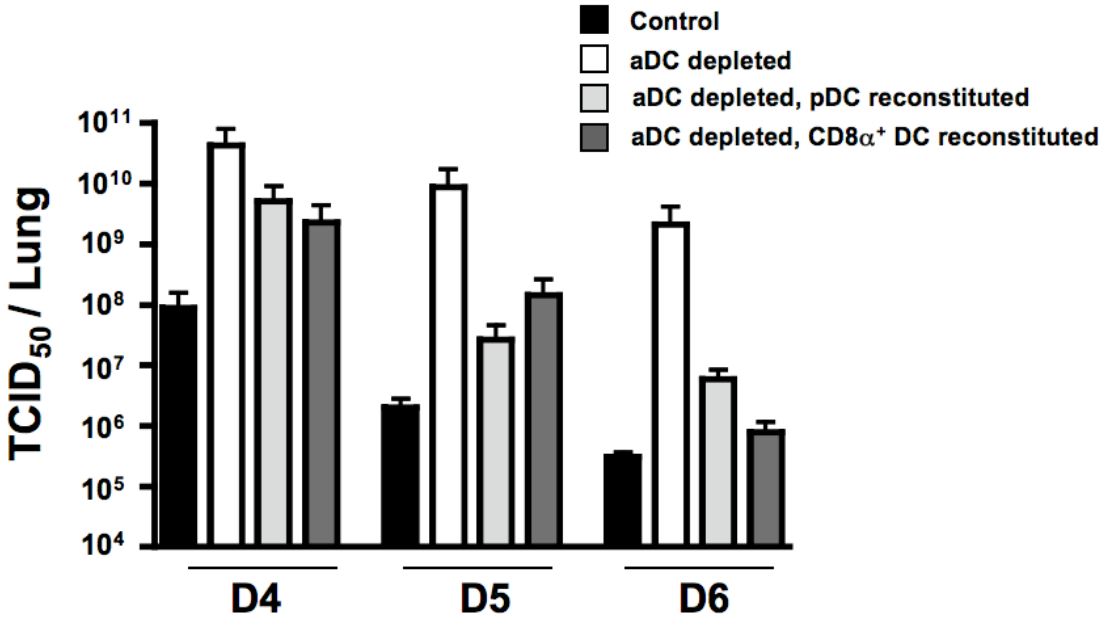
Control
aDC depleted
aDC depleted, pDC reconstituted
aDC depleted, CD8α+ DC reconstituted
TCID50 / Lung
10^11
10^10
10^9
10^8
10^7
10^6
10^5
10^4
D4
D5
D6

Figure 34. Oseltamivir treatment of aDC depleted mice results in reduced pulmonary antigen loads. Groups of BALB/c mice were infected with a sublethal dose of IAV +/- aDC depletion as in Figure 5. On days 2, 3 and 4 p.i., mice were treated with 2 mg/kg/day Oseltamivir by oral gavage. On day 5 p.i., mice were sacrificed and their lungs assessed for antigen load as measured by ELISA for IAV NP protein. Data are representative of 1 experiment with n= 3 mice/group. Shown are means ± SEM.

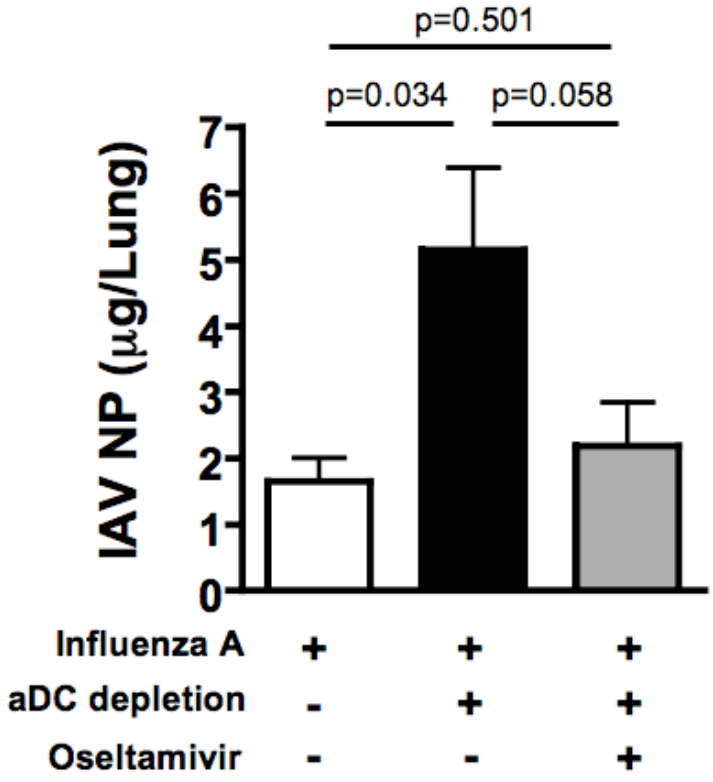
p=0.501
p=0.034
p=0.058
IAV NP (μg/Lung)
0
1
2
3
4
5
6
7
Influenza A + + +
aDC depletion - + +
Oseltamivir - - +

Figure 35. The effects of altering pulmonary antigen load on the CD8 T cell response in the lungs following IAV infection. Groups of BALB/c mice were infected with a sublethal dose of IAV +/- aDC depletion as in Figure 5. On days 2, 3 and 4 p.i., one group was treated with Oseltamivir Phosphate by oral gavage as in Figure 34 (dark grey bars). On day 3, one group of mice received a second dose of live IAV i.n. (light grey bars). Control mice received only one dose of IAV (white bars) or received IAV plus aDC depletion at 48 hours p.i. without Oseltamivir treatement (black bars). On day 5 p.i., the mice were sacrificed and their lungs assessed by flow cytometry for total numbers of virus-specific CD8 T cells (A) and apoptosis of virus-specific CD8 T cells as measured by the presence of active caspase 3/7 (B). Data are pooled from 2 independent experiments and represent means ± SEM. n= 7-9 mice/group.

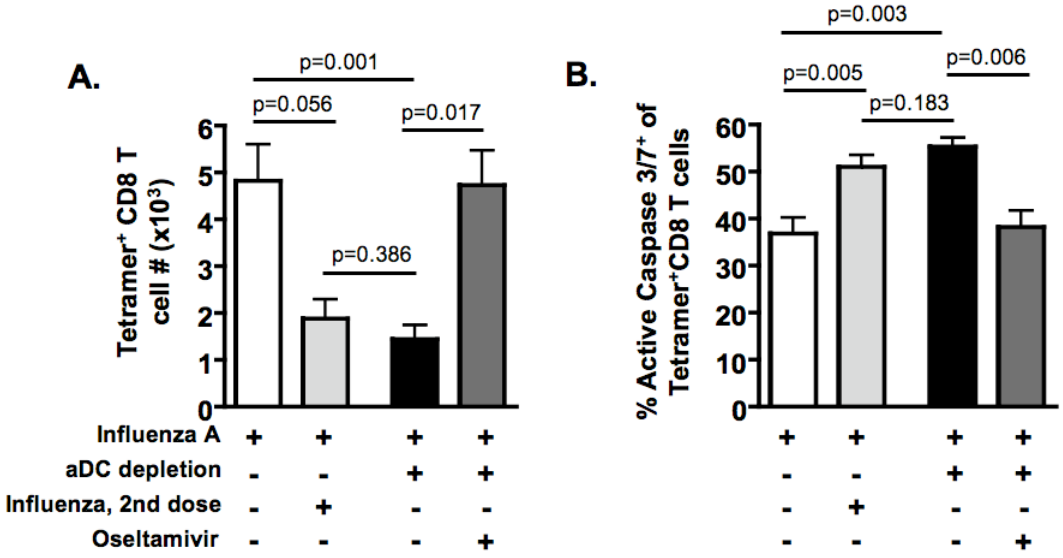
A.
p=0.001
p=0.056
p=0.017
p=0.386
Tetramer+ CD8 T cell # (x10³)
0
1
2
3
4
5
6
Influenza A + + + +
aDC depletion - - + +
Influenza, 2nd dose - + - -
Oseltamivir - - - +
B.
p=0.003
p=0.005
p=0.183
p=0.006
% Active Caspase 3/7+ of Tetramer+CD8 T cells
0
10
20
30
40
50
60
+ + + +
- - + +
- + - -
- - - +

Figure 36. The effects of altering pulmonary antigen load on the CD8 T cell response in the LN following IAV infection. Groups of BALB/c mice were infected with a sublethal dose of IAV as in Figure 5. On day 3, one group of mice received a second dose of live IAV i.n. (black bars) as in Figure 35. Control mice received only one dose of IAV (white bars). On day 5 p.i., the mice were sacrificed and their LN analyzed by flow cytometry for total numbers of virus-specific CD8 T cells. Data are pooled from 2 independent experiments and represent means ± SEM. n= 8 mice/group.

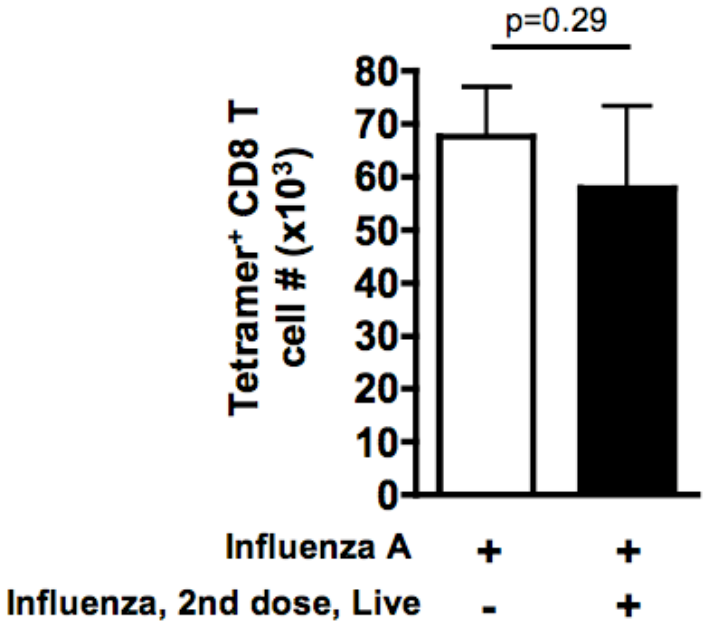
p=0.29
Tetramer+ CD8 T cell # (x10³)
80
70
60
50
40
30
20
10
0
Influenza A + +
Influenza, 2nd dose, Live - +

Figure 37. The effects of antigen load on pulmonary DC numbers in the lungs following IAV infection. Groups of BALB/c mice were infected with a sublethal dose of IAV +/- aDC depletion as in Figure 5. On days 2, 3 and 4 p.i., one group was treated with Oseltamivir Phosphate by oral gavage as in Figure 34 (dark grey bars). On day 3, one group of mice received a second dose of live IAV i.n. (light grey bars). Control mice received only one dose of IAV (white bars) or received IAV plus aDC depletion at 48 hours p.i. without Oseltamivir treatement (black bars). On day 5 p.i., the mice were sacrificed and their lungs assessed by flow cytometry for total numbers of pDC (A), $CD8\alpha^+$ DC (B), aDC (C) and iDC (D). Data are pooled from 2 independent experiment and represent means ± SEM. n= 9-10 mice/group.

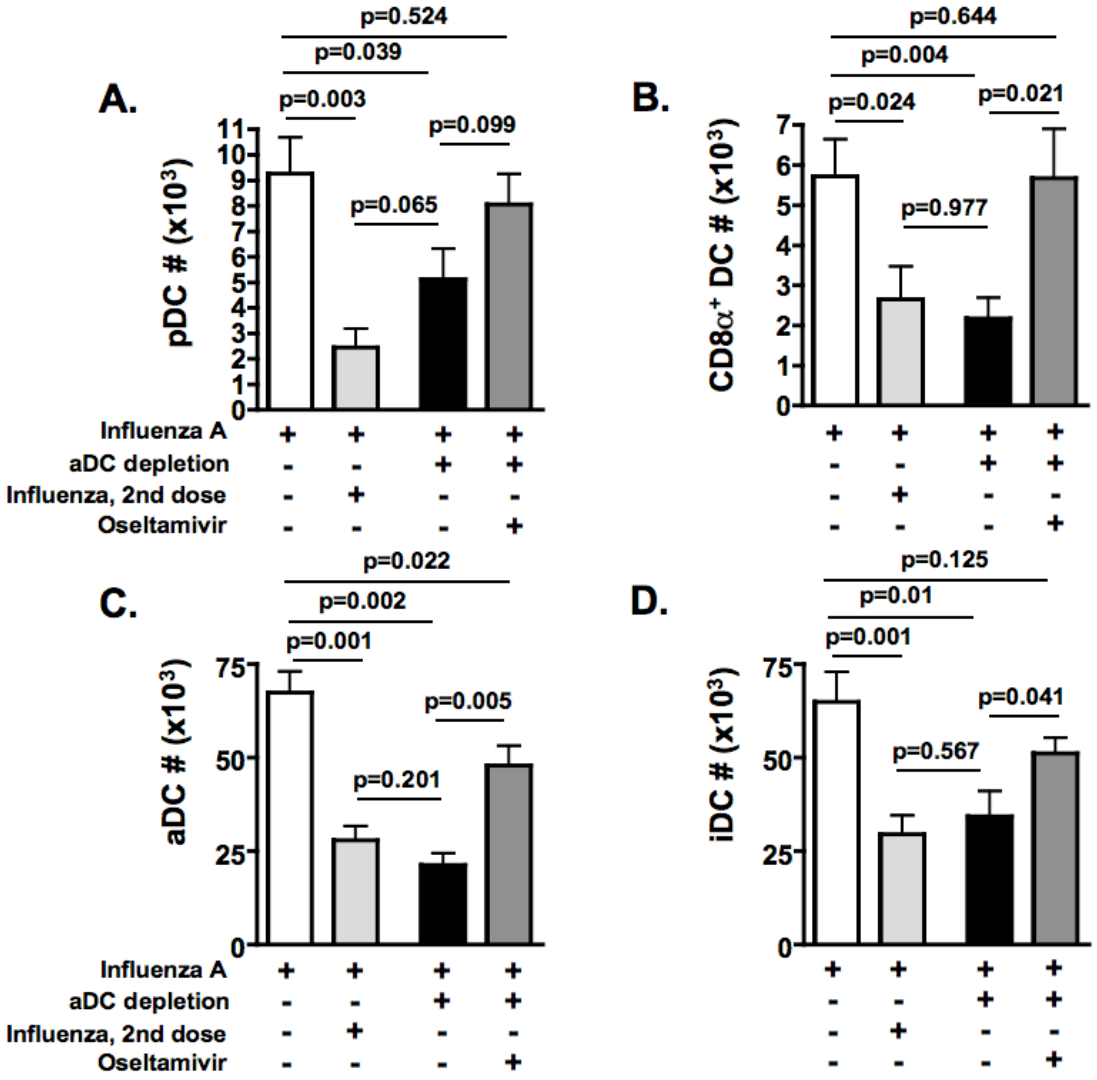
A.
p=0.524
p=0.039
p=0.003
p=0.099
p=0.065
pDC # (x10³)
B.
p=0.644
p=0.004
p=0.024
p=0.021
p=0.977
CD8α⁺ DC # (x10³)
C.
p=0.022
p=0.002
p=0.001
p=0.005
p=0.201
aDC # (x10³)
D.
p=0.125
p=0.01
p=0.001
p=0.041
p=0.567
iDC # (x10³)
Influenza A
aDC depletion
Influenza, 2nd dose
Oseltamivir

Figure 38. Blocking Fas/FasL interactions in aDC depleted mice rescues the virus-specific CD8 T cell response in the lungs. Groups of BALB/c mice were infected with a sublethal dose of IAV +/- aDC depletion as in Figure 5. On days 4 and 5 p.i., mice received Fas:Fc or control Fc chimeras i.n.. On days 5 (A and B) and 6 p.i. (C), the mice were sacrificed and their lungs assessed by flow cytometry for apoptosis of virus-specific CD8 T cells as measured by the frequency of active caspase $3/7^{+}$ of IAV-specific CD8 T cells (A) and total numbers of virus-specific CD8 T cells as measured by MHC I tetramers (B and C). No significant differences were observed between non-depleted control mice that received Fas:Fc or control Fc chimeras. Data are pooled from 2 independent experiments and represent means ± SEM. n= 6-8 mice/group.

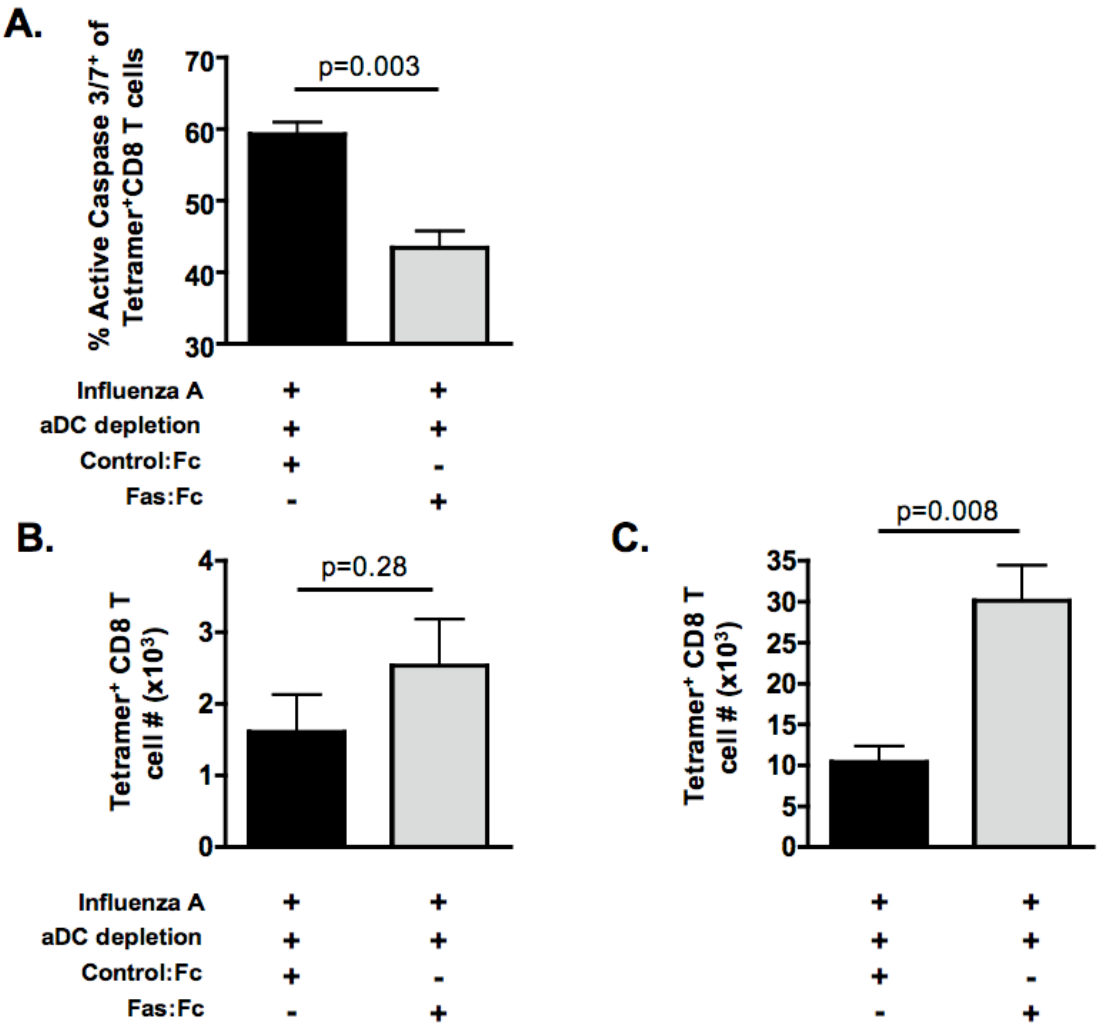
A.
% Active Caspase 3/7+ of Tetramer+CD8 T cells
70
60
50
40
30
p=0.003
Influenza A + +
aDC depletion + +
Control:Fc + -
Fas:Fc - +
B.
Tetramer+ CD8 T cell # (x10³)
4
3
2
1
0
p=0.28
Influenza A + +
aDC depletion + +
Control:Fc + -
Fas:Fc - +
C.
Tetramer+ CD8 T cell # (x10³)
35
30
25
20
15
10
5
0
p=0.008
+ +
+ +
+ -
- +

CHAPTER VI CONCLUSIONS

Synopsis

The overall purpose of this study was to achieve a detailed understanding of the pulmonary DC-mediated mechanisms that regulate virus-specific CD8 T cell immunity in the lungs following IAV infection. We previously demonstrated that the absence of specific pulmonary DC subsets, including pDC and CD8α^+ DC, from the lungs leads to a significant decrease in the number of virus-specific CD8 T cells (53). Reconstitution of the lungs with physiologic numbers of pDC or CD8α^+ DC is able to restore the pulmonary IAV-specific CD8 T cell response to near normal levels via a mechanism that is dependent upon direct DC:T cell interactions, DC-expressed MHC I and the presence of viral antigen (53). Herein, we demonstrate that the pulmonary DC subset-mediated rescue of IAV-specific CD8 T cell responses does not require DC costimulation via CD40, nor does in require CD8 T cell costimulation via CD28. Interestingly, however, pulmonary DC-mediated CD8 T cell rescue does appear to require costimulation via CD27, as blockade of DC-expressed CD70 results in a significant reduction in virus-specific CD8 T cell numbers that subsequently accumulate in the lungs. Further, it appears that "late" costimulation via OX40L and 4-1BBL can promote pulmonary pDC mediated rescue of virus-specific CD8 T cell responses in the C57BL/6 model, but not the BALB/c model, of IAV infection.

Importantly, we have previously observed that the reduction in T cell numbers observed in the lungs of aDC depleted mice following IAV challenge results not from impaired proliferation within the lungs, but instead is due to increased levels of apoptosis of virus-specific CD8 T cells compared to non-depleted controls (264). We demonstrate here that virus-specific CD8 T cells in the lungs of aDC depleted mice express alterations in several pro- and anti-apoptotic molecules compared to CD8 T cells from control lungs, including reduced levels of the pro-survival molecules Bcl-2 and Bcl-X_L and increased

levels of the pro-apoptotic molecules Bim, and active caspase 8 and 9. Together these results indicate that T cells from aDC depleted lungs undergo apoptosis via both ACAD- and AICD-mediated mechanisms. We further demonstrate that over-expression of Bcl-2, which can block both ACAD and AICD (20, 136, 137), is sufficient to rescue virus-specific CD8 T cells from apoptosis in the lungs of aDC depleted mice. Together, the results indicate that interactions between pulmonary DC and virus-specific CD8 T cells may provide key T cell survival signals that can induce upregulation of Bcl-2 or other anti-apoptotic molecules, hence promoting increased T cell survival.

In our model of IAV infection followed by aDC depletion at 48 hours p.i., we are altering both the antigen load and the inflammatory cytokine environment in the lungs, suggesting an important functional role for both ACAD and AICD. We demonstrate here that IAV infection induces upregulation of both IL-15 mRNA and protein in the lungs, while depletion of aDC at 48 hours p.i. results in a significant reduction in pulmonary IL-15 expression. Pulmonary DC reconstitution of aDC depleted lungs prevents virus-specific CD8 T cell apoptosis and induces increased expression of Bcl-2. Others have shown that IL-15 induces effector T cells to upregulate several pro-survival molecules, including Bcl-2 and Bcl-X_L (152). In conjunction with previous studies, we demonstrate that the rescue of CD8 T cell apoptosis and Bcl-2 expression is partially a result of DC-mediated trans-presentation of IL-15, as blockade of IL-15 or IL-15Rα on the surface of pulmonary DC prior to adoptive transfer, or transfer of IL-$15^{-/-}$ pulmonary DC subsets ablates the rescue of the virus-specific CD8 T cell response in the lungs of aDC depleted mice. Together our results demonstrate that virus-specific CD8 T cells require trans-presentation of IL-15 by pulmonary DC subsets in the lungs following IAV infection in order to avoid ACAD-mediated apoptosis.

Our previous studies have shown that aDC depleted mice express higher viral titers in the lungs compared to their non-depleted control counterparts (53), suggesting an increased likelihood for virus-specific CD8 T cells to encounter antigen in the absence of

the proper costimulatory molecules, and hence an increased likelihood of T cell apoptosis by AICD. We demonstrate here that altering the antigen burden and/or levels of viral replication in the lungs following IAV infection has an effect on CD8 T cell survival therein, possibly by altering the number of pDC and CD8α^+ DC available for interaction with the T cells. Increased antigen burden in the lungs results in reduced pulmonary DC subset accumulation, increased CD8 T cell apoptosis and subsequently reduced pulmonary CD8 T cell numbers; while a reduction in the pulmonary antigen burden results in increased pulmonary DC subset accumulation, decreased CD8 T cell apoptosis and increased CD8 T cell accumulation in the lungs. Together, these results suggest an important role for excessive antigen presentation in the lungs in promoting increased AICD-mediated T cell apoptosis in the lungs of aDC depleted mice. We further demonstrate that blockade of FasL, a molecule that is often associated with AICD (20, 136, 137), results in reduced apoptosis and increased numbers of virus-specific CD8 T cells in the lungs of aDC depleted mice. Together, our results demonstrate a functional role for antigen burden and FasL-associated AICD in regulating CD8 T cell immunity in the lungs following IAV infection.

Future Directions

We have made several novel observations concerning the role of pulmonary DC in regulating CD8 T cell immunity that require further studies. Our studies have described several components of the immune response that appear to contribute to the ability of pulmonary DC to regulate CD8 T cell accumulation in the lungs following IAV infection, including the late costimulatory molecules 4-1BBL, OX40L and CD70 in Chapter II, and the important survival cytokine IL-15 in Chapter IV. While the experiments discussed herein address each component individually, there is likely a complex interplay between these immune components, and even additional, as yet to be identified components, that can promote enhanced CD8 T cell immunity in the lungs.

For example, IL-15 signaling has been demonstrated to promote increased expression of CD70 and 4-1BBL (162, 280). It is conceivable that the reduced levels of IL-15 observed in the lungs of aDC depleted mice may contribute to reduced expression of 4-1BBL or CD70 on the few pulmonary DC present therein, and hence, result in a reduction in the subsequent CD8 T cell response in the lungs. Further, type I IFN has been described to promote both increased IL-15 production (162) and increased expression of 4-1BBL and CD70 (178-180, 207). Not surprisingly, given the reduction in pulmonary APC numbers, our preliminary results suggest that levels of type I IFN are reduced in the lungs of aDC depleted mice compared to their control counterparts. This initial reduction in type I IFN in aDC depleted lungs could contribute to the striking reduction in IL-15 expression observed in Figure 25, and similarly, contribute to reduced expression of the costimulatory molecules CD70 and 4-1BBL in the lungs, together resulting in the reduced CD8 T cell response therein. Importantly, we demonstrate that Bcl-2 and Bcl-X_L expression is reduced in virus-specific CD8 T cells in the lungs of aDC depleted mice (Chapter III), but that pulmonary DC reconstitution rescues Bcl-2 expression to normal levels (Chapter IV). Bcl-2 and Bcl-X_L expression by effector T cells is upregulated by numerous factors, including type I IFN, IL-15 and costimulation via 4-1BB and CD70 (57, 58, 113, 114, 175, 176, 193), suggesting that any one or combination of these factors may be contributing to the pulmonary DC mediated rescue of Bcl-2 expression and hence, CD8 T cell survival. As an added complexity, our experiments in Chapter V revealed a novel role for antigen burden in regulating both pDC and CD8α^+ DC accumulation and CD8 T cell survival in the lungs, suggesting that the viral load may dictate the nature of the evolving immune response and the availability of/necessity for many of the factors identified herein. Ultimately, our model of IAV-infection and aDC depletion has elucidated the complex and dynamic system of local regulation of T cell responses by pulmonary DC *in vivo*. However, much remains to be understood and in the future, it will be essential to determine how individual molecules

and cytokines interact and coexist to promote the development of an effective virus-specific CD8 T cell response, and ultimately mediate viral clearance and recovery.

We have demonstrated in Chapters II, III and IV that pulmonary pDC and CD8α^+ DC interact with virus-specific CD8 T cells to promote their increased survival and accumulation in the lungs following IAV infection. It is thought that these DC subsets localize to different locations within the lungs; CD8α^+ DC have been suggested to localize to iBALT (281, 282), while pDC are suggested to localize to the alveolar interstitium (106, 283). However, relatively little is known about the location of pulmonary pDC or CD8α^+ DC in the lungs during IAV infections, and it is unclear if these subsets interact with virus-specific CD8 T cells in the same or distinct locations within the lungs. In the future it will be necessary to perform a detailed microscopic analysis on the lungs following IAV infection to determine the location of pulmonary DC:T cell interactions in the lungs.

The rescue of virus-specific CD8 T cell immunity in aDC depleted lungs requires a direct interaction between T cells and pulmonary pDC or CD8α^+ DC (53). However, the kinetics of these interactions remain undefined. The length of T cell: DC contact in the LN can lead to diverse responses such as tolerance, proliferation without effector molecule expression, or full activation (284), suggesting that the kinetics of pulmonary DC:T cell interactions in the lungs may also result in differing immune outcomes. Further, it remains unclear if virus-specific CD8 T cells require a single interaction with pulmonary DC in the lungs, or if continuous or serial engagements are required in order to promote T cell survival and accumulation. We have demonstrated that reconstitution of aDC depleted lungs with pulmonary pDC and CD8α^+ DC results in increased Bcl-2 expression by virus-specific CD8 T cells (Figure 24). Conceivably, a single interaction with pulmonary DC trans-presenting IL-15 or expressing costimulatory CD70 or 4-1BBL could result in a sustained up-regulation of Bcl-2 that ensures T cell survival for the duration of the effector phase. However, it is equally likely that multiple interactions

with DC are required to promote the continued expression of pro-survival molecules such as Bcl-2. In this way, the immune system could utilize pulmonary DC:T cell interactions to titrate the length and magnitude of the effector response in the lungs. The continued presence of antigen-bearing DC subsets in the lungs would ensure the availability of key survival signals for virus-specific T cells therein and promote their continued survival and clearance of infected cells. With the resolution of the immune response, the antigen-bearing DC would eventually be cleared by the effector cells, thus limiting the survival signals and promoting T cell contraction. In the future it will be important to characterize these important parameters of pulmonary DC:T cell interactions and determine the requirements for promoting an effective, but not overly exuberant, virus-specific CD8 T cell response in the lungs following IAV infection.

We demonstrate in Chapter V that alterations in antigen burden in the lungs following IAV infection results in differential accumulation of pulmonary pDC and CD8α^+ DC to the lungs (Figure 37). In mice that received a second infection with live IAV, and therefore have increased antigen loads in the lungs, we observe a reduction in the numbers of pDC and CD8α^+ DC that accumulate therein. We observed a similar reduction in pDC and CD8α^+ DC accumulation in the lungs following a lethal infection with IAV compared to that accumulation observed following a sublethal infection (264). This suggests an important role for antigen levels, and likely, the inflammatory environment in the lungs, in regulating the accumulation of pulmonary DC subsets in the lungs following IAV infection. As discussed in Chapter V, while it remains unclear what specific factors are contributing to pulmonary pDC and CD8α^+ DC recruitment, our preliminary experiments suggest that aDC may recruit pDC via CXCL12 and CXCL1 interactions with CXCR4 and CXCR3, respectively, while iDC may recruit CD8α^+ DC via CCL2 interactions with CCR5 and CCRL-1. Future studies should be aimed at confirming the cell types and chemokines that are contributing to pDC and CD8α^+ DC recruitment to the lungs, and, more importantly, given the integral role of pDC and

CD8α^+ DC in regulating effector CD8 T cell immunity in the lungs, how changes in pathogen burden contribute to alterations in this recruitment.

Overall, we have described a novel role for pulmonary DC in regulating CD8 T cell immunity in the lungs during IAV infection. However, the role of these pulmonary DC subsets following infection with other respiratory pathogens, or in settings such as asthma or allergies, remains undefined. In addition, humans, unlike laboratory mice, encounter numerous infections during the course of their lifetime. It has been suggested in a model of asthma that pDC can be found in the lungs long after pulmonary insult (50). In separate studies, iBALT, and therefore potentially CD8α^+ DC, has been shown to be likewise retained at times well after pulmonary insult (281, 282). At this time it remains unclear how long pDC and CD8α^+ DC numbers remain elevated in the lungs following IAV infection; however, it will be important in the future to determine what effects the increased presence these essential pulmonary DC subsets have on both the regulation of IAV memory responses, as well as on the regulation of immune responses to other primary pathogen challenges.

Conclusions

Pulmonary pDC and CD8α^+ DC are integral to promoting effective CD8 T cell immunity in the lungs following IAV infection. In their absence, virus-specific CD8 T cells undergo increased apoptosis via both AICD and ACAD mediated mechanisms, resulting in a decrease in the magnitude of the effector CD8 T cell response in the lungs, and, subsequently, increased pulmonary viral titers and increased IAV-associated mortality. Pulmonary pDC and CD8α^+ DC utilize "late" costimulatory molecules such as CD70, 4-1BBL and OX40L and trans-presentation of IL-15 in order to promote the increased survival and accumulation of virus-specific CD8 T cells in the lungs following IAV infection.

The results detailed in Chapters II-V led us to propose the model outlined in Figure 39. Following a primary IAV infection, pulmonary DC migrate from the lungs to the LN where they, and LN-resident DC, interact with naïve, virus-specific CD8 T cells to iniate a program of activation, proliferation and differentiation into cytotoxic effector cells. These activated effector cells then migrate from the LN to the lungs. Therein, they require a second interaction with pulmonary pDC or CD8α^+ DC via a mechanism that requires direct DC:T cell contact, MHC I and viral antigen, trans-presentation of IL-15 (Chapter IV) and costimulation via CD70 and, in some cases 4-1BBL or OX40L (Chapter II). In the absence of these pulmonary DC-mediated survival signals, virus-specific CD8 T cells express reduced levels of the pro-survival molecule Bcl-2 and undergo increased apoptosis as a result of both ACAD and AICD- mediated pathways (Chapter III). However, interactions with pulmonary DC subsets promote increased expression of Bcl-2 by virus-specific CD8 T cells and hence, their increased survival in the lungs following IAV infection. The increased survival of CD8 T cells in the lungs results in enhanced viral clearance, and ultimately, recovery from infection.

Collectively, the results detailed here suggest that DC subsets recruited to the lungs during IAV infection play an essential role in promoting productive IAV- specific CD8 T cell responses and therefore, more effective viral clearance and recovery from disease. Specifically, this knowledge furthers our understanding of antiviral immune responses in the lungs. Importantly, these results suggest a critical role for pulmonary DC is shaping the lung environment and the immune responses therein. In the future, manipulating the numbers and types of DC subsets recruited into the lungs may be a valuable therapeutic approach for promoting more efficient protection from or control of respiratory diseases, such as viral and bacterial infections and asthma, while minimizing damaging lung immunopathology.

Figure 39. Model for the role of pulmonary DC in the lungs following IAV infection. 1) rDC lining the airways and alveolar spaces of the lungs acquire influenza antigen either through direct infection or uptake of apoptotic bodies from infected epithelial cells. rDC undergo maturation and migration to the lung draining LN. 2) Once in the LN, rDC pass on antigen to LN-resident $CD8\alpha^+$ DC. Both LN-resident $CD8\alpha^+$ DC and rDC interact with naïve antigen-specific CD8 T cells in the LN and initiate a program of activation, proliferation and differentiation into cytotoxic effector cells. 3) Activated effector CD8 T cells migrate from the LN to the lungs. 4) CD8 T cells undergo a second direct interaction with MHC I expressing, viral antigen-presenting pulmonary pDC or $CD8\alpha^+$ DC and receive survival signals via "late" costimulation of CD27, 4-1BB, or OX40 and trans-presentation of IL-15. These survival signals inhibit CD8 T cell apoptosis via AICD- and ACAD- mediated mechanisms and induce upregulation of Bcl-2, thus promoting increased T cell accumulation, enhanced viral clearance and ultimately, disease recovery and protection.

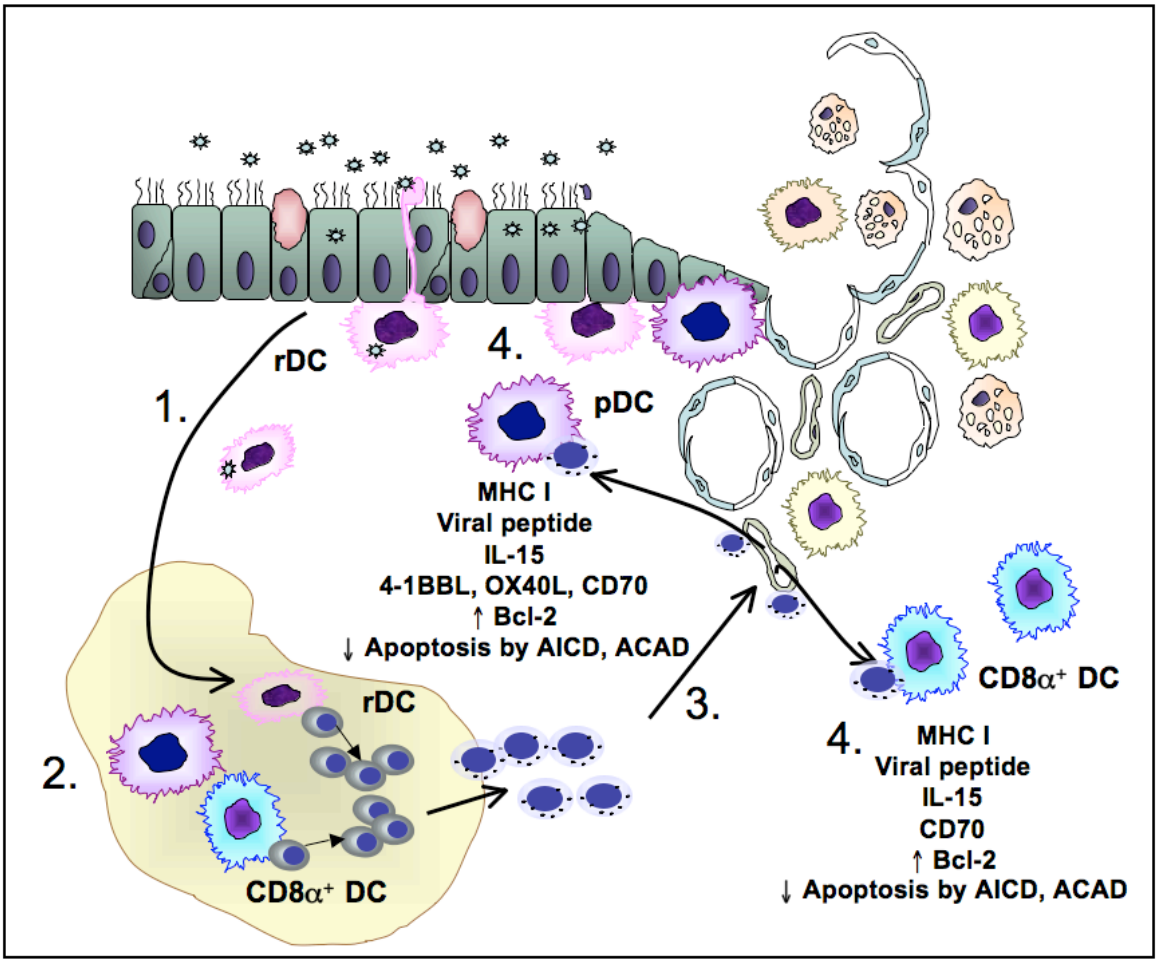
1.
rDC
2.
rDC
CD8α⁺ DC
3.
4.
pDC
MHC I
Viral peptide
IL-15
4-1BBL, OX40L, CD70
↑ Bcl-2
↓ Apoptosis by AICD, ACAD
4.
CD8α⁺ DC
MHC I
Viral peptide
IL-15
CD70
↑ Bcl-2
↓ Apoptosis by AICD, ACAD

REFERENCES

1. Barker, W. H., and J. P. Mullooly. 1980. Impact of epidemic type A influenza in a defined adult population. *J Epidemiol.* 112:798-811.

2. Barker, W. H., and J. P. Mullooly. 1982. Pneumonia and influenza deaths during epidemics: implications for prevention. *Arch Intern Med.* 142:85-89.

3. Singleton, J. A., P. Wortley, and P. J. Lu. 2004. Influenza vaccination of persons with cardiovascular disease in the United States. *Tex Heart Inst J.* 31:22-27.

4. Thompson, W. W., L. Comanor, and D. K. Shay. 2006. Epidemiology of seasonal influenza: use of surveillance data and statistical models to estimate the burden of disease. *J Infect Dis* 194 Suppl 2:S82-91.

5. Horimoto, T., and Y. Kawaoka. 2001. Pandemic threat posed by avian influenza A viruses. *Clin Microbiol Rev* 14:129-149.

6. Palese, P. 2004. Influenza: old and new threats. *Nat Med* 10:82-87.

7. Tumpey, T. M., A. Garcia-Sastre, J. K. Taubenberger, P. Palese, D. E. Swayne, and C. F. Basler. 2004. Pathogenicity and immunogenicity of influenza viruses with genes from the 1918 pandemic virus. *Proc Natl Acad Sci USA* 101:3166-3171.

8. Subbarao, K., B. R. Murphy, and A. S. Fauci. 2006. Development of effective vaccines against pandemic influenza. *Immunity* 24:5-9.

9. Horimoto, T., and Y. Kawaoka. 2005. Influenza: lessons from past pandemics, warnings from current incidents. *Nat Rev Microbiol.* 3:591-600.

10. Nayak, D. P., E. K. Hui, and S. Barman. 2004. Assembly and budding of influenza virus. *Virus Res* 106:147-165.

11. Lamb, R. A. a. R. M. K. 2001. *Orthomyxoviridae:* The Viruses and Their Replication. In *Fields Virology*. D. M. a. P. M. H. Knipe, ed. Lippincott Williams & Wilkins, Philadelphia, PA.

12. Phipps-Yonas, H., J. Seto, S. C. Sealfon, T. M. Moran, and A. Fernandez-Sesma. 2008. Interferon-beta pretreatment of conventional and plasmacytoid human dendritic cells enhances their activation by influenza virus. *PLoS Pathog* 4:e1000193.

13. Lawrence, C. W., and T. J. Braciale. 2004. Activation, differentiation, and migration of naive virus-specific CD8+ T cells during pulmonary influenza virus infection. *J Immunol.* 173:1209-1218.

14. Lawrence, C. W., R. M. Ream, and T. J. Braciale. 2005. Frequency, specificity, and sites of expansion of CD8+ T cells during primary pulmonary influenza virus infection. *J Immunol.* 174:5332-5340.

15. Stambas, J., C. Guillonneau, K. Kedzierska, J. D. Mintern, P. C. Doherty, and N. L. La Gruta. 2008. Killer T cells in influenza. *Pharmacol Ther* 120:186-196.

16. Hale, B. G., R. A. Albrecht, and A. Garcia-Sastre. Innate immune evasion strategies of influenza viruses. *Future Microbiol* 5:23-41.

17. Hamilton-Easton, A., and M. Eichelberger. 1995. Virus-specific antigen presentation by different subsets of cells from lung and mediastinal lymph node tissues of influenza virus-infected mice. *J Virol* 69:6359-6366.

18. Der, S. D., A. Zhou, B. R. Williams, and R. H. Silverman. 1998. Identification of genes differentially regulated by interferon alpha, beta, or gamma using oligonucleotide arrays. *Proc Natl Acad Sci U S A* 95:15623-15628.

19. Kang, D. C., R. V. Gopalkrishnan, Q. Wu, E. Jankowsky, A. M. Pyle, and P. B. Fisher. 2002. mda-5: An interferon-inducible putative RNA helicase with double-stranded RNA-dependent ATPase activity and melanoma growth-suppressive properties. *Proc Natl Acad Sci U S A* 99:637-642.

20. Marrack, P., and J. Kappler. 2004. Control of T cell Viability. *Annu Rev Immunol.* 22:765-787.

21. Marrack, P., J. Kappler, and T. Mitchell. 1999. Type I interferons keep activated T cells alive. *J Exp Med.* 189:521-530.

22. Price, G. E., A. Gaszewska-Masterlzar, and D. Moskophidis. 2000. The role of alpha/beta and gamma interferons in development of immunity to influenza A virus in mice. *J Virol.* 74:3996-4003.

23. Curtsinger, J. M., D. C. Lins, and M. F. Mescher. 2005. Signal 3 tolerant CD8 T cells degranulate in response to antigen but lack granzyme B to mediate cytolysis. *J Immunol.* 175:4392-4399.

24. Curtsinger, J. M., C. S. Schmidt, A. Mondino, D. C. Lins, R. M. Kedl, and et al. 1999. Inflammatory cytokines provide a third signal for activation of naive CD4+ and CD8+ T cells. *J Immunol.* 162:3256-3262.

25. Durbin, J. E., A. Fernandez-Sesma, C. K. Lee, T. D. Rao, A. B. Frey, T. M. Moran, S. Vukmanovic, A. Garcia-Sastre, and D. E. Levy. 2000. Type I IFN modulates innate and specific antiviral immunity. *J Immunol.* 164:4220-4228.

26. Horisberger, M. A. 1995. Interferons, Mx genes, and resistance to influenza virus. *Am J Respir Crit Care Med* 152:S67-71.

27. Horisberger, M. A., and H. K. Hochkeppel. 1985. An interferon-induced mouse protein involved in the mechanism of resistance to influenza viruses. Its purification to homogeneity and characterization by polyclonal antibodies. *J Biol Chem.* 260:1730-1733.

28. Kolumam, G. A., S. Thomas, L. J. Thompson, J. Sprent, and K. Murali-Krishna. 2005. Type I interferons act directly on CD8 T cells to allow clonal expansion and memory formation in response to viral infection. *J Exp Med.* 202:637-650.

29. Le Bon, A., V. Durand, E. Kamphuis, C. Thompson, S. Bulfone-Paus, and et al. 2006. Direct stimulation of T cells by type I IFN enhances the CD8+ T cell response during cross-priming. *J Immunol.* 176:4682-4689.

30. Le Bon, A., N. Etchart, C. Rossmann, M. Ashton, S. Hou, and et al. 2003. Cross-priming of CD8+ T cells stimulated by virus-induced type I interferon. *Nat Immunol.* 4:1009-1015.

31. Yamada, Y. K., A. Meager, A. Yamada, and F. A. Ennis. 1986. Human interferon alpha and gamma production by lymphocytes during the generation of influenza virus-specific cytotoxic T lymphocytes. *J Gen Virol.* 67 (Pt 11):2325-2334.

32. Garcia-Sastre, A., A. Egorov, D. Matassov, S. Brandt, D. E. Levy, J. E. Durbin, P. Palese, and T. Muster. 1998. Influenza A virus lacking the NS1 gene replicates in interferon-deficient systems. *Virology* 252:324-330.

33. Fernandez-Sesma, A., S. Marukian, B. J. Ebersole, D. Kaminski, M. S. Park, T. Yuen, S. C. Sealfon, A. Garcia-Sastre, and T. M. Moran. 2006. Influenza virus evades innate and adaptive immunity via the NS1 protein. *J Virol* 80:6295-6304.

34. Kochs, G., A. Garcia-Sastre, and L. Martinez-Sobrido. 2007. Multiple anti-interferon actions of the influenza A virus NS1 protein. *J Virol* 81:7011-7021.

35. Wang, X., M. Li, H. Zheng, T. Muster, P. Palese, A. A. Beg, and A. Garcia-Sastre. 2000. Influenza A virus NS1 protein prevents activation of NF-kappaB and induction of alpha/beta interferon. *J Virol* 74:11566-11573.

36. Lopez, C. B., A. Garcia-Sastre, B. R. Williams, and T. M. Moran. 2003. Type I interferon induction pathway, but not released interferon, participates in the maturation of dendritic cells induced by negative-strand RNA viruses. *J Infect Dis* 187:1126-1136.

37. Holt, P. G., D. J. Nelson, and A. S. McWilliam. 1995. Population dynamics and functions of respiratory tract dendritic cells in the rat. *Adv Exp Med Biol.* 378:177-181.

38. Vermaelen, K., and R. Pauwels. 2004. Accurate and simple discrimination of mouse pulmonary dendritic cell and macrophage populations by flow cytometry: methodology and new insights. *Cytometry A* 61:170-177.

39. Vermaelen, K., and R. Pauwels. 2005. Pulmonary dendritic cells. *Am J Respir Cell Mol Biol.* 172:530-551.

40. Vermaelen, K. Y., I. Carro-Muino, B. N. Lambrecht, and R. A. Pauwels. 2001. Specific migratory dendritic cells rapidly transport antigen from the airways to the thoracic lymph nodes. *J Exp Med.* 193:51-60.

41. von Garnier, C., L. Filgueira, M. Wikstrom, M. Smith, J. A. Thomas, D. H. Strickland, P. G. Holt, and P. A. Stumbles. 2005. Anatomical location determines the distribution and function of dendritic cells and other APCs in the respiratory tract. *J Immunol.* 175:1609-1618.

42. Pollard, A. M., and M. F. Lipscomb. 1990. Characterization of murine lung dendritic cells: similarities to Langerhans cells and thymic dendritic cells. *J Exp Med.* 172:159-167.

43. Holt, P. G., M. A. Schon-Hegrad, and J. Oliver. 1988. MHC class II antigen-bearing dendritic cells in pulmonary tissues of the rat. Regulation of antigen presentation activity by endogenous macrophage populations. *J Exp Med.* 167:262-274.

44. Stumbles, P. A., J. W. Upham, and P. G. Holt. 2003. Airway dendritic cells: co-ordinators of immunological homeostasis and immunity in the respiratory tract. *APMIS* 111:741-755.

45. Lambrecht, B. N., and H. Hammad. 2003. Taking our breath away: dendritic cells in the pathogenesis of asthma. *Nat Rev Immunol.* 3:994-1003.

46. Shortman, K., and Y. J. Liu. 2002. Mouse and Human Dendritic Cell Subtypes. *Nat Rev Immunol.* 2:151-161.

47. McWilliam, A. S., S. Napoli, A. M. Marsh, F. L. Pemper, D. J. Nelson, C. L. Pimm, P. A. Stumbles, T. N. Wells, and P. G. Holt. 1996. Dendritic cells are recruited into the airway epithelium during the inflammatory response to a broad spectrum of stimuli. *J Exp Med.* 184:2429-2432.

48. McWilliam, A. S., D. Nelson, J. A. Thomas, and P. G. Holt. 1994. Rapid dendritic cell recruitment is a hallmark of the acute inflammatory response at mucosal surfaces. *J Exp Med.* 179:1331-1336.

49. Byersdorfer, C. A., and D. D. Chaplin. 2001. Visualization of early APC/T cell interactions in the mouse lung following intranasal challenge. *J Immunol.* 167:6756-6764.

50. De Heer, H. J., H. Hammad, T. Soullie, D. Hijdra, N. Vos, M. A. Willart, H. C. Hoogsteden, and B. N. Lambrecht. 2004. Essential role of lung plasmacytoid dendritic cells in preventing asthmatic reactions to harmless inhaled antigen. *J Exp Med.* 200:89-98.

51. Legge, K. L., and T. J. Braciale. 2003. Accelerated Migration of Respiratory Dendritic Cells to the Regional Lymph Nodes is Limited to the Early Phase of Pulmonary Infection. *Immunity.* 18:265-277.

52. Lin, K. L., Y. Suzuki, H. Nakano, E. Ramsburg, and M. D. Gunn. 2008. CCR2+ monocyte-derived dendritic cells and exudate macrophages produce influenza-induced pulmonary immune pathology and mortality. *J Immunol.* 180:2562-2572.

53. McGill, J., van Rooijen, N., Legge, K.L. 2008. Protective influenza-specific CD8 T cell responses require interactions with dendritic cells in the lungs. *J Exp Med.* 205:1635-1646.

54. Xia, W., C. E. Pinto, and R. L. Kradin. 1995. The antigen-presenting activities of Ia+ dendritic cells shift dynamically from lung to lymph node after an airway challenge with soluble antigen. *J Exp Med.* 181:1275-1283.

55. Yamamoto, N., S. Suzuki, A. Shirai, M. Suzuki, M. Nakazawa, Y. Nagashima, and T. Okubo. 2000. Dendritic cells are associated with augmentation of antigen sensitization by influenza A virus infection in mice. *Eur J Immunol* 30:316-326.

56. Doherty, P. C., and J. P. Christensen. 2000. Accessing complexity: the dynamics of virus-specific T cell responses. *Annu Rev Immunol.* 18:561-592.

57. Doherty, P. C., D. J. Topham, R. A. Tripp, R. D. Cardin, J. W. Brooks, and P. G. Stevenson. 1997. Effector CD4+ and CD8+ T cell mechanisms in the control of respiratory virus infections. *Immunol Rev.* 159:105-117.

58. Topham, D. J., R. A. Tripp, and P. C. Doherty. 1997. CD8+ T cells clear influenza virus by perforin or Fas-dependent processes. *J Immunol.* 159:5197-5200.

59. Wong, P., and E. G. Pamer. 2003. CD8 T cell responses to infectious pathogens. *Annu Rev Immunol.* 21:29-70.

60. Banchereau, J., F. Briere, C. Caux, J. Davoust, S. Lebecque, Y. J. Liu, B. Pulendran, and K. Palucka. 2000. Immunobiology of dendritic cells. *Annu Rev Immunol.* 18:767-811.

61. Banchereau, J., and R. M. Steinman. 1998. Dendritic cells and the control of immunity. *Nature* 392:245-252.

62. Guermonprez, P., J. Valladeau, L. Zitvogel, C. Thery, and S. Amigorena. 2002. Antigen presentation and T cell stimulation by dendritic cells. *Annu Rev Immunol.* 20:621-667.

63. Norbury, C. C., D. Malide, J. S. Gibbs, J. R. Bennink, and J. W. Yewdell. 2002. Visualizing priming of virus-specific CD8 T cells by infected dendritic cells in vivo. *Nat Immunol.* :265-271.

64. Bhardwaj, N., A. Bender, N. Gonzalez, L. K. Bui, M. C. Garrett, and R. M. Steinman. 1994. Influenza virus-infected dendritic cells stimulate strong proliferative and cytolytic responses from human CD8+ T cells. *J Clin Invest.* 94:797-807.

65. Bender, A., L. K. Bui, M. A. Feldman, M. Larsson, and N. Bhardwaj. 1995. Inactivated influenza virus, when presented on dendritic cells, elicits human CD8+ cytolytic T cell responses. *J Exp Med.* 182:1663-1671.

66. Bhardwaj, N., A. Bender, N. Gonzalez, L. K. Bui, M. C. Garrett, and R. M. Steinman. 1995. Stimulation of human anti-viral CD8+ cytolytic T lymphocytes by dendritic cells. *Adv Exp Med Biol.* 378:375-379.

67. Macatonia, S. E., P. M. Taylor, S. C. Knight, and B. A. Askonas. 1989. Primary stimulation by dendritic cells induces antiviral proliferative and cytotoxic T cell responses in vitro. *J Exp Med.* 169:1255-1264.

68. Nonacs, R., C. Humborg, J. P. Tam, and R. M. Steinman. 1992. Mechanisms of mouse spleen dendritic cell function in the generation of influenza-specific, cytolytic T lymphocytes. *J Exp Med.* 176:519-529.

69. Albert, M. L., B. Sauter, and N. Bhardwaj. 1998. Dendritic cells acquire antigen from apoptotic cells and induce class I-restricted CTLs. *Nature* 392:86-89.

70. Brydon, E. W., J. Smith, and C. Sweet. 2003. Influenza A virus-induced apoptosis in brochiolar epithelial cells limits pro-inflammatory cytokine release. *J Gen Virol.* 84:2389-2400.

71. Mori, I., T. Komatsu, K. Takeuchi, K. Nakakuki, M. Sudo, and Y. Kimua. 1996. In vivo induction of apoptosis by influenza virus. *J Gen Virol.* 76:2869-2873.

72. Sauter, B., M. Albert, L. Francisco, M. Larsson, S. Somersan, and N. Bhardwaj. 2000. Consequences of cell death: exposure to necrotic tumor cells, but not primary tissue cells or apoptotic cells, induces the maturation of immunostimulatory dendritic cells. *J Exp Med.* 191:434.

73. Gallucci, S., M. Lolkema, and P. Matzinger. 1999. Natural adjuvants: endogenous activators of dendritic cells. *Nat Med.* 5:1249-1255.

74. Wolff, A., A. Technau, C. Ihling, K. Technau-Ihling, R. Erber, F. X. Bosch, and G. Brandner. 2001. Evidence that wild-type p53 in neuroblastoma cells is in a conformation refractory to integration into the transcriptional complex. *Oncogene* 20:1307-1317.

75. Hao, X., T. S. Kim, and T. J. Braciale. 2008. Differential response of respiratory dendritic cell subsets to influenza virus infection. *J Virol* 82:4908-4919.

76. Legge, K. L., and T. J. Braciale. 2005. Lymph node dendritic cells control CD8+ T cell responses through regulated FasL expression. *Immunity* 23:649-659.

77. Technau-Ihling, K., C. Ihling, J. Kromeier, and G. Brandner. 2001. Influenza A virus infection of mice induces nuclear accumulation of the tumorsuppressor protein p53 in the lung. *Arch Virol* 146:1655-1666.

78. Dhodapkar, M. V., and R. M. Steinman. 2002. Antigen-bearing immature dendritic cells induce peptide-specific CD8+ regulatory T cells in vivo in humans. *Blood* 100:174-177.

79. Dhodapkar, M. V., R. M. Steinman, J. Krasovsky, C. Munz, and N. Bhardwaj. 2001. Antigen-specific inhibition of effector T cell function in humans after injection of immature dendritic cells. *J Exp Med.* 193:233-238.

80. Albert, M. L., S. F. Pearce, L. M. Francisco, B. Sauter, P. Roy, R. L. Silverstein, and N. Bhardwaj. 1998. Immature dendritic cells phagocytose apoptotic cells via alphavbeta5 and CD36, and cross-present antigens to cytotoxic T lymphocytes. *J Exp Med.* 188:1359-1368.

81. Belz, G. T., C. M. Smith, L. Kleinert, P. Reading, A. Brooks, K. Shortman, F. R. Carbone, and W. R. Heath. 2004. Distinct migrating and nonmigrating dendritic cell populations are involved in MHC class I-restricted antigen presentation after lung infection with virus. *Proc Natl Acad Sci USA.* 101:8670-8675.

82. Jakubzick, C., F. Tacke, J. Llodra, N. van Rooijen, and G. J. Randolph. 2006. Modulation of dendritic cell trafficking to and from the airways. *J Immunol.* 176:3578-3584.

83. Hammad, H., H. J. de Heer, T. Soullie, H. C. Hoogsteden, F. Trottein, and B. N. Lambrecht. 2003. Prostaglandin D2 inhibits airway dendritic cell migration and function in steady state conditions by selective activation of the D prostanoid receptor 1. *J Immunol.* 171:3936-3940.

84. Kim, T. S., and T. J. Braciale. 2009. Respiratory dendritic cell subsets differ in their capacity to support the induction of virus-specific cytotoxic CD8+ T cell responses. *PLoS ONE* 4:e4204.

85. Lambrecht, B. N., M. De Veerman, A. J. Coyle, J. C. Butierrez-Ramos, K. Thielemans, and R. A. Pauwels. 2000. Myeloid dendritic cells induce Th2 responses to inhaled antigen, leading to eosinophilic airway inflammation. *J Clin Invest.* 106:551-559.

86. Holt, P. G., and P. A. Stumbles. 2000. Regulation of immunologic homeostasis in peripheral tissues by dendritic cells: the respiratory tract as a paradigm. *J Allergy Clin Immunol* 105:421-429.

87. Holt, P. G. 2005. Pulmonary dendritic cells in local immunity to inert and pathogenic antigens in the respiratory tract. *Proc Am Thorac Soc* 2:116-120.

88. Yoon, H., K. L. Legge, S. S. Sung, and T. J. Braciale. 2007. Sequential activation of CD8+ T cells in the draining lymph nodes in response to pulmonary virus infection. *J Immunol* 179:391-399.

89. GeurtsvanKessel, C. H., M. A. Willart, L. S. van Rijt, F. Muskens, M. Kool, C. Baas, K. Thielemans, C. Bennett, B. E. Clausen, H. C. Hoogsteden, A. D. Osterhaus, G. F. Rimmelzwaan, and B. N. Lambrecht. 2008. Clearance of influenza virus from the lung depends on migratory langerin+CD11b- but not plasmacytoid dendritic cells. *J Exp Med* 205:1621-1634.

90. Belz, G. T., C. M. Smith, D. Eichner, K. Shortman, G. Karupiah, F. R. Carbone, and W. R. Heath. 2004. Cutting edge: conventional CD8 alpha+ dendritic cells are generally involved in priming CTL immunity to viruses. *J Immunol.* 172:1996-2000.

91. Carbone, F. R., G. T. Belz, and W. R. Heath. 2004. Transfer of antigen between migrating and lymph node-resident DCs in peripheral T-cell tolerance and immunity. *Trends Immunol.* 25:655-658.

92. Allan, R. S., J. Waithman, S. Bedoui, C. M. Jones, J. A. Villadangos, Y. Zhan, A. M. Lew, K. Shortman, W. R. Heath, and F. R. Carbone. 2006. Migratory dendritic cells transfer antigen to a lymph node-resident dendritic cell population for efficient CTL priming. *Immunity.* 25:153-162.

93. Allan, R. S., C. M. Smith, G. T. Belz, A. L. van Lint, L. M. Wakim, W. R. Heath, and F. R. Carbone. 2003. Epidermal viral immunity induced by CD8alpha+ dendritic cells but not by Langerhans cells. *Science.* 301:1925-1928.

94. Smith, C. M., G. T. Belz, N. S. Wilson, J. A. Villadangos, K. Shortman, F. R. Carbone, and W. R. Heath. 2003. Cutting edge: conventional CD8 alpha+ dendritic cells are preferentially involved in CTL priming after footpad infection with herpes simplex virus-1. *J Immunol.* 170:4437-4440.

95. Belz, G. T., K. Shortman, M. J. Bevan, and W. R. Heath. 2005. CD8alpha+ dendritic cells selectively present MHC Class I-restricted noncytolytic viral and intracellular bacterial antigens in vivo. *J Immunol.* 175:196-200.

96. Belz, G. T., S. Bedoui, F. Kupresanin, F. R. Carbone, and W. R. Heath. 2007. Minimal activation of memory CD8(+) T cell by tissue-derived dendritic cells favors the stimulation of naive CD8(+) T cells. *Nat Immunol.* 8:1060-1066.

97. Mount, A. M., C. M. Smith, F. Kupresanin, K. Stoermer, W. R. Heath, and G. T. Belz. 2008. Multiple dendritic cell populations activate CD4+ T cells after viral stimulation. *PLoS ONE.* 3:e1691.

98. Ingulli, E., C. Funatake, E. L. Jacovetty, and M. Zanetti. 2009. Cutting edge: antigen presentation to CD8 T cells after influenza A virus infection. *J Immunol.* 182:29-33.

99. Eichelberger, M. C., M. L. Wang, W. Allan, R. G. Webster, and P. C. Doherty. 1991. Influenza virus RNA in the lung and lymphoid tissue of immunologically intact and CD4-depleted mice. *J Gen Virol.* 72 (Pt 7):1695-1698.

100. Flynn, K. J., J. M. Riberdy, J. P. Christensen, J. D. Altman, and P. C. Doherty. 1999. In vivo proliferation of naive and memory influenza-specific CD8(+) T cells. *Proc Natl Acad Sci U S A.* 96:8597-8602.

101. Jelley-Gibbs, D. M., J. P. Dibble, D. M. Brown, T. M. Strutt, K. K. McKinstry, and S. L. Swain. 2007. Persistent depots of influenza antigen fail to induce a cytotoxic CD8 T cell response. *J Immunol.* 178:7563-7570.

102. Zammit, D. J., D. L. Turner, K. D. Klonowski, L. Lefrancois, and L. S. Cauley. 2006. Residual antigen presentation after influenza virus infection affects CD8 T cell activation and migration. *Immunity.* 24:439-449.

103. Mintern, J. D., S. Bedoui, G. M. Davey, J. M. Moffat, P. C. Doherty, and S. J. Turner. 2009. Transience of MHC Class I-restricted antigen presentation after influenza A virus infection. *Proc Natl Acad Sci U S A.* 106:6724-6729.

104. Jelley-Gibbs, D. M., D. M. Brown, J. P. Dibble, L. Haynes, S. M. Eaton, and S. L. Swain. 2005. Unexpected prolonged presentation of influenza antigens promotes CD4 T cell memory generation. *J Exp Med.* 202:697-706.

105. Khanna, K. M., C. C. Aguila, J. M. Redman, J. E. Suarez-Ramirez, L. Lefrancois, and L. S. Cauley. 2008. In situ imaging reveals different responses by naive and memory CD8 T cells to late antigen presentation by lymph node DC after influenza virus infection. *Eur J Immunol.* 38:3304-3315.

106. de Heer, H. J., H. Hammad, M. Kool, and B. N. Lambrecht. 2005. Dendritic cell subsets and immune regulation in the lung. *Sem Immunol.* 17:295-303.

107. Aldridge, J. R., Jr., C. E. Moseley, D. A. Boltz, N. J. Negovetich, C. Reynolds, J. Franks, S. A. Brown, P. C. Doherty, R. G. Webster, and P. G. Thomas. 2009. TNF/iNOS-producing dendritic cells are the necessary evil of lethal influenza virus infection. *Proc Natl Acad Sci U S A.* 106:5306-5311.

108. Smit, J. J., D. M. Lindell, L. Boon, M. Kool, B. N. Lambrecht, and N. W. Lukacs. 2008. The balance between plasmacytoid DC versus conventional DC determines pulmonary immunity to virus infections. *PLoS ONE.* 3:e1720.

109. Holt, P. G. 1978. Inhibitory activity of unstimulated alveolar macrophages on T-lymphocyte blastogenic response. *Am Rev Respir Dis.* 118:791-793.

110. Holt, P. G., J. Oliver, N. Bilyk, C. McMenamin, P. G. McMenamin, G. Kraal, and T. Thepen. 1993. Downregulation of the antigen presenting cell function(s) of pulmonary dendritic cells in vivo by resident alveolar macrophages. *J Exp Med.* 177:397-407.

111. Bilyk, N., and P. G. Holt. 1995. Cytokine modulation of the immunosuppressive phenotype of pulmonary alveolar macrophage populations. *Immunology.* 86:231-237.

112. Strickland, D. H., T. Thepen, U. R. Kees, G. Kraal, and P. G. Holt. 1993. Regulation of T-cell function in lung tissue by pulmonary alveolar macrophages. *Immunology.* 80:266-272.

113. Thepen, T., N. Van Rooijen, and G. Kraal. 1989. Alveolar macrophage elimination in vivo is associated with an increase in pulmonary immune response in mice. *J Exp Med.* 170:499-509.

114. Becker, S., J. Quay, and J. Soukup. 1991. Cytokine (tumor necrosis factor, IL-6, and IL-8) production by respiratory syncytial virus-infected human alveolar macrophages. *J Immunol.* 147:4307-4312.

115. Dawson, T. C., M. A. Beck, W. A. Kuziel, F. Henderson, and N. Maeda. 2000. Contrasting effects of CCR5 and CCR2 deficiency in the pulmonary inflammatory response to influenza A virus. *Am J Pathol.* 156:1951-1959.

116. Perrone, L. A., J. K. Plowden, A. Garcia-Sastre, J. M. Katz, and T. M. Tumpey. 2008. H5N1 and 1918 pandemic influenza virus infection results in early and excessive infiltration of macrophages and neutrophils in the lungs of mice. *PLoS Pathog.* 4:e1000115.

117. Wareing, M. D., A. L. Shea, C. A. Inglis, P. B. Dias, and S. R. Sarawar. 2007. CXCR2 is required for neutrophil recruitment to the lung during influenza virus infection, but is not essential for viral clearance. *Viral Immunol.* 20:369-378.

118. Wareing, M. D., A. Lyon, C. Inglis, F. Giannoni, I. Charo, and S. R. Sarawar. 2007. Chemokine regulation of the inflammatory response to a low-dose influenza infection in CCR2-/- mice. *J Leukoc Biol.* 81:793-801.

119. Herold, S., W. von Wulffen, M. Steinmueller, S. Pleschka, W. A. Kuziel, M. Mack, M. Srivastava, W. Seeger, U. A. Maus, and J. Lohmeyer. 2006. Alveolar epithelial cells direct monocyte transepithelial migration upon influenza virus infection: impact of chemokines and adhesion molecules. *J Immunol.* 177:1817-1824.

120. Bilyk, N., and P. G. Holt. 1993. Inhibition of the immunosuppressive activity of resident pulmonary alveolar macrophages by granulocyte/macrophage colony-stimulating factor. *J Exp Med.* 177:1773-1777.

121. Taut, K., C. Winter, D. E. Briles, J. C. Paton, J. W. Christman, R. Maus, R. Baumann, T. Welte, and U. A. Maus. 2008. Macrophage Turnover Kinetics in the Lungs of Mice Infected with Streptococcus pneumoniae. *Am J Respir Cell Mol Biol.* 38:105-113.

122. Baskin, C. R., H. Bielefeldt-Ohmann, T. M. Tumpey, P. J. Sabourin, J. P. Long, A. Garcia-Sastre, A. E. Tolnay, R. Albrecht, J. A. Pyles, P. H. Olson, L. D. Aicher, E. R. Rosenzweig, K. Murali-Krishna, E. A. Clark, M. S. Kotur, J. L. Fornek, S. Proll, R. E. Palermo, C. L. Sabourin, and M. G. Katze. 2009. Early and sustained innate immune response defines pathology and death in nonhuman primates infected by highly pathogenic influenza virus. *Proc Natl Acad Sci U S A.* 106:3455-3460.

123. Kobasa, D., S. M. Jones, K. Shinya, J. C. Kash, J. Copps, H. Ebihara, Y. Hatta, J. H. Kim, P. Halfmann, M. Hatta, F. Feldmann, J. B. Alimonti, L. Fernando, Y. Li, M. G. Katze, H. Feldmann, and Y. Kawaoka. 2007. Aberrant innate immune response in lethal infection of macaques with the 1918 influenza virus. *Nature.* 445:319-323.

124. Tumpey, T. M., A. Garcia-Sastre, J. K. Taubenberger, P. Palese, D. E. Swayne, M. J. Pantin-Jackwood, S. Schultz-Cherry, A. Solorzano, N. Van Rooijen, J. M. Katz, and C. F. Basler. 2005. Pathogenicity of influenza viruses with genes from the 1918 pandemic virus: functional roles of alveolar macrophages and neutrophils in limiting virus replication and mortality in mice. *J Virol.* 79:14933-14944.

125. Kim, H. M., Y. W. Lee, K. J. Lee, H. S. Kim, S. W. Cho, N. van Rooijen, Y. Guan, and S. H. Seo. 2008. Alveolar macrophages are indispensable for controlling influenza viruses in lungs of pigs. *J Virol.* 82:4265-4274.

126. Hashimoto, Y., T. Moki, T. Takizawa, A. Shiratsuchi, and Y. Nakanishi. 2007. Evidence for phagocytosis of influenza virus-infected, apoptotic cells by neutrophils and macrophages in mice. *J Immunol.* 178:2448-2457.

127. Xu, L., H. Yoon, M. Q. Zhao, J. Liu, C. V. Ramana, and R. I. Enelow. 2004. Cutting edge: pulmonary immunopathology mediated by antigen-specific expression of TNF-alpha by antiviral CD8+ T cells. *J Immunol.* 173:721-725.

128. Hussell, T., A. Pennycook, and P. J. Openshaw. 2001. Inhibition of tumor necrosis factor reduces the severity of virus-specific lung immunopathology. *Eur J Immunol.* 31:2566-2573.

129. Peper, R. L., and H. Van Campen. 1995. Tumor necrosis factor as a mediator of inflammation in influenza A viral pneumonia. *Microb Pathog.* 19:175-183.

130. Karupiah, G., J. H. Chen, C. F. Nathan, S. Mahalingam, and J. D. MacMicking. 1998. Identification of nitric oxide synthase 2 as an innate resistance locus against ectromelia virus infection. *J Virol.* 72:7703-7706.

131. Jayasekera, J. P., C. G. Vinuesa, G. Karupiah, and N. J. King. 2006. Enhanced antiviral antibody secretion and attenuated immunopathology during influenza virus infection in nitric oxide synthase-2-deficient mice. *J Gen Virol.* 87:3361-3371.

132. Snelgrove, R. J., L. Edwards, A. J. Rae, and T. Hussell. 2006. An absence of reactive oxygen species improves the resolution of lung influenza infection. *Eur J Immunol.* 36:1364-1373.

133. Akaike, T., and H. Maeda. 2000. Nitric oxide and virus infection. *Immunology.* 101:300-308.

134. Davis, I., and S. Matalon. 2001. Reactive species in viral pneumonitis: lessons from animal models. *News Physiol Sci.* 16:185-190.

135. Herold, S., M. Steinmueller, W. von Wulffen, L. Cakarova, R. Pinto, S. Pleschka, M. Mack, W. A. Kuziel, N. Corazza, T. Brunner, W. Seeger, and J. Lohmeyer. 2008. Lung epithelial apoptosis in influenza virus pneumonia: the role of macrophage-expressed TNF-related apoptosis-inducing ligand. *J Exp Med.* 205:3065-3077.

136. Krammer, P. H., R. Arnold, and I. N. Lavrik. 2007. Life and death in peripheral T cells. *Nat Rev Immunol.* 7:532-542.

137. Brenner, D., P. H. Krammer, and R. Arnold. 2008. Concepts of activated T cell death. *Crit Rev Oncol Hematol.* 66:52-64.

138. Krammer, P. H. 2000. CD95's deadly mission in the immune system. *Nature* 407:789-795.

139. Hildeman, D. A., Y. Zhu, T. C. Mitchell, J. Kappler, and P. Marrack. 2002. Molecular mechanisms of activated T cell death in vivo. *Curr Opin Immunol.* 14:354-359.

140. Karin, M., and A. Lin. 2002. NF-kappaB at the crossroads of life and death. *Nat Immunol.* 3:221-227.

141. Gulow, K., M. Kaminski, K. Darvas, D. Suss, M. Li-Weber, and P. H. Krammer. 2005. HIV-1 trans-activator of transcription substitutes for oxidative signaling in activation-induced T cell death. *J Immunol.* 174:5249-5260.

142. Cui, H., K. Matsui, S. Omura, S. L. Schauer, R. A. Matulka, G. E. Sonenshein, and S. T. Ju. 1997. Proteasome regulation of activation-induced T cell death. *Proc Natl Acad Sci U S A.* 94:7515-7520.

143. Lenardo, M. J. 1991. Interleukin-2 programs mouse alpha beta T lymphocytes for apoptosis. *Nature.* 353:858-861.

144. Van Parijs, L., Y. Refaeli, J. D. Lord, B. H. Nelson, A. K. Abbas, and D. Baltimore. 1999. Uncoupling IL-2 signals that regulate T cell proliferation, survival, and Fas-mediated activation-induced cell death. *Immunity.* 11:281-288.

145. Refaeli, Y., L. Van Parijs, C. A. London, J. Tschopp, and A. K. Abbas. 1998. Biochemical mechanisms of IL-2-regulated Fas-mediated T cell apoptosis. *Immunity.* 8:615-623.

146. Zhang, J., T. Bardos, Q. Shao, J. Tschopp, K. Mikecz, T. T. Glant, and A. Finnegan. 2003. IL-4 potentiates activated T cell apoptosis via an IL-2-dependent mechanism. *J Immunol.* 170:3495-3503.

147. Refaeli, Y., L. Van Parijs, S. I. Alexander, and A. K. Abbas. 2002. Interferon gamma is required for activation-induced death of T lymphocytes. *J Exp Med.* 196:999-1005.

148. Marks-Konczalik, J., S. Dubois, J. M. Losi, H. Sabzevari, N. Yamada, L. Feigenbaum, T. A. Waldmann, and Y. Tagaya. 2000. IL-2-induced activation-induced cell death is inhibited in IL-15 transgenic mice. *Proc Natl Acad Sci U S A.* 97:11445-11450.

149. Ku, C. C., M. Murakami, A. Sakamoto, J. Kappler, and P. Marrack. 2000. Control of homeostasis of CD8+ memory T cells by opposing cytokines. *Science.* 288:675-678.

150. Zhang, X., S. Sun, I. Hwang, D. F. Tough, and J. Sprent. 1998. Potent and selective stimulation of memory-phenotype CD8+ T cells in vivo by IL-15. *Immunity.* 8:591-599.

151. Yajima, T., K. Yoshihara, K. Nakazato, S. Kumabe, S. Koyasu, S. Sad, H. Shen, H. Kuwano, and Y. Yoshikai. 2006. IL-15 regulates CD8+ T cell contraction during primary infection. *J Immunol.* 176:507-515.

152. Akbar, A. N., N. J. Borthwick, R. G. Wickremasinghe, P. Panayoitidis, D. Pilling, M. Bofill, S. Krajewski, J. C. Reed, and M. Salmon. 1996. Interleukin-2 receptor common gamma-chain signaling cytokines regulate activated T cell apoptosis in response to growth factor withdrawal: selective induction of anti-apoptotic (bcl-2, bcl-xL) but not pro-apoptotic (bax, bcl-xS) gene expression. *Eur J Immunol.* 26:294-299.

153. Kim, H. R., K. A. Hwang, S. H. Park, and I. Kang. 2008. IL-7 and IL-15: biology and roles in T-Cell immunity in health and disease. *Crit Rev Immunol.* 28:325-339.

154. Budagian, V., E. Bulanova, R. Paus, and S. Bulfone-Paus. 2006. IL-15/IL-15 receptor biology: a guided tour through an expanding universe. *Cytokine Growth Factor Rev.* 17:259-280.

155. Sandau, M. M., K. S. Schluns, L. Lefrancois, and S. C. Jameson. 2004. Cutting edge: transpresentation of IL-15 by bone marrow-derived cells necessitates expression of IL-15 and IL-15R alpha by the same cells. *J Immunol.* 173:6537-6541.

156. Kobayashi, H., S. Dubois, N. Sato, H. Sabzevari, Y. Sakai, T. A. Waldmann, and Y. Tagaya. 2005. Role of trans-cellular IL-15 presentation in the activation of NK cell-mediated killing, which leads to enhanced tumor immunosurveillance. *Blood.* 105:721-727.

157. Schluns, K. S., K. D. Klonowski, and L. Lefrancois. 2004. Transregulation of memory CD8 T-cell proliferation by IL-15Ralpha+ bone marrow-derived cells. *Blood.* 103:988-994.

158. Schluns, K. S., T. Stoklasek, and L. Lefrancois. 2005. The roles of interleukin-15 receptor alpha: trans-presentation, receptor component, or both? *Int J Biochem Cell Biol.* 37:1567-1571.

159. Burkett, P. R., R. Koka, M. Chien, S. Chai, D. L. Boone, and A. Ma. 2004. Coordinate expression and trans presentation of interleukin (IL)-15Ralpha and IL-15 supports natural killer cell and memory CD8+ T cell homeostasis. *J Exp Med.* 200:825-834.

160. Burkett, P. R., R. Koka, M. Chien, S. Chai, F. Chan, A. Ma, and D. L. Boone. 2003. IL-15R alpha expression on CD8+ T cells is dispensable for T cell memory. *Proc Natl Acad Sci U S A.* 100:4724-4729.

161. Ma, A., R. Koka, and P. Burkett. 2006. Diverse functions of IL-2, IL-15, and IL-7 in lymphoid homeostasis. *Annu Rev Immunol.* 24:657-679.

162. Mattei, F., G. Schiavoni, F. Belardelli, and D. F. Tough. 2001. IL-15 is expressed by dendritic cells in response to type I IFN, double-stranded RNA, or lipopolysaccharide and promotes dendritic cell activation. *J Immunol.* 167:1179-1187.

163. Musso, T., L. Calosso, M. Zucca, M. Millesimo, D. Ravarino, M. Giovarelli, F. Malavasi, A. N. Ponzi, R. Paus, and S. Bulfone-Paus. 1999. Human monocytes constitutively express membrane-bound, biologically active, and interferon-gamma-upregulated interleukin-15. *Blood.* 93:3531-3539.

164. Doherty, T. M., R. A. Seder, and A. Sher. 1996. Induction and regulation of IL-15 expression in murine macrophages. *J Immunol.* 156:735-741.

165. Dubois, S. P., T. A. Waldmann, and J. R. Muller. 2005. Survival adjustment of mature dendritic cells by IL-15. *Proc Natl Acad Sci U S A.* 102:8662-8667.

166. Liu, T., H. Nishimura, T. Matsuguchi, and Y. Yoshikai. 2000. Differences in interleukin-12 and -15 production by dendritic cells at the early stage of Listeria monocytogenes infection between BALB/c and C57 BL/6 mice. *Cell Immunol.* 202:31-40.

167. Ohteki, T., K. Suzue, C. Maki, T. Ota, and S. Koyasu. 2001. Critical role of IL-15-IL-15R for antigen-presenting cell functions in the innate immune response. *Nat Immunol.* 2:1138-1143.

168. Jinushi, M., T. Takehara, T. Tatsumi, T. Kanto, V. Groh, T. Spies, T. Suzuki, T. Miyagi, and N. Hayashi. 2003. Autocrine/paracrine IL-15 that is required for type I IFN-mediated dendritic cell expression of MHC class I-related chain A and B is impaired in hepatitis C virus infection. *J Immunol.* 171:5423-5429.

169. Pulendran, B., S. Dillon, C. Joseph, T. Curiel, J. Banchereau, and M. Mohamadzadeh. 2004. Dendritic cells generated in the presence of GM-CSF plus IL-15 prime potent CD8+ Tc1 responses in vivo. *Eur J Immunol.* 34:66-73.

170. Schluns, K. S., K. Williams, A. Ma, X. X. Zheng, and L. Lefrancois. 2002. Cutting edge: requirement for IL-15 in the generation of primary and memory antigen-specific CD8 T cells. *J Immunol.* 168:4827-4831.

171. Becker, T. C., E. J. Wherry, D. Boone, K. Murali-Krishna, R. Antia, A. Ma, and R. Ahmed. 2002. Interleukin 15 is required for proliferative renewal of virus-specific memory CD8 T cells. *J Exp Med.* 195:1541-1548.

172. Goldrath, A. W., P. V. Sivakumar, M. Glaccum, M. K. Kennedy, M. J. Bevan, C. Benoist, D. Mathis, and E. A. Butz. 2002. Cytokine requirements for acute and Basal homeostatic proliferation of naive and memory CD8+ T cells. *J Exp Med.* 195:1515-1522.

173. Rausch, A., M. Hessmann, A. Holscher, T. Schreiber, S. Bulfone-Paus, S. Ehlers, and C. Holscher. 2006. Interleukin-15 mediates protection against experimental tuberculosis: a role for NKG2D-dependent effector mechanisms of CD8+ T cells. *Eur J Immunol.* 36:1156-1167.

174. Vella, A. T., S. Dow, T. A. Potter, J. Kappler, and P. Marrack. 1998. Cytokine-induced survival of activated T cells in vitro and in vivo. *Proc Natl Acad Sci U S A.* 95:3810-3815.

175. Bulfone-Paus, S., D. Ungureanu, T. Pohl, G. Lindner, R. Paus, R. Ruckert, H. Krause, and U. Kunzendorf. 1997. Interleukin-15 protects from lethal apoptosis in vivo. *Nat Med.* 3:1124-1128.

176. Lenschow, D. J., T. L. Walunas, and J. A. Bluestone. 1996. CD28/B7 system of T cell costimulation. *Annu Rev Immunol.* 14:233-258.

177. Sharpe, A. H., and G. J. Freeman. 2002. The B7-CD28 superfamily. *Nat Rev Immunol.* 2:116-126.

178. Croft, M. 2003. Costimulation of T cells by OX40, 4-1BB, and CD27. *Cytokine Growth Factor Rev.* 14:265-273.

179. Watts, T. H. 2005. TNF/TNFR family members in costimulation of T cell responses. *Annu Rev Immunol.* 23:23-68.

180. Croft, M. 2009. The role of TNF superfamily members in T-cell function and diseases. *Nat Rev Immunol.* 9:271-285.

181. DeBenedette, M. A., A. Shahinian, T. W. Mak, and T. H. Watts. 1997. Costimulation of CD28- T lymphocytes by 4-1BB ligand. *J Immunol.* 158:551-559.

182. Ohshima, Y., Y. Tanaka, H. Tozawa, Y. Takahashi, C. Maliszewski, and G. Delespesse. 1997. Expression and function of OX40 ligand on human dendritic cells. *J Immunol.* 159:3838-3848.

183. Murata, K., N. Ishii, H. Takano, S. Miura, L. C. Ndhlovu, M. Nose, T. Noda, and K. Sugamura. 2000. Impairment of antigen-presenting cell function in mice lacking expression of OX40 ligand. *J Exp Med.* 191:365-374.

184. Futagawa, T., H. Akiba, T. Kodama, K. Takeda, Y. Hosoda, H. Yagita, and K. Okumura. 2002. Expression and function of 4-1BB and 4-1BB ligand on murine dendritic cells. *Int Immunol.* 14:275-286.

185. Diehl, L., G. J. van Mierlo, A. T. den Boer, E. van der Voort, M. Fransen, L. van Bostelen, P. Krimpenfort, C. J. Melief, R. Mittler, R. E. Toes, and R. Offringa. 2002. In vivo triggering through 4-1BB enables Th-independent priming of CTL in the presence of an intact CD28 costimulatory pathway. *J Immunol.* 168:3755-3762.

186. Tesselaar, K., Y. Xiao, R. Arens, G. M. van Schijndel, D. H. Schuurhuis, R. E. Mebius, J. Borst, and R. A. van Lier. 2003. Expression of the murine CD27 ligand CD70 in vitro and in vivo. *J Immunol.* 170:33-40.

187. Grewal, I. S., and R. A. Flavell. 1998. CD40 and CD154 in cell-mediated immunity. *Annu Rev Immunol.* 16:111-135.

188. Borrow, P., A. Tishon, S. Lee, J. Xu, I. S. Grewal, M. B. Oldstone, and R. A. Flavell. 1996. CD40L-deficient mice show deficits in antiviral immunity and have an impaired memory CD8+ CTL response. *J Exp Med.* 183:2129-2142.

189. Edelmann, K. H., and C. B. Wilson. 2001. Role of CD28/CD80-86 and CD40/CD154 costimulatory interactions in host defense to primary herpes simplex virus infection. *J Virol.* 75:612-621.

190. Lee, B. O., L. Hartson, and T. D. Randall. 2003. CD40-deficient, influenza-specific CD8 memory T cells develop and function normally in a CD40-sufficient environment. *J Exp Med.* 198:1759-1764.

191. Carreno, B. M., and M. Collins. 2002. The B7 family of ligands and its receptors: new pathways for costimulation and inhibition of immune responses. *Annu Rev Immunol.* 20:29-53.

192. Bachmann, M. F., R. M. Zinkernagel, and A. Oxenius. 1998. Immune responses in the absence of costimulation: viruses know the trick. *J Immunol.* 161:5791-5794.

193. Lee, B. J., S. K. Reiter, M. Anderson, and S. R. Sarawar. 2002. CD28(-/-) mice show defects in cellular and humoral immunity but are able to control infection with murine gammaherpesvirus 68. *J Virol.* 76:3049-3053.

194. Kundig, T. M., A. Shahinian, K. Kawai, H. W. Mittrucker, E. Sebzda, M. F. Bachmann, T. W. Mak, and P. S. Ohashi. 1996. Duration of TCR stimulation determines costimulatory requirement of T cells. *Immunity.* 5:41-52.

195. Sigal, L. J., H. Reiser, and K. L. Rock. 1998. The role of B7-1 and B7-2 costimulation for the generation of CTL responses in vivo. *J Immunol.* 161:2740-2745.

196. Shahinian, A., K. Pfeffer, K. P. Lee, T. M. Kundig, K. Kishihara, A. Wakeham, K. Kawai, P. S. Ohashi, C. B. Thompson, and T. W. Mak. 1993. Differential T cell costimulatory requirements in CD28-deficient mice. *Science.* 261:609-612.

197. McAdam, A. J., E. A. Farkash, B. E. Gewurz, and A. H. Sharpe. 2000. B7 costimulation is critical for antibody class switching and CD8(+) cytotoxic T-lymphocyte generation in the host response to vesicular stomatitis virus. *J Virol.* 74:203-208.

198. Kim, S. K., K. S. Schluns, and L. Lefrancois. 1999. Induction and visualization of mucosal memory CD8 T cells following systemic virus infection. *J Immunol.* 163:4125-4132.

199. Thebeau, L. G., and L. A. Morrison. 2003. Mechanism of reduced T-cell effector functions and class-switched antibody responses to herpes simplex virus type 2 in the absence of B7 costimulation. *J Virol.* 77:2426-2435.

200. Chen, W., J. R. Bennink, P. A. Morton, and J. W. Yewdell. 2002. Mice deficient in perforin, CD4+ T cells, or CD28-mediated signaling maintain the typical immunodominance hierarchies of CD8+ T-cell responses to influenza virus. *J Virol.* 76:10332-10337.

201. Bertram, E. M., P. Lau, and T. H. Watts. 2002. Temporal segregation of 4-1BB versus CD28-mediated costimulation: 4-1BB ligand influences T cell numbers late in the primary response and regulates the size of the T cell memory response following influenza infection. *J Immunol.* 168:3777-3785.

202. Lumsden, J. M., J. M. Roberts, N. L. Harris, R. J. Peach, and F. Ronchese. 2000. Differential requirement for CD80 and CD80/CD86-dependent costimulation in the lung immune response to an influenza virus infection. *J Immunol.* 164:79-85.

203. Halstead, E. S., Y. M. Mueller, J. D. Altman, and P. D. Katsikis. 2002. In vivo stimulation of CD137 broadens primary antiviral CD8+ T cell responses. *Nat Immunol.* 3:536-541.

204. Hendriks, J., Y. Xiao, and J. Borst. 2003. CD27 promotes survival of activated T cells and complements CD28 in generation and establishment of the effector T cell pool. *J Exp Med.* 198:1369-1380.

205. Suresh, M., J. K. Whitmire, L. E. Harrington, C. P. Larsen, T. C. Pearson, J. D. Altman, and R. Ahmed. 2001. Role of CD28-B7 interactions in generation and maintenance of CD8 T cell memory. *J Immunol.* 167:5565-5573.

206. Bertram, E. M., W. Dawicki, B. Sedgmen, J. L. Bramson, D. H. Lynch, and T. H. Watts. 2004. A switch in costimulation from CD28 to 4-1BB during primary versus secondary CD8 T cell response to influenza in vivo. *J Immunol.* 172:981-988.

207. Bertram, E. M., W. Dawicki, and T. H. Watts. 2004. Role of T cell costimulation in anti-viral immunity. *Semin Immunol.* 16:185-196.

208. Cooper, D., P. Bansal-Pakala, and M. Croft. 2002. 4-1BB (CD137) controls the clonal expansion and survival of CD8 T cells in vivo but does not contribute to the development of cytotoxicity. *Eur J Immunol.* 32:521-529.

209. Chu, N. R., M. A. DeBenedette, B. J. Stiernholm, B. H. Barber, and T. H. Watts. 1997. Role of IL-12 and 4-1BB ligand in cytokine production by CD28+ and CD28- T cells. *J Immunol.* 158:3081-3089.

210. Cannons, J. L., P. Lau, B. Ghumman, M. A. DeBenedette, H. Yagita, K. Okumura, and T. H. Watts. 2001. 4-1BB ligand induces cell division, sustains survival, and enhances effector function of CD4 and CD8 T cells with similar efficacy. *J Immunol.* 167:1313-1324.

211. Gramaglia, I., D. Cooper, K. T. Miner, B. S. Kwon, and M. Croft. 2000. Co-stimulation of antigen-specific CD4 T cells by 4-1BB ligand. *Eur J Immunol.* 30:392-402.

212. Hurtado, J. C., Y. J. Kim, and B. S. Kwon. 1997. Signals through 4-1BB are costimulatory to previously activated splenic T cells and inhibit activation-induced cell death. *J Immunol.* 158:2600-2609.

213. Takahashi, C., R. S. Mittler, and A. T. Vella. 1999. Cutting edge: 4-1BB is a bona fide CD8 T cell survival signal. *J Immunol.* 162:5037-5040.

214. Lee, H. W., S. J. Park, B. K. Choi, H. H. Kim, K. O. Nam, and B. S. Kwon. 2002. 4-1BB promotes the survival of CD8+ T lymphocytes by increasing expression of Bcl-xL and Bfl-1. *J Immunol.* 169:4882-4888.

215. DeBenedette, M. A., T. Wen, M. F. Bachmann, P. S. Ohashi, B. H. Barber, K. L. Stocking, J. J. Peschon, and T. H. Watts. 1999. Analysis of 4-1BB ligand (4-1BBL)-deficient mice and of mice lacking both 4-1BBL and CD28 reveals a role for 4-1BBL in skin allograft rejection and in the cytotoxic T cell response to influenza virus. *J Immunol.* 163:4833-4841.

216. Tan, J. T., J. K. Whitmire, R. Ahmed, T. C. Pearson, and C. P. Larsen. 1999. 4-1BB ligand, a member of the TNF family, is important for the generation of antiviral CD8 T cell responses. *J Immunol.* 163:4859-4868.

217. Kwon, B. S., J. C. Hurtado, Z. H. Lee, K. B. Kwack, S. K. Seo, B. K. Choi, B. H. Koller, G. Wolisi, H. E. Broxmeyer, and D. S. Vinay. 2002. Immune responses in 4-1BB (CD137)-deficient mice. *J Immunol.* 168:5483-5490.

218. Lin, G. H., B. J. Sedgmen, T. J. Moraes, L. M. Snell, D. J. Topham, and T. H. Watts. 2009. Endogenous 4-1BB ligand plays a critical role in protection from influenza-induced disease. *J Immunol.* 182:934-947.

219. Chen, A. I., A. J. McAdam, J. E. Buhlmann, S. Scott, M. L. Lupher, Jr., E. A. Greenfield, P. R. Baum, W. C. Fanslow, D. M. Calderhead, G. J. Freeman, and A. H. Sharpe. 1999. Ox40-ligand has a critical costimulatory role in dendritic cell:T cell interactions. *Immunity.* 11:689-698.

220. Kopf, M., C. Ruedl, N. Schmitz, A. Gallimore, K. Lefrang, B. Ecabert, B. Odermatt, and M. F. Bachmann. 1999. OX40-deficient mice are defective in Th cell proliferation but are competent in generating B cell and CTL Responses after virus infection. *Immunity.* 11:699-708.

221. Pippig, S. D., C. Pena-Rossi, J. Long, W. R. Godfrey, D. J. Fowell, S. L. Reiner, M. L. Birkeland, R. M. Locksley, A. N. Barclay, and N. Killeen. 1999. Robust B cell immunity but impaired T cell proliferation in the absence of CD134 (OX40). *J Immunol.* 163:6520-6529.

222. Humphreys, I. R., G. Walzl, L. Edwards, A. Rae, S. Hill, and T. Hussell. 2003. A critical role for OX40 in T cell-mediated immunopathology during lung viral infection. *J Exp Med.* 198:1237-1242.

223. Bansal-Pakala, P., B. S. Halteman, M. H. Cheng, and M. Croft. 2004. Costimulation of CD8 T cell responses by OX40. *J Immunol.* 172:4821-4825.

224. Gramaglia, I., A. Jember, S. D. Pippig, A. D. Weinberg, N. Killeen, and M. Croft. 2000. The OX40 costimulatory receptor determines the development of CD4 memory by regulating primary clonal expansion. *J Immunol.* 165:3043-3050.

225. Evans, D. E., R. A. Prell, C. J. Thalhofer, A. A. Hurwitz, and A. D. Weinberg. 2001. Engagement of OX40 enhances antigen-specific CD4(+) T cell mobilization/memory development and humoral immunity: comparison of alphaOX-40 with alphaCTLA-4. *J Immunol.* 167:6804-6811.

226. De Smedt, T., J. Smith, P. Baum, W. Fanslow, E. Butz, and C. Maliszewski. 2002. Ox40 costimulation enhances the development of T cell responses induced by dendritic cells in vivo. *J Immunol.* 168:661-670.

227. Maxwell, J. R., A. Weinberg, R. A. Prell, and A. T. Vella. 2000. Danger and OX40 receptor signaling synergize to enhance memory T cell survival by inhibiting peripheral deletion. *J Immunol.* 164:107-112.

228. Nolte, M. A., R. W. van Olffen, K. P. van Gisbergen, and R. A. van Lier. 2009. Timing and tuning of CD27-CD70 interactions: the impact of signal strength in setting the balance between adaptive responses and immunopathology. *Immunol Rev.* 229:216-231.

229. Hendriks, J., L. A. Gravestein, K. Tesselaar, R. A. van Lier, T. N. Schumacher, and J. Borst. 2000. CD27 is required for generation and long-term maintenance of T cell immunity. *Nat Immunol.* 1:433-440.

230. Tesselaar, K., R. Arens, G. M. van Schijndel, P. A. Baars, M. A. van der Valk, J. Borst, M. H. van Oers, and R. A. van Lier. 2003. Lethal T cell immunodeficiency induced by chronic costimulation via CD27-CD70 interactions. *Nat Immunol.* 4:49-54.

231. Dolfi, D. V., and P. D. Katsikis. 2007. CD28 and CD27 costimulation of CD8+ T cells: a story of survival. *Adv Exp Med Biol.* 590:149-170.

232. Kaech, S. M., and R. Ahmed. 2001. Memory CD8+ T cell differentiation: initial antigen encounter triggers a developmental program in naive cells. *Nat Immunol.* 2:415-422.

233. Wong, P., and E. G. Pamer. 2001. Cutting edge: antigen-independent CD8 T cell proliferation. *J Immunol.* 166:5864-5868.

234. Wong, P., and E. G. Pamer. 2004. Disparate in vitro and in vivo requirements for IL-2 during antigen-independent CD8 T cell expansion. *J Immunol.* 172:2171-2176.

235. Trinchieri, G. 2003. Interleukin-12 and the regulation of innate resistance and adaptive immunity. *Nat Rev Immunol.* 3:133-146.

236. Curtsinger, J. M., C. M. Johnson, and M. F. Mescher. 2003. CD8 T cell clonal expansion and development of effector function require prolonged exposure to antigen, costimulation, and signal 3 cytokine. *J Immunol.* 171:5165-5171.

237. Curtsinger, J. M., D. C. Lins, and M. F. Mescher. 2003. Signal 3 determines tolerance versus full activation of naive CD8 T cells: dissociating proliferation and development of effector function. *J Exp Med.* 197:1141-1151.

238. Van Rooijen, N., and A. Sanders. 1994. Liposome mediated depletion of macrophages: mechanism of action, preparation of liposomes and applications. *J Immunol Methods.* 174:83-93.

239. Rogers, P. R., J. Song, I. Gramaglia, N. Killeen, and M. Croft. 2001. OX40 promotes Bcl-xL and Bcl-2 expression and is essential for long-term survival of CD4 T cells. *Immunity.* 15:445-455.

240. Song, J., S. Salek-Ardakani, P. R. Rogers, M. Cheng, L. Van Parijs, and M. Croft. 2004. The costimulation-regulated duration of PKB activation controls T cell longevity. *Nat Immunol.* 5:150-158.

241. Vitiello, A., L. Yuan, R. W. Chesnut, J. Sidney, S. Southwood, P. Farness, M. R. Jackson, P. A. Peterson, and A. Sette. 1996. Immunodominance analysis of CTL responses to influenza PR8 virus reveals two new dominant and subdominant Kb-restricted epitopes. *J Immunol.* 157:5555-5562.

242. Chen, W., C. C. Norbury, Y. Cho, J. W. Yewdell, and J. R. Bennink. 2001. Immunoproteasomes shape immunodominance hierarchies of antiviral CD8(+) T cells at the levels of T cell repertoire and presentation of viral antigens. *J Exp Med.* 193:1319-1326.

243. Chen, W., L. C. Anton, J. R. Bennink, and J. W. Yewdell. 2000. Dissecting the multifactorial causes of immunodominance in class I-restricted T cell responses to viruses. *Immunity.* 12:83-93.

244. La Gruta, N. L., S. J. Turner, and P. C. Doherty. 2004. Hierarchies in cytokine expression profiles for acute and resolving influenza virus-specific CD8+ T cell responses: correlation of cytokine profile and TCR avidity. *J Immunol.* 172:5553-5560.

245. La Gruta, N. L., P. C. Doherty, and S. J. Turner. 2006. A correlation between function and selected measures of T cell avidity in influenza virus-specific CD8+ T cell responses. *Eur J Immunol.* 36:2951-2959.

246. Turner, S. J., P. C. Doherty, J. McCluskey, and J. Rossjohn. 2006. Structural determinants of T-cell receptor bias in immunity. *Nat Rev Immunol.* 6:883-894.

247. Messaoudi, I., J. A. Guevara Patino, R. Dyall, J. LeMaoult, and J. Nikolich-Zugich. 2002. Direct link between mhc polymorphism, T cell avidity, and diversity in immune defense. *Science.* 298:1797-1800.

248. Turner, S. J., K. Kedzierska, H. Komodromou, N. L. La Gruta, M. A. Dunstone, A. I. Webb, R. Webby, H. Walden, W. Xie, J. McCluskey, A. W. Purcell, J. Rossjohn, and P. C. Doherty. 2005. Lack of prominent peptide-major histocompatibility complex features limits repertoire diversity in virus-specific CD8+ T cell populations. *Nat Immunol.* 6:382-389.

249. La Gruta, N. L., K. Kedzierska, K. Pang, R. Webby, M. Davenport, W. Chen, S. J. Turner, and P. C. Doherty. 2006. A virus-specific CD8+ T cell immunodominance hierarchy determined by antigen dose and precursor frequencies. *Proc Natl Acad Sci U S A.* 103:994-999.

250. Turner, S. J., G. Diaz, R. Cross, and P. C. Doherty. 2003. Analysis of clonotype distribution and persistence for an influenza virus-specific CD8+ T cell response. *Immunity.* 18:549-559.

251. Kedzierska, K., S. J. Turner, and P. C. Doherty. 2004. Conserved T cell receptor usage in primary and recall responses to an immunodominant influenza virus nucleoprotein epitope. *Proc Natl Acad Sci U S A.* 101:4942-4947.

252. Williams, M. A., J. Trambley, J. Ha, A. B. Adams, M. M. Durham, P. Rees, S. R. Cowan, T. C. Pearson, and C. P. Larsen. 2000. Genetic characterization of strain differences in the ability to mediate CD40/CD28-independent rejection of skin allografts. *J Immunol.* 165:6849-6857.

253. Maldonado-Lopez, R., T. De Smedt, P. Michel, J. Godfroid, B. Pajak, C. Heirman, K. Thielemans, O. Leo, J. Urbain, and M. Moser. 1999. CD8alpha+ and CD8alpha- subclasses of dendritic cells direct the development of distinct T helper cells in vivo. *J Exp Med.* 189:587-592.

254. Maldonado-Lopez, R., C. Maliszewski, J. Urbain, and M. Moser. 2001. Cytokines regulate the capacity of CD8alpha(+) and CD8alpha(-) dendritic cells to prime Th1/Th2 cells in vivo. *J Immunol.* 167:4345-4350.

255. Fujimoto, N., H. Ishida, I. Nakamura, K. Ogasawara, and Y. Itoh. 2003. Quantities of interleukin-12p40 in mature CD8alpha negative dendritic cells correlate with strength of TCR signal and determine Th cell development. *Microbiol Immunol.* 47:1017-1024.

256. Winkel, K. D., V. Kronin, M. F. Krummel, and K. Shortman. 1997. The nature of the signals regulating CD8 T cell proliferative responses to CD8alpha+ or CD8alpha- dendritic cells. *Eur J Immunol.* 27:3350-3359.

257. Schulz, O., and C. Reis e Sousa. 2002. Cross-presentation of cell-associated antigens by CD8alpha+ dendritic cells is attributable to their ability to internalize dead cells. *Immunology* 107:183-189.

258. Barchet, W., M. Cella, and M. Colonna. 2005. Plasmacytoid dendritic cells- virus experts of innate immunity. *Semin Immunol.* 17:253-261.

259. Nakano, H., M. Yanagita, and M. D. Gunn. 2001. Cd11c+B220+Gr-1+ cells in mouse lymph nodes and spleen display characteristics of plasmacytoid dendritic cells. *J Exp Med.* 194:1171-1178.

260. Martin, P., G. Martinez del Hoyo, F. Anjuere, F. C. Arias, H. H. Vargas, A. Fernandez-L, V. Parrillas, and C. Ardavin. 2002. Characterization of a new subpopulation of mouse CD8a+ B220+ dendritic cells endowed with type 1 interferon production capacity and tolerogenic potential. *Blood.* 100:383-390.

261. Asselin-Paturel, C., A. Boonstra, M. Dalod, I. Durand, N. Yessaad, C. Dezutter0Dambuyant, and et al. 2001. Mouse type I IFN-producing cells are immature APCs with plasmacytoid morphology. *Nat Immunol.* 200:1144-1150.

262. McGill, J., Legge, K.L.L. . 2009. Contribution of lung-resident T cell proliferation to the overall magnitude of the antigen-specific CD8 T cell response in the lungs following murine influenza virus infection. *J Immunol*. 183:4177-4181.

263. McGill, J., and K. L. L. Legge. 2008. Continued proliferation of influenza-specific T cell in the lungs during the early stages of influenza virus infections. *Options for the Control of Influenza*.

264. McGill, J. 2007. The role of pulmonary DC in the lungs during influenza infection. In *Pathology*. University of Iowa, Iowa City.

265. Breitschopf, K., A. M. Zeiher, and S. Dimmeler. 2000. Ubiquitin-mediated degradation of the proapoptotic active form of bid. A functional consequence on apoptosis induction. *J Biol Chem.* 275:21648-21652.

266. Hailfinger, S., F. Rebeaud, and M. Thome. 2009. Adapter and enzymatic functions of proteases in T-cell activation. *Immunol Rev.* 232:334-347.

267. Alam, A., L. Y. Cohen, S. Aouad, and R. P. Sekaly. 1999. Early activation of caspases during T lymphocyte stimulation results in selective substrate cleavage in nonapoptotic cells. *J Exp Med.* 190:1879-1890.

268. Kennedy, N. J., T. Kataoka, J. Tschopp, and R. C. Budd. 1999. Caspase activation is required for T cell proliferation. *J Exp Med.* 190:1891-1896.

269. Salmena, L., B. Lemmers, A. Hakem, E. Matysiak-Zablocki, K. Murakami, P. Y. Au, D. M. Berry, L. Tamblyn, A. Shehabeldin, E. Migon, A. Wakeham, D. Bouchard, W. C. Yeh, J. C. McGlade, P. S. Ohashi, and R. Hakem. 2003. Essential role for caspase 8 in T-cell homeostasis and T-cell-mediated immunity. *Genes Dev.* 17:883-895.

270. Overbergh, L., D. Valckx, M. Waer, and C. Mathieu. 1999. Quantification of murine cytokine mRNAs using real time quantitative reverse transcriptase PCR. *Cytokine.* 11:305-312.

271. Abebe, F., T. Mustafa, A. H. Nerland, and G. A. Bjune. 2006. Cytokine profile during latent and slowly progressive primary tuberculosis: a possible role for interleukin-15 in mediating clinical disease. *Clin Exp Immunol.* 143:180-192.

272. Castro, J. E., J. A. Listman, B. A. Jacobson, Y. Wang, P. A. Lopez, S. Ju, P. W. Finn, and D. L. Perkins. 1996. Fas modulation of apoptosis during negative selection of thymocytes. *Immunity.* 5:617-627.

273. Janssen, E. M., N. M. Droin, E. E. Lemmens, M. J. Pinkoski, S. J. Bensinger, B. D. Ehst, T. S. Griffith, D. R. Green, and S. P. Schoenberger. 2005. CD4+ T-cell help controls CD8+ T-cell memory via TRAIL-mediated activation-induced cell death. *Nature.* 434:88-93.

274. Lamhamedi-Cherradi, S. E., S. J. Zheng, K. A. Maguschak, J. Peschon, and Y. H. Chen. 2003. Defective thymocyte apoptosis and accelerated autoimmune diseases in TRAIL-/- mice. *Nat Immunol.* 4:255-260.

275. Martinez-Lorenzo, M. J., M. A. Alava, S. Gamen, K. J. Kim, A. Chuntharapai, A. Pineiro, J. Naval, and A. Anel. 1998. Involvement of APO2 ligand/TRAIL in activation-induced death of Jurkat and human peripheral blood T cells. *Eur J Immunol.* 28:2714-2725.

276. Speiser, D. E., E. Sebzda, T. Ohteki, M. F. Bachmann, K. Pfeffer, T. W. Mak, and P. S. Ohashi. 1996. Tumor necrosis factor receptor p55 mediates deletion of peripheral cytotoxic T lymphocytes in vivo. *Eur J Immunol.* 26:3055-3060.

277. Zheng, L., G. Fisher, R. E. Miller, J. Peschon, D. H. Lynch, and M. J. Lenardo. 1995. Induction of apoptosis in mature T cells by tumour necrosis factor. *Nature.* 377:348-351.

278. Devadas, S., J. Das, C. Liu, L. Zhang, A. I. Roberts, Z. Pan, P. A. Moore, G. Das, and Y. Shi. 2006. Granzyme B is critical for T cell receptor-induced cell death of type 2 helper T cells. *Immunity.* 25:237-247.

279. Jewell, N. A., N. Vaghefi, S. E. Mertz, P. Akter, R. S. Peebles, Jr., L. O. Bakaletz, R. K. Durbin, E. Flano, and J. E. Durbin. 2007. Differential type I interferon induction by respiratory syncytial virus and influenza a virus in vivo. *J Virol.* 81:9790-9800.

280. Pulle, G., M. Vidric, and T. H. Watts. 2006. IL-15-dependent induction of 4-1BB promotes antigen-independent CD8 memory T cell survival. *J Immunol.* 176:2739-2748.

281. Moyron-Quiroz, J. E., J. Rangel-Moreno, K. Kusser, L. Hartson, F. Sprague, S. Goodrich, D. L. Woodland, F. E. Lund, and T. D. Randall. 2004. Role of inducible bronchus associated lymphoid tissue (iBALT) in respiratory immunity. *Nature Medicine.* 10:927-934.

282. Woodland, D. L., and T. D. Randall. 2004. Anatomical features of anti-viral immunity in the respiratory tract. *Semin Immunol.* 16:163-170.

283. Sung, S. S., S. M. Fu, C. E. Rose, Jr., F. Gaskin, S. T. Ju, and S. R. Beaty. 2006. A major lung CD103 (alphaE)-beta7 integrin-positive epithelial dendritic cell population expressing Langerin and tight junction proteins. *J Immunol.* 176:2161-2172.

284. Hugues, S., L. Fetler, L. Bonifaz, J. Helft, F. Amblard, and S. Amigorena. 2004. Distinct T cell dynamics in lymph nodes during the induction of tolerance and immunity. *Nat Immunol* 5:1235-1242.